Connecting Archimedean and non-Archimedean AdS/CFT

Sarthak Parikh

A Dissertation

Presented to the Faculty

of Princeton University

in Candidacy for the Degree

of Doctor of Philosophy

Recommended for Acceptance

by the Department of

Physics

Advisor: Steven S. Gubser

September 2017

Abstract

This thesis develops a non-Archimedean analog of the usual Archimedean anti-de Sitter (AdS)/conformal field theory (CFT) correspondence. AdS space gets replaced by a Bruhat–Tits tree, which is a regular graph with no cycles. The boundary of the Bruhat–Tits tree is described by an unramified extension of the p-adic numbers, which replaces the real valued Euclidean vector space on which the CFT lives. Conformal transformations on the boundary act as linear fractional transformations.

In the first part of the thesis, correlation functions are computed in the simple case of massive, interacting scalars in the bulk. They are found to be surprisingly similar to standard holographic correlation functions down to precise numerical coefficients, when expressed in terms of local zeta functions. Along the way, we show that like in the Archimedean case, CFT conformal blocks are dual to geodesic bulk diagrams, which are bulk exchange diagrams with the bulk points of integration restricted to certain geodesics. Other than these intriguing similarities, significant simplifications also arise. Notably, all derivatives disappear from the operator product expansion, and the conformal block decomposition of the four-point function. Finally, a minimal bulk action is constructed on the Bruhat–Tits tree for a single scalar field with nearest neighbor interactions, which reproduces the two-, three-, and four-point functions of the free $O(N)$ model.

In the second part, the p-adic $O(N)$ model is studied at the interacting fixed

point. Leading order results for the anomalous dimensions of low dimension operators are obtained in two separate regimes: the ϵ-expansion and the large N limit. Remarkably, formulae for anomalous dimensions in the large N limit are valid equally for Archimedean and non-Archimedean field theories, when expressed in terms of local zeta functions. Finally, higher derivative versions of the $O(N)$ model in the Archimedean case are considered, where the general formula for anomalous dimensions obtained earlier is still valid. Analogies with two-derivative theories hint at the existence of some interesting new field theories in four real Euclidean dimensions.

Acknowledgements

I would like to deeply thank my advisor Steve Gubser for his exceptional guidance, support and encouragement during my graduate studies. Steve has been an incredibly inspiring mentor, advisor and collaborator. I have benefited immensely from my interactions with him over these years, and learnt so much. His enthusiasm for, and insightful approach to research has been awe-inspiring and deeply influential.

I am grateful to the Physics department for their full support and for providing a wonderful environment to work in. I would like to especially thank Herman Verlinde for his guidance and support over the past five years. I thank the high energy theory group at Princeton for a great and exciting five years! I would like to thank Igor Klebanov for offering stimulating courses in QFT and string theory, and also for being on my pre-thesis committee. I also thank David Huse for being on my pre-thesis committee, and Shivaji Sondhi for many helpful discussions, advice and his sense of humor. I am grateful to Herman Verlinde for agreeing to be a reader for this thesis, and to Silviu Pufu and Josh Shaevitz for agreeing to be on my FPO committee. I also thank the Physics department staff, especially Jessica Heslin, Kate Brosowsky, Kim Dawidowski and Toni Sarchi for all their help and their excellent and timely management of all academic needs.

I wish to thank all my amazing collaborators for intense collaborations and discussions over the past five years (including on projects which could not make

it to this thesis): Steve Gubser, Matt Heydeman, Bart Horn, Christian Jepsen, Johannes Knaute, Matilde Marcolli, Revant Nayar, Ingmar Saberi, Andreas Samberg, Bogdan Stoica, Brian Trundy and Przemek Witaszczyk. I am deeply indebted to the team behind Wolfram Mathematica. Grad school in general, and much work in this thesis in particular, would have been quite complicated without `FullSimplify` (and all the other incredibly useful commands and capabilities).

I want to thank all my friends at Princeton for everything, especially the great class of 2012 physics grads. You all made my grad school experience so much better, in your own unique ways, so I want to take the time to thank each of you individually. A proper thanks would, however, make the acknowledgements section the size of a full length chapter, which is not ideal. Also, each additional page in this thesis sets me back by a dime or two. So I will limit myself to sharing a few memorable, old and personal incidents which immediately come to my mind (and which you probably don't even remember). Unforgettable memories are flooding my mind even as my aching fingers try to keep up on the keyboard:

Aaron, it was always a pleasure to watch you engage in arguments with others, and I confess I sometimes used to feel if it were me, I would have destroyed you. But in reality it was actually very draining to try, and almost impossible to beat you at. Thanks for being an awesome office-mate. I won't forget those two long days of intense and non-stop calculations – it was really enjoyable! Aitor, thanks for teaching me (unsuccessfully) how to do backflips and somersaults on the trampoline. You were a great office-mate and fun to hang out with. Go 24D! Bin, thanks for sharing with me the ultimate strategy on how to survive on the Block 95 meal plan: Pay for lunches and use the meals on dinner! Dave, thanks for driving us out of town to safety (and eventually to the movies to watch *The Great Gatsby*) when the university was evacuated following a hoax call. I also look back fondly at the fun evening post-prelims in NYC. Thanks for being

a great floor-mate in 24D! Debayan, you never hesitate to stand up for others, including myself and thanks for that! You bring so much energy and enthusiasm to every party I've seen you at, but sometimes you ooze energy and lethargy at the same time - and I haven't quite figured out how. I have also never cooked as much food as I once did one fateful evening in the NGC kitchen (with you and Zach). DJ, your double at NGC was quite a set-up! I see you on average once a year, but it is always a pleasure. Farzan, thanks for your unwavering enthusiasm for soccer, and sorry I couldn't make it to many pick-up games. One of the first ever prelim problems we set forth to do, one fine naive afternoon in the NGC common room early in the term, we declared we could handle by simply balancing forces based on Newton's laws. Little did we know then we had to solve the Laplace equation in spherical coordinates with special boundary conditions until much, much later when we finally got back around to it again. Grisha, thinking about all those counter-intuitive and confusing aspects of GR during our first term was fun! Also thanks (to you and Debayan) for making the filing of first year taxes so entertaining. Ilya, thanks for your enthusiasm for learning, and your constant presence in Jadwin. I really enjoyed attempting to answer your penetrating questions about various things in physics. But the most memorable moment for me was the epiphany I had at the eve of the GR finals about you and you-know-what, which took me a substantial amount of time to bring to life. Joaquin, my good neighbor at 24D, your (and Josh's) birthdays were always very fun to celebrate! I enjoyed that long road trip to Boston! Josh, you are the reason why I ever ordered a meat burrito – I have never done it before or ever since. I hope you enjoyed it! You were hardly here after the second year (go 24D anyway!), and I sometimes used to miss hearing all the snide remarks you like to make. Lauren, thanks for being such a great office-mate from start to finish. I wish you had performed at a few more recitals, because your pieces

were so good! And the beautiful wedding was such a treat to attend! Lin, I haven't forgotten our intense games of squash at Dillon – I used to look forward to those! Thank you (to also HaoQi and an unsuspecting Helen) for being so enthusiastic about my "magic" tricks! Patty, the "natural refrigerator" you and your room-mates set-up during an extended power-cut in the middle of a snow blizzard was ingenious! You're always fun to talk to, but unfortunately I don't see you on the fourth floor that often. Steve, your prowess at basketball during the intra-murals came to our rescue more than once. Thanks buddy! Suerfu, thanks for agreeing to drive a U-Haul and help me with moving, after another friend had to cancel on me last second. You're a life saver! Yu, it was always fun to chat with you. You also unwittingly led to a lot of confusion during one of the physics undergrad labs. We were teaching different sections on the same day and shared the undergraduate teaching assistant (UTA) between us. One day he came up to me, and this is what happened:

UTA, "Yu said that the correction from the moment of inertia was small."

Me, "Really? I don't remember..."

UTA, "Well Yu did. So I want–"

Me, "I'm pretty sure I didn't because in the last lab I actually found big corrections from taking the moment of inertia into account..."

UTA, "Hmmm... But Yu found it didn't really factor in that much..."

Me, "Uhh wait no, I *didn't* –"

UTA, "Oh I'm talking about Yu, the graduate TA in the lab next door."

Facepalm!

And finally, Zach, I had the pleasure of seeing first-hand the early days of the Z-Bar as it shot to fame and glory. Thanks for being my vegetarian buddy on many occasions (except when you would order sea-food which is *not* vegetarian). Thanks also for single-handedly bringing together many BBQs, and immortalizing

"Ball in a Cylinder."

I also want to thank everyone else who I had the pleasure of hanging out with at Princeton and share memorable moments with, especially Chandra, Jon, Kenan, Logan, MdCI, members of the Juggling club, and *you*, the reader who I most likely forgot to acknowledge. A special thanks to Akshay and Sanjay for going beyond their call of duty by agreeing to take part in a superbly complicated housing application, designed to address my housing woes.

Outside Princeton, I'd like to thank all members of the Herd, M.T.S. and O.Z., especially Krits and Surro for always being there whenever I needed to escape from something. I am grateful to Sud for being a reminder of what the important things in life are. I also greatly thank Mitesh uncle, Neel, Rushang, Shobhana aunty and Vidhi for making me feel at home, away from home.

No words can do justice to how much I am grateful to my parents, Deepak and Suhasini Parikh, and all other members of my family. This thesis would not have been possible without your constant love, support, encouragement and patience.

The work in this thesis was supported in part by the Department of Energy under Grant No. DE-FG02-91ER40671, and in part by the Bershadsky Family Fellowship Fund in Mathematics or Physics.

To Ma, Papa and Dada.

Contents

Chapter 1

Introduction

1.1 An invitation to the thesis

The Standard Model of particle physics and Einstein's theory of General Relativity are the two theoretical pillars of physics which describe the four known fundamental forces of Nature: electromagnetism, weak interactions, strong interactions, and gravity, and all observed particles. While the Standard Model is a quantum field theory governed by the gauge group $SU(3) \times SU(2) \times U(1)$, which describes the quantum phenomena associated with electromagnetism, weak and strong interactions at small length scales, Einstein's General Relativity is a classical theory of gravity based on the principle of general covariance, describing gravitation at large length scales. Both these theories have found incredible success with experiments. The Standard Model (see [1] for the latest survey of the theory), which is currently being tested at the Large Hadron Collider (LHC) at CERN, has exceeded all expectations and shown exceptional agreement with experimental observations over the past few decades, with a recent high point the discovery of the Higgs boson five years ago [2, 3]. General Relativity too has survived intense experimental scrutiny both in the weak field regime, as well as

the strong field, highly non-linear regime, which most recently is being probed by studying black hole mergers and the direct detection of gravitational waves generated in such events [4, 5, 6] (the latest experimental confirmation coming as recently as June 2017). While individually very successful,[1] these theoretical frameworks remain disconnected from each other, and have so far evaded all attempts at a unification, leading to a consistent theory of quantum gravity. How then does gravity behave at the quantum level? This is one of the biggest and deepest open problems in theoretical physics at the moment. Experiments too have been unable to provide direction, as experimental signatures of quantum gravity have stayed out of reach thus far. On the one hand the LHC continues to carefully probe the Standard Model and physicists await experimental clues on what lies beyond the Standard Model. On the other, several recent experiments in cosmology are probing early Universe physics, where quantum gravity effects may turn out to play an important role. I remain hopeful that breakthroughs in experiments in the near future will provide us theoretical directions and shed light on new, unexplored ideas, and hints about quantum gravity.

Precision tests of the Standard Model at particle accelerators require the computation of cross-sections of many scattering processes, so that theoretical predictions can be compared with experimental observations. This way mismatches signalling deviations from the Standard Model can be uncovered with sufficient statistical significance. However, many scattering processes at energy scales of interest involve the strong interactions, and computations involving the strong force become incredibly unwieldy at low enough energies of interest, due to that fact that quantum chromodynamics (QCD), the theory of strong interactions becomes very strongly coupled and goes outside the regime of validity of

[1] Some experimental results point already to the fact that these theories are incomplete: the detection of neutrino masses [7, 8, 9], and the lack of understanding of dark matter and dark energy which together combine to form 95% of the Universe, to name a few.

perturbation theory. This serves as a major obstacle in probing the strong interactions sector of the Standard Model. Thus finding new computational tools and techniques for predicting scattering amplitudes of processes at strong couplings is desirable.

Two related theoretical revolutions of the last few decades, namely string theory and the gauge/gravity duality, have led to incredible insight into understanding the dynamics of quantum field theories at strong coupling, as well as quantum gravity. These advances form the backbone of this dissertation. Essentially, string theory describes the quantum mechanics of extended objects, the simplest ones being one-dimensional "strings". Historically, string theory was born as a candidate theory of strong interactions [10], but found limited success and was abandoned in favor of QCD. However, soon it was realized that the framework of string theory allowed the construction of mathematically consistent quantum theories of gravity [11, 12, 13]. Unfortunately, so far they have not had success in describing our physical world — for instance consistent theories live in spacetimes with the number of dimensions higher than the observed four. It is not clear precisely how the extra dimensions should be compactified or otherwise gotten rid of so as to describe our four-dimensional world. Additionally, the theories involve supersymmetry, and particles with quantum numbers not yet observed in any experiments. On top of this, a complete theoretical understanding of string theory is still lacking, although the "second superstring revolution" led to a lot of non-perturbative insight into string theory (see for example, [14, 15, 16, 17, 18]). However, these theories provide examples of (mathematically consistent) unification of quantum mechanics with gravity, and provide a concrete framework for learning more about quantum gravity. Moreover, the non-perturbative exploration of string theory gave us D-branes [19], the study of which eventually led to the gauge-string duality.

This brings us to the second revolution, the discovery of the holographic principle (or the gauge/gravity duality, or the anti-de Sitter (AdS)/conformal field theory (CFT) correspondence) [20, 21, 22, 23, 24]. It equates a quantum theory of gravity with a quantum field theory in one lower dimension. Such a duality came as a big surprise, given that it equates very different kinds of theories. Many examples of the duality include the equivalence between a string theory and a conformal field theory (CFT). It is often a weak/strong duality, which means that a string theory in the weak coupling limit is dual to a strongly interacting conformal field theory and vice versa. This makes the AdS/CFT duality a very useful tool for learning about quantum field theories at strong couplings (by studying instead the more tractable semi-classical limit of a string theory), and learning about quantum gravity (by studying instead a weakly coupled quantum field theory). We will discuss this correspondence in more detail in the next section.

Over time, several surprising mathematical structures in quantum field theories (QFTs) have come to light, thanks to the AdS/CFT correspondence as well as many other complimentary approaches (see [25] for one example), but much more remains undiscovered. In chapter 4 we study quantum field theories in a non-Archimedean spacetime motivated by this goal of uncovering interesting aspects of the structure of QFTs. Archimedean field theories are the ones usually studied in textbooks, based on fields defined on the spacetime $\mathbb{R}^n$ or $\mathbb{R}^{n-1,1}$. More precisely, the Archimedean property (of real numbers) is that if $0 < |a| < |b|$, then there is some integer n such that $|na| > |b|$. This property fails to hold in non-Archimedean metrics.[2] The remarkable simplicity and other surprising properties of non-Archimedean field theories, as well as their intimate connection

[2]In this dissertation the term Archimedean will always refer to any construction based entirely on real numbers, and the non-Archimedean spacetime will be constructed out of p-adic numbers, which are explained in section 1.3.

with Archimedean field theories forms the subject of chapter 4.

On the gravity side, it is the general expectation that the notion of spacetime will be drastically different at the Planck length ($\ell_p = \sqrt{\hbar G/c^3} \approx 10^{-33}$ cm in four dimensions), which is the length scale at which effects of quantum gravity disrupt the very structure of spacetime. Spacetime is thought to be emergent at these distances. Could it be that at Planck scales, spacetime is no longer continuous but discrete? Various aspects of gravity in a "discrete spacetime" have been explored in the literature (see, for example [26, 27, 28]). Recently, Refs. [29, 30] formulated an exact discretization of the evolution of strings in curved spacetimes, with a purely algebraic evolution law governing the classical dynamics. It was proposed [29] and later explicitly demonstrated [31], that the target spacetime could be suported on algebraic number fields, for example the rationals $\mathbb{Q}$ or an algebraic extension of $\mathbb{Q}$. We will develop yet another discretization approach in chapters 2-3 based on the local field of p-adic numbers, and study scalar field theories in a fixed gravitational background with a tree-like graph theoretic topology. (This was recently extended [32] to include a fluctuating spacetime.) In fact, such gravity theories are interesting to study for another reason: via the (non-Archimedean) AdS/CFT correspondence which will be developed in chapter 2, these theories of gravity share many features with the putative bulk duals of non-Archimedean field theories, such as the one discussed in chapter 4.

In the rest of this chapter, we briefly review some of the basic ingredients which go into this dissertation, namely the AdS/CFT correspondence, and the notion of number fields, particularly the non-Archimedean field of p-adic numbers. We end the chapter with a brief outline and summary of this dissertation.

1.2 The AdS/CFT correspondence

In this section we give a brief introduction to the AdS/CFT correspondence [22, 23, 24] (for a comprehensive review, see for example [33]). Loosely, it says that a quantum field theory in an n-dimensional spacetime is equivalent to a theory of quantum gravity in an $(n+1)$-dimensional spacetime. This is sometimes called a "holographic duality" because using this duality we may in principle "reconstruct" a higher dimensional theory entirely by studying its dual theory in lower dimensions. The simplest examples of this correspondence equate certain special quantum field theories called conformal field theories (CFTs), with theories of gravity in anti-de Sitter (AdS) space, hence the name AdS/CFT. Moreover, in many examples the quantum field theory is a gauge theory, and for this reason this is also often referred to as the gauge/gravity duality. The AdS/CFT correspondence is a conjectural statement, so although there are now many well studied examples providing strong evidence in its support, a proof remains elusive. The goal of the rest of this section is to explain this duality in some detail.

What is meant by the statement that a quantum field theory and a theory of gravity are "equivalent" or "holographically dual" to each other?

Broadly, a quantum field theory and a theory of gravity in a higher dimensional spacetime are holographically dual if all the information in one theory is encoded in some way in its dual. Here by a theory of gravity we do not necessarily mean Einstein's theory of General Relativity, which as we mentioned earlier has found incredible success in describing our Universe at cosmological length scales. Any mathematically consistent (quantum) theory of gravity which may or may not

have Einstein's General Relativity as its classical limit is welcome. That such a theory might not describe our real world should not be a disincentive to study the AdS/CFT correspondence — we will explain why later in this section in the answer to the question: *"Why is it useful?"*

To appreciate the profundity of the statement of the AdS/CFT correspondence, one should note that naively, a (quantum) theory of gravity is expected to describe physics fundamentally different from the physics of any quantum field theory, which is a theory *without* gravity. In particular, in a theory of gravity spacetime itself is dynamical, thus all matter in the theory must live on and interact with this dynamical spacetime. In fact, due to general coordinate invariance of gravity, it is impossible to define local observables. Remarkably by the AdS/CFT correspondence, a theory of gravity describes the *same* physics as its dual quantum field theory, which is a local field theory defined on a fixed background spacetime! To the untrained eye, these theories couldn't have been more different from each other, yet quite unexpectedly they are precisely equal or dual to each other by the holographic duality. Precisely how all the information of one theory is encoded in its dual is thus an important question, but not always easy to answer. We understand some aspects of this encoding, which we can use to develop a "holographic dictionary" that helps translate results in the language of one theory to results in the language of its dual. In other words, such a dictionary demonstrates explicit examples of how a theory with gravity and a theory without gravity can conceivably convey the same physics. The task of figuring out the full dictionary remains far from complete; we will give some examples of entries in this dictionary later in this section.

Even finding examples of holographically dual theories is not usually easy or obvious. By now we have many (conjectural) examples of such dual pairs, and a lot of non-trivial evidence in support of the respective dualities. Evidence comes

in many forms, such as calculating quantities in one theory, and the same quantities in the dual theory (more precisely, quantities related via the holographic dictionary) and verifying that they agree. As more and more agreements are uncovered, evidence in support of the duality grows. However, often it turns out if computations are easy to perform in one theory, they are almost intractable in the dual.[3] This means testing these dualities can be hard; on the other hand this also means that the holographic duality can be incredibly powerful — calculations which were completely inaccessible in one theory become very easy after translating to the language of the dual theory. We will say more about this later in this section.

Having painted a rough picture, let us turn to some concrete details. It helps to recall that the (Euclidean) partition function of a theory, which in a sense captures all available information in the theory, is given by

$$\mathcal{Z} = \int [\mathcal{D}\phi] \exp\left(-S[\phi]/\hbar\right), \tag{1.1}$$

where $S[\phi]$ denotes the action functional which depends on the field content ϕ of the theory. The partition function represents the sum over all possible field configurations, weighted by the value of the action at each configuration. Equivalently, it represents the quantum mechanical vacuum to vacuum transition amplitude. The integration measure $[\mathcal{D}\phi]$ implements the sum over all possible phase space configurations, which in the classical limit, $\hbar \to 0$ leads (via the saddle point approximation) to the evaluation of the partition function simply at the extremum of the action,[4]

$$\mathcal{Z}_{\text{classical}} \sim \exp\left(-S_{\text{extremum}}[\phi]\right). \tag{1.2}$$

Returning to the AdS/CFT correspondence, at its heart it is a duality between

[3] This is a consequence of the weak/strong nature of the correspondence which we alluded to earlier.

[4] From here on we will work in the units where $c = \hbar = 1$.

a theory of gravity in an $(n+1)$-dimensional spacetime (sometimes referred to as the "bulk") that has an n-dimensional asymptotic boundary, and a quantum field theory which "lives on that boundary". It may be expressed schematically as the equality of the partition functions of the two theories [23, 24]

$$\left\langle \exp\left(\int d^n x\, \phi_0(\vec{x})\mathcal{O}(\vec{x})\right)\right\rangle_{\text{QFT}} = \mathcal{Z}_{\text{gravity}}^{\left[\phi(z,\vec{x})\big|_{z=0}=\phi_0(\vec{x})\right]}, \tag{1.3}$$

where on the QFT side, we take the vacuum expectation value of the exponential of an operator $\mathcal{O}$ sourced by an independently chosen function $\phi_0(\vec{x})$. Thus the left hand side is the generating function of all correlators of the operator $\mathcal{O}$, generated via taking successive functional derivatives of the left hand side with respect to ϕ_0 and setting $\phi_0 = 0$ at the end. On the gravity side, we write the full partition function for the gravitational theory, where $\phi(z, \vec{x})$ is a dynamical field "dual to $\mathcal{O}$", and z is the extra "radial" direction (*i.e.* the additional dimension in the gravity theory), with the asymptotic boundary of the spacetime situated at $z = 0$. The field ϕ is subject to the boundary condition that at the asymptotic boundary ($z = 0$), it takes the value specified by the source function $\phi_0(\vec{x})$. By (1.3), computing M-point correlators of $\mathcal{O}$ in the field theory is equivalent to computing M-point Feynman diagrams of the field ϕ in the gravity theory, subject to appropriate boundary conditions.

In a holographically dual pair, for every field in the gravitational theory, there exists an operator in the QFT such that (1.3) holds. This field $\leftrightarrow$ operator correspondence represents one of the basic entries of the holographic dictionary. More can be said about the relation between the bulk field ϕ and the dual operator on the boundary $\mathcal{O}$; for example the relation between the mass of ϕ and the (scaling) dimension of $\mathcal{O}$. We will explain this in more detail later in this section in the answer to the question: *"What are some examples of the AdS/CFT correspondence?"* Here we note a related correspondence: for every local conserved

current in the boundary QFT, there is a massless gauge field in the bulk theory of gravity; for example a local (conserved) stress-tensor operator is dual to the graviton field in the gravity theory. At this stage, we can mention one more example of an entry in the holographic dictionary: moving the radial coordinate z, which measures the distance from the asymptotic boundary of the spacetime, is dual to performing renormalization in the dual quantum field theory. We will explain this in more detail soon.

As stated earlier, the simplest versions of the duality involve a gravitational theory in an AdS background and a conformal field theory as the dual quantum field theory. Before we present explicit examples of the duality, let us briefly review these constructions in more detail.

What is anti-de Sitter (AdS) space?

AdS space is the unique space which is maximally symmetric and negatively curved. It is a solution to Einstein's field equations (with a negative cosmological constant term) in the theory of General Relativity, described by the Einstein-Hilbert action,

$$S_{\rm EH} = \frac{1}{16\pi G}\int d^{n+1}x\sqrt{-g}\,(R-2\Lambda)\,, \tag{1.4}$$

where $g = \det g_{\mu\nu}$ is the determinant of the metric, R is the Ricci scalar, G is the $(n+1)$-dimensional version of Newton's gravitational constant, and Λ is the cosmological constant. The field equations following from (1.4) are

$$R_{\mu\nu} - \frac{1}{2}Rg_{\mu\nu} + \Lambda g_{\mu\nu} = 0\,, \tag{1.5}$$

where $R_{\mu\nu}$ is the Ricci curvature. The maximally symmetric solution to these equations for negative Λ is

$$ds^2 = -\left(1+\frac{r^2}{L^2}\right)dt^2 + \frac{1}{\left(1+\frac{r^2}{L^2}\right)}dr^2 + r^2 d\Omega_{n-1}^2\,, \tag{1.6}$$

with

$$\Lambda = -\frac{n(n-1)}{2L^2} \qquad R = g_{\mu\nu}R^{\mu\nu} = -\frac{n(n+1)}{L^2}\,, \tag{1.7}$$

where L is the radius of curvature of AdS_{n+1} (*i.e.* $(n+1)$-dimensional AdS space), and $d\Omega_{n-1}^2$ is the metric on an S^{n-1} sphere. Here is $r \in [0, \infty)$ and $t \in \mathbb{R}$. With the coordinate transformation

$$r = L\sinh\rho \qquad t = L\tau\,, \tag{1.8}$$

the metric takes the form

$$ds^2 = L^2\left(-\cosh^2\rho\, d\tau^2 + d\rho^2 + \sinh^2\rho\, d\Omega_{n-1}^2\right). \tag{1.9}$$

This metric is referred to as the (universal cover) of AdS space in global coordinates.

AdS space may also be parametrized as the equation of a hyperboloid in a flat $\mathbb{R}^{2,n}$ spacetime endowed with a $(--+\ldots+)$ signature. In equations, this means AdS_{n+1} is the hyperboloid

$$-X_{-1}^2 - X_0^2 + \sum_{j=1}^{n} X_j^2 = -L^2\,, \tag{1.10}$$

in $\mathbb{R}^{2,n}$ which has the metric

$$ds^2 = -dX_{-1}^2 - dX_0^2 + \sum_{j=1}^{n} dX_j^2\,. \tag{1.11}$$

It's easy to verify that

$$\begin{aligned} X_{-1} &= L\cosh\rho\,\cos\tau \\ X_0 &= L\cosh\rho\,\sin\tau \\ X_j &= L\sinh\rho\,\Omega_j \qquad \text{with } j = 1,\ldots,n \quad \text{and} \quad \sum_{j=1}^{n}\Omega_j^2 = 1 \end{aligned} \tag{1.12}$$

is a solution to (1.10). These are referred to as the global coordinates of AdS. Substituting them in (1.11), we recover (1.9) (once we "unwrap" the τ direction

to cover whole of $\mathbb{R}$ rather than just the interval $[0, 2\pi]$). The $SO(n,2)$ isometry of AdS_{n+1} is apparent from (1.10)-(1.11), while the $SO(2) \times SO(n)$ subgroup of $SO(n,2)$ is manifest in (1.9). Another way to parametrize AdS is:

$$\begin{aligned} X_{-1} &= \frac{1}{2u}\left(1 + u^2(L^2 + \vec{x}^2 - t^2)\right) \\ X_0 &= Lut \\ X^j &= Lux^j \qquad \text{with } j = 1, \ldots, n-1 \\ X^n &= \frac{1}{2u}\left(1 - u^2(L^2 - \vec{x}^2 + t^2)\right), \end{aligned} \tag{1.13}$$

where $u > 0$ and $\vec{x} \in \mathbb{R}^{n-1}$. Substituting this in (1.11), we get the AdS metric in the following form,

$$ds^2 = L^2\left(\frac{du^2}{u^2} + u^2(-dt^2 + d\vec{x}^2)\right). \tag{1.14}$$

These coordinates cover only half of the AdS hyperboloid, and are referred to as the Poincaré coordinates or the Poincaré patch. The isometry subgroups manifest in this metric are the Poincaré group $ISO(1, n-1)$ and the dilatations transforming the metric under $SO(1,1)$.

Since anti-de Sitter space features prominently in this dissertation, we take this opportunity to highlight some features of AdS which will be important for us later. In chapters 2-4, we will be working in the Euclidean signature. Wick rotating the global time direction in (1.9) or the Poincaré time coordinate in (1.14), we get Euclidean AdS (also simply called hyperbolic space $\mathbb{H}^{n+1}$). It is the hyperboloid,

$$-X_{-1}^2 + X_0^2 + \sum_{j=1}^{n} X_j^2 = -L^2\,, \tag{1.15}$$

in $\mathbb{R}^{1,n+1}$, which has the metric

$$ds^2 = -dX_{-1}^2 + dX_0^2 + \sum_{j=1}^{n} dX_j^2\,. \tag{1.16}$$

Thus it is clear that the isometry group of Euclidean AdS_{n+1} space is $SO(n+1,1)$. The metric (1.9) in global coordinates becomes

$$ds^2 = L^2 \left(\cosh^2\rho\, d\tau^2 + d\rho^2 + \sinh^2\rho\, d\Omega_{n-1}^2\right), \tag{1.17}$$

while the Poincaré patch metric becomes

$$ds^2 = L^2 \left(\frac{du^2}{u^2} + u^2(dt^2 + d\vec{x}^2)\right), \tag{1.18}$$

where now τ and t are the Wick rotated Euclidean time coordinates. A more convenient coordinate choice for us is obtained by sending $u = 1/z$, which gives

$$ds^2 = \frac{L^2}{z^2}\left(dz^2 + dt^2 + d\vec{x}^2\right). \tag{1.19}$$

In chapters 2-4, we will differ slightly in our notation by renaming the "radial direction" z as z_0 with the boundary of Euclidean AdS at $z_0 = 0$, and the flat $\mathbb{R}^n$ directions $(t, \vec{x})$ as $\vec{z}$, in which case (1.19) becomes

$$ds^2 = \frac{L^2}{z_0^2}\left(dz_0^2 + d\vec{z}^2\right). \tag{1.20}$$

AdS is a space of infinite volume, but light rays can reach its boundary in finite time, thus one must specify boundary conditions at the asymptotic boundaries of AdS space. This is essentially why we need to specify boundary conditions for the field ϕ in the evaluation of the gravity partition function in (1.3). Note that at the boundary of Eucliedean AdS space $\mathbb{H}^{n+1}$, the metric is conformally flat, being conformally equivalent to $\mathbb{R}^n$. Compactifying the boundary by adding a point at infinity we obtain S^n. On the other hand, the conformal compactification of $\mathbb{H}^{n+1}$ is the Poincaré ball $\mathbb{D}^{n+1}$, whose boundary once again is S^n. This is an essential ingredient of the AdS/CFT correspondence.

For $n = 1$, the metric (1.20) represents the upper half plane. The upper half plane is the coset space $\mathbb{H}^2 = SL(2,\mathbb{R})/SO(2)$ where $SO(2)$ is the maximal

compact subgroup of $SL(2,\mathbb{R}) \cong SO(2,1)$. [5] The isometries $SL(2,\mathbb{R})$ act as Mobius transformations on the upper half plane (where $z \in \mathbb{R}$ and $z_0 \in \mathbb{R}^+$),

$$w = z + iz_0 \to \frac{aw+b}{cw+d} \qquad a,b,c,d \in \mathbb{R} \qquad ad-bc=1\,. \tag{1.21}$$

By adding a point at infinity, we may compactify the upper half plane to the Poincaré disk. Then the boundary of the disk is the real projective line $\mathbb{P}^1(\mathbb{R}) = \mathbb{R} \cup \{\infty\}$. Isometries of the upper half plane act as linear fractional transformations on the projective line at the boundary:

$$z \to \frac{az+b}{cz+d} \qquad a,b,c,d \in \mathbb{R} \qquad z \in \mathbb{P}^1(\mathbb{R}) \qquad ad-bc=1\,. \tag{1.22}$$

What are conformal field theories (CFTs)?

Conformal field theories are quantum field theories with conformal symmetry, comprising Poincaré invariance (which includes Lorentz invariance and translational invariance) and invariance under angle preserving transformations. Angle preserving transformations include but are not restricted to scaling transformations.[6] Quantum field theories in general exhibit renormalization group (RG) flows, and the fixed points of these flows correspond to CFTs. Thus roughly speaking, conformal invariance means the physics described by a CFT looks the same at all length/energy scales. The fixed points can be massless and free CFTs or interacting fixed points. Many statistical systems, such as water at the critical point, exhibit IR interacting fixed points; thus CFTs prove useful for describing the long-distance behaviour of these statistical systems at criticality, and can accurately predict, for example the critical exponents.

[5] In much the same way, for $n = 2$, we have $\mathrm{EAdS}_3 = \mathbb{H}^3 = SL(2,\mathbb{C})/SO(3)$ with $SO(3)$ the maximal compact subgroup of $SL(2,\mathbb{C}) \cong SO(3,1)$.

[6] We will not concern ourselves with issue of conformal invariance versus the smaller group of scale invariance. It suffices to say that under suitable assumptions, scale invariance in a large number of quantum field theories automatically implies conformal invariance, at least in lower dimensional examples. There exist exceptions, and a full understanding is still lacking. See, for instance [34, 35] and references therein for more details.

The conformal group on $\mathbb{R}^{1,n-1}$ (for $n > 2$) includes Poincaré transformations: $x^\mu \to \Lambda^\mu_\nu x^\nu + a^\mu$, where Λ is the Lorentz transformation matrix and $\mu = 0, 1, \ldots n-1$, scaling (dilatation) transformations $x^\mu \to \lambda x^\mu$ and special conformal transformations:

$$x^\mu \to \frac{x^\mu + a^\mu x^\nu x_\nu}{1 + 2x^\nu a_\nu + a^\rho a_\rho x^\sigma x_\sigma}\,. \tag{1.23}$$

The special conformal transformations can be thought of as the composition of an inversion: $x^\mu \to x^\mu/x^2$, followed by a translation and then an inversion once again, thus they leave the origin invariant.

Denoting the generators of translations by P_μ, Lorentz transformations by $M_{\mu\nu}$, scaling by D and special conformal transformations by K_μ, the commutation relations amongst the generators are

$$\begin{gathered}
[M_{\mu\nu}, P_\rho] = -(\eta_{\mu\rho}P_\nu - \eta_{\nu\rho}P_\mu) \qquad [M_{\mu\nu}, K_\rho] = -(\eta_{\mu\rho}K_\nu - \eta_{\nu\rho}K_\mu) \\
[D, P_\mu] = -P_\mu \qquad [D, K_\mu] = K_\mu \qquad [P_\mu, K_\nu] = 2M_{\mu\nu} - 2\eta_{\mu\nu}D \\
[M_{\mu\nu}, M_{\rho,\sigma}] = -\eta_{\mu\rho}M_{\nu\sigma} - \eta_{\rho\nu}M_{\sigma\mu} - \eta_{\nu\sigma}M_{\mu\rho} - \eta_{\sigma\mu}M_{\rho\nu}\,,
\end{gathered} \tag{1.24}$$

where all other commutators vanish, and $\eta_{\mu\nu} = \mathrm{diag}\{-1, 1, \ldots, 1\}$. To show that the conformal group is the same as $SO(n, 2)$, we define the generators J_{MN} where $M, N = \{0, \ldots, n+1\}$ and $\eta_{MN} = \mathrm{diag}\{-1, 1, \ldots, 1, -1\}$:

$$J_{\mu\nu} = M_{\mu\nu} \qquad J_{\mu n} = \frac{1}{2}(K_\mu - P_\mu) \qquad J_{\mu(n+1)} = \frac{1}{2}(K_\mu + P_\mu) \qquad J_{(n+1)n} = D\,, \tag{1.25}$$

and then check that

$$[J_{MN}, J_{RS}] = -\eta_{MR}J_{NS} - \eta_{RN}J_{SM} - \eta_{NS}J_{MR} - \eta_{SM}J_{RN}\,, \tag{1.26}$$

which is indeed the algebra of $SO(n, 2)$. Recall that this was also the isometry group of AdS_{n+1}. The match between the symmetry group of the boundary QFT and the isometry group of the bulk theory is an essential part of the AdS/CFT

dictionary. In Euclidean signature, the conformal group becomes $SO(n+1,1)$ which matches the isometry group of Euclidean AdS_{n+1}.

For low values of n, *i.e.* $n = 1$ or $n = 2$, $SO(n+1,1)$ is isomorphic to the linear fractional transformations generated by $SL(2,\mathbb{R})$ and $SL(2,\mathbb{C})$ respectively. However, linear fractional transformations capture only the global part of conformal transformations, for recall that at $n = 1, 2$, the full conformal symmetry is enhanced to the infinite dimensional Virasoro symmetry (to be precise, two copies of Virasoro for $n = 2$). In this dissertation however, we restrict ourselves to a study of just global conformal transformations, and avoid any further discussion of the Virasoro algebra.

Representations of the conformal group $SO(n+1,1)$ are labelled by representations of the Lorentz group and the scaling dimension Δ, which is the eigenvalue under a dilatation:

$$[D, \mathcal{O}(0)] = \Delta \mathcal{O}(0)\,. \tag{1.27}$$

The operators transform under a dilatation (suppressing Lorentz indices) $z \to \lambda z$, as $\mathcal{O}(z) \to \lambda^{\Delta}\mathcal{O}(\lambda z)$. The operators which are annihilated by special conformal transformations at the origin are called primary operators. The descendants of a primary operator can be built by systematically acting on the primaries with the "raising" operators P_μ. This increases the scaling dimension Δ by integral values, one for each action of P_μ.

Conformal invariance strongly constrains the form of the correlators. For a scalar operator of scaling dimension Δ, its two-point function with any operator of scaling dimension unequal to Δ vanishes, while

$$\langle \mathcal{O}(z)\mathcal{O}(0)\rangle \propto \frac{1}{(z^2)^{\Delta}}\,. \tag{1.28}$$

The three-point function is also completely fixed by conformal invariance, up to an overall constant. The four-point functions are determined upto a function of

the conformally invariant cross-ratios built out of the four points of insertion. We will discuss this in more detail in chapter 3.

Some simple examples of CFTs include free massless scalars in any number of dimensions, and IR critical ϕ^4 theories between two and four dimensions. These include the so-called vector models, which are theories with $O(N)$ symmetry. Such theories will be the subject of chapters 3-4. Another classic example is the maximally supersymmetric $\mathcal{N} = 4$ super-Yang-Mills theory in $(3+1)$-dimensions.

What are some examples of the AdS/CFT correspondence?

The original example of the AdS/CFT correspondence [22] is the conjectured duality between the $\mathcal{N} = 4$ super-Yang-Mills (SYM) theory in $(3+1)$-dimensions with the gauge group $SU(N)$ and the coupling constant g_{YM} on the CFT side, and the Type IIB superstring theory in $\mathrm{AdS}_5 \times S^5$ (with the radius of AdS and S^5 given by L) and with the five-form field strength having flux N through S^5. This duality came from studying a stack of N coincident D3-branes, whose near horizon geometry is empty $\mathrm{AdS}_5 \times S^5$ spacetime and whose low-energy dynamics on the worldvolume is described by the $\mathcal{N} = 4$ $SU(N)$ super-Yang-Mills. The string coupling g_s is related to the field theory coupling via $g_s = g_{YM}^2$, while the AdS radius is related to N via $L^4 = 4\pi g_s N \ell_s^4$ where ℓ_s is the string length. Describing these theories in detail will take us too far afield, so we will limit ourselves to describing just the weak/strong aspect of this duality. The strongest version of the conjecture is that these theories are dual to each other at all values of $\lambda \equiv g_{YM}^2 N$ (which is the effective coupling in the field theory) and N, thus it is an equivalence between two fully quantum theories. This includes, but is not limited to, a one-to-one correspondence between all gauge invariant operators in the SYM theory and fields or states in Type IIB string theory, and the equality between appropriate correlators.

A weaker form of the conjecture states that the two theories are dual in the limit of $N \to \infty$ with λ held fixed. On the SYM side, this corresponds to the 't Hooft limit of large N gauge theory at fixed coupling λ. On the string theory side, fixed λ translates to fixed L/ℓ_s but g_s small since N is large; thus this limit corresponds to a weak coupling classical string perturbation theory.

In the weakest form of the correspondence, we first take the 't Hooft limit followed by sending $\lambda \to \infty$. On the SYM side, this corresponds to a strongly coupled, large N gauge theory while on the string theory side, a large λ corresponds to a large L/ℓ_s leading to a weakly coupled classical Type IIB supergravity theory in an $\ell_s^2 = \alpha'$ expansion. The weakest form of the correspondence is of great practical utility, for it allows us a chance to explore the previously inaccessible regime of strongly coupled dynamics of gauge theories by studying classical supergravity in the weak coupling limit. In this case, for example, the equivalence of the partition functions in (1.3) simplifies on the gravity side to become

$$\left\langle \exp\left(d^n x\, \phi_0(\vec{x})\mathcal{O}_\Delta(\vec{x})\right) \right\rangle_{\mathcal{N}=4 \text{ SYM}} = \exp\left(-S_{\text{IIB sugra}}[\phi]\right) , \tag{1.29}$$

with appropriate boundary conditions, for every field in the supergravity dual to a gauge-invariant operator $\mathcal{O}_\Delta$ of scaling dimension Δ. If instead, we take the 't Hooft limit, followed by $\lambda \to 0$, we obtain a weakly coupled large N gauge theory on the field theory side, while a strongly coupled classical Type IIB string theory on the gravity side. Thus this duality is an example of a weak/strong duality, where a theory is weakly coupled when its dual is strongly coupled, and vice versa.

We now explicitly demonstrate some aspects of AdS/CFT with a simple toy model involving a scalar degree of freedom in a weakly coupled classical gravity theory. This is also of relevance to later chapters in this dissertation. We work in the (Euclidean) AdS background in the Poincaré patch, with $ds^2 = g_{\mu\nu}dx^\mu dx^\nu =$

$\frac{L^2}{z^2}(dz^2 + d\vec{x}^2)$, where $\vec{x}$ labels the n Euclidean boundary directions and $z = 0$ is the boundary of AdS. The minimal quadratic action of a scalar field in curved background is

$$S = \int d^{n+1}x\sqrt{g}\left(\frac{1}{2}g^{\mu\nu}\partial_\mu\phi\partial_\nu\phi + \frac{1}{2}m^2\phi^2\right). \tag{1.30}$$

The equation of motion for ϕ is

$$\frac{1}{\sqrt{g}}\partial_\mu\left(\sqrt{g}g^{\mu\nu}\partial_\nu\right)\phi - m^2\phi = 0\,. \tag{1.31}$$

The solution to this equation has the asymptotics:

$$\phi(z,\vec{x}) \sim A(\vec{x})z^{n-\Delta}(1+\cdots) + B(\vec{x})z^{\Delta}(1+\cdots)\,, \tag{1.32}$$

at small z, where the exponent satisfies $\Delta(\Delta - n) = m^2L^2$, and the ellipses indicate terms with higher powers of z. The mass-scaling dimension relation (for scalar operators) $\Delta(\Delta - n) = m^2L^2$, or equivalently

$$\Delta_\pm = \frac{n}{2} \pm \sqrt{\frac{n^2}{4} + m^2L^2} \tag{1.33}$$

is one of the basic entries in the holographic dictionary. Which of the two roots should we use? If $m^2 > 0$, then we must pick $\Delta = \Delta_+$ as $\Delta_- < 0$ which is not allowed by the unitarity bound for scalar operators in conformal field theories, which restricts $\Delta > n/2 - 1$. In this case $\Delta_+ > n$, so that near the boundary of AdS space, where $z \to 0$, the second term in (1.32) vanishes, and we are left with $\lim_{z\to 0}\phi(z,\vec{x}) \sim A(\vec{x})z^{n-\Delta_+}$ which diverges near the boundary. However this is the standard UV divergence of the boundary theory, which can be regulated. So the boundary condition in (1.3) which properly accounts for the UV divergences should more precisely be written as $\phi(z,\vec{x}) = \phi_0(\vec{x})z^{n-\Delta_+}$ as $z \to 0$, where we identify $A(\vec{x})$ with the source function on the boundary $\phi_0(\vec{x})$, and $\Delta = \Delta_+$ is identified with the scaling dimension of the operator $\mathcal{O}$ in (1.3). We call this the "standard quantization," and use it exclusively in chapters 2-3. In chapter

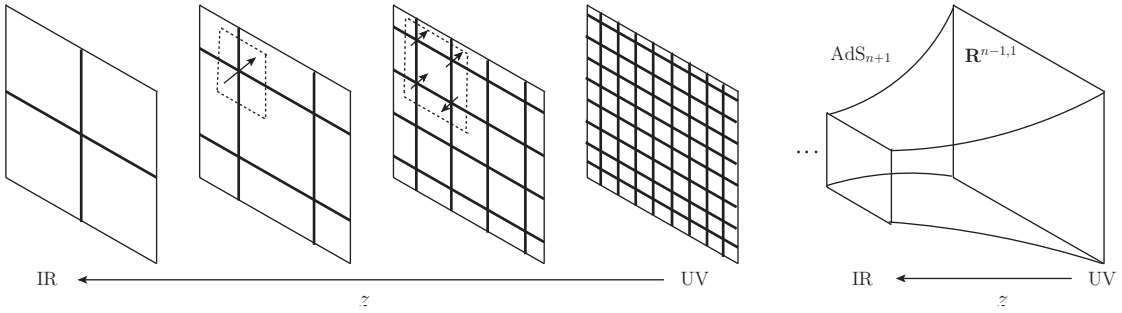

Figure 1.1: Holographic renormalization. Left: Going deeper in the radial direction z corresponds to course graning (block spin transformations). Right: A cartoon of AdS with its conformally flat boundary. (Figure source [38].)

2 we present details on how to compute the two-point function and higher-point correlators in this setup.

The mass-squared of the scalar field can actually be made slightly negative in AdS space without causing instabilities, because the gravitational background makes an additional contribution to the potential in curved space. It turns out the bound is $m^2L^2 > -n^2/4$ (called the BF bound [36]), and this precisely corresponds to real scaling dimensions with $\Delta_+ > n/2$ and $0 < \Delta_- < n/2$. Now we can choose between Δ_+ and Δ_- for the choice of Δ. Note that Δ_+ never falls below the BF bound, but for a narrow range of mass-squared we can arrange $n/2 - 1 < \Delta_- < n/2$; the corresponding mass range is $-n^2/4 < m^2L^2 < -n^2/4 + 1$. Choosing $\Delta = \Delta_-$ (which is usually called "alternative quantization" [37]), the asymptotic solution near the boundary, (1.32), becomes $\phi(z, \vec{x}) \to B(\vec{x})z^{\Delta_-} = B(\vec{x})z^{n-\Delta_+}$ as $z \to 0$. Now the scaling dimension of the operator dual to the bulk field ϕ is $\Delta = \Delta_-$.

Let us also briefly discuss holographic renormalization. The radial coordinate z probes short or long distance physics of the boundary QFT depending on whether it is nearer to or farther away from the boundary. This is the essence of holographic renormalization group flow. One can start with a boundary CFT and add a relevant deformation. For a relevant deformation, the scaling dimension of

the operator must be $\Delta < n$, which means in the bulk theory, the dual scalar field must have negative mass-squared. This triggers an RG flow in the boundary theory. On the gravity side, moving deeper into the bulk corresponds to decreasing the energy scale in the boundary QFT, and the geometry deep inside the bulk changes to reflect the IR structure of the dual field theory (see figure 1.1).

Finally, let us present some more examples of pairs of theories dual to each other by the AdS/CFT correspondence. One duality is between the (single trace sector of) the non-supersymmetric free $O(N)$ vector model in n-dimensions on the CFT side, and a Vasiliev higher spin gauge theory in AdS_{n+1} on the gravity side with the bulk coupling constant, $G \propto 1/N$ [39] (see [40] for a review). The free $O(N)$ vector model has the action

$$S = \int d^n x \, \frac{1}{2} (\partial_\mu \phi^i)^2 \,, \tag{1.34}$$

where $i = 1, \ldots, N$. The spectrum of single trace operators in the theory consists of a scalar operator $J_0 = \phi^i \phi^i$ which has scaling dimension $n-2$, and an infinite tower of even-spin conserved currents J_s with scaling dimensions $n-2+s$, schematically of the form $J_s \sim \sum_k \partial^k \phi^i \partial^{s-k} \phi^i$. By the AdS/CFT correspondence, the single trace operators of the free $O(N)$ model are in one-to-one correspondence with single particle states in the dual gravity theory. Thus the dual gravity theory must have a scalar field of mass $m^2 L^2 = -2(n-2)$,[7] and an infinite tower of higher (even) spin massless gauge fields.[8] This is the spectrum of the so-called minimal bosonic Vasiliev theory in AdS_{n+1} [41]. Since by the AdS/CFT correspondence correlators of operators in the CFT are to be matched with Feynman diagrams in AdS space, and since the three-point functions of higher-spin currents are obviously non-zero, we must have interacting higher spin gauge fields

[7] Note that the negative mass-squared lies above the BF bound, since $-2(n-2) < -n^2/4$.

[8] In the case of spin-s fields, the mass-scaling dimension relation becomes $m^2 L^2 = (\Delta + s - 2)(\Delta - s + 2 - n)$.

in the bulk theory, to be able to reproduce the three-point function obtained from simple Wick contractions on the boundary. Indeed, the Vasiliev theory is a strongly coupled, non-linear theory of interacting higher spin gauge fields and a scalar, whose classical equations of motions are known but no satisfactory action principle exists at the moment. In this duality, the CFT side is weakly coupled which can be used to learn more about the strongly coupled gravity side. A generalization of this construction to complex vector models with $U(N)$ symmetry leads to a Vasiliev theory which involves higher spin gauge fields of all integral spins.

Let us move to the critical $O(N)$ vector model. We start with the interacting $O(N)$ model,

$$S = \int d^n x \left(\frac{1}{2} (\partial_\mu \phi^i)^2 + \frac{\lambda}{4} (\phi^i \phi^i)^2 \right), \tag{1.35}$$

where the mass term is tuned to zero. The renormalization group flow of this theory in the Wilson-Fisher ϵ expansion as well as the large N expansion, is discussed in detail in chapter 4. Here we just note that between $2 < n < 4$, the $(\phi^i \phi^i)^2$ term is relevant and the model flows from a free theory in the UV to a non-trivial interacting theory in the IR, called the critical $O(N)$ model (with the mass parameter suitably tuned away). The critical $O(N)$ model may be viewed as the double trace deformation of the free $O(N)$ model, by the operator J_0^2 where $J_0 = \phi^i \phi^i$ [42]. The AdS dual of double trace deformations are well known [37, 43]. In this case, the AdS dual of the critical $O(N)$ model is the *same* Vasiliev theory as the one dual to the free $O(N)$ model, but with a different choice of boundary condition on the bulk scalar field [39]. Indeed, the mass-squared of the scalar field, $m^2 L^2 = -2(n-2)$ falls precisely in the window $-n^2/4 + 1 < m^2 L^2 < -n^2/4$ where both the roots of $\Delta(\Delta - n) = m^2 L^2$ lead to unitary theories. The free $O(N)$ model corresponds to choice $\Delta = \Delta_+ = n - 2$ while the critical $O(N)$ model corresponds to the choice $\Delta = \Delta_- = 2$. From the point of view of RG

flow in the boundary, the dimension of the operator J_0 goes from $n-2$ in the UV to $2+O(1/N)$ in the large N limit in the IR [42]. Correspondingly, higher spin operators are no longer conserved currents; current conservation laws are weakly broken in the large N limit, which comes from operators picking up anomalous dimensions in the IR. We will return to the computation of anomalous dimensions in chapter 4.

Why is it useful?

We have briefly described the AdS/CFT correspondence in this section, and shown some glimpses of how it captures the equivalence between a quantum field theory and a theory of gravity. In most cases, one can take various limits so that the correspondence becomes a duality between a weakly coupled theory and a strongly coupled theory. It is precisely in these cases that AdS/CFT is incredibly powerful, allowing us easy access to strong coupling regimes of theories of interest via their weakly coupled duals. In fact, this is perhaps how one could conceivably have such a counter-intuitive equality (or duality) between a theory with gravity and a theory without gravity. In most cases we do not really understand the strong coupling limits of theories, and how the degrees of freedom are arranged; the AdS/CFT duality gives a precise prescription how this happens whenever the dual theory is known.

Applications of AdS/CFT is a vast topic and outside the purview of this dissertation. Let us just point out that applications extend to condensed matter systems (see, for example [44]), whether at criticality or away from criticality, as well as the strong coupling limit of various quantum field theories, such as QCD, via string theory/gravity constructions (see, for example [45]). In this way AdS/CFT has revived the original reason for studying string theory: to describe strong interactions between gluons and quarks. The "AdS/CFT" correspondence

is not just limited to gravity theories in AdS space and conformal field theories on the boundary. Gravity in more general background spaces, and quantum field theories without conformal invariance are also welcome. In applications to physical systems of interest, if the dual gravity theory turns out to be highly contrived and unphysical, so be it; the goal in that case is not to learn about how gravity works in the real world, but how that particular physical system can be conveniently expressed in a language where calculations become possible.

Little is known about the quantum theory of gravity experimentally, and while string dualities give insight into non-perturbative phenomena in theories of quantum gravity, those insights tend to focus on objects preserving some fraction of supersymmetry. On the other hand, the AdS/CFT correspondence is better at giving access in principle to all the dynamics of bulk quantum gravity in terms of a well-defined (perhaps weakly coupled) boundary theory.

In this section we restricted ourselves to a discussion of the AdS/CFT correspondence over $\mathbb{R}$, the real number field. By this we mean that we assumed the coordinates of the n-dimensional spacetime over which the quantum field theory is defined are real numbers. It turns out this assumption is not crucial for AdS/CFT to work. Indeed it is possible to extend the correspondence to other number fields, such as the p-adic numbers, $\mathbb{Q}_p$ or their extensions. (For a brief account on the application of p-adic numbers to different branches of physics, see for example [46].) When the spacetime of the boundary quantum field theory is p-adic rather than real, the dual gravitational theory lives in a spacetime which has a discrete tree-like geometry that serves as the analog of AdS space. Such a p-adic construction will be the subject of chapters 2, 3 and 4. In the next section, we review some basic facts about number fields in general and p-adic numbers in particular, which will play an important role in this dissertation.

1.3 Global and local fields

The goal of this section is to give a short, non-rigorous account of algebraic number fields (which we'll simply call global fields) and locally compact fields (simply called local fields), directed towards physicists who may be unfamiliar with these topics. While the subject of local and global fields is extremely vast and interesting, here we will briefly discuss (without proofs) topics only of *direct* relevance to this dissertation. At first this section will likely seem unrelated to the previous section, but towards the end, we will draw attention to interesting connections between the two which form the basis for the rest of the dissertation.

Before we proceed with definitions, let us give some intuition: Roughly speaking, a *field* is a set which comes with an operation of addition and multiplication, such that any two elements of the set when added, subtracted, multiplied or divided together (excluding division by zero) result in an element which belongs to the same set. Some examples of fields are: the rational numbers $\mathbb{Q}$, the real numbers $\mathbb{R}$, the complex numbers $\mathbb{C}$, and the p-adic numbers $\mathbb{Q}_p$ (which we describe in section 1.3.2).

Textbooks in physics mostly restrict attention to theories where spacetime is a real manifold, and where fields (fields as in physical fields, *e.g.* scalar fields, fermionic fields) and operators are real or complex valued, so that correlation functions and scattering amplitudes are real or complex valued. In this dissertation, we will be studying the consequences of defining theories where the spacetime is a p-adic manifold. We begin with some basic definitions.

Groups

A group G is a set, together with an operation $+$ such that

- G is closed under the operation: $\forall a, b \in G$, $a + b \in G$,

- the operation is associative: $\forall a, b, c \in G, (a + b) + c = a + (b + c)$,
- there is a unique identity element $e \in G$ such that for all $a \in G$, $e + a = a + e = a$
- for each element $a \in G$, there exists an element $b \in G$, called the inverse of a, such that $a + b = b + a = e$.

Some common examples of groups include the integers $\mathbb{Z}$ under the operation of addition, $\mathbb{Z}/m\mathbb{Z}$ the additive group of integers modulo m, S_m the symmetric group on a set of m elements with the group operation the composition of permutations, and $SO(m)$ the group of orthogonal $m \times m$ matrices of unit determinant.

Rings

A ring R is a set together with two operations, $+$ and $\times$ such that

- R is an abelian (*i.e.* commutative) group under $+$ where we denote the "additive" identity element by $0 \in R$ (commutativity means if $a, b \in R$, then $a + b = b + a$),
- R is closed under $\times$,
- the operation $\times$ is associative,
- there exists a unique "multiplicative" identity element $1 \in R$ under $\times$ such that $\forall a \in R$, $a \times 1 = 1 \times a = a$,
- distributivity holds: $\forall a, b, c \in R$, $a \times (b + c) = (a \times b) + (a \times c)$ and $(b + c) \times a = (b \times a) + (c \times a)$.

Some common examples of rings include the integers $\mathbb{Z}$ under addition ($+$) and multiplication ($\times$), $\mathbb{Z}/m\mathbb{Z}$ the additive ($+$) group of integers modulo m together

with multiplication ($\times$), $M(m, \mathbb{R})$ the ring of $m \times m$ matrices with real entries under matrix addition ($+$) and matrix multiplication ($\times$), and $SL(m, \mathbb{R})$ the ring of $m \times m$ matrices with real entries and unit determinant under matrix addition ($+$) and matrix multiplication ($\times$). Note that in the final two examples, the operation $\times$ is not commutative (*i.e.* $\exists A, B \in R$, such that $A \times B \neq B \times A$).

Fields

A field F is a commutative ring (meaning commutative under $\times$) such that all nonzero elements in F (*i.e.* all $a \in F$ with $a \neq 0$) have a "multiplicative" inverse under $\times$. $\mathbb{Q}, \mathbb{R}$ and $\mathbb{C}$ together with addition and multiplication are all examples of fields.

Another important class of examples of fields are the finite fields. There exists a unique finite field with q elements for every $q = p^n$ where n is any positive integer and p is a prime. We will refer to this unique field as the finite field $\mathbb{F}_q$. For $n = 1$, $\mathbb{F}_p$ is isomorphic to $\mathbb{Z}/p\mathbb{Z}$. Later in this section we will spend some time discussing the *non-Archimedean* field of p-adic numbers, $\mathbb{Q}_p$.

Field extensions

Let K be a field. If K contains L as a subfield, that is, L is a subset of K such that L is a field with respect to the field operations inherited from K, then (the larger field) K is a field extension of L. Sometimes, this is denoted as $K : L$ and read as K is a field extension of L. An example of a field extension is the field of complex numbers $\mathbb{C}$ over the reals $\mathbb{R}$. We may write it as $\mathbb{C} = \mathbb{R}(\sqrt{-1})$, which means that $\mathbb{C}$ is obtained by adjoining to $\mathbb{R}$ a root of the polynomial $X^2 + 1 = 0$, which is an irreducible polynomial of degree two (more precisely, irreducible in $\mathbb{R}$).

The larger field K may be considered as a vector space over the smaller field

L. The dimension of the vector space, denoted $[K : L]$ is referred to as the degree of extension of K over L. The degree of extension is the same as the degree of the irreducible polynomial whose root is adjoined to L to construct K. For example, the complex numbers are a degree two extension over the reals. In this dissertation, we will only consider field extensions of finite degree.

Another example of a simple field extension of degree 2 is $\mathbb{Q}(\sqrt{2})$, which is the smallest field including both $\mathbb{Q}$ and $\sqrt{2}$. Any element may be expressed as $z = x + y\sqrt{2}$. If we adjoin the root of $X^2 - 3 = 0$ to $\mathbb{Q}(\sqrt{2})$, we get a degree four field extension $\mathbb{Q}(\sqrt{2}, \sqrt{3}) = \{a + b\sqrt{2} + c\sqrt{3} + d\sqrt{6} : a, b, c, d \in \mathbb{Q}\}$.

Usually, we need to specify multiplication rules for multiplying two elements of the field extension. This can be specified by providing the multiplication table for the elements adjoined to the base field to construct the larger field. For example, in $\mathbb{C} = \mathbb{R}(\sqrt{-1})$, we have $(\sqrt{-1})^2 = -1 \in \mathbb{R}$. In $\mathbb{Q}(\sqrt{2})$, we have $(\sqrt{2})^2 = 2 \in \mathbb{Q}$. In $\mathbb{Q}(\sqrt{2}, \sqrt{3})$, we have $(\sqrt{2})^2 = 2 \in \mathbb{Q}$, $(\sqrt{3})^2 = 3 \in \mathbb{Q}$, and $\sqrt{2}\sqrt{3} = \sqrt{6} \notin \mathbb{Q}$. Using these rules, any two elements in $\mathbb{Q}(\sqrt{2}, \sqrt{3})$ may be multiplied together, to give another element of the form $a + b\sqrt{2} + c\sqrt{3} + d\sqrt{6}$, where $a, b, c, d \in \mathbb{Q}$.

Alternately, we could have specified the field extension $\mathbb{Q}(\sqrt{2}, \sqrt{3})$ as the degree four extension of $\mathbb{Q}$ obtained by adjoining to $\mathbb{Q}$ one of the roots of the irreducible polynomial $f(X) = X^4 - 10X^2 + 1$. To see why, let K be the field extension over $\mathbb{Q}$ obtained by adjoining to $\mathbb{Q}$ one of the roots of the polynomial $f(X) = X^4 - 10X^2 + 1$. Let $r \in K$ be one of those roots, so that $f(r) = 0$. Then any element $z \in K$ has the form $z = a_0 + a_1 r + a_2 r^2 + a_3 r^3$ where $a_0, a_1, a_2, a_3 \in \mathbb{Q}$. We multiply two elements $z, w \in K$ by "reducing" using the defining polynomial $f(r) = 0$. For example, if $w = b_0 + b_1 r + b_2 r^2 + b_3 r^3$, with $b_0, b_1, b_2, b_3 \in \mathbb{Q}$, then the product zw involves powers of r which are higher than r^3, which can be iteratively removed by substituting the equation $r^4 - 10r^2 + 1 = 0$. We now show that K contains $\sqrt{2}$ and $\sqrt{3}$. Let's pick $r = \sqrt{5 + 2\sqrt{6}}$, which is allowed since

it is one of the four roots of $f(r) = 0$. Now note that $\sqrt{5+2\sqrt{6}} = \sqrt{2}+\sqrt{3}$, because $(\sqrt{2}+\sqrt{3})^2 = 5+2\sqrt{6}$, and we picked the positive root. So, $r = \sqrt{2}+\sqrt{3}$, which means $r^2 = 5+2\sqrt{6}$ and $r^3 = 11\sqrt{2}+9\sqrt{3}$. Thus $z = a_0+a_1r+a_2r^2+a_3r^3$ has an equivalent representation as $z = c_0 + c_1\sqrt{2} + c_2\sqrt{3} + c_3\sqrt{6}$ where $c_i \in \mathbb{Q}$ are related to the $a_i \in \mathbb{Q}$. Thus we have shown that $K = \mathbb{Q}(\sqrt{2}, \sqrt{3})$. In mathematical terms, K is the quotient of the polynomial ring $\mathbb{Q}[X]$ by the ideal generated by the irreducible polynomial $f(X) = X^4 - 10X^2 + 1$.

Another important example of a finite extension is $\mathbb{F}_{p^n}$, the finite field with p^n elements, which is the unique extension of $\mathbb{F}_p$ (the finite field with p elements) of degree n. We will not explain the construction of $\mathbb{F}_{p^n}$ in detail, but just note that the construction is similar to the one outlined in the previous paragraph: $\mathbb{F}_{p^n}$ is the quotient of the polynomial ring $\mathbb{F}_p[X]$ by the ideal generated by an irreducible polynomial in $\mathbb{F}_p$ of degree n. An alternate construction of $\mathbb{F}_{p^n}$ will be discussed near the end of this section.

1.3.1 Global fields

The simplest examples of global fields are algebraic number fields, or simply number fields, and the most basic of them is the field of rational numbers $\mathbb{Q}$. More generally, an algebraic number field is a finite degree field extension of the field of rational numbers. $\mathbb{Q}(\sqrt{2})$ and $\mathbb{Q}(\sqrt{2}, \sqrt{3})$ are examples of algebraic number fields, of degrees two and four respectively. We gave an example of the construction of the algebraic number field $\mathbb{Q}(\sqrt{2}, \sqrt{3})$ in the previous section. For our purposes, we will not need to delve deeper into the theory of algebraic number fields, so we move on to consider local fields.

1.3.2 Local fields and p-adic numbers

Local fields, also called locally compact fields, arise as completions of global fields. In this section we focus on the local fields $\mathbb{R}$ and $\mathbb{Q}_p$, obtained by completing the global field $\mathbb{Q}$ with respect to the (usual) absolute value norm and the p-adic norm, respectively. Here, by completion we mean that every Cauchy sequence with elements in $\mathbb{Q}$ converges in $\mathbb{R}$ with respect to the absolute value norm, and in $\mathbb{Q}_p$ with respect to the p-adic norm.

Are other completions of $\mathbb{Q}$ possible? Ostrowski's theorem states that every non-trivial norm on $\mathbb{Q}$ is equivalent to either the absolute value norm (denoted $|\cdot|_\infty$) or the p-adic norm $|\cdot|_p$ for some prime p.[9] Thus by Ostrowski's theorem, $\mathbb{R}$ and $\mathbb{Q}_p$ exhaust the list of possible completions of $\mathbb{Q}$. $\mathbb{Q}_p$ is sometimes referred to as the completion of $\mathbb{Q}$ at the finite places (one at every prime p), and $\mathbb{R}$ as the completion of $\mathbb{Q}$ at "the place at infinity," which explains the notation $|\cdot|_\infty$ for the norm on $\mathbb{R}$.

Let us now turn to Archimedean and non-Archimedean norms. A norm on a field K is a function $|\cdot| : K \to \mathbb{R}$ such that

- $|x| \geq 0$ with equality iff $x = 0$
- $|xy| = |x||y|$
- Triangle inequality: $|x + y| \leq |x| + |y|$.

An Archimedean norm has the property that given any $a, b \in K$ with $a \neq 0$, there exists a positive integer n such that $|na| > |b|$. This property does not hold for a non-Archimedean norm. Alternately (but equivalently), one can distinguish between Archimedean and non-Archimedean norms by the following property:

[9] The trivial norm is the one with $|x| = 0$ if $x = 0$ and $|x| = 1$ otherwise. Two norms $|\cdot|_1, |\cdot|_2$ on a field K are equivalent if there exists a positive real number s such that $|x|_1 = |x|_2^s$ for all $x \in K$.

For an Archimedean norm, $\sup\{|n| : n \in \mathbb{Z}\} = +\infty$, while for a non-Archimedean norm, $\sup\{|n| : n \in \mathbb{Z}\} = 1$.

It is obvious the absolute value norm on $\mathbb{R}$ is Archimedean, for if $a, b \in \mathbb{R}$ with $0 < |a|_\infty < |b|_\infty$, then for some $n \in \mathbb{Z}$ we have $|na|_\infty > |b|_\infty$. By contrast, if $a, b \in \mathbb{Q}_p$, we will show this property no longer holds, thus the p-adic norm is non-Archimedean. The key difference between Archimedean and non-Archimedean norms may be summed up in the property of ultrametricity. A non-Archimedean norm (which satisfies by definition all the properties of a norm listed above) satisfies a *stronger* version of the triangle inequality: $|x + y| \leq \sup(|x|, |y|)$. This is the property of ultrametricity. An important consequence of ultrametricity is that all triangles are 'tall isosceles'. That is, if $x + y + z = 0$ in a non-Archimedean field K, then after relabelling x, y and z if necessary, we always have $|x| = |y| \geq |z|$.

How do norms work in field extensions? In general, if K is a degree n extension of a field L, then we remind the reader that K can be represented as an n-dimensional vector space over L. Given an element $a \in K$, the map $v \to av$ for any other element $v \in K$ amounts to a linear map on L^n; so we can calculate its determinant $N_{K:L}(a)$. The determinant of this map is the field norm $N(a)$, or in more precise notation $N_{K:L}(a)$ where $K : L$ specifies the field extension under consideration. $N_{K:L}$ is a homogeneous map from K to L of degree n, in the sense that $N_{K:L}(\lambda a) = \lambda^n N_{K:L}(a)$ when $\lambda \in L$. Note that $N_{K:L}(1) = 1$ because multiplying an element of K by 1 is represented as multiplying the associated vector in L^n by the $n \times n$ identity matrix. The norm $|\cdot| : K \to \mathbb{R}$ may then be defined as $|a| = |N_{K:L}(a)|_L^s$ for some fixed positive real number s, where $|\cdot|_L$ is the norm on the base field L. Returning to algebraic number fields for a moment, in the field extension $\mathbb{Q}(\sqrt{2})$ of degree 2, any element may be expressed as $z = x + y\sqrt{2}$, and the natural field norm is $N(z) = x^2 - 2y^2$. In this case,

$N(z) = z\bar{z}$ where $\bar{z} = x - y\sqrt{2}$ can be characterized as the conjugate of z.[10]

p-adic numbers

Let's finally turn our attention to the p-adic numbers $\mathbb{Q}_p$. Every non-zero p-adic number in $\mathbb{Q}_p$ has a unique series decomposition,

$$x = p^{v_p(x)} \sum_{m=0}^{\infty} a_m p^m \qquad a_0 \neq 0\,, \tag{1.36}$$

where $a_m \in \{0, 1, \ldots, p-1\}$ are the digits and $v_p(x) \in \mathbb{Z}$ is called the p-adic valuation of x, which basically measures the divisibility of x by p. The p-adic norm is then defined to be,

$$|x|_p \equiv p^{-v_p(x)}\,. \tag{1.37}$$

We define $|0|_p = 0$, and correspondingly $v_p(0) = \infty$. The sum in (1.36) is convergent with respect to the norm $|\cdot|_p$. Intuitively, the p-adic norm is based on regarding p as small but non-zero, while integers prime to p are all the same size. To define addition and multiplication on $\mathbb{Q}_p$, we can define them in the standard manner (as rationals) for series that terminate, and then extend the definition to all of $\mathbb{Q}_p$ by insisting that addition and multiplication should be continuous maps with respect to $|\cdot|_p$.

Since $\mathbb{Q}_p$ is a completion of the rationals, all rational numbers belong to $\mathbb{Q}_p$; in fact, $\mathbb{Q}$ is dense in $\mathbb{Q}_p$. It is obvious that every positive integer has a unique decomposition of the form (1.36). For example, for $p = 3$, the integer 11 has the representation: $11 = 2\cdot 3^0 + 0\cdot 3^1 + 1\cdot 3^2 + 0\cdot 3^2 + 0\cdot 3^3 + \cdots$, with $v_3(11) = 0$. Thus $|11|_3 = 1$. As a second example in $\mathbb{Q}_3$, consider $27 = 3^3(1\cdot 3^0 + 0)$, so $|27|_3 = 3^{-3}$. Note that $54 = 3^3(2\cdot 3^0 + 0)$ so $|54|_3 = 3^{-3}$ as well.

To write negative integers, or fractions in the series representation of (1.36), the key point to note is that the series in (1.36) can be an infinite series. So for

[10] More generally, if the field extension is a Galois field, then the field norm of an element in the extension is obtained by multiplying all its conjugates together with itself.

example,

$$-1 = \frac{p-1}{1-p} = (p-1)(1+p+p^2+\cdots)\,. \tag{1.38}$$

Thus -1 can be written as an infinite series with coefficients $a_m = p-1$ for all $m \geq 0$, and $v_p(-1) = 0$. The series in (1.38), and more generally in (1.36) converges p-adically, because higher powers of p get smaller and smaller in the p-adic norm.

It turns out every rational number may be written in the form (1.36), and its series representation either terminates ($a_m = 0$ for all $m > N$ for some non-negative integer N) or it has a non-terminating but repeating series representation (the digits a_m repeat in a pattern after some $m > N$ for some non-negative integer N). For example, in $\mathbb{Q}_3$, $1/9 = 3^{-2}(1 \cdot 3^0 + 0)$, with $v_3(1/9) = -2$, $2/9 = 3^{-2}(2 \cdot 3^0 + 0)$, with $v_3(2/9) = -2$, and,

$$\frac{1}{2} = 1 - \frac{1}{2} = 1 + \frac{1}{1-3} = 2 + 3 + 3^2 + 3^3 + 3^4 + 3^5 + O(3^6)\,. \tag{1.39}$$

In the final example, $v_3(1/2) = 0$, and all $a_m = 1$ for $m > 0$. Also, note that the r.h.s. of (1.39) corresponds to specifying $1/2$ with a p-adic accuracy of $O(3^6)$. All non-terminating non-repeating series expansions are p-adic "irrational" numbers.

p-adic numbers may also be written in a "decimal representation" (more precisely, a p-nary representation), which is read from right to left. For example, in Q_3, $1 = 1.$, $3 = 10.$, $11 = 102.$, $27 = 1000.$ and $54 = 2000.$. Any digits to the right of the decimal point multiply negative powers of p. For example in $\mathbb{Q}_3$, $1/9 = 0.01$ and $2/9 = 0.02$. p-adic numbers with non-terminating decimal representation continue to the left infinitely. For example, $-1 = \ldots 222222. = 222222. + O(3^6)$, and $1/2 = \ldots 111112. = 111112. + O(3^6)$. [11]

[11] Amusingly, $\mathbb{Q}_p$ can also contain roots of -1 depending on the value of the prime p. For example, $\mathbb{Q}_5$ contains the two primitive fourth roots of unity. They are $\zeta_1 = \ldots 140223032431212.$ and $\zeta_2 = \zeta_1^3 = \ldots 304221412013233.$. They both square to -1: $\zeta_1^2 = \zeta_2^2 = \ldots 444444444.$ and their fourth power gives unity.

Let's mention two important subsets of $\mathbb{Q}_p$. The ring of p-adic integers, $\mathbb{Z}_p$ is defined to be

$$\mathbb{Z}_p = \{x \in \mathbb{Q}_p : |x|_p \leq 1\}\,. \tag{1.40}$$

Note that the set of all integers $\mathbb{Z}$ is dense in $\mathbb{Z}_p$. (It is clear all integers belong to $\mathbb{Z}_p$ because if an integer is relatively prime to p, then it has unit norm, and if it is divisible by p then its norm will be p^N for some negative integer N, thus smaller than 1.) We conclude $\sup\{|n|_p : n \in \mathbb{Z}\} = 1$. Earlier in the section, we claimed that this is the defining property of non-Archimedean norms. Equivalently, if $a, b \in \mathbb{Q}_p$ with $0 < |a|_p < |b|_p$, then since $|na|_p = |n|_p|a|_p \leq |a|_p$ for all $n \in \mathbb{Z}$, we have $|na|_p < |b|_p$ for all $n \in \mathbb{Z}$. Thus the p-adic norm is non-Archimedean. In fact, starting with the definition of the p-adic norm, it is easy to directly check that it is ultrametric, *i.e.* $|x + y|_p \leq \sup(|x|_p, |y|_p)$.

The other important subset of $\mathbb{Q}_p$ is the set of units in $\mathbb{Z}_p$, *i.e.* elements of $\mathbb{Z}_p$ that have a multiplicative inverse (so form a multiplicative group). This set is given by

$$\mathbb{U}_p = \{x \in \mathbb{Q}_p : |x|_p = 1\}, \tag{1.41}$$

and we will simply refer to it as the "units." Note that $1/2 \in \mathbb{Z}_3$, in fact $1/2 \in \mathbb{U}_3$.

We may now re-express (1.36) as

$$x = p^{v_p(x)}\hat{x}\,, \tag{1.42}$$

where $\hat{x}$ is a unit ($\hat{x} \in \mathbb{U}_p$), uniquely determined by non-zero x. Intuitively, we think of $\mathbb{Z}_p$ as the unit ball in $\mathbb{Q}_p$, while $\mathbb{U}_p$ is the unit sphere. Because the decomposition (1.42) is unique, we may express the non-zero p-adic numbers as

$$\mathbb{Q}_p^\times = \bigsqcup_{m\in\mathbb{Z}} p^m \mathbb{U}_p\,, \tag{1.43}$$

where $\sqcup$ indicates a disjoint union and $\mathbb{Q}_p^\times$ is the multiplicative group of units in $\mathbb{Q}_p$, namely $\mathbb{Q}_p \setminus \{0\}$.

Adelic products

A striking consequence of defining the p-adic norm as in (1.37) is that the product of norms of a rational number over all the local places (*i.e.* over the p-adics for all prime p and the reals) is simply unity:

$$|x|_\infty \prod_p |x|_p = \prod_v |x|_v = 1 \qquad x \in \mathbb{Q}\,, \tag{1.44}$$

where v runs over all primes p and ∞. This is the simplest example of an adelic product, and is straightforward to prove by writing out x in it's prime factor decomposition.

In chapters 2-4, we will encounter some more adelic products, the simplest versions of which can be constructed out of local zeta and Gamma functions defined as follows:

$$\Gamma_v(s) \equiv \frac{\zeta_v(s)}{\zeta_v(1-s)} \qquad v = \infty, p\,, \tag{1.45}$$

where

$$\zeta_\infty(s) \equiv \pi^{-s/2}\Gamma_{\text{Euler}}(s/2) \qquad \zeta_p(s) \equiv \frac{1}{1-p^{-s}}\,. \tag{1.46}$$

Here $\Gamma_{\text{Euler}}(s)$ is the usual Euler Gamma function (so, for example, $\Gamma_{\text{Euler}}(N) = (N-1)!$ for positive integer N). Then the adelic (or global) zeta function is given by the product [12]

$$\zeta_{\mathbb{A}}(s) \equiv \prod_v \zeta_v(s)\,, \tag{1.47}$$

and it can be checked that it satisfies the functional equation

$$\zeta_{\mathbb{A}}(s) = \zeta_{\mathbb{A}}(1-s)\,. \tag{1.48}$$

From (1.48) and (1.45), it is clear that

$$\Gamma_{\mathbb{A}}(s) \equiv \prod_v \Gamma_v(s) = 1\,. \tag{1.49}$$

[12]Note that the restricted product, $\prod_p \zeta_p(s) = \zeta(s)$ is the usual Riemann zeta function.

Thus the local zeta and Gamma functions over the finite places ($\mathbb{Q}_p$) and the place at infinity ($\mathbb{R}$) are tied together via adelic products. Incredibly, we show in chapters 2-4 that correlators in the Archimedean (respectively non-Archimedean) AdS/CFT may be written entirely in terms of these local ζ_∞ and Γ_∞ (respectively ζ_p and Γ_p) functions, thus hinting at some unexplored, and possibly deep number theoretic connections between these constructions!

The Bruhat–Tits tree as AdS space

We will now argue that p-adic numbers provide a natural setting for holography. Let's first introduce the Bruhat–Tits tree (perhaps better known amongst physicists as the infinite Bethe lattice). The Bruhat–Tits tree, associated with the p-adic numbers $\mathbb{Q}_p$, is an infinite regular graph with no cycles, having the coordination number $p+1$. We begin by establishing the relation between the p-adic numbers and the tree. Consider first an element of $\mathbb{U}_p$. The first (rightmost) digit is non-zero, so there are $p-1$ choices for it. Once that choice is made, there are p choices for the next digit, and the next, and so forth. A convenient graphical way to depict the relation (1.43) is to show the sets $p^m\mathbb{U}_p$ as bushes rooted in a trunk, with each root corresponding to some fixed power p^m. Each non-zero p-adic number x is the terminus of a unique upward path through one of the bushes, and the magnitude $|x|_p$ corresponds to the bush in which the path lies. It is natural to go further and include points 0 and ∞ as the terminal points on each end of the trunk. Altogether, the resulting graph is precisely the Bruhat–Tits tree, T_p, with coordination number $p+1$. See figure 1.2.

The boundary of the Bruhat–Tits tree is $\mathbb{Q}_p \sqcup \{\infty\}$, which more properly is the projective line $\mathbb{P}^1(\mathbb{Q}_p)$. We can realize $\mathbb{P}^1(\mathbb{Q}_p)$ as all pairs $(x,y) \in \mathbb{Q}_p^2 \setminus \{(0,0)\}$ modulo the relation $(x,y) \sim (\lambda x, \lambda y)$ for $\lambda \in \mathbb{Q}_p^\times$. There is a natural action of

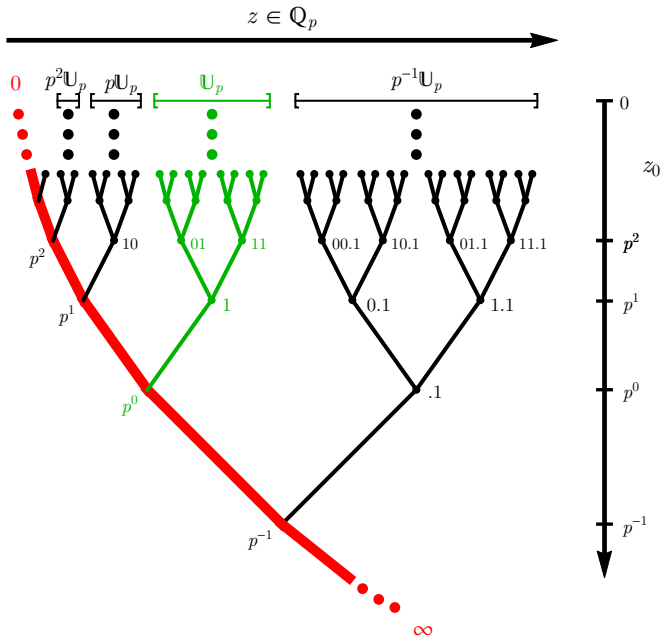

Figure 1.2: The Bruhat–Tits tree for $\mathbb{Q}_p$ with $p = 2$, with a coordinate system (z_0, z) shown. (Figure source [47].)

$\mathrm{PGL}(2, \mathbb{Q}_p)$ on $\mathbb{P}^1(\mathbb{Q}_p)$, most simply realized as linear fractional transformations

$$x \to \frac{\alpha x + \beta}{\gamma x + \delta}\,, \tag{1.50}$$

where α, β, γ, and δ are all elements in $\mathbb{Q}_p$, satisfying $\alpha\delta - \beta\gamma \neq 0$. The maximal compact subgroup of $\mathrm{PGL}(2, \mathbb{Q}_p)$ is $\mathrm{PGL}(2, \mathbb{Z}_p)$ and a remarkable fact is that the Bruhat–Tits tree, T_p, is naturally identified as the quotient $\mathrm{PGL}(2, \mathbb{Q}_p)/\mathrm{PGL}(2, \mathbb{Z}_p)$.

Thus every node on the tree is in a one-to-one correspondence with a coset of $\mathrm{PGL}(2, \mathbb{Q}_p)/\mathrm{PGL}(2, \mathbb{Z}_p)$. The nodes transform under the action of the group $\mathrm{PGL}(2, \mathbb{Q}_p)$, which is an isometry of T_p. Thus the graph distance between nodes is invariant under the action of $\mathrm{PGL}(2, \mathbb{Q}_p)$.

The alert reader might have started noticing similarities between the Bruhat–Tits tree and low dimensional (Euclidean) AdS spaces (in particular AdS_2 and AdS_3). Recall that AdS_{n+1} is the quotient space $SO(n+1, 1, \mathbb{R})/SO(n+1, \mathbb{R})$ where $SO(n+1, \mathbb{R})$ is the maximal compact subgroup of $SO(n+1, 1, \mathbb{R})$. For

$n = 1$, the isometry group $SO(2,1,\mathbb{R}) \cong \mathrm{SL}(2,\mathbb{R})/\mathbb{Z}_2 \cong \mathrm{PSL}(2,\mathbb{R})$, while for $n = 2$, the isometry group is isomorphic to $SO(3,1,\mathbb{R}) \cong \mathrm{SL}(2,\mathbb{C})/\mathbb{Z}_2 \cong \mathrm{PSL}(2,\mathbb{C})$. This is to be compared with $\mathrm{PGL}(2,\mathbb{Q}_p)$ in the case of the Bruhat–Tits tree. The boundary of AdS_{n+1} is $S^1 = \mathbb{P}^1(\mathbb{R})$ for $n = 1$ and $S^2 = \mathbb{P}^1(\mathbb{C})$ for $n = 2$, where linear fractional transformations act.

Thus by intent, the Bruhat–Tits tree is a discrete analog of a Riemannian symmetric space. The analogy can be summarized in tabular form as follows:

symmetry group	maximal compact subgroup	quotient space	boundary
$\mathrm{PGL}(2,\mathbb{Q}_p)$	$\mathrm{PGL}(2,\mathbb{Z}_p)$	T_p	$\mathbb{P}^1(\mathbb{Q}_p)$
$\mathrm{PSL}(2,\mathbb{R})$	$\mathrm{SO}(2,\mathbb{R})$	$\mathbb{D}$	$\mathbb{P}^1(\mathbb{R})$
$\mathrm{PSL}(2,\mathbb{C})$	$\mathrm{SO}(3,\mathbb{R})$	$\mathbb{B}$	$\mathbb{P}^1(\mathbb{C})$

(1.51)

where $\mathbb{D}$ is the Poincaré disk and $\mathbb{B}$ is the Poincaré ball.[13] The volume of both AdS and the Bruhat–Tits tree scales exponentially with radius. A precise comparison between the scalings of the respective volumes is made in section 2.5.2 of chapter 2.

We should be encouraged by this table to think that some p-adic version of the $\mathrm{AdS}_2/\mathrm{CFT}_1$ or $\mathrm{AdS}_3/\mathrm{CFT}_2$ correspondence can be formulated. Indeed, we will develop a p-adic AdS/CFT correspondence in chapter 2.

In fact a natural form of holographic renormalization is manifest on the Bruhat–Tits shown in figure 1.2, as we explain now. We find it natural to refer to a particular depth coordinate z_0 on the Bruhat–Tits tree, where $z_0 = p^\omega$ and $\omega \in \mathbb{Z}$. Along the trunk of the tree, z_0 is p^m at the point where the bush terminating in $p^m\mathbb{U}_p$ is rooted. At a node of the tree not on the trunk, we have chosen some finite number of p-adic digits, and z_0 is the first power of p corresponding

[13] The tree drawn in figure 1.2 is closer to the upper-half-plane $\mathbb{H}^2$ (the Poincaré patch picture) for $n = 1$ or $\mathbb{H}^3$ for $n = 2$, rather than the Poincaré disk or ball

to a digit we have *not* chosen. For instance, at the point 10.1 on the 2-adic tree shown in figure 1.2, $z_0 = p^2$ because in writing 10.1 we have specified the $1/p$-place digit, the ones-place digit, and the p-place digit, but not the p^2-place digit. In short, z_0 is p-adic accuracy. [14] [15] Thus the "deeper" a node is in the bulk, meaning the larger the value of $|z_0|_p$, the lower its p-adic accuracy in describing a specific boundary point. In fact, specifying a bulk node specifies an open subset of p-adic numbers on the boundary to which the particular bulk node provides an approximation. This open set is the set of all boundary points which lie at the terminus of the bush which originates at the node. Moving deeper and deeper in the bulk corresponds to a larger and larger open set on the boundary. This is the essence of holographic renormalization.

Bruhat–Tits tree associated with field extensions

We would like to inquire whether there is a natural generalization of the Bruhat–Tits tree for $\mathbb{Q}_p$ which allows us to formulate a p-adic version of $\mathrm{AdS}_{n+1}/\mathrm{CFT}_n$. For $n = 2$, our goal is captured pictorially in figure 1.3. To eventually discuss n-dimensional p-adic field theories on the boundary, we will need to define some natural norm $|x|$ for vectors x in a vector space $\mathbb{Q}_p^n$.

There are in fact natural norms on the vector space $\mathbb{Q}_p^n$. A surprise, however, is that they are formulated rather differently from the usual $\mathrm{O}(n)$ symmetric norm on $\mathbb{R}^n$, and they are non-unique. To construct these norms, we start with

[14] More formally, any point on the tree can be considered an equivalence class of p-adic numbers, where the equivalence relation is equality up to $O(z_0)$ corrections. The equivalence classes all take the form $z + z_0\mathbb{Z}_p$, where $z \in \mathbb{Q}_p$. To say it another way: if z is any p-adic number, then the point (z_0, z) on the tree is the point whose digits up to $p^{v_p(z_0)}$ match the corresponding digits of z. This even works for points along the trunk if we think of all their chosen digits as 0.

[15] To bring this discussion closer to the standard mathematical description of the Bruhat–Tits tree (see e.g. [48]), we can rephrase our definition of a point on T_p so that each point is an equivalence class in $\mathbb{Q}_p \times \mathbb{Q}_p$, where elements (z_0, z) and (z_0', z') in $\mathbb{Q}_p \times \mathbb{Q}_p$ are identified if $|z_0| = |z_0'|$ and $z \in z' + z_0'\mathbb{Z}_p$.

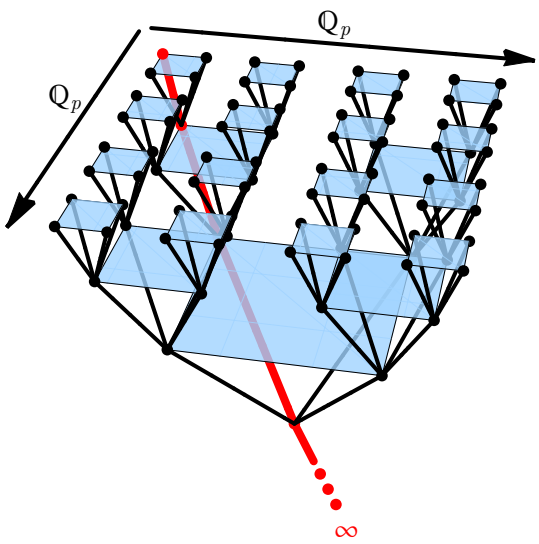

Figure 1.3: A variant of the Bruhat–Tits tree for the unramified extension $\mathbb{Q}_{p^2}$ with $p = 2$. Notice the parallels with figure 1.1. (Figure source [47].)

a field extension K of $\mathbb{Q}_p$ of degree n. Using the associated field norm $N(x)$ for $x \in K$, we can define a norm

$$|x|_K = |N(x)|_p^{1/n} . \tag{1.52}$$

This is the unique norm on K satisfying $|x|_K = |x|_p$ for any $x \in \mathbb{Q}_p$ and $|xy|_K = |x|_K|y|_K$ for any $x, y \in K$. Since $K = \mathbb{Q}_p^n$ as a vector space, (1.52) defines a natural norm on $\mathbb{Q}_p^n$, and it turns out to be an ultrametric norm; so in particular it satisfies the tall isosceles property. Different field extensions of the same degree define inequivalent norms on $\mathbb{Q}_p^n$. We will be most interested in the unramified extension of degree n, which we will denote by $\mathbb{Q}_{p^n}$. By definition, it is the field extension (which turns out to be unique) such that $|x|_K$ as defined in (1.52) is always an integer power of p for non-zero x. Other field extensions of $\mathbb{Q}_p$ can be labeled (though not always uniquely) by the smallest integer divisor e of n such that $|x|_K^e$ is an integer power of p for all non-zero x. One refers to e as the ramification index, and $e = 1$ corresponds to the unramified case.

Given a field extension K of $\mathbb{Q}_p$ (not necessarily unramified), we can introduce

analogs of $\mathbb{Z}_p$ and $\mathbb{U}_p$, namely

$$\mathbb{Z}_K \equiv \{x \in K \colon |x|_K \leq 1\} \qquad \text{and} \qquad \mathbb{U}_K \equiv \{x \in K \colon |x|_K = 1\}\,. \tag{1.53}$$

Like the p-adic integers, $\mathbb{Z}_K$ is a ring but not a field. If we define $\mathfrak{p}_K \equiv \{x \in K \colon |x|_K < 1\}$, then it can be shown that $\mathfrak{p}_K$ is a maximal ideal in $\mathbb{Z}_K$, so that $\mathbb{Z}_K/\mathfrak{p}_K$ is a field, called the residue field. It is in fact the finite field $\mathbb{F}_{p^f}$ with p^f elements, where $f = n/e$. It can also be shown that one can find an element $\pi \in K$ with $|\pi|_K = p^{-1/e}$, and that once such an element (called a "uniformizer") is chosen, the polar decomposition summarized in (1.36) and (1.42) can be generalized to a unique representation of any non-zero element of K:

$$x = \pi^{v_K(x)} \sum_{m=0}^{\infty} a_m \pi^m\,, \quad a_0 \neq 0\,, \tag{1.54}$$

where $v_K(x) \in \mathbb{Z}$ is the valuation of x in K, and the a_k are elements of the residue field, with $a_0 \neq 0$. From the perspective of a tree representation, we see from (1.54) that we can represent the sets $\pi^m \mathbb{U}_K$ as bushes rooted in a trunk, with each root marked by a power π^m of the uniformizer. Starting on the trunk, the first step up into a chosen bush amounts to choosing $a_0 \neq 0$, and subsequent steps amount to choosing successive "digits" a_k in the residue field. We see that the tree has uniform coordination number $p^f + 1$.

Two examples may help make the discussion of the previous paragraph clearer. First, the totally ramified extension of $\mathbb{Q}_p$ of degree n comes from extending $\mathbb{Q}_p$ by $p^{1/n}$. Then $e = n$ and $f = 1$, and the uniformizer can be chosen as $p^{1/n}$ itself. The tree is identical to the original Bruhat–Tits tree, only the natural depth coordinate z_0 now takes values $p^{m/n}$ where $m \in \mathbb{Z}$. Thus it can be thought of as a refinement of the Bruhat–Tits tree for $\mathbb{Q}_p$ itself. Second, the unique unramified extension $\mathbb{Q}_{p^n}$ of $\mathbb{Q}_p$ of degree n can be obtained by adjoining to $\mathbb{Q}_p$ a primitive $(p^n - 1)$-th root of unity. This non-trivial assertion is demonstrated, for example,

on pp. 167ff of [49]. The obvious choice of uniformizer is p, and the natural tree structure associated with $\mathbb{Q}_{p^n}$ is shown in figure 1.3. The depth coordinate z_0 takes values p^ω with $\omega \in \mathbb{Z}$. The boundary is $\mathbb{Q}_{p^n} \sqcup \{\infty\}$, which more properly is $\mathbb{P}^1(\mathbb{Q}_{p^n})$. We will denote this modified Bruhat–Tits tree by T_{p^n}. It can be realized as a group quotient, $T_{p^n} = \mathrm{PGL}(2, \mathbb{Q}_{p^n})/\mathrm{PGL}(2, \mathbb{Z}_{p^n})$, where $\mathbb{Z}_{p^n} = \mathbb{Z}_{\mathbb{Q}_{p^n}}$ [50]. We can use the same parametrization (z_0, z) of points in T_{p^n} as we did for T_p, and it is made precise by uniquely associating a point on the tree with the set $z + z_0\mathbb{Z}_{p^n}$ of points on the boundary that can be reached by traveling upward from it.

We will only consider unramified extensions in this dissertation. Since the isometry group of T_{p^n} is $\mathrm{PGL}(2, \mathbb{Q}_{p^n})$, which is more like $\mathrm{PSL}(2, \mathbb{R})$ and $\mathrm{PSL}(2, \mathbb{C})$, than $SO(n+1, 1, \mathbb{R})$, the non-Archimedean $\mathrm{AdS}_{n+1}/\mathrm{CFT}_n$ correspondence we will develop will have many features of a low dimensional AdS/CFT, and in fact n may sometimes serve merely as a tunable parameter. On the other hand, we will discover surprising connections with results obtained in higher dimensional Archimedean $\mathrm{AdS}_{n+1}/\mathrm{CFT}_n$ correspondence.

1.4 Outline of the dissertation

This dissertation is organized as follows. In chapter 2, we set up a non-Archimedean AdS/CFT correspondence. The AdS bulk gets replaced by a discrete regular graph, and its boundary is described by p-adic numbers. We compute various simple holographic correlators in a simple bulk theory of interacting scalar fields in a fixed background, and find the first hints of adelic relations between the Archimedean and the non-Archimedean AdS/CFT. This involves expressing final expressions for the various correlators in terms of local zeta functions. We take the first steps towards a description of p-adic Wilson loops, and discuss

the relation between the discrete Bruhat–Tits tree, and the geometry of chordal distances.

In chapter 3, we continue our investigation of the non-Archimedean AdS/CFT correspondence by focussing on the computation of the complete four-point function of scalar operators of arbitrary dimensions. We develop various computational techniques which help simplify the evaluation of complicated bulk Feynman diagrams. These techniques include the identification of the bulk dual of the p-adic scalar conformal blocks. Just like in the Archimedean case, the bulk dual turns out to be the so-called "geodesic bulk diagram," which is a bulk exchange diagram where the bulk points of integration are restricted to lie along specific geodesics. This identification, together with various useful propagator identities, helps us write down the full conformal block decomposition of the four-point function. Not only do we obtain closed-form expressions for the four-point function, we are able to discover striking (adelic) similarities between the Archimedean and non-Archimedean four-point functions, down to precise coefficients. That the p-adic expressions are simpler than the Archimedean ones can be attributed to the fact that the p-adic operator product expansion is significantly simpler, importantly lacking derivative expansions.

Finally, we write down a minimal bulk action which reproduces the two-, three-, and four-point functions of a free $O(N)$ model at leading order in large N. The bulk action describes a single massive scalar field on the Bruhat–Tits tree, with an on-site cubic, on-site quartic and a nearest neighbor quartic interaction vertex. We demonstrate precise agreement between a computation done both on the bulk and the boundary sides, to test the proposed duality. This is the first instance of a (non-trivial) check of the non-Archimedean AdS/CFT duality.

In chapter 4, we switch gears and turn to a purely field theoretic treatment of the p-adic interacting $O(N)$ model in n-dimensions and its IR fixed point. We

begin by reviewing the $O(N)$ model over the p-adic numbers and the discrete renormalization group transformations, which can be understood as spin blocking in an ultrametric context. We discuss an important property of ultrametric field theories: a non-renormalization theorem for the kinetic terms. We then obtain leading order results for the anomalous dimensions of low dimension operators near the Wilson-Fisher fixed point in the ϵ expansion. We next turn to large N methods, and obtain universal formulae for anomalous dimensions of low dimension operators which are equally valid for both (non-Archimedean) field theories over the p-adic numbers as well as (Archimedean) field theories on $\mathbb{R}^n$. These universal formulae are expressible in terms of local Beta functions (which are eventually constructed out of local zeta functions), and have an adelic flavor associated with them. Results for anomalous dimensions agree between the ϵ expansion and large N methods when they can be meaningfully compared, as well as with previous results from the literature. Finally, we consider higher derivative versions of the (Archimedean) $O(N)$ model on $\mathbb{R}^n$, the simplest of which has been studied in connection with spatially modulated phases. Our general formula for anomalous dimensions can still be applied. Finally, we comment on the existence of some interesting new field theories in four real Euclidean dimensions.

The overarching theme in this dissertation has been the search for methods which afford computational simplicity on the one hand, and uncover intriguing mathematical structures in physical theories on the other. We have taken a few steps towards connecting known formalisms with new ones and discovered surprising mathematical connections which are teaching us new lessons. We end with some concluding remarks and outlook for the future in chapter 5. I am optimistic the greatest surprises in the research direction pursued in this dissertation are yet to come and lie just around the corner.

Chapter 2

Non-Archimedean AdS/CFT

This chapter is based on a lightly edited version of a paper with Steven S. Gubser, Johannes Knaute, Andreas Samberg and Przemek Witaszczyk [47]. This work was also presented at the conferences [51, 52, 53].

2.1 Introduction and summary

We pointed out in chapter 1 several hints of holography already apparent in the description of p-adic numbers and the Bruhat–Tits tree. In fact, p-adic numbers and Bruhat–Tits tree have already appeared in the literature in connection with dS/CFT, in the context of a statistical mechanical model capturing certain aspects of eternal inflation [54]. We would like to pursue this in a different direction and develop a (Euclidean) AdS/CFT correspondence based on p-adic numbers, where real spacetime coordinates of the boundary theory are replaced by p-adic coordinates, and the bulk AdS geometry gets replaced by the Bruhat–Tits tree, so we might call this the BT/CFT correspondence, the p-adic AdS/CFT correspondence or simply the non-Archimedean AdS/CFT correspondence.

Considering a discrete bulk geometry (such as that of the Bruhat–Tits tree)

is also interesting from the point of view of tensor networks and holography [55, 56, 57, 58]. Indeed, shortly after the publication of the work on which this chapter is based [47], connections between p-adic AdS/CFT and tensor networks were pointed out in [59] and more recently in [60].

In fact, even from the point of view of a formulation of a discrete string worldsheet with the target space based on (global) algebraic number fields [61, 62, 63, 30, 29, 31, 31, 64]), one might ask whether there is a worldsheet formulation based on the (local) field of p-adic numbers. (Of course, a description in terms of real coordinates exists, and it is the standard framework of string theory.) Indeed the framework of p-adic string theory was developed in [65, 66, 48] (see [67] for a review), where the open string worldsheet was described as a Bruhat–Tits tree of coordination number $p+1$ [68], and the boundary of the string worldsheet was described by p-adic numbers (more precisely, the projective line $\mathbb{P}^1(\mathbb{Q}_p)$). Let us discuss a remarkable aspect of p-adic string theory, which will serve as a useful guide to us while formulating p-adic AdS/CFT. In the standard formulation of open strings, the (crossing symmetric) Veneziano amplitude (*i.e.* the four tachyon open string tree amplitude symmetrized over all channels) is given by

$$A_\infty^{(4)} = \int_{\mathbb{R}} dz |z|_\infty^{k_1\cdot k_2} |1-z|_\infty^{k_1\cdot k_3}\,, \tag{2.1}$$

where as in chapter 1 the norm $|\cdot|_\infty$ means the usual absolute value norm on the reals, and the tachyon momenta satisfy

$$k_i^2 = 2 \qquad \sum_{i=1}^4 k_i = 0\,. \tag{2.2}$$

Defining the Mandelstam variables

$$s \equiv -(k_1+k_2)^2 \qquad t \equiv -(k_1+k_3)^2 \qquad u \equiv -(k_1+k_4)^2\,, \tag{2.3}$$

so that $s+t+u=-8$, the integral in (2.1) evaluates

$$\begin{aligned} A_\infty^{(4)} &= B_{\rm Euler}(-\alpha(s),-\alpha(t)) + B_{\rm Euler}(-\alpha(t),-\alpha(u)) + B_{\rm Euler}(-\alpha(u),-\alpha(s)) \\ &= B_\infty(-\alpha(s),-\alpha(t))\,, \end{aligned} \tag{2.4}$$

where $\alpha(x) \equiv 1 + x/2$, and

$$B_{\rm Euler}(t_1,t_2) \equiv \frac{\Gamma_{\rm Euler}(t_1)\Gamma_{\rm Euler}(t_2)}{\Gamma_{\rm Euler}(t_1+t_2)}\,, \tag{2.5}$$

where $\Gamma_{\rm Euler}$ is the (usual) Euler Gamma function. [1] In the second line of (2.4), we have rewritten the Veneziano amplitude in terms of the local Beta, Gamma and zeta functions, defined as follows: [2]

$$B_\infty(t_1,t_2) \equiv \frac{\Gamma_\infty(t_1)\Gamma_\infty(t_2)}{\Gamma_\infty(t_1+t_2)} \tag{2.9}$$

with

$$\Gamma_\infty(s) \equiv \frac{\zeta_\infty(s)}{\zeta_\infty(1-s)} \qquad \zeta_\infty(s) \equiv \pi^{-s/2}\Gamma_{\rm Euler}(s/2)\,. \tag{2.10}$$

Analogously in p-adic string theory, the p-adic (or non-Archimedean) Veneziano amplitude is given by

$$A_p^{(4)} = \int_{\mathbb{Q}_p} dz |z|_p^{k_1\cdot k_2} |1-z|_p^{k_1\cdot k_3}\,, \tag{2.11}$$

with the momenta satisfying (2.2) like in the Archimedean case. The difference with the Archimedean case is stems from the fact that $z \in \mathbb{Q}_p$, so that the

[1] The Euler Gamma function is defined via the integral

$$\Gamma_{\rm Euler}(s) \equiv \int_0^\infty dx\, \exp(-x)|x|_\infty^{s-1}\,. \tag{2.6}$$

[2] The $B_\infty(t_1,t_2)$ and $\Gamma_\infty(s)$ functions are actually defined by the integrals

$$B_\infty(t_1,t_2) \equiv \int_{\mathbb{R}} dx\, |x|_\infty^{t_1-1}|1-x|_\infty^{t_2-1}\,, \tag{2.7}$$

$$\Gamma_\infty(s) \equiv \int_{\mathbb{R}} dx\, \exp(2\pi i x)\, |x|_\infty^{s-1}\,, \tag{2.8}$$

which can be evaluated to verify (2.9)-(2.10).

absolute value norms are now replaced with p-adic norms and the integration is now performed over $\mathbb{Q}_p$. Performing the p-adic integrals (we discuss p-adic integration in detail in section 2.2), we obtain [3]

$$A_p^{(4)} = B_p(-\alpha(s), -\alpha(t))\,, \tag{2.15}$$

where

$$B_p(t_1, t_2) \equiv \frac{\Gamma_p(t_1)\Gamma_p(t_2)}{\Gamma_p(t_1 + t_2)} \tag{2.16}$$

with

$$\Gamma_p(s) \equiv \frac{\zeta_p(s)}{\zeta_p(1-s)} \qquad \zeta_p(s) \equiv \frac{1}{1-p^{-s}}\,. \tag{2.17}$$

The authors of [66] showed that the following remarkable product formula holds:

$$A_\infty^{(4)} \prod_p A_p^{(4)} = 1\,, \tag{2.18}$$

where the product is over all primes p (with the key observation being that $\Gamma_{\mathbb{A}}(s) \equiv \Gamma_\infty(s)\prod_p \Gamma_p(s) = 1$). This product is similar to the simple adelic product $|x|_\infty \prod_p |x|_p = 1$, mentioned in chapter 1. [4] This observation that the

[3] Like in footnote 2, $B_p(t_1, t_2)$ and $\Gamma_p(s)$ functions are actually defined by the integrals

$$B_p(t_1, t_2) \equiv \int_{\mathbb{Q}_p} dx\, |x|_p^{t_1 - 1} |1-x|_p^{t_2 - 1}\,, \tag{2.12}$$

$$\Gamma_p(s) \equiv \int_{\mathbb{Q}_p} dx\, \exp(2\pi i[x])\, |x|_p^{s-1}\,, \tag{2.13}$$

where $[x]$ is the "fractional part" of $x \in \mathbb{Q}_p$. The precise details are not important for now and will be explained in more detail in section 2.2, but the upshot is that one can verify (2.16)-(2.17) starting from the integrals in (2.12)-(2.13). In fact even the local zeta functions in (2.10) and (2.17) have integral representations:

$$\begin{aligned} \zeta_\infty(s) &\equiv \zeta_\infty(1) \int_{\mathbb{R}} dx\, \exp(-\pi x^2) |x|_\infty^{s-1} \\ \zeta_p(s) &\equiv \zeta_p(1) \int_{\mathbb{Q}_p} dx\, \gamma_p(x) |x|_p^{s-1}\,, \end{aligned} \tag{2.14}$$

where $\zeta_\infty(1) = 1, \zeta_p(1) = 1/(1-p^{-1})$ and $\gamma_p(x)$ is the characteristic function of $\mathbb{Z}_p$, which we will describe in section 2.2. A key property of $\gamma_p(x)$ is that it is it's own Fourier transform.

[4] The generalization of this adelic product to higher point tachyon amplitudes involves a recursive relation between the N- and $(N-1)$-point amplitudes [69].

amplitudes at the finite places (local fields at all primes p as well as the "prime at infinity") are related to each other is quite tantalizing. We could even say that the Archimedean Venziano amplitude can be "reconstructed" starting from the p-adic amplitudes via the adelic product. Could something along these lines hold in AdS/CFT? In fact, it is worth pointing out that in retrospect, we can recognize the derivation in [68] of an effective non-local action on the boundary of the p-adic string worldsheet, for a classical theory of massless scalars on the Bruhat–Tits tree as already in the spirit of $\mathrm{AdS}_2/\mathrm{CFT}_1$. In this chapter and the next, we provide evidence that something similar happens in holography, in fact almost just as well.

The bulk of the present chapter is devoted to a detailed account of how to formulate AdS/CFT when the boundary is not $\mathbb{R}^n$ but instead an n-dimensional vector space $\mathbb{Q}_p^n$. More precisely, we take the boundary to be the unramified extension of $\mathbb{Q}_p$ of degree n,[5] and the bulk is a modification of the Bruhat–Tits tree for $\mathbb{Q}_p$ such that each vertex has $p^n + 1$ nearest neighbors.[6] We will formulate a version of AdS/CFT that relates classical dynamics on the Bruhat-Tits tree of $\mathbb{Q}_{p^n}$ to a conformal field theory on $\mathbb{Q}_{p^n}$. We will find it to be similar

[5]One reason for sticking with the case of unramified extensions is that it is simpler than the case of ramified extensions, where conflicting notions of dimension may arise. Starting with the unramified field extension $\mathbb{Q}_{p^f}$, we may extend further by adjoining $p^{1/e}$ for some $e > 1$. The residue field is still $\mathbb{F}_{p^f}$, and the natural uniformizer is $p^{1/e}$. The Bruhat–Tits tree is unchanged from T_{p^f}, except in that the depth coordinate on the Bruhat–Tits tree z_0 takes values $p^{m/e}$ for $m \in \mathbb{Z}$; thus it is a refinement of the Bruhat–Tits tree for $\mathbb{Q}_{p^f}$ in the sense of [70]. This ramified extension has two conflicting notions of dimensionality: The residue field $\mathbb{F}_{p^f}$ has dimension f as a vector space over $\mathbb{F}_p$, but the full field extension has dimension ef as a vector space over $\mathbb{Q}_p$. Possibly the resulting holographic dynamics will show a mix of f-dimensional and ef-dimensional behaviors.

[6]Quadratic field extensions appeared already in [65] in connection with closed strings, which is to say two-dimensional conformal field theory. Ramified extensions have been considered in the context of the p-adic string in [70], following work of [71], and other field extensions of the p-adics have also been considered for some time in the program of Gervais [72] to generalize p-adic string amplitudes. Field extensions of $\mathbb{Q}_p$, the modified Bruhat–Tits tree and its Schottky uniformization were also discussed in [73] in the context of tachyon multiloop amplitudes in p-adic string theory, and in [74] (building on work of [75]) in the context of black holes in $\mathrm{AdS}_3/\mathrm{CFT}_2$.

in many regards to the usual Euclidean $\mathrm{AdS}_{n+1}/\mathrm{CFT}_n$ duality, although we are limited in this work to scalar fields and operators. One significant difference, however, is that the symmetry group of the Bruhat-Tits tree is $\mathrm{PGL}(2,\mathbb{Q}_{p^n})$, which is closer to $\mathrm{SL}(2,\mathbb{R})$ than to the group $\mathrm{O}(n{+}1,1,\mathbb{R})$ of isometries of AdS_{n+1}. Correspondingly, conformal field theories over $\mathbb{Q}_{p^n}$ can be expected to have some common algebraic features independent of the value of n. For simplicity, our discussion will be limited to the simplest possible action on the modified Bruhat–Tits tree (which corresponds to the gravity side of the AdS/CFT correspondence), namely a nearest neighbor action for a single real scalar defined on the vertices of the Bruhat–Tits tree (which serves as the fixed background geometry). with a mass and possibly some cubic or quartic self-interactions,

$$S[\phi] = \eta_p \sum_{\langle ab \rangle} \frac{1}{2}(\phi_a - \phi_b)^2 + \eta_p \sum_a \left(\frac{1}{2} m_p^2 \phi_a^2 + \frac{g_3}{3!}\phi_a^3 + \frac{g_4}{4!}\phi_a^4 \right) , \tag{2.19}$$

where η_p, g_3, and g_4 are coupling constants. The seemingly "missing" factor of $\sqrt{g}$ in the action, which for example is present in the Archimedean case (see, for instance (1.30) in chapter 1) is actually implicit in (2.19). Essentially, starting with a continuum (Euclidean) pAdS space given by the product space $p\mathrm{AdS}_{n+1} = \mathbb{Q}_p^\times \times \mathbb{Q}_{p^n}$, where $\mathbb{Q}_p^\times$ corresponds to the radial direction in the bulk, and an action defined on this space (which does include an explicit factor of $\sqrt{g}$), (roughly speaking) after consistently identifying points "within one AdS radius distance" of each other as belonging to the universality class, the geometry of $p\mathrm{AdS}_{n+1}$ can be shown to become that of the Bruhat–Tits tree T_{p^n}, with the continuum integral over all of AdS space in the action becoming the discrete tree sum shown in (2.19). We explain this point in detail in section 2.5.3.

So starting with the action in (2.19), where the sum $\sum_{\langle ab \rangle}$ represents a sum over all nearest neighbor vertices and the sum $\sum_a$ is over all vertices of the tree, we will express Green's functions in terms of bulk-to-boundary and bulk-to-bulk

propagators, and a number of formal similarities to ordinary AdS/CFT will be noted. In general — up to subtleties with regularization as discussed in section 2.4.1 — the expression for p-adic correlators is found from the prescription

$$-\log\left\langle \exp\left\{\int_{\mathbb{Q}_q} dz\,\phi_0(z)\mathcal{O}(z)\right\}\right\rangle_p = \underset{\phi\to\phi_0}{\text{extremum}}\, S[\phi] \tag{2.20}$$

where by $\phi \to \phi_0$ we mean

$$\lim_{z_0\to 0} |z_0|_p^{\Delta-n}\phi(z_0,z) = \phi_0(z)\,, \tag{2.21}$$

and $S[\phi]$ is the bulk action (2.36) or some generalization thereof. The formula (2.20) is closely analogous to the standard AdS/CFT prescription of [23, 24] as discussed in chapter 1, and it should be understood as receiving corrections from loops in the bulk, so that the full story is that the partition functions of the bulk and boundary coincide when appropriately sourced.

Final expressions for two- and three-point correlators are computed using (2.20) in section 2.4 and are found to be mostly, but not entirely, amenable to being assembled into adelic products. The main feature of p-adic four-point amplitudes is a remarkably simple closed form expression for the p-adic amplitudes as compared to their real counterparts. A detailed account of the complete four-point function of operators of arbitrary dimensions (which includes both contact as well as exchange diagrams) is postponed to chapter 3. A remarkable feature of the p-adic correlators is their striking similarities with the Archimedean results when the standard expressions found in the literature are reexpressed in term of the local zeta functions ζ_∞ (rather than Γ_{Euler}). In fact all explicit factors of π disappear, and the final Archimedean expressions take considerably simpler (and almost universal) forms in terms of local zeta functions. (Universal in the sense independent of the choice of the local field — whether p-adic or real.) This continues to hold for more complicated calculations presented in chapters

3 and 4, where we rewrite standard expressions for the full four-point function and anomalous dimensions in terms of local Beta, Gamma and zeta functions. On top of their remarkable resemblance with the Archimedean results, the p-adic results are also associated with great simplicity. For example, the exact bulk-to-boundary propagator is a linear combination of precisely two terms associated with the two power laws allowed by the equations of motion, upto a certain depth in the bulk beyond which it vanishes exactly. The Archimedean bulk-to-boundary propagator instead has subleading correction terms near the boundary, and an exponentially fall-off deeper in the bulk. As another example, the p-adic four-point function admits a closed form expression, in contrast to the Archimedean four-point function (a detailed analysis of the four-point function, along with a discussion on what causes the p-adic correlators to have simpler final expressions will be undertaken in chapter 3). Finally, the simplicity of CFT correlators can also be seen as the simplicity of the bulk. The discrete tree geometry of the bulk causes the holographic computation of correlators to reduce to simple geometric sums rather than complicated integrals in the Archimedean case. In fact, any diagram in the bulk, be it higher-point functions or loop corrections, should be exactly calculable in closed form because it may be reduced to a combination of geometric sums.

The organization of the rest of this chapter is as follows. In section 2.2 we summarize some aspects of p-adic integration that we will need. Most of our account is standard, and more thorough treatments can be found, for example, in [48, 49]. In section 2.3, we introduce the classical scalar dynamics that we are interested in on the Bruhat–Tits tree, and we explain how to compute bulk-to-bulk and bulk-to-boundary propagators. We then pass in section 2.4 to the computation of holographic m-point amplitudes for $m = 2$, 3, and 4. In section 2.5 we touch upon the relation of p-adic correlators to their real counterparts, the

geometry of chordal distance on p-adic AdS_{n+1}, and a brief account of Wilson loops, and finally conclude in section 2.6 with some future directions.

We will simplify notation by setting $q = p^n$ so that $\mathbb{Q}_q$ is the unramified extension of degree n. We will abbreviate the norm $|\cdot|_{\mathbb{Q}_q}$ to $|\cdot|_q$ and the valuation $v_{\mathbb{Q}_q}$ to v_q.

2.2 p-adic integration

We will need to perform integrals over $\mathbb{Q}_p$ or over the unramified extension $\mathbb{Q}_q$. Such integrals may be approximated as Riemann sums built by sampling a typical value of the integrand at each point in the Bruhat–Tits tree T_q, and then summing these typical values over all points at a fixed depth z_0. In practice, we will often work with integrands which are piecewise constant over easily enumerated subsets of $\mathbb{Q}_q$, and then the integral can be replaced by a discrete sum.

In order to write down the Riemann sums of interest explicitly, it is helpful to define the sets

$$S_\mu^\omega \equiv \left\{ x \in \mathbb{Q}_q \colon x = \sum_{m=\mu}^{\omega-1} a_m p^m \text{ where all } a_m \in \mathbb{F}_q \right\} \tag{2.22}$$

for $\omega > \mu$, and $S_\mu^\omega = \{0\}$ for $\omega \leq \mu$. If $\omega > \mu$, then the elements of S_μ^ω uniquely label the $q^{\omega-\mu}$ points in T_q at depth $z_0 = p^\omega$ which can be accessed by going upward $\omega - \mu$ steps from the point $(p^\mu, 0)$. Given a function $f : \mathbb{Q}_q \to \mathbb{R}$ which is continuous and tends swiftly to 0 when its argument is large in the $|\cdot|_q$ norm, we may approximate

$$\int_{\mathbb{Q}_q} dx\, f(x) \approx \sum_{x \in S_\mu^\omega} q^{-\omega} f(x)\,, \tag{2.23}$$

where we usually require $\omega > \mu$. The approximate equality in (2.23) becomes an exact equality in the limit where $\mu \to -\infty$ and $\omega \to \infty$. We should think of μ as an infrared cutoff which essentially tells us to replace the integral over $\mathbb{Q}_q$

by an integral over $p^\mu \mathbb{Z}_q$. The ultraviolet cutoff ω tells us to sample the integral at evenly spaced points, with a small volume $q^{-\omega}$ assigned to each point. We observe that for fixed ω and fixed μ with $\omega \geq \mu$, we can split up $p^\mu \mathbb{Z}_q$ into many copies of $p^\omega \mathbb{Z}_q$, each shifted by an element of S_μ^ω. Explicitly, we can write $p^\mu \mathbb{Z}_q$ as a disjoint union:[7]

$$p^\mu \mathbb{Z}_q = \bigsqcup_{x \in S_\mu^\omega} (x + p^\omega \mathbb{Z}_q) \qquad \text{for fixed } \omega \geq \mu \,. \tag{2.25}$$

The disjoint union (2.25) helps motivate the form of the right hand side of (2.23). Using (2.23), one can show that

$$\int_{\mathbb{Z}_q} dx = 1 \,, \tag{2.26}$$

and that

$$\int_{\xi S} dx = |\xi|_q^n \int_S dy \tag{2.27}$$

for any measurable set $S \subset \mathbb{Q}_q$ and any fixed non-zero element $\xi \in \mathbb{Q}_q$. Then $\xi S = \{\xi s : s \in S\}$. We think of the prefactor in (2.27) as coming from $|dx/dy|_q^n = |N(dx/dy)|_p$ where $x = \xi y$. Since $\mathbb{U}_q = \mathbb{Z}_q \setminus p\mathbb{Z}_q$, we see by combining (2.26) and (2.27) that

$$\int_{\mathbb{U}_q} dx = 1 - \frac{1}{q} \,. \tag{2.28}$$

In later sections we will need the Fourier transform over $\mathbb{Q}_q$. The first ingredient is an additive character $\chi : \mathbb{Q}_q \to S^1$, where we think of S^1 as a complex phase. The key properties of χ are $\chi(\xi + \eta) = \chi(\xi)\chi(\eta)$, $\chi(0) = 1$, and $\chi(\xi)^* = \chi(-\xi)$,

[7] We will have enough occasion in this chapter to use both ordinary unions, represented by $\cup$, and disjoint unions, represented by $\sqcup$, that we emphasize the distinction. By definition,

$$\bigcup_{\alpha \in S} A_\alpha \equiv \{x : x \in A_\alpha \text{ and } \alpha \in S\} \qquad \text{while} \qquad \bigsqcup_{\alpha \in S} A_\alpha \equiv \{(x, \alpha) : x \in A_\alpha \text{ and } \alpha \in S\} \,. \tag{2.24}$$

Note that the ordinary union and disjoint union of sets can be naturally identified if and only if all the sets A_α are disjoint. Sometimes, as in (1.43), we use $\sqcup$ to indicate a union of obviously disjoint sets; elsewhere, as in (2.118), we use $\sqcup$ on overlapping sets when the multiplicity of elements in the final union matters. We reserve $\cup$ for use in situations where we want the ordinary union of sets which may overlap.

where * means complex conjugation. The standard additive character on $\mathbb{R}$ is $\chi(\xi) = \mathrm{e}^{2\pi i\xi}$. On $\mathbb{Q}_p$, the standard choice is $\chi(\xi) = \mathrm{e}^{2\pi i[\xi]}$, where $[\xi]$ is the fractional part of ξ: That is, $[\xi] \in [0,1)$, and $\xi = [\xi] + m$ for some $m \in \mathbb{Z}_p$. Note that $[\xi]$ is a rational number whose denominator is a power of p. To handle an unramified extension $\mathbb{Q}_q$, we start with an arbitrary non-zero element

$$\xi = \sum_{m=v_q(\xi)}^{\infty} b_m p^m \,, \tag{2.29}$$

where each $b_m \in \mathbb{F}_q$ and $b_{v_q(\xi)} \neq 0$, and define the fractional part as $[\xi] = 0$ if $\xi \in \mathbb{Z}_q$, and

$$[\xi] = \sum_{m=v_q(\xi)}^{-1} \mathrm{Tr}_{\mathbb{F}_q:\mathbb{F}_p}(b_m) p^m \tag{2.30}$$

otherwise. To make sense of (2.30), recall that $\mathrm{Tr}_{\mathbb{F}_q:\mathbb{F}_p} : \mathbb{F}_q \to \mathbb{F}_p$ is a homomorphism of the additive group structures on $\mathbb{F}_q$ and $\mathbb{F}_p$, and $\mathbb{F}_p$ can be identified with the set $\{0, 1, 2, \ldots, p-1\}$, so the right hand side of (2.30) is a rational number in $[0,1)$ whose denominator is a power of p. Now we can define $\chi(\xi) = \mathrm{e}^{2\pi i[\xi]}$ as in the case of $\mathbb{Q}_p$.

The Fourier and inverse Fourier transforms over $\mathbb{Q}_q$ can be defined as

$$f(x) = \int_{\mathbb{Q}_q} dk\, \chi(kx) \tilde{f}(k) \qquad\qquad \tilde{f}(k) = \int_{\mathbb{Q}_q} dx\, \chi(kx)^* f(x)\,. \tag{2.31}$$

A key feature of the p-adic Fourier transform is that

$$\gamma_q(x) \equiv \begin{cases} 1 & \text{for } x \in \mathbb{Z}_q \\ 0 & \text{otherwise} \end{cases} \tag{2.32}$$

is its own Fourier transform. Indeed, if $k \in \mathbb{Z}_q$, then for all $x \in \mathbb{Z}_q$, we have $[kx] = 0$, so $\chi(kx) = 1$ and the second integral of (2.31) reduces to the integral of 1 over $\mathbb{Z}_q$, which is 1; whereas, if instead $k \notin \mathbb{Z}_q$, the character $\chi(kx)$ takes values symmetrically distributed around the unit circle in $\mathbb{C}$, so that the average

is 0. Using (2.27) and (2.32), we can show that

$$\int_{\xi\mathbb{U}_q} dy\,\chi(y) = |\xi|_q^n \left(\gamma_q(\xi) - \frac{1}{q}\gamma_q(p\xi)\right) = \begin{cases} |\xi|_q^n \left(1 - \dfrac{1}{q}\right) & \text{if } v_q(\xi) \geq 0 \\ -1 & \text{if } v_q(\xi) = -1 \\ 0 & \text{if } v_q(\xi) < -1\,. \end{cases} \tag{2.33}$$

With the formula (2.33) in hand, we can find the Fourier transform of any function $f(x)$ which depends only on the norm $|x|_q$.

In the computation of two-point functions we will use

$$\int_{\mathbb{Q}_q} dx\,\chi(k_1 x)\chi(k_2 x) = \delta(k_1 + k_2)\,. \tag{2.34}$$

This formal relation is rendered meaningful by integrating both sides against a smooth function $\tilde{f}(k_1)$ which decreases rapidly for large argument:

$$\begin{aligned} \int_{\mathbb{Q}_q} dk_1\,\tilde{f}(k_1) \int_{\mathbb{Q}_q} dx\,\chi(k_1 x)\chi(k_2 x) &= \int_{\mathbb{Q}_q} dx\,\chi(k_2 x) \int_{\mathbb{Q}_q} dk_1\,\tilde{f}(k_1)\chi(k_1 x) \\ &= \int_{\mathbb{Q}_q} dx\,\chi(k_2 x) f(x) = \tilde{f}(-k_2)\,, \end{aligned} \tag{2.35}$$

where in the first step we switched order of integrations (still as a formal manipulation), and the remaining steps are rigorously defined examples of Fourier transforms.

2.3 Propagators

Following the philosophy of AdS/CFT, we would like to study a classical action on the modified Bruhat–Tits tree T_q, where $q = p^n$. From the behavior of classical fields on this p-adic version of AdS_{n+1}, we expect to obtain correlators on the boundary, $\partial T_q = \mathbb{Q}_q$ (more precisely, $\partial T_q = \mathbb{P}^1(\mathbb{Q}_q)$). Readers interested in the simplest examples may consistently set $n = 1$ and $q = p$, so that the whole

discussion reduces to the unmodified $(p+1)$-regular Bruhat–Tits tree and the boundary is just $\mathbb{Q}_p$ (more precisely, $\mathbb{P}^1(\mathbb{Q}_p)$).

2.3.1 Action, bulk-to-bulk propagator, and mass formula

Consider the following discrete bulk Euclidean action on the tree,

$$S = \sum_{\langle ab \rangle} \frac{1}{2} \left(\phi_a - \phi_b\right)^2 + \sum_a \left(\frac{1}{2} m_p^2 \phi_a^2 - J_a \phi_a \right) , \tag{2.36}$$

where a and b label vertices on the tree. The notation $\langle ab \rangle$ indicates that the sum is over nearest neighboring lattice sites, or in other words over all edges of the tree. The equation of motion derived from (2.36) is

$$(\Box + m_p^2)\phi_a = J_a \,, \tag{2.37}$$

where the laplacian on the tree is

$$\Box \, \phi_a = \sum_{\substack{\langle ab \rangle \\ a \text{ fixed}}} \left(\phi_a - \phi_b\right) . \tag{2.38}$$

The choice of sign in (2.38) corresponds to the choice $\Box = -\frac{1}{\sqrt{g}} \partial_\mu \sqrt{g} g^{\mu\nu} \partial_\nu$ on a real manifold, i.e. $\Box$ is positive definite as an operator acting on functions with swift fall-off at infinity. A solution to (2.37) is

$$\phi_a = \sum_b G(a,b) J_b \,, \tag{2.39}$$

where the Green's function $G(a,b)$ satisfies

$$(\Box_a + m_p^2) G(a,b) = \delta(a,b) \,. \tag{2.40}$$

In (2.40) the laplacian $\Box_a$ is understood to act on the first index of G, and

$$\delta(a,b) = \begin{cases} 1 & \text{if } a = b \\ \\ 0 & \text{otherwise} \,. \end{cases} \tag{2.41}$$

A solution to (2.40) depending only on the distance $d(a,b)$ between vertices a and b on the tree is

$$G(a,b) = \frac{\zeta_p(2\Delta)}{p^{\Delta}} p^{-\Delta d(a,b)}\,, \tag{2.42}$$

where Δ satisfies the relation

$$m_p^2 = -\frac{1}{\zeta_p(\Delta - n)\,\zeta_p(-\Delta)}\,. \tag{2.43}$$

We have introduced the p-adic zeta functions

$$\zeta_p(s) \equiv \frac{1}{1-p^{-s}}\,. \tag{2.44}$$

Results on bulk-to-bulk propagators for a massless scalar on the Bruhat–Tits tree were obtained in [68], both for asymptotic Dirichlet and Neumann boundary conditions. The result for Dirichlet boundary conditions matches exactly with the $n = \Delta = 1$ case of (2.42), up to an overall sign due to a notational difference in the definition of the tree Laplacian.

If $m_p^2 = m_{BF,p}^2 \equiv -1/\,\zeta_p(-n/2)^2$, then the unique real solution to (2.43) is $\Delta = n/2$. If $m_p^2 > m_{BF,p}^2$, there are two real solutions $\Delta_\pm$ to (2.43) with $\Delta_+ + \Delta_- = n$ and $\Delta_+ > \Delta_-$. If $m_{BF,p}^2 < m_p^2 < 0$, then $\Delta_\pm$ are both positive, whereas if $m_p^2 > 0$, $\Delta_+ > 0$ while $\Delta_- < 0$. This is similar to the situation for real AdS_{n+1} of radius L, where $m_\infty^2 L^2 = \Delta(\Delta - n)$ as discussed in chapter 1. Following standard terminology, we will refer to constructions based on $\mathbb{R}$ as the Archimedean place. In either the Archimedean or p-adic places, we will assume $\Delta = \Delta_+ > n/2$ from here on and leave aside considerations of alternative quantization.

2.3.2 Bulk-to-boundary propagator

Next we want to formulate the bulk-to-boundary propagator $K(a,x)$, where $a \in T_q$ is a bulk point and $x \in \mathbb{Q}_q$ is a boundary point. $K(a,x)$ should be a limit

of $G(a,b)$ where b is taken to the boundary point $x \in \mathbb{Q}_q$. As this limit is taken with a held fixed, we must multiply by some function of b to keep the result finite while preserving the property

$$(\Box_a + m_p^2)K(a,x) = 0 \tag{2.45}$$

throughout the bulk. An obvious adaptation of the standard normalization convention is

$$\int_{\mathbb{Q}_q} dx\, K(z_0, z; x) = |z_0|_p^{n-\Delta}\,, \tag{2.46}$$

where the power on the right hand side makes sense because then the right hand side itself is annihilated by $\Box + m_p^2$, and we remember that the bulk point a can be expressed as (z_0, z).

We insist on translation invariance in the $\mathbb{Q}_q$ direction: that is, $K(z_0, z; x)$ depends on z and x only through the difference $z - x$. We propose the form

$$K(z_0, z; x) = \frac{\zeta_p(2\Delta)}{\zeta_p(2\Delta - n)} \frac{|z_0|_p^{\Delta}}{|(z_0, z-x)|_s^{2\Delta}}\,. \tag{2.47}$$

By $|\cdot|_s$ we mean the supremum norm:

$$|(z_0, z-x)|_s = \sup\{|z_0|_p, |z-x|_q\}\,, \tag{2.48}$$

where $|z_0|_p = p^{-\omega}$ when $z_0 = p^\omega$.

To check that (2.47) is correct, it is enough to start by setting $z = 0$ and holding z_0 fixed. Then the bulk point is precisely the point along the trunk labeled by $z_0 = p^\omega$, which is to say the point at which the bush below $z_0\mathbb{U}_q$ is rooted. For points $x \in z_0\mathbb{Z}_q = \bigsqcup_{m \geq \omega} p^m \mathbb{U}_q \sqcup \{0\}$, a path from x to the bulk point $(z_0, 0)$ goes straight down. By contrast, to go from a boundary point $x \in p^{-1}z_0\mathbb{U}_q$ to the bulk point $(z_0, 0)$ we must go down to the root point $p^{-1}z_0$ and then back up one step to z_0. This means there are two extra steps in the paths from points $x \in p^{-1}z_0\mathbb{U}_q$ as compared to paths from points $x \in z_0\mathbb{Z}_q$. There are $2m$ extra

steps if $x \in p^{-m} z_0 \mathbb{U}_q$, since we must go down to the root point $p^{-m} z_0$ and then back up m steps to z_0.[8] Because $G(a,b) \propto p^{-\Delta d(a,b)}$, we are penalized by a factor of $p^{-2\Delta}$ for each extra step we take. Hence $K(z_0, 0; x)$ is constant for $x \in z_0 \mathbb{Z}_q$, whereas $K(z_0, 0; x) = p^{-2\Delta m} K(z_0, 0; 0)$ when $|x|_q = p^m |z_0|_q$ for $m > 0$. Observing that

$$|(z_0, x)|_s = \begin{cases} |z_0|_p & \text{for } |x|_q \leq |z_0|_p \\ p^m |z_0|_p & \text{for } |x|_q = p^m |z_0|_p \text{ and } m > 0\,, \end{cases} \tag{2.49}$$

we see that the factor $|(z_0, z-x)|_s^{2\Delta}$ in the denominator of the right hand side of (2.47) is just what we need to account for the x-dependence of K.

To figure out the z_0 dependence of K, let's set $x = z = 0$. Then the number of steps from the boundary point to the bulk point (that is, from $x = 0$ to the point marked $z_0 = p^\omega$ on the tree) increases by 1 every time we decrease ω by 1. Each such step should decrease K by a factor of $p^{-\Delta}$. So we conclude that $K(z_0, 0; 0) \propto |z_0|_p^{-\Delta}$. Together with the considerations of the previous paragraph, we see that $K(z_0, z; x) \propto |z_0|_p^{\Delta} / |(z_0, z-x)|_s^{2\Delta}$. At this point one can explicitly verify the property (2.45).

All that remains is to check that the overall normalization of K in (2.47) matches the condition (2.46). To this end we calculate the integral

$$\begin{aligned} \int_{\mathbb{Q}_q} \frac{dx}{|(z_0, x)|_s^{2\Delta}} &= \int_{z_0 \mathbb{Z}_q} \frac{dx}{|z_0|_p^{2\Delta}} + \sum_{m=1}^{\infty} \int_{p^{-m} z_0 \mathbb{U}_q} \frac{dx}{p^{2m\Delta} |z_0|_p^{2\Delta}} \\ &= |z_0|_p^{n-2\Delta} \left[1 + \left(1 - \frac{1}{q}\right) \sum_{m=1}^{\infty} q^m p^{-2m\Delta} \right] \\ &= |z_0|_p^{n-2\Delta} \left[1 + \left(1 - \frac{1}{p^n}\right) \left(\frac{1}{1 - p^{n-2\Delta}} - 1 \right) \right] \\ &= |z_0|_p^{n-2\Delta} \frac{\zeta_p(2\Delta - n)}{\zeta_p(2\Delta)}\,, \end{aligned} \tag{2.50}$$

[8] The number of steps from a boundary point to a bulk point is always infinite, so the careful reader may prefer the more precise statement that if we start counting steps at some fixed depth w_0, with $|w_0|_p < |z_0|_p$, then the number of steps is the same for all $x \in z_0 \mathbb{Z}_q$, and increases by $2m$ for $x \in p^{-m} z_0 \mathbb{Z}_q$.

where the key step was to split the integral over all of $\mathbb{Q}_q$ to integrals over disjoint domains across which the integrand is constant. The final result in (2.50) confirms the normalization in (2.47).

It is interesting to note that the normalized bulk-to-boundary propagator for a scalar field in Euclidean AdS_{n+1} is

$$K(z_0, \vec{z}; \vec{x}) = \frac{\zeta_\infty(2\Delta)}{\zeta_\infty(2\Delta - n)} \frac{z_0^\Delta}{(z_0^2 + (\vec{z} - \vec{x})^2)^\Delta}\,, \tag{2.51}$$

where we have used the normalization condition

$$\int_{\mathbb{R}^n} d^n x\, K(z_0, \vec{z}; \vec{x}) = z_0^{n-\Delta} \tag{2.52}$$

and introduced the local zeta function

$$\zeta_\infty(s) = \pi^{-s/2} \Gamma_{\text{Euler}}(s/2)\,. \tag{2.53}$$

2.3.3 Bulk-to-boundary propagator in Fourier space

Recall in the real case that we may express

$$K(z_0, \vec{z}; \vec{x}) = \int_{\mathbb{R}^n} d^n k\, \mathrm{e}^{2\pi i \vec{k}\cdot(\vec{x}-\vec{z})} K(z_0, \vec{k})\,, \tag{2.54}$$

where

$$K(z_0, \vec{k}) = \frac{2}{\zeta_\infty(2\Delta - n)} k^{\Delta - \frac{n}{2}} z_0^{\frac{n}{2}} K_{\Delta - \frac{n}{2}}(2\pi k z_0)\,, \tag{2.55}$$

where K_ν is a modified Bessel function of the second kind. The positioning of the factors of 2π in (2.54) is non-standard, but it is easily understood if $\vec{k}$ is thought of as momentum as the result of setting Planck's constant $h = 1$ instead of the usual $\hbar = 1$. It is useful to note the asymptotics

$$K(z_0, \vec{k}) = z_0^{n-\Delta}\,[1 + \ldots] + \frac{\zeta_\infty(-2\Delta + n)}{\zeta_\infty(2\Delta - n)} k^{2\Delta - n} z_0^\Delta\,[1 + \ldots] \tag{2.56}$$

for small kz_0, while

$$K(z_0, \vec{k}) = \frac{k^{\Delta - \frac{n}{2} - \frac{1}{2}} z_0^{\frac{n}{2} - \frac{1}{2}}}{\zeta_\infty(2\Delta - n)} \mathrm{e}^{-2\pi k z_0} + \ldots \tag{2.57}$$

for large kz_0. In (2.56), $[1 + \ldots]$ denotes a Taylor series in $(kz_0)^2$. Readers familiar with the standard formulas for bulk-to-boundary propagators in Fourier space may be amused to note that by using ζ_∞ in favor of Γ_{Euler} and following the $h = 1$ convention rather than $\hbar = 1$, we obtain simpler expressions for the coefficients than the usual ones.

Now we would like to generalize (2.55) to the p-adic case. Explicitly,

$$K(z_0, k) \equiv \int_{\mathbb{Q}_q} dx\, \chi(kx)^* K(z_0, 0; x) = \frac{\zeta_p(2\Delta)}{\zeta_p(2\Delta - n)} |z_0|_p^\Delta \sum_{m\in\mathbb{Z}} \int_{p^m \mathbb{U}_q} dx \frac{\chi(kx)^*}{|(z_0, x)|_s^{2\Delta}}\,. \tag{2.58}$$

In the second equality, we have split $\mathbb{Q}_q$ into nested spheres $p^m\mathbb{U}_q$. We were able to drop integration over the point 0 because this point has zero measure and the integrand is finite there. $|(z_0, x)|_s^{2\Delta}$ depends on x only through its norm $|x|_q$, so each integrand in the last expression in (2.58) is constant over its domain $p^m\mathbb{U}_q$ of integration. As a result we may use (2.33). After some work, we obtain the simple result

$$K(z_0, k) = \left(|z_0|_p^{n-\Delta} + |k|_q^{2\Delta - n} |z_0|_p^\Delta \frac{\zeta_p(-2\Delta + n)}{\zeta_p(2\Delta - n)} \right) \gamma_q(kz_0)\,. \tag{2.59}$$

(We could simplify (2.59) further using $\zeta_p(-2\Delta + n)/\,\zeta_p(2\Delta - n) = -p^{-2\Delta+n}$, but for comparison with (2.56) it is best to leave (2.59) in terms of p-adic zeta functions.) A remarkable point about (2.59) is that $K(z_0, k)$ is *exactly* a linear combination of the two power laws $|z_0|_p^{n-\Delta}$ and $|z_0|_p^\Delta$ down to the point where $|kz_0|_q = 1$, and then for larger $|kz_0|_q$ (meaning, further from the boundary of the Bruhat–Tits tree), $K(z_0, k)$ vanishes exactly, instead of the exponentially small behavior (2.57) observed in the real case. The exact vanishing explains a point that may have been puzzling the reader: an on-shell scalar with momentum k should take the form

$$\phi(z_0, z) = K(z_0, k)\chi(kz)\,, \tag{2.60}$$

but how can this be a well-defined function on the Bruhat–Tits tree when $\chi(kz)$

itself is not? The answer is that $\chi(kz)$ is well-defined at points on the tree (z_0, z) precisely if $|kz_0|_q \leq 1$. To see that this is true, remember that for a point (z_0, z) on the tree, the p-adic coordinate z can only be specified up to $O(z_0)$ corrections. That means that kz is determined up to $O(p^{v_q(kz_0)})$ corrections. $\chi(kz)$ is well-defined if and only if the fractional part $[kz]$ is well-defined, which is the same as saying that kz is determined up to $O(p^m)$ corrections for some $m \geq 0$. We conclude that the condition for $\chi(kz)$ to be well-defined at (z_0, z) is $v_q(kz_0) \geq 0$, and that is the same condition as $|kz_0|_q \leq 1$. In other words, $\chi(kz)$ is not defined on the whole tree, but $\chi(kz)\gamma_q(kz_0)$ is, and that is enough for the expression (2.60) to be well-defined.

It is possible to go further and verify not only that (2.60) is well-defined, but also that it is a solution of $(\Box + m_p^2)\phi = 0$. There are four cases to consider:

- $|kz_0|_q > p$. Trivial because $\phi(z_0, z) = \phi(pz_0, z) = \phi(z_0/p, z) = 0$ for all z in this case.

- $|kz_0|_q < 1$. In this case, ϕ is a sum of the two power laws permitted by the mass formula (2.43), so the result is again trivial.

- $|kz_0|_q = p$. This case is straightforward because $\phi(z_0, z) = \phi(z_0/p, z) = 0$ for all z, whereas for fixed z, $\phi(a)$ ranges over a non-trivial character of $\mathbb{F}_q$ as its argument a ranges over the q nearest neighbors of (z_0, z) in the upward direction.

- $|kz_0|_q = 1$. An explicit calculation starting from $(\Box + m_p^2)\phi = 0$ leads to

$$-qK(p|k|_q, k) + (q + 1 + m_p^2)K(|k|_q, k) = 0\,, \tag{2.61}$$

  which is easily verified by direct substitution.

In fact, using (2.43) one can show from (2.61) that the relative coefficient between the two terms in parentheses in (2.59) must be as written there. If we further

require that $K(z_0, 0) = |z_0|_p^{n-\Delta}$, which is the same as the normalization condition (2.46), we can conclude that (2.59) is the only possible answer for $K(z_0, k)$, independently of the Fourier transform calculation given in (2.58).

2.3.4 Cross-ratios and limiting procedures

It will sometimes be useful to have expressions for propagators which are less attached to the particular choice of depth coordinate, and correspondingly to a particular $\mathbb{Q}_q$ patch of the projective space $\mathbb{P}^1(\mathbb{Q}_q)$. For this purpose, a key formula expresses the distance $d(a, b)$ between two points a and b on T_q in terms of points x, y, u, and v in $\mathbb{P}^1(\mathbb{Q}_q)$ such that the paths on T_q from x to y and from u to v intersect precisely along the path from a to b, as in figure 2.1:

$$p^{-d(a,b)} = \left|\frac{(x-u)(y-v)}{(x-y)(u-v)}\right|_q = \left|\frac{(x-u)(y-v)}{(x-v)(u-y)}\right|_q . \tag{2.62}$$

In writing (2.62), we are assuming that none of x, y, u, and v are at ∞. The second and third expressions in (2.62) are easily seen to be invariant under $\mathrm{PGL}(2, \mathbb{Q}_q)$. If one of x, y, u, and v is at ∞, then we must first apply a suitable $\mathrm{PGL}(2, \mathbb{Q}_q)$ transformation to all four points so that they all are mapped to $\mathbb{Q}_q$, and then use (2.62).

From (2.42) and (2.62) it is clear that we may express the bulk-to-bulk Green's function as

$$G(a, b) = \frac{\zeta_p(2\Delta)}{p^\Delta} \left|\frac{(x-u)(y-v)}{(x-y)(u-v)}\right|_q^\Delta . \tag{2.63}$$

A little less obvious is the expression for the bulk-to-boundary propagator:

$$K(a, y) = \frac{\zeta_p(2\Delta)}{\zeta_p(2\Delta - n)} \left|\frac{x-u}{(x-y)(u-y)}\right|_q^\Delta , \tag{2.64}$$

where a is the unique point where paths from x, y, and u meet: see figure 2.1. It is obvious that K should be a limit of $G(a, b)$ as b approaches the boundary:

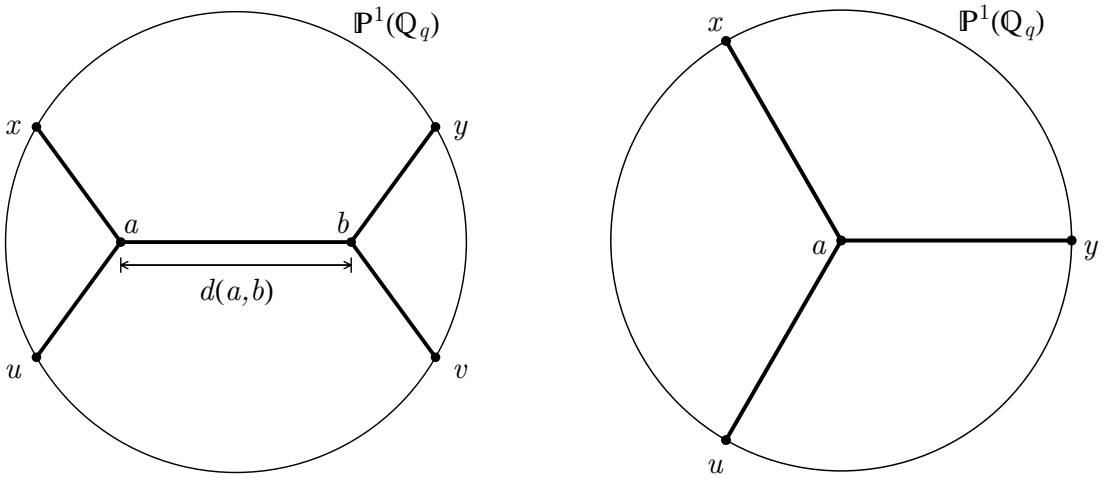

Figure 2.1: Left: The distance $d(a,b)$ between a and b is the number of steps along T_q in the path from a to b. The path from x to y in T_q goes through a and then b; likewise the path from u to v. The intersection of the paths from x to y and from u to v is precisely the path from a to b. Right: Paths on T_q from three boundary points x, y, and u meet at a unique bulk point a.

Explicitly,

$$K(a,y) = 2\nu_p \lim_{v\to y} |y-v|_q^{-\Delta} G(a,b)\,, \tag{2.65}$$

where $G(a,b)$ is written in the form (2.63) and ν_p is some constant. The most straightforward way to obtain the prefactor written in (2.64) is to explicitly compare with (2.47) using $y = 0$, $x \in \mathbb{Q}_q^\times$, and $u \in \mathbb{Q}_q^\times$ with $|u|_q > |x|_q$. Then, using the tall isosceles property of $|\cdot|_q$, we have from (2.65) the relation $K(a,y) = 2\nu_p \frac{\zeta_p(2\Delta)}{p^\Delta}|x|_q^{-\Delta}$, and from (2.47) it is clear that $K(a,y) = \frac{\zeta_p(2\Delta)}{\zeta_p(2\Delta-n)}|x|_q^{-\Delta}$. The prefactor claimed in (2.64) follows immediately.

An alternative derivation of the prefactor in (2.65) proceeds by comparison with the Archimedean case, where in order to derive the relation analogous to (2.65) together with the correct prefactor, the natural starting point is the relation

$$K(z_0,\vec{z};\vec{x}) = \lim_{x_0\to 0} \sqrt{h}\, x_0^{\Delta-} n\cdot\partial G(z_0,\vec{z};x_0,\vec{x})\,, \tag{2.66}$$

where h is the determinant of the induced metric and n is the outward facing normal vector at the boundary $x_0 = 0$. (The relation (2.66) is essentially in the

spirit of the treatment of [76].) Here we are using the short-hand $\Delta_- = n - \Delta_+ = n - \Delta$. Then using Green's second identity

$$\int_{\mathcal{M}} d^{n+1}x\sqrt{g}\left(\phi(\Box + m_\infty^2)\psi - \psi(\Box + m_\infty^2)\phi\right) = -\int_{\partial\mathcal{M}} d^n y\sqrt{h}\left(\phi n\cdot\partial\psi - \psi n\cdot\partial\phi\right) \tag{2.67}$$

with the substitutions $\phi(z_0,\vec{z}) = G(z_0,\vec{z};x_0,\vec{x})$ and $\psi(z_0,\vec{z}) = K(z_0,\vec{z};\vec{x})$, together with the scalings near the boundary

$$z_0\partial_{z_0}G(z_0,\vec{z};x_0,\vec{x}) = \Delta_+ G(z_0,\vec{z};x_0,\vec{x}) \qquad \lim_{z_0\to 0} K(z_0,\vec{z};\vec{x}) = z_0^{\Delta_-}\delta(\vec{z}-\vec{x})\,, \tag{2.68}$$

it follows that

$$K(z_0,\vec{z};\vec{x}) = 2\nu_\infty \lim_{x_0\to 0} x_0^{-\Delta_+} G(z_0,\vec{z};x_0,\vec{x}) \quad \text{where} \quad 2\nu_\infty \equiv \Delta_+ - \Delta_- = 2\Delta - n\,. \tag{2.69}$$

In the p-adics, to derive (2.65) together with the coefficient ν_p, it is more convenient to start instead with the identity

$$\phi_a = \sum_{b\in T_q}\left(\phi_b\left(\Box_b + m_p^2\right)G(a,b) - G(a,b)\left(\Box_b + m_p^2\right)\phi_b\right) \tag{2.70}$$

where $a = (w_0, w)$ and $b = (z_0, z)$ are vertices on T_q, and rewrite ϕ_a on the l.h.s. using

$$\phi_a = \int_{\mathbb{Q}_q} dz\, K(a,z)\phi_0(z) \approx \sum_{z\in S_\mu^\Omega} q^{-\Omega} K(a,z)\phi_0(z)\,, \tag{2.71}$$

where μ and Ω are the infrared and ultraviolet cutoffs, respectively (see the discussion following (2.23)), chosen such that $p^{-\Omega} < |w_0|_p < p^{-\mu}$. With some work, the r.h.s. of (2.70) can be partially integrated, and using the scalings

$$G(a;z_0/p,z)\Big|_{z_0=p^\Omega} = p^{\Delta_+} G(a;z_0,z)\Big|_{z_0=p^\Omega} \qquad \lim_{|z_0|_p\to 0}\phi(z_0,z) = |z_0|_p^{\Delta_-}\phi_0(z)\,, \tag{2.72}$$

we arrive at

$$K(z_0,z;x) = 2\nu_p \lim_{|x_0|_p\to 0} |x_0|_p^{-\Delta_+} G(z_0,z;x_0,x) \tag{2.73}$$

where

$$2\nu_p \equiv p^{\Delta_+} - p^{\Delta_-} = \frac{p^\Delta}{\zeta_p(2\Delta - n)}\,. \tag{2.74}$$

Using (2.74), the final result of taking the limit (2.73) agrees with (2.47) and (2.64).

When computing correlators, it will sometimes be convenient to refer to the unnormalized propagators

$$\begin{aligned} \hat{G}(a,b) &\equiv \left|\frac{(x-u)(y-v)}{(x-y)(u-v)}\right|_q^\Delta = p^{-\Delta d(a,b)} \\ \hat{K}(a,y) &\equiv \left|\frac{x-u}{(x-y)(u-y)}\right|_q^\Delta = \frac{|z_0|_p^\Delta}{|(z_0, z-y)|_s^{2\Delta}}\,, \end{aligned} \tag{2.75}$$

where in the first line the arrangement of a, b, x, y, u, and v are as described around (2.62), and in the second line $a = (z_0, z)$ is the unique point where paths from x, y, and u meet.

2.4 Correlators

Let's start with a naive approach to p-adic AdS/CFT two-point correlator, which misses some overall factors but nevertheless gives us some interesting partial guidance on what to expect. In this naive approach, the two-point function is extracted as the limit of the bulk-to-boundary propagator, where the bulk point is taken to the boundary. Explicitly, starting from (2.47),

$$\begin{aligned} \langle \mathcal{O}(x)\mathcal{O}(y)\rangle_{p,\text{naive}} &= \lim_{x_0\to 0} |x_0|_p^{-\Delta} K(x_0, x; z) = \frac{\zeta_p(2\Delta)}{\zeta_p(2\Delta - n)} \lim_{x_0\to 0} \frac{1}{|(x_0, x-y)|_s^{2\Delta}} \\ &= \frac{\zeta_p(2\Delta)}{\zeta_p(2\Delta - n)} \frac{1}{|x-y|_q^{2\Delta}}\,, \end{aligned} \tag{2.76}$$

where $\lim_{x_0\to 0}$ refers to setting $x_0 = p^\omega$ and sending $\omega \to +\infty$ so that x_0 becomes small in the p-adic norm $|\cdot|_p$. (The same answer could be obtained by starting from (2.64), multiplying by $|x-u|_q^{-\Delta}$, and taking the limit $u \to x$ in the topology

of $\mathbb{Q}_q$.) An equally naive calculation in the Archimedean case starts with (2.51) and works the same way:

$$\langle \mathcal{O}(x)\mathcal{O}(y)\rangle_{\infty,\text{naive}} = \lim_{x_0\to 0} x_0^{-\Delta} K(x_0,\vec{x};\vec{y}) = \frac{\zeta_\infty(2\Delta)}{\zeta_\infty(2\Delta-n)}\frac{1}{|\vec{x}-\vec{y}|^{2\Delta}}\,. \tag{2.77}$$

We can add a bit of formal polish in the unextended case $n = 1$ by noting that if x and y are rational, then we can define

$$\langle \mathcal{O}(x)\mathcal{O}(y)\rangle_{v,\text{naive}} = \frac{\zeta_v(2\Delta)}{\zeta_v(2\Delta-1)}\frac{1}{|x-y|_v^{2\Delta}} \tag{2.78}$$

equally for $v = p$ and $v = \infty$, where $|\cdot|_\infty$ is the ordinary absolute value. We are led to the adelic relation

$$\langle \mathcal{O}(x)\mathcal{O}(y)\rangle_{\mathbb{A},\text{naive}} \equiv \prod_v \langle \mathcal{O}(x)\mathcal{O}(y)\rangle_{v,\text{naive}} = \frac{\zeta_{\mathbb{A}}(2\Delta)}{\zeta_{\mathbb{A}}(2\Delta-1)} \qquad \text{for unequal } x, y \in \mathbb{Q}\,, \tag{2.79}$$

where the product is over all primes as well as ∞, and we used the key relation

$$\prod_v |\xi|_v = 1 \qquad \text{for } \xi \in \mathbb{Q}\,. \tag{2.80}$$

We have also introduced the adelic zeta function,

$$\zeta_{\mathbb{A}}(s) \equiv \prod_v \zeta_v(s) = \pi^{-s/2}\Gamma_{\text{Euler}}(s/2)\,\zeta(s)\,, \tag{2.81}$$

where $\zeta(s) = \sum_{n=1}^{\infty}\frac{1}{n^s}$ is the ordinary Riemann zeta function. The adelic zeta function obeys the simple functional relation $\zeta_{\mathbb{A}}(s) = \zeta_{\mathbb{A}}(1-s)$, and its non-trivial zeros are the same as the non-trivial zeros of $\zeta(s)$, i.e. a discrete sequence at $\operatorname{Re} s = 1/2$ according to the Riemann Hypothesis.

The above treatment of the two-point correlator is wrong (or, at least, against the usual spirit of AdS/CFT) because it leaves the on-shell action entirely out of the story. We tackle the two-point function more in the next section.

2.4.1 Two-point function

As a warmup to p-adic calculations, let's review the standard account for Archimedean AdS_{n+1}, using Fourier space since it's easier to sort out prefactors reliably in Fourier space than in position space. The on-shell scalar configuration we are interested in is

$$\phi(z_0, \vec{z}) = \lambda_1 \mathrm{e}^{2\pi i \vec{k}_1 \cdot \vec{z}} K_\epsilon(z_0, \vec{k}_1) + \lambda_2 \mathrm{e}^{2\pi i \vec{k}_2 \cdot \vec{z}} K_\epsilon(z_0, \vec{k}_2)\,. \tag{2.82}$$

We have defined

$$K_\epsilon(z_0, \vec{k}) \equiv \frac{K(z_0, \vec{k})}{K(\epsilon, \vec{k})} = \frac{z_0^{n-\Delta} + \zeta_R k^{2\Delta - n} z_0^\Delta}{\epsilon^{n-\Delta} + \zeta_R k^{2\Delta-n}\epsilon^\Delta} + \dots \quad \text{where} \quad \zeta_R \equiv \frac{\zeta_\infty(-2\Delta + n)}{\zeta_\infty(2\Delta - n)}\,. \tag{2.83}$$

The notation $+\dots$ in the third expression of (2.83) reminds us that we have dropped terms which are subleading to the ones shown in both the numerator and the denominator by positive even powers of kz_0 or $k\epsilon$. The point of (2.83) is that we have arranged to have $\phi(\epsilon, \vec{z}) = \lambda_1 \mathrm{e}^{2\pi i \vec{k}_1 \cdot \vec{z}} + \lambda_2 \mathrm{e}^{2\pi i \vec{k}_2 \cdot \vec{z}}$, which we use as source for a regulated version of the operator of interest, call it $\mathcal{O}_\epsilon$. Then the prescription we will use for Green's functions is

$$-\log \left\langle \exp\left\{ \int_{\mathbb{R}^n} d^n z\, \phi_\epsilon(\vec{z}) \mathcal{O}_\epsilon(\vec{z}) \right\} \right\rangle_\infty = \underset{\phi(\epsilon,\vec{z}) = \phi_\epsilon(\vec{z})}{\text{extremum}} S_\epsilon[\phi]\,, \tag{2.84}$$

where

$$S_\epsilon[\phi] = \eta_\infty \int_{z_0 > \epsilon} d^{n+1} z \, \sqrt{\det g_{\mu\nu}} \left[\frac{1}{2} g^{\mu\nu} \partial_\mu \phi \partial_\nu \phi + \frac{1}{2} m_\infty^2 \phi^2 \right]\,, \tag{2.85}$$

and the AdS_{n+1} metric is $ds^2 = g_{\mu\nu} dz^\mu dz^\nu = \frac{L^2}{z_0^2}\left(dz_0^2 + d\vec{z}^2\right)$. The prefactor η_∞ is related to the gravitational coupling in string theory realizations of AdS/CFT. In order to make it easy to compute the extremum, we add to the action a multiple

of the equation of motion:

$$\begin{aligned} S_{\text{on-shell}} &= \eta_\infty \int_{z_0>\epsilon} d^{n+1}z\,\sqrt{\det g_{\mu\nu}}\left[\frac{1}{2}g^{\mu\nu}\partial_\mu\phi\partial_\nu\phi+\frac{1}{2}m_\infty^2\phi^2-\frac{1}{2}\phi(\Box+m_\infty^2)\phi\right] \\ &= -\frac{\eta_\infty}{4}\int_{z_0>\epsilon} d^{n+1}z\,\sqrt{\det g_{\mu\nu}}\,\Box\,\phi^2 \\ &= -\frac{\eta_\infty}{4}\left(\frac{L}{\epsilon}\right)^{n-1}\int_{z_0=\epsilon} d^n z\,\partial_{z^0}\phi^2\,, \end{aligned} \tag{2.86}$$

where $\Box = -\frac{1}{\sqrt{g}}\partial_\mu\sqrt{g}g^{\mu\nu}\partial_\nu$. In order to extract the desired two-point function, we compute

$$\begin{aligned} \langle\mathcal{O}_\epsilon(\vec{k}_1)\mathcal{O}_\epsilon(\vec{k}_2)\rangle_\infty &= -\left.\frac{\partial^2 S_{\text{on-shell}}}{\partial\lambda_1\partial\lambda_2}\right|_{\lambda_1=\lambda_2=0} \\ &= \frac{\eta_\infty}{2}\left(\frac{L}{\epsilon}\right)^{n-1}\left(\int_{\mathbb{R}^n} d^n z\,\mathrm{e}^{2\pi i(\vec{k}_1+\vec{k}_2)\cdot\vec{z}}\right)\Big[\partial_{z_0}\Big(K_\epsilon(z_0,\vec{k}_1)K_\epsilon(z_0,\vec{k}_2)\Big)\Big]_{z_0=\epsilon} \\ &= \eta_\infty\frac{L^{n-1}}{\epsilon^n}\delta(\vec{k}_1+\vec{k}_2)\left[-\Delta+n+(2\Delta-n)(k_1\epsilon)^{2\Delta-n}\zeta_R+\ldots\right]. \end{aligned} \tag{2.87}$$

We discard the k_1-independent term from inside square brackets in the last expression of (2.87) on grounds that its Fourier transform is a pure contact term in position space. The terms we have omitted by writing $\ldots$ inside square brackets are suppressed by positive integer powers of $(k_1\epsilon)^{2\Delta-n}$ relative to the last term shown, so for small ϵ and fixed k_1 we may discard them too. (We are ignoring the possibility of alternative quantization.) Thus, if we ignore contact terms and also drop terms subleading in ϵ, we find

$$\begin{aligned} \langle\mathcal{O}_\epsilon(\vec{x}_1)\mathcal{O}_\epsilon(\vec{x}_2)\rangle_\infty &= \int_{\mathbb{R}^n} d^n k_1 d^n k_2\,\mathrm{e}^{2\pi i(\vec{k}_1\cdot\vec{x}_1+\vec{k}_2\cdot\vec{x}_2)}\langle\mathcal{O}_\epsilon(\vec{k}_1)\mathcal{O}_\epsilon(\vec{k}_2)\rangle_\infty \\ &= \eta_\infty L^{n-1}\epsilon^{2(\Delta-n)}(2\Delta-n)\zeta_R\int_{\mathbb{R}^n} d^n k_1\,\mathrm{e}^{2\pi i\vec{k}_1\cdot\vec{x}_{12}}k_1^{2\Delta-n} \\ &= \eta_\infty L^{n-1}\epsilon^{2(\Delta-n)}(2\Delta-n)\frac{\zeta_\infty(2\Delta)}{\zeta_\infty(2\Delta-n)}\frac{1}{|\vec{x}_{12}|^{2\Delta}}\,, \end{aligned} \tag{2.88}$$

where we have set $\vec{x}_{12}=\vec{x}_1-\vec{x}_2$. In the last equality of (2.88) we started with (2.51) and (2.56) and expanded at small z_0 to obtain

$$\zeta_R\int_{\mathbb{R}^n} d^n k\,\mathrm{e}^{2\pi i\vec{k}\cdot\vec{x}}k^{2\Delta-n} = \frac{\zeta_\infty(2\Delta)}{\zeta_\infty(2\Delta-n)}\frac{1}{|\vec{x}|^{2\Delta}}\,. \tag{2.89}$$

Note that the precise value of ζ_R doesn't matter, since it enters the holographic calculation (2.87) from the Fourier-space bulk-to-boundary propagator, and from precisely the same propagator we can extract (2.89). The overall normalization of this propagator *does* enter, and it leads to the $\zeta_\infty(2\Delta)/\,\zeta_\infty(2\Delta-n)$ factor in the last expression of (2.88). The factor $2\nu_\infty = 2\Delta - n$ arises when passing from the second line of (2.87) to the third line: That is, it is related to evaluating the z_0 derivative of ϕ^2 at $z_0 = \epsilon$. This is similar to the way the normal derivative in (2.66) leads to a factor of $2\nu_\infty$ in (2.69). We will therefore refer to $2\Delta - n$ as a boundary factor. To obtain the final form of the two-point function, we note that $K(\epsilon, \vec{k}) \approx \epsilon^{n-\Delta}$ for small ϵ. Thus the solution $\phi(z_0, \vec{z})$ in (2.82) contains an extra factor of $\epsilon^{\Delta-n}$, which can be regarded as a leg factor for defining a truly local operator:

$$\mathcal{O}(\vec{x}) = \lim_{\epsilon\to 0} \epsilon^{n-\Delta}\mathcal{O}_\epsilon(\vec{x})\,. \tag{2.90}$$

Using (2.90), we obtain the final answer

$$\langle \mathcal{O}(\vec{x}_1)\mathcal{O}(\vec{x}_2)\rangle_\infty = \eta_\infty L^{n-1}(2\Delta-n)\frac{\zeta_\infty(2\Delta)}{\zeta_\infty(2\Delta-n)}\frac{1}{|\vec{x}_{12}|^{2\Delta}}\,. \tag{2.91}$$

This expression is valid only up to contact terms. The more general expression for fully local correlators is

$$-\log\left\langle \exp\left\{\int_{\mathbb{R}^n} d^n z\,\phi_0(\vec{z})\mathcal{O}(\vec{z})\right\}\right\rangle_\infty = \operatorname*{extremum}_{\phi\to\phi_0} S[\phi] \tag{2.92}$$

where by $\phi \to \phi_0$ we mean

$$\lim_{z_0\to 0} z_0^{\Delta-n}\phi(z_0,\vec{z}) = \phi_0(\vec{z})\,, \tag{2.93}$$

and $S[\phi]$ is the same as $S_\epsilon[\phi]$ in (2.85) but integrated over all of AdS_{n+1}.

Now let's consider the analogous computation on the Bruhat–Tits tree, using the action (2.19). Only the quadratic terms are of interest to us since, for now, we only want the two-point function and are not concerned with loop corrections.

The on-shell scalar configuration of interest is

$$\phi(z_0, z) = \lambda_1 \chi(k_1 z) K_\epsilon(z_0, k_1) + \lambda_2 \chi(k_2 z) K_\epsilon(z_0, k_2)\,. \tag{2.94}$$

We have defined

$$K_\epsilon(z_0, k) \equiv \frac{|z_0|_p^{n-\Delta} + \zeta_R |k|_q^{2\Delta - n} |z_0|_p^\Delta}{|\epsilon|_p^{n-\Delta} + \zeta_R |k|_q^{2\Delta - n} |\epsilon|_p^\Delta} \gamma_q(k z_0) \tag{2.95}$$

where now

$$\zeta_R \equiv \frac{\zeta_p(-2\Delta + n)}{\zeta_p(2\Delta - n)} = -p^{-2\Delta + n}\,. \tag{2.96}$$

Note that we cannot quite follow (2.83) because $K(z_0, k)/K(\epsilon, k)$ is ill-defined for $|\epsilon k|_q > 1$. In practice, we aim to keep momenta fixed while we take a limit $\epsilon \to 0$ (in the p-adic sense), so we will never encounter a situation where $|\epsilon k|_q > 1$. As compared to (2.83), it is notable that in (2.95) we are not discarding any subleading terms at all. This makes the structure of contact terms simpler. Note that $\phi(\epsilon, z) = \lambda_1 \chi(k_1 z) + \lambda_2 \chi(k_2 z)$ (on the assumption $|\epsilon k|_q \leq 1$), so the obvious adaptation of (2.84) is

$$-\log \left\langle \exp\left\{ \int_{\mathbb{Q}_q} dz\, \phi_\epsilon(z) \mathcal{O}_\epsilon(z) \right\} \right\rangle_p = \underset{\phi(\epsilon, z) = \phi_\epsilon(z)}{\text{extremum}} S_\epsilon[\phi] \tag{2.97}$$

where

$$S_\epsilon[\phi] = \eta_p \sum_{|\epsilon|_p < |a_0|_p} \left[\frac{1}{4} \sum_{\substack{\langle ab \rangle \\ a \text{ fixed}}} (\phi_a - \phi_b)^2 + \frac{1}{2} m_p^2 \phi_a^2 \right], \tag{2.98}$$

where in a slight abuse of notation we use a_0 to mean the value of the depth coordinate z_0 at the point $a \in T_q$. The reader should be forewarned that the cutoff procedure has an $O(1)$ impact on the normalization of the two-point function. We are following what seems like the most sensible approach in (2.98) of first writing the sum $\sum_{\langle ab \rangle}$ over edges as a sum over vertices with an inner sum over the edges coming off of each vertex, and then restricting only the outer sum over vertices. We have chosen to restrict the sum to points a with $|\epsilon|_p < |a_0|_p$; later we

will consider what happens if we say instead $|\epsilon|_p \leq |a_0|_p$. It would be interesting to explore more systematically the full range of possible cutoffs for the sum.

The next step is to reduce the sum (2.98) to a boundary term. Toward this end, we note

$$\frac{1}{4} \sum_{\substack{\langle ab \rangle \\ a \text{ fixed}}} (\phi_a - \phi_b)^2 + \frac{1}{2} m_p^2 \phi_a^2 - \frac{1}{2} \phi_a (\Box + m_p^2) \phi_a = -\frac{1}{4} \Box \phi_a^2 \,. \tag{2.99}$$

Thus, by adding a multiple of the equation of motion to the action (2.98), we obtain

$$S_{\text{on-shell}} = -\frac{\eta_p}{4} \sum_{\substack{|\epsilon|_p < |a_0|_p \leq |M|_p \\ \text{restricted}}} \Box \phi_a^2 \,, \tag{2.100}$$

where we have imposed an infrared cutoff by restricting the sum to run over only those points in the subtree rooted at $p^{v_q(M)}$. To simplify notation, it helps to consistently set

$$z_0 = p^\omega \qquad M = p^\mu \qquad \epsilon = p^\Omega \,, \tag{2.101}$$

with μ large and negative while Ω is large and positive. Denoting a point $a \in T_q$ by $a = (z_0, z)$, we can enumerate the points in the sum (2.100) first by letting ω run over the integers in $[\mu, \Omega)$ and then, for each fixed ω, letting z run over S_μ^ω. Next we need to have an explicit way of labeling the points b which are the nearest neighbors of a. Writing

$$z = \sum_{m=\mu}^{\omega-1} \kappa_m p^m \in S_\mu^\omega \qquad \text{where each } \kappa_m \in \mathbb{F}_q \,, \tag{2.102}$$

we see that

$$z \to [z]_{\omega-1} \equiv \sum_{m=\mu}^{\omega-2} \kappa_m p^m \tag{2.103}$$

is a q-to-1 map from S_μ^ω to $S_\mu^{\omega-1}$ provided $\omega > \mu$, and if $\omega \leq \mu$ it is the trivial 1-to-1 map—since in this latter case $S_\mu^\omega = S_\mu^{\omega-1} = \{0\}$. Note that for $\mathbb{Q}_p$, $[z]_0$ is just the fractional part of z. The map $(z_0, z) \to (z_0/p, [z]_{\omega-1})$ takes a point (z_0, z)

to its nearest neighbor in the downward direction (i.e. the nearest neighbor one step closer to ∞). We can also define q 1-to-1 maps from S_μ^ω to $S_\mu^{\omega+1}$ as follows:

$$z \to z + p^\omega \kappa \tag{2.104}$$

where $\kappa \in \mathbb{F}_q$. Then the maps $(z_0, z) \to (pz_0, z + p^\omega\kappa)$ take a point (z_0, z) to its nearest neighbors in the upward direction. Now we can rewrite (2.100) as

$$\begin{aligned} S_{\text{on-shell}} &= -\frac{\eta_p}{4} \sum_{\omega=\mu}^{\Omega-1} \sum_{z\in S_\mu^\omega} \left[(q+1)\phi(p^\omega, z)^2 - \phi(p^{\omega-1}, [z]_{\omega-1})^2 - \sum_{\kappa\in\mathbb{F}_q} \phi(p^{\omega+1}, z + p^\omega\kappa)^2 \right] \\ &= -\frac{\eta_p}{4} \left[\sum_{\omega=\mu}^{\Omega-1} \sum_{z\in S_\mu^\omega} (q+1)\phi(p^\omega, z)^2 - \sum_{\omega=\mu}^{\Omega-2} \sum_{z\in S_\mu^\omega} q\phi(p^\omega, z)^2 - \phi(p^{\mu-1}, 0)^2 \right. \\ &\qquad \left. - \sum_{\omega=\mu+1}^{\Omega} \sum_{z\in S_\mu^\omega} \phi(p^\omega, z)^2 \right] \\ &= -\frac{\eta_p}{4} \left[\sum_{z\in S_\mu^{\Omega-1}} q\phi(p^{\Omega-1}, z)^2 - \sum_{z\in S_\mu^\Omega} \phi(p^\Omega, z)^2 + \phi(p^\mu, 0)^2 - \phi(p^{\mu-1}, 0)^2 \right] . \end{aligned} \tag{2.105}$$

Because the Fourier space propagator vanishes identically for sufficiently large $|kz_0|_q$, we can drop the last two terms in square brackets in the last line of (2.105). The resulting expression is the discrete version of the last line of (2.86).

We now compute the two-point function as

$$\begin{aligned} \langle \mathcal{O}_\epsilon(k_1)\mathcal{O}_\epsilon(k_2)\rangle_p &= -\frac{\partial^2 S_{\text{on-shell}}}{\partial\lambda_1\partial\lambda_2} \\ &= \frac{\eta_p}{2} \left(q \sum_{z\in S_\mu^{\Omega-1}} \chi((k_1+k_2)z) \right) \\ &\qquad \times \left[p^{2n-2\Delta} \frac{1 + \zeta_R p^{2\Delta-n} |k_1\epsilon|_q^{2\Delta-n}}{1 + \zeta_R |k_1\epsilon|_q^{2\Delta-n}} \frac{1 + \zeta_R p^{2\Delta-n} |k_2\epsilon|_q^{2\Delta-n}}{1 + \zeta_R |k_2\epsilon|_q^{2\Delta-n}} \right] \\ &\quad - \frac{\eta_p}{2} \left(\sum_{z\in S_\mu^\Omega} \chi((k_1+k_2)z) \right) . \end{aligned} \tag{2.106}$$

To obtain (2.106) we have assumed that $|k_i\epsilon|_q \leq 1/p$ for $i = 1, 2$. Now we use (2.23) to obtain

$$q \sum_{z \in S_\mu^{\Omega-1}} \chi((k_1+k_2)z) \approx \sum_{z \in S_\mu^{\Omega}} \chi((k_1+k_2)z) \approx q^\Omega \int_{\mathbb{Q}_q} dz\, \chi((k_1+k_2)z) = q^\Omega \delta(k_1+k_2), \tag{2.107}$$

where the approximate equalities become exact in the limit where the cutoffs are removed. Of course, we mean (2.107) in the sense that if we integrate either of the discrete sums with respect to k_1 against a continuous test function $\tilde{f}(k_1)$ with bounded support, the result is $\tilde{f}(-k_2)$. Simplifying also the quantity in square brackets in (2.106) by expanding through first order in $|\epsilon|_q^{2\Delta-n}$ (where we assume $\Delta > n/2$), we obtain

$$\langle \mathcal{O}_\epsilon(k_1)\mathcal{O}_\epsilon(k_2)\rangle_p = \frac{\eta_p}{|\epsilon|_p^n}\delta(k_1+k_2)\left[-\frac{1}{2\,\zeta_p(2\Delta-2n)} + \frac{p^n\zeta_R}{\zeta_p(2\Delta-n)}|k_1\epsilon|_q^{2\Delta-n} + \ldots\right]. \tag{2.108}$$

The omitted terms, indicated as …, are suppressed by positive integer powers of $|k_1\epsilon|_q^{2\Delta-n}$ relative to the last term shown. To return from Fourier space to position space, we start by inverting the Fourier transform (2.59) and then take $z_0 \to 0$ (p-adically) to obtain

$$\zeta_R \int_{\mathbb{Q}_q} dk\, \chi(kx)|k|_q^{2\Delta-n} = \frac{\zeta_p(2\Delta)}{\zeta_p(2\Delta-n)}\frac{1}{|x|_q^{2\Delta}}\,, \tag{2.109}$$

up to a divergent term proportional to $\delta(x)$. Thus (for separated points) we find

$$\langle \mathcal{O}_\epsilon(x_1)\mathcal{O}_\epsilon(x_2)\rangle_p = \eta_p|\epsilon|_p^{2\Delta-2n}\frac{p^n\,\zeta_p(2\Delta)}{\zeta_p(2\Delta-n)^2}\frac{1}{|x_{12}|^{2\Delta}}\,. \tag{2.110}$$

Because $K(\epsilon, k) \approx |\epsilon|_p^{n-\Delta}$ for small ϵ, we introduce a leg factor in the p-adic case,

$$\mathcal{O}(x) = \lim_{\epsilon\to 0}|\epsilon|_p^{n-\Delta}\mathcal{O}_\epsilon(x)\,, \tag{2.111}$$

and correspondingly the two-point function for the local operator $\mathcal{O}(x)$ is

$$\langle \mathcal{O}(x_1)\mathcal{O}(x_2)\rangle_{p,\text{exclusive}} = \eta_p\frac{p^n\,\zeta_p(2\Delta)}{\zeta_p(2\Delta-n)^2}\frac{1}{|x_{12}|^{2\Delta}}\,, \tag{2.112}$$

up to contact terms. We use the notation "p, exclusive" in (2.112) as a reminder that we employed a specific cutoff procedure, namely to restrict $|\epsilon|_p < |a_0|_p$ in the outer sum of (2.98), which excludes the points right at the boundary $|\epsilon|_p = |a_0|_p$. Carrying through the whole computation with the restriction $|\epsilon|_p \leq |a_0|_p$ which includes these boundary points, we obtain instead

$$\langle \mathcal{O}(x_1)\mathcal{O}(x_2)\rangle_{p,\text{inclusive}} = p^{2\Delta-2n}\langle \mathcal{O}(x_1)\mathcal{O}(x_2)\rangle_{p,\text{exclusive}}\,. \tag{2.113}$$

We see no reason to prefer the condition $|\epsilon|_p \leq |a_0|_p$ over $|\epsilon|_p < |a_0|_p$, or vice versa. We therefore take the democratic approach of taking the geometric mean of (2.112) and (2.113) to get our final result:

$$\langle \mathcal{O}(x_1)\mathcal{O}(x_2)\rangle_p = \eta_p \frac{p^\Delta\,\zeta_p(2\Delta)}{\zeta_p(2\Delta-n)^2}\frac{1}{|x_{12}|^{2\Delta}}\,, \tag{2.114}$$

again up to contact terms. We will comment further on the prefactor in (2.114) in section 2.6.

2.4.2 Contact diagrams and higher-point correlators

A crucial ingredient in higher-point correlation functions is contact diagrams, which in the Archimedean place are diagrammatic representations of amplitudes

$$\begin{aligned} A_\infty(\vec{x}_1,\vec{x}_2,\vec{x}_3) &\equiv \int \frac{d^{n+1}y}{y_0^{n+1}}\prod_{i=1}^{3}\hat{K}(y_0,\vec{y}-\vec{x}_i) \\ &= \frac{\zeta_\infty(\Delta)^3\,\zeta_\infty(3\Delta-n)}{2\,\zeta_\infty(2\Delta)^3}\frac{1}{|\vec{x}_{12}|^\Delta|\vec{x}_{23}|^\Delta|\vec{x}_{13}|^\Delta} \end{aligned} \tag{2.115}$$

for three-point functions, and

$$D_\infty(\vec{x}_1,\vec{x}_2,\vec{x}_3,\vec{x}_4) \equiv \int \frac{d^{n+1}y}{y_0^{n+1}}\prod_{i=1}^{4}\hat{K}(y_0,\vec{y}-\vec{x}_i) \tag{2.116}$$

for four-point functions. We would like to consider the analogous p-adic amplitudes. We will consider the exchange diagram for four-point functions in chapter 3.

For the three-point function, the first observation is that three non-coincident points x_1, x_2, and x_3 in $\mathbb{P}^1(\mathbb{Q}_q)$ determine a unique point $c \in T_q$ as the point where paths from x_1, x_2, and x_3 meet. We may therefore express

$$A_p(x_1, x_2, x_3) \equiv \sum_{a \in T_q} \prod_{i=1}^{3} \hat{K}(a, x_i) = \left[\prod_{i=1}^{3} \hat{K}(c, x_i) \right] \sum_{a \in T_q} \hat{G}(c, b) \hat{G}(b, a)^3 \,, \quad (2.117)$$

where in every term of the sum, b is the point where a path from a to c first joins one of the paths from the x_i to c: see the so-called subway diagram, figure 2.2a. To demonstrate the second equality in (2.117), let the path (with no backtracking) in $T_q \sqcup \partial T_q$ from x to y be denoted $(x : y)$. Consider a path to be a collection of edges. Then for every $a \in T_q$, we have

$$\bigsqcup_{i=1}^{3} (x_i : a) = \bigsqcup_{i=1}^{3} (x_i : c) \sqcup (b : c) \sqcup 3(a : b) \,. \quad (2.118)$$

Here we are using $\sqcup$ to form a union in which the multiplicity of each element is counted. For example, if an edge e is in A with multiplicity 2 and B with multiplicity 1, it is in $A \sqcup B$ with multiplicity 3. Of course, $3(a : b)$ means $(a : b) \sqcup (a : b) \sqcup (a : b)$. Noting that each edge leads to a factor of $p^{-\Delta}$, we arrive at (2.117). Figure 2.2a illustrates how this works for a particular point $a \in T_q$. Using (2.75), we see that

$$\hat{K}(c, x_1) = \left| \frac{x_{23}}{x_{12} x_{13}} \right|_q^{\Delta} \,, \quad (2.119)$$

with similar expressions for $\hat{K}(c, x_2)$ and $\hat{K}(c, x_3)$. Thus, straightforwardly we find

$$\prod_{i=1}^{3} \hat{K}(c, x_i) = \frac{1}{|x_{12} x_{23} x_{13}|_q^{\Delta}} \,. \quad (2.120)$$

We will refer to the union of the three paths (x_i, c) as the main tree, and then b can be thought of as the projection of a onto the main tree.

In order to work out the sum in (2.117), we denote

$$\ell = d(a, b) \qquad\qquad m = d(b, c) \,. \quad (2.121)$$

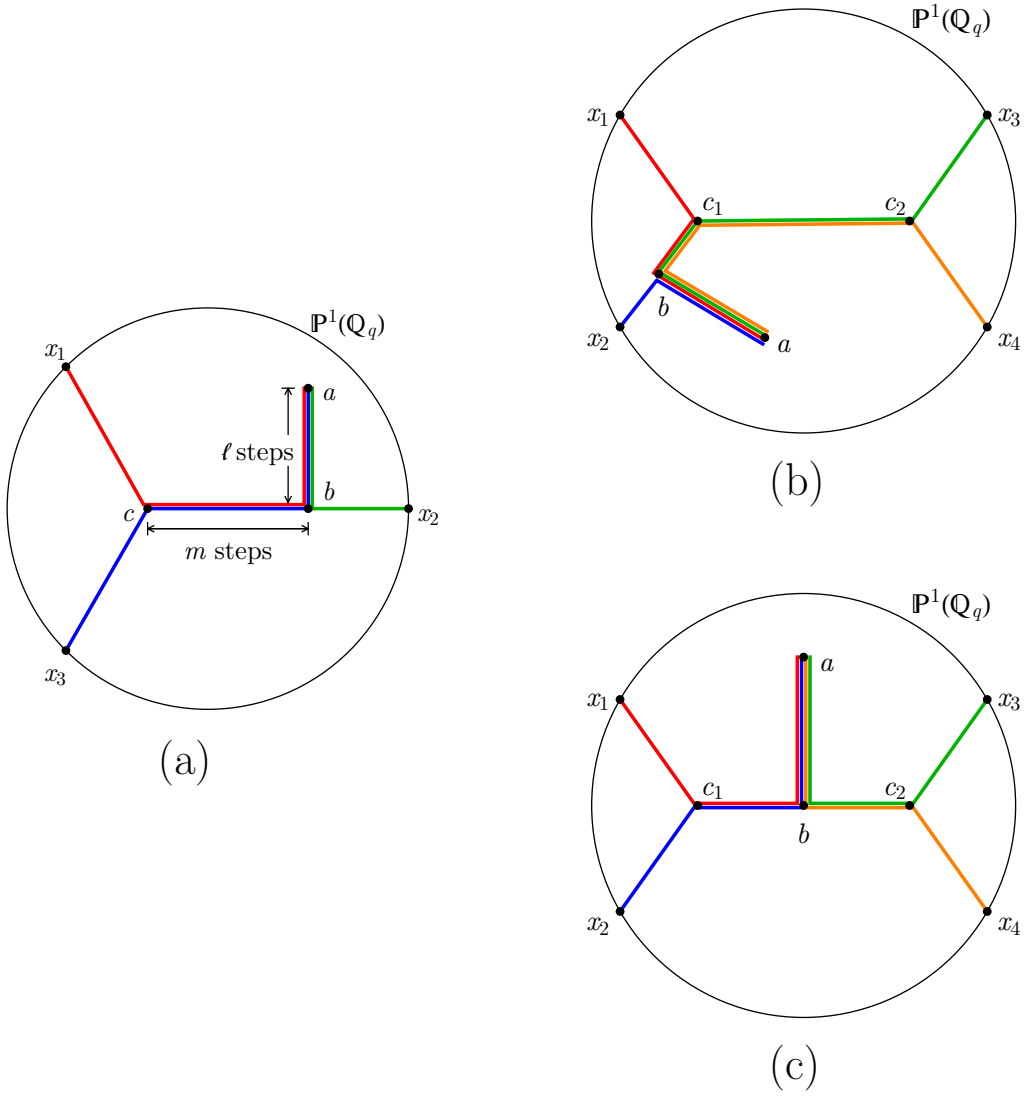

Figure 2.2: Subway diagrams, indicating disjoint unions of paths on $T_q \sqcup \partial T_q$. (a) Paths from x_1, x_2, and x_3 meet at the bulk point $c \in T_q$ and comprise what we refer to as the main tree. The product $\prod_{i=1}^{3} \hat{K}(a, x_i)$ relates to paths from the x_i which all go to the point a after first passing through the point b, which is the projection of a onto the main tree. (b) and (c): Paths from x_1 and x_2 to x_3 and x_4 overlap between c_1 and c_2. There are two classes of subway diagrams contributing to the four-point amplitude, depending on whether the projection b of a onto the main trunk falls between c_1 and c_2 or on a leg between some x_i and the appropriate c_j.

Then if $m = 0$, meaning that b and c coincide, there is one point with $\ell = 0$ (namely $a = c$), and there are $(p^n - 2)p^{n(\ell-1)}$ points a at a fixed distance $\ell > 0$ from c whose projection onto the main tree is c. On the other hand, if $m > 0$, then there are three possible choices for b. Once the choice of b is made, there is a single point with $\ell = 0$ (namely $a = b$), and there are $(p^n - 1)p^{n(\ell-1)}$ points a at a fixed distance $\ell > 0$ from b whose projection onto the main tree is b. Therefore

$$\begin{aligned}\sum_{a\in T_q} \hat{G}(c,b)\hat{G}(b,a)^3 &= 3\sum_{m=1}^{\infty} p^{-\Delta m}\left[1+\sum_{\ell=1}^{\infty}(q-1)q^{\ell-1}\left(p^{-\Delta\ell}\right)^3\right] \\ &\quad + \left[1+\sum_{\ell=1}^{\infty}(q-2)q^{\ell-1}\left(p^{-\Delta l}\right)^3\right] \\ &= \frac{\zeta_p(\Delta)^3\,\zeta_p(3\Delta-n)}{\zeta_p(2\Delta)^3}\,,\end{aligned} \tag{2.122}$$

where for convergence we must require $\Delta > n/3$, which is certainly true since we choose the root $\Delta = \Delta_+ > n/2$. To summarize,

$$A_p(x_1,x_2,x_3) = \frac{\zeta_p(\Delta)^3\,\zeta_p(3\Delta-n)}{\zeta_p(2\Delta)^3}\frac{1}{|x_{12}x_{23}x_{13}|_q^{\Delta}}\,. \tag{2.123}$$

With the three-point amplitude (2.123) in hand, we can give an account of three-point correlators of the operator $\mathcal{O}$ dual to ϕ. By the same arguments as used in the real case [76, 77], one finds

$$\langle \mathcal{O}(x_1)\mathcal{O}(x_2)\mathcal{O}(x_3)\rangle_p = -\eta_p g_3 \frac{\zeta_p(2\Delta)^3}{\zeta_p(2\Delta-n)^3} A_p(x_1,x_2,x_3)\,. \tag{2.124}$$

To study the four point amplitude

$$D_p(x_1,x_2,x_3,x_4) = \sum_{a\in T_q}\prod_{i=1}^{4}\hat{K}(a,x_i)\,, \tag{2.125}$$

let us first stipulate that $|(x_{12}x_{34})/(x_{13}x_{24})|_q < 1$, so that the paths among the x_i on T_q have the topology shown in figures 2.2b and 2.2c: The paths from x_1 and x_2 meet at c_1; the paths from x_3 and x_4 meet at c_2; and the separation of the bulk points c_1 and c_2 is

$$d(c_1,c_2) = -\log_p\left|\frac{x_{12}x_{34}}{x_{13}x_{24}}\right|_q = -\log_p\left|\frac{x_{12}x_{34}}{x_{14}x_{23}}\right|_q\,, \tag{2.126}$$

where $\log_p$ is the base p logarithm. (Note that the middle expression in (2.126) is also the valuation of $(x_{12}x_{34})/(x_{13}x_{24})$.) Just as in (2.117), we may decompose the amplitude into the product of an x_i–dependent part based on the main tree $(x_1 : c_1) \sqcup (x_2 : c_1) \sqcup 2(c_1 : c_2) \sqcup (x_3 : c_2) \sqcup (x_4 : c_2)$ times a prefactor expressed as a sum over T_q:

$$D_p(x_1, x_2, x_3, x_4) = \left[\hat{K}(c_1, x_1)\hat{K}(c_1, x_2)\hat{K}(c_2, x_3)\hat{K}(c_2, x_4)\hat{G}(c_1, c_2)^2\right] \hat{D}_p \quad (2.127)$$

where

$$\begin{aligned}\hat{D}_p &= 4\sum_{m=1}^{\infty} p^{-2\Delta m}\left[1 + \sum_{\ell=1}^{\infty}(q-1)q^{\ell-1}(p^{-\Delta\ell})^4\right] \\ &\quad + (d(c_1, c_2) - 1)\left[1 + \sum_{\ell=1}^{\infty}(q-1)q^{\ell-1}(p^{-\Delta\ell})^4\right] \\ &\quad + 2\left[1 + \sum_{\ell=1}^{\infty}(q-2)q^{\ell-1}(p^{-\Delta\ell})^4\right] \\ &= \left[-\frac{1}{\zeta_p(4\Delta)}\log_p\left|\frac{x_{12}x_{34}}{x_{13}x_{24}}\right|_q + \left(\frac{\zeta_p(2\Delta)}{\zeta_p(4\Delta)} + 1\right)^2 - 3\right]\zeta_p(4\Delta - n)\,,\end{aligned} \quad (2.128)$$

and we need $\Delta > n/4$ for convergence, which is always the case for $\Delta = \Delta_+$. The first line of (2.128) comes from configurations where b is on one of the legs $(x_i : c_j)$ of the main trunk, as in figure 2.2b. The second line of (2.128) comes from configurations where b is on the connecting leg $(c_1 : c_2)$, as in figure 2.2c. The third line comes from configurations where $b = c_1$ or $b = c_2$. To simplify the factor in square brackets in (2.127), we use relations

$$\hat{K}(c_1, x_1) = \left|\frac{x_{23}}{x_{12}x_{13}}\right|_q^{\Delta} = \left|\frac{x_{24}}{x_{12}x_{14}}\right|_q^{\Delta} \qquad \hat{G}(c_1, c_2) = \left|\frac{x_{12}x_{34}}{x_{13}x_{24}}\right|_q^{\Delta} = \left|\frac{x_{12}x_{34}}{x_{14}x_{23}}\right|_q^{\Delta}. \quad (2.129)$$

There are similar relations for the other factors of $\hat{K}$ in (2.127). Combining them, we find

$$D_p(x_1, x_2, x_3, x_4) = \left[-\frac{1}{\zeta_p(4\Delta)}\log_p\left|\frac{x_{12}x_{34}}{x_{13}x_{24}}\right|_q + \left(\frac{\zeta_p(2\Delta)}{\zeta_p(4\Delta)} + 1\right)^2 - 3\right]\frac{\zeta_p(4\Delta - n)}{|x_{13}x_{24}|_q^{2\Delta}}\,. \quad (2.130)$$

We derived (2.130) on the assumption $|(x_{12}x_{34})/(x_{13}x_{24})|_q < 1$. If instead it were $|(x_{12}x_{34})/(x_{13}x_{24})|_q = 1$, then all four paths from the x_i meet at a common vertex c, and by an explicit calculation similar to (2.122), it is straightforward to check that (2.130) still holds as written. (Of course, the $\log_p$ term vanishes identically.) Amusingly, this degeneration is impossible for $q = 2$. By relabeling the x_i if necessary, we can always reach a situation where $|(x_{12}x_{34})/(x_{13}x_{24})|_q \leq 1$, so (2.130) is in fact a general result. Note that it is also an exact result, which shows that D_p is considerably simpler than D_∞. In chapter 3, we will undertake a detailed comparison between the Archimedean and p-adic four-point functions, and point to remarkable similarities between them. In this chapter, we restrict ourselves to noting that the leading logarithmic term of D_∞ for extreme values of the argument of the log essentially agrees with the $\log_p$ term in (2.130), as we now show.

The leading logarithmic part of D_∞ can be extracted from the expression for D_∞ in [78] written as a series expansion in powers of conformally invariant variables s and t,

$$s \equiv \frac{1}{2}\frac{|\vec{x}_{13}|^2|\vec{x}_{24}|^2}{|\vec{x}_{12}|^2|\vec{x}_{34}|^2 + |\vec{x}_{14}|^2|\vec{x}_{23}|^2} \qquad t \equiv \frac{|\vec{x}_{12}|^2|\vec{x}_{34}|^2 - |\vec{x}_{14}|^2|\vec{x}_{23}|^2}{|\vec{x}_{12}|^2|\vec{x}_{34}|^2 + |\vec{x}_{14}|^2|\vec{x}_{23}|^2}\,. \tag{2.131}$$

Specializing to identical operators of dimension Δ in equations (A.1), (A.3) and (6.30) of [78], we obtain

$$\begin{aligned} D_\infty(\vec{x}_1,\vec{x}_2,\vec{x}_3,\vec{x}_4)_{\log} = {} & \frac{-(2s)^\Delta 2^{\Delta-2}}{|\vec{x}_{13}|^{2\Delta}|\vec{x}_{24}|^{2\Delta}}\,\frac{\zeta_\infty(4\Delta-n)}{\zeta_\infty(2\Delta)^2}\,\log(1-t^2) \\ & \times \sum_{\ell=0}^{\Delta-1}\sum_{k=0}^{\infty} \frac{(-2)^{-\ell}\Gamma_{\text{Euler}}(k+1)\,s^{\Delta-\ell-1}(1-2s)^{k+\ell-2\Delta+2}}{\Gamma_{\text{Euler}}(\Delta-\ell)^2\,\ell!\Gamma_{\text{Euler}}(k+\ell-2\Delta+3)}\,\alpha_k(t) \end{aligned} \tag{2.132}$$

where

$$\alpha_k(t) = \sum_{\ell=0}^{\infty} \frac{\Gamma_{\text{Euler}}(\ell+1/2)}{\Gamma_{\text{Euler}}(1/2)\,\ell!}\,\frac{(1-t^2)^\ell}{2\ell+k+1}\,, \tag{2.133}$$

and now log indicates a natural logarithm. It is noteworthy that if $|\vec{x}_{12}||\vec{x}_{34}| \ll$

$|\vec{x}_{13}||\vec{x}_{24}|$,

$$s \to \frac{1}{2} \qquad t \to -1 \qquad (1-t^2) \to 4\frac{|\vec{x}_{12}|^2|\vec{x}_{34}|^2}{|\vec{x}_{14}|^2|\vec{x}_{23}|^2} \approx 4\frac{|\vec{x}_{12}|^2|\vec{x}_{34}|^2}{|\vec{x}_{13}|^2|\vec{x}_{24}|^2}\,, \tag{2.134}$$

$$\alpha_k(t) = \frac{1}{1+k} + O(1-t^2) \tag{2.135}$$

and the leading logarithmic singularity in (2.132) arises at $k = -\ell+2\Delta-2$ in the infinite sum. Then the leading order contribution from the second line of (2.132) evaluates to

$$\sum_{\ell=0}^{\Delta-1} \frac{(-2)^{-\ell}\Gamma_{\text{Euler}}(2\Delta-\ell-1)}{2^{\Delta-\ell-1}\Gamma_{\text{Euler}}(\Delta-\ell)^2\,\ell!}\,\frac{1}{2\Delta-\ell-1} = 2^{2-3\Delta}\frac{\zeta_\infty(2\Delta)}{\zeta_\infty(2\Delta+1)}\,. \tag{2.136}$$

Combining (2.136) with the first line of (2.132), we obtain to leading logarithmic order

$$D_\infty(\vec{x}_1,\vec{x}_2,\vec{x}_3,\vec{x}_4)_{\log} = -\frac{\zeta_\infty(4\Delta-n)}{\zeta_\infty(4\Delta)}\left(\log\frac{|\vec{x}_{12}||\vec{x}_{34}|}{|\vec{x}_{13}||\vec{x}_{24}|}\right)\frac{1}{|\vec{x}_{13}|^{2\Delta}|\vec{x}_{24}|^{2\Delta}} \tag{2.137}$$

for $|\vec{x}_{12}||\vec{x}_{34}| \ll |\vec{x}_{13}||\vec{x}_{24}|$. The corresponding expressions in the $|\vec{x}_{14}||\vec{x}_{23}| \ll |\vec{x}_{13}||\vec{x}_{24}|$ and $|\vec{x}_{13}||\vec{x}_{24}| \ll |\vec{x}_{12}||\vec{x}_{34}|$ limits can be obtained by appropriately relabeling the $\vec{x}_i$ in (2.137).

If $g_3 = 0$ so that only the contact diagram contributes to the four-point function, then standard reasoning leads to

$$\langle\mathcal{O}(x_1)\mathcal{O}(x_2)\mathcal{O}(x_3)\mathcal{O}(x_4)\rangle_p = -\eta_p g_4\frac{\zeta_p(2\Delta)^4}{\zeta_p(2\Delta-n)^4}D_p(x_1,x_2,x_3,x_4)\,. \tag{2.138}$$

If $g_3 \neq 0$, then there are exchange diagrams. We expect that, analogous to the real case [78], the full four-point function can be reduced to a sum of contact diagrams, some of them generalizing the D_p amplitude we have worked out explicitly. Indeed we work this out explicitly in chapter 3.

2.5 Taking stock

In this section, we collect the main technical results of this chapter: expressions for the non-Archimedean propagators and correlators, and contrast them with

their Archimedean analogs. The resemblance between the two is striking! We continue in section 2.5.2 with further comparisons between standard Archimedean results and our new p-adic results and show how some strange factors in the p-adic results presented in section 2.5.1 reduce to the standard Archimedean counterparts upon taking a $p \to 1$ limit. Then we discuss the geometry of chordal distance in section 2.5.3 and explain the origin of the tree-sum, and finally give a brief account of long thin Wilson loops in section 2.5.4.

2.5.1 Main results

Here are our main results on propagators and correlators:

- The relationship between mass and dimension is

$$\begin{aligned} m_\infty^2 L^2 &= \Delta(\Delta - n) && \text{for } v = \infty \\ m_p^2 &= -\frac{1}{\zeta_p(\Delta - n)\,\zeta_p(-\Delta)} && \text{for } v = p\,. \end{aligned} \tag{2.139}$$

  (The local zeta functions ζ_∞ and ζ_p were introduced in (2.53) and (2.44), respectively.)

- The bulk-to-boundary propagator is

$$\begin{aligned} K(z_0, \vec{z}; \vec{x}) &= \frac{\zeta_\infty(2\Delta)}{\zeta_\infty(2\Delta - n)} \frac{z_0^\Delta}{(z_0^2 + (\vec{z} - \vec{x})^2)^\Delta} && \text{for } v = \infty \\ K(z_0, z; x) &= \frac{\zeta_p(2\Delta)}{\zeta_p(2\Delta - n)} \frac{|z_0|_p^\Delta}{|(z_0, z - x)|_s^{2\Delta}} && \text{for } v = p\,, \end{aligned} \tag{2.140}$$

- The bulk-to-bulk propagator is

$$\begin{aligned} G(z_0, \vec{z}; w_0, \vec{w}) &= \frac{1}{2\Delta - n} \frac{\zeta_\infty(2\Delta)}{\zeta_\infty(2\Delta - n)} u_\infty^{-\Delta} \\ &\qquad \times {}_2F_1\left(\Delta, \Delta - n + \frac{1}{2}; 2\Delta - n + 1; -\frac{4}{u_\infty}\right) && \text{for } v = \infty \\ G(z_0, z; w_0, w) &= \frac{\zeta_p(2\Delta - n)}{p^\Delta} \frac{\zeta_p(2\Delta)}{\zeta_p(2\Delta - n)} u_p^{-\Delta} && \text{for } v = p\,, \end{aligned} \tag{2.141}$$

where we define

$$u_\infty \equiv \frac{(z_0-w_0)^2+(\vec{z}-\vec{w})^2}{z_0 w_0} \qquad\qquad u_p \equiv p^{d(z_0,z;w_0,w)}\,. \tag{2.142}$$

- The two-point function is

$$\begin{aligned}\langle \mathcal{O}(\vec{x}_1)\mathcal{O}(\vec{x}_2)\rangle_\infty &= \eta_\infty L^{n-1}(2\Delta-n)\frac{\zeta_\infty(2\Delta)}{\zeta_\infty(2\Delta-n)}\frac{1}{|\vec{x}_{12}|^{2\Delta}} \qquad \text{for } v=\infty \\ \langle \mathcal{O}(x_1)\mathcal{O}(x_2)\rangle_p &= \eta_p \frac{p^\Delta}{\zeta_p(2\Delta-n)}\frac{\zeta_p(2\Delta)}{\zeta_p(2\Delta-n)}\frac{1}{|x_{12}|_q^{2\Delta}} \qquad \text{for } v=p\,.\end{aligned} \tag{2.143}$$

Recall that in computing the two-point function for the p-adics, we faced some arbitrariness in the prefactor based on the precise cutoff scheme we employed. The result in (2.143) is based on the democratic approach of geometrically averaging over the inclusive and exclusive cutoff scheme as explained around (2.112)–(2.113).

- The three-point function is

$$\begin{aligned}&\langle \mathcal{O}(\vec{x}_1)\mathcal{O}(\vec{x}_2)\mathcal{O}(\vec{x}_3)\rangle_\infty \\ &\qquad = -\eta_\infty L^{n-1} g_3 \frac{\zeta_\infty(\Delta)^3\,\zeta_\infty(3\Delta-n)}{2\,\zeta_\infty(2\Delta-n)^3}\frac{1}{|\vec{x}_{12}|^\Delta|\vec{x}_{23}|^\Delta|\vec{x}_{13}|^\Delta} \qquad \text{for } v=\infty \\ &\langle \mathcal{O}(x_1)\mathcal{O}(x_2)\mathcal{O}(x_3)\rangle_p \\ &\qquad = -\eta_p g_3 \frac{\zeta_p(\Delta)^3\,\zeta_p(3\Delta-n)}{\zeta_p(2\Delta-n)^3}\frac{1}{|x_{12}x_{23}x_{13}|_q^\Delta} \qquad \text{for } v=p\,.\end{aligned} \tag{2.144}$$

- The four-point function is built from contact diagrams, the simplest of

which have leading logarithmic singularities of the form

$$\begin{aligned} &D_\infty(\vec{x}_1,\vec{x}_2,\vec{x}_3,\vec{x}_4)_{\log} \\ &\qquad = -\frac{\zeta_\infty(4\Delta-n)}{\zeta_\infty(4\Delta)}\left(\log\frac{|\vec{x}_{12}||\vec{x}_{34}|}{|\vec{x}_{13}||\vec{x}_{24}|}\right)\frac{1}{|\vec{x}_{13}|^{2\Delta}|\vec{x}_{24}|^{2\Delta}} \qquad \text{for } v=\infty \\ &D_p(x_1,x_2,x_3,x_4)_{\log} \\ &\qquad = -\frac{\zeta_p(4\Delta-n)}{\zeta_p(4\Delta)}\left(\log_p\left|\frac{x_{12}x_{34}}{x_{13}x_{24}}\right|_q\right)\frac{1}{|x_{13}x_{24}|_q^{2\Delta}} \qquad \text{for } v=p\,. \end{aligned} \tag{2.145}$$

The Archimedean results in (2.139)–(2.145) are standard in the literature, although their simplified presentation in terms of the local zeta function $\zeta_\infty(s)$ is new as far as we are aware.

There are some natural simplifying features of p-adic AdS/CFT. To begin with, all quantities of interest lie in the field extension $\mathbb{Q}(p^\Delta)$: that is, rational numbers combined with integer powers of p^Δ. Many of the powers of p can be efficiently packaged in the p-adic zeta function ζ_p, and Archimedean results can be (almost) recovered by replacing p by ∞. The reason why the p-adic formulas we derived are valued in $\mathbb{Q}(p^\Delta)$ is that they come from sums of products of propagators over the Bruhat–Tits tree, and these sums typically reduce to geometric series, $\sum_{\ell=1}^\infty x^\ell = \frac{x}{1-x}$, with $x \in \mathbb{Q}(p^\Delta)$, and the map $x \to \frac{x}{1-x}$ involves only field operations. In the Archimedean place, we are struck by the complete absence of factors of π when we express correlators in terms of ζ_∞ rather than Γ_{Euler}. This is analogous to seeing p-adic correlators taking values in $\mathbb{Q}(p^\Delta)$.

2.5.2 Comparing Archimedean and p-adic results

It is clear from (2.139)–(2.145) that we generally cannot write closed-form expressions for physical quantities which are valid equally for $v=\infty$ and $v=p$. We are often close to being able to do so, as in the cases of the bulk-to-boundary

propagator (2.140), the three-point function (2.144), and the leading-log term in the four-point amplitude (2.145); note however the mismatched factor of 2 in (2.144), which is operationally related to the fact that we integrate over $y_0 > 0$ in the Archimedean calculations, whereas the sum over T_q can be thought of as including an integral over all non-zero p-adic numbers y_0 (more on this later).

To better understand the relation between $v = \infty$ and $v = p$, consider first the growth of volume in Euclidean AdS_{n+1} with radius as compared to the growth in the number of vertices of T_q with radius. The volume of a ball $\mathcal{B}_{n+1}(R)$ of radius R in AdS_{n+1} is

$$\mathrm{vol}(\mathcal{B}_{n+1}(R)) \sim \text{constant} \times \mathrm{e}^{nR/L} \qquad \text{for } R \gg L\,, \tag{2.146}$$

where L is the radius of curvature of AdS_{n+1}. On the other hand, introducing a lattice spacing a on the Bruhat–Tits tree, the volume of a ball $\mathcal{B}_{T_q}(R)$ of radius R in T_q—meaning all points within a graph distance R/a of a specified point—is given by

$$\mathrm{vol}(\mathcal{B}_{T_q}(R)) \sim \text{constant} \times p^{nR/a} = \text{constant} \times \mathrm{e}^{nR/L_p} \qquad \text{for } R \gg a\,, \tag{2.147}$$

where we have introduced a length scale

$$L_p \equiv \frac{a}{\log p}\,, \tag{2.148}$$

which stands in place of the radius of curvature L and makes (2.146) and (2.147) directly comparable. It is helpful to see in (2.147)–(2.148) how dimensions work, but elsewhere we set $a = 1$. (Changing this to $a = 1/e$ where e is the ramification index could be helpful in discussing ramified extensions.)

With the length scale L_p in hand, we can better understand the apparent mismatch in the two-point functions (2.143) between the boundary factor $2\Delta - n$ in the Archimedean place and $p^{\Delta}/\,\zeta_p(2\Delta - n)$ for the p-adics. If we set $p = \mathrm{e}^{\log p}$

and formally treat $\log p$ as small, as in [71, 70], then the p-adic results become, to leading order in $\log p$,

$$m_p^2 L_p^2 \approx \Delta(\Delta - n) \qquad \frac{p^\Delta L_p}{\zeta_p(2\Delta - n)} \approx 2\Delta - n\,. \tag{2.149}$$

An improved discussion along these lines is probably possible if we extend $\mathbb{Q}_q$ by including $p^{1/e}$ and using the uniformizer $\pi = p^{1/e} = \mathrm{e}^{(\log p)/e}$. In addition to (2.149), we have

$$\begin{aligned} \frac{d(m_\infty^2 L^2)}{d\Delta} &= 2\Delta - n \qquad && \text{for } v = \infty \\ \frac{d(m_p^2 L_p^2)}{d\Delta} &= \frac{p^\Delta L_p}{\zeta_p(2\Delta - n)} \qquad && \text{for } v = p\,, \end{aligned} \tag{2.150}$$

where we have not made any formal expansion in small $\log p$. Finally, we note that the same factor of $p^\Delta / \zeta_p(2\Delta - n) = 2\nu_p$ also appears in the normalizations of the p-adic two-point function and bulk-to-bulk propagator, and in this latter context there is no cutoff-related ambiguity: See the discussion ending in (2.74).

In short, the results of p-adic and Archimedean calculations have strong affinities, but we are not generally in a position to write down adelic products. Perhaps we should not be too surprised by the mismatches between p-adic and Archimedean calculations, since our starting point on the p-adic side was only the simplest lattice action. It seems possible that a more informed treatment of the bulk action will lead to progress toward an adelic version of AdS/CFT.

2.5.3 The geometry of chordal distance

We believe that a good first step toward adelic AdS/CFT is to re-examine the geometry of T_q from a point of view that makes its similarities to ordinary AdS_{n+1} more transparent. Indeed, the Bruhat–Tits tree T_q is a natural bulk construction both from the perspective of the representation of p-adic numbers as a string of digits, and from the more geometric point of view of a coset construction

$\mathrm{PGL}(2,\mathbb{Q}_q)/\mathrm{PGL}(2,\mathbb{Z}_q)$, where the denominator is the maximal compact subgroup of the numerator. But from the point of view of classical AdS/CFT, it is a bit surprising, especially since the bulk T_q has a smaller cardinality than the boundary $\mathbb{Q}_q$. Our parametrization of T_q in terms of (z_0, z), where $z_0 = p^\omega$ and $z \in \mathbb{Q}_q$ is known up to $O(z_0)$ corrections, suggests that it might be more natural to let the bulk be all of

$$p\mathrm{AdS}_{n+1} \equiv \mathbb{Q}_p^\times \times \mathbb{Q}_q \,, \tag{2.151}$$

with coordinates (z_0, z) where now $z_0 \in \mathbb{Q}_p^\times$ (a non-zero p-adic number) and $z \in \mathbb{Q}_q$. Introduce a chordal distance function between any two points (w_0, w) and (z_0, z):[9]

$$u_p = \frac{|(z_0 - w_0, z - w)|_s^2}{|z_0 w_0|_p} \,, \tag{2.153}$$

where $|\cdot|_s$ indicates the supremum norm (2.48). It is easy to show that if (z_0, z) and (w_0, w) parametrize different points on T_q in the sense explained in chapter 1, with z_0 and w_0 restricted to integer powers of p, then $u_p = p^{d(z_0,z;w_0,w)}$, in agreement with (2.142). On the other hand, u_p can be an arbitrarily small power of p if (w_0, w) and (z_0, z) are p-adically very close to one another. So we can ask, how is T_q related to the larger space $p\mathrm{AdS}_{n+1}$?

It turns out there is a simple and pleasing answer: To get T_q, we must coarse-grain $p\mathrm{AdS}_{n+1}$ at the AdS scale. Specifically, we can form an equivalence relation

$$(z_0, z) \sim (w_0, w) \qquad \text{iff} \qquad u_p(z_0, z; w_0, w) \leq 1 \,. \tag{2.154}$$

[9]The Archimedean quantity u_∞ introduced in (2.142) is actually the square of the chordal distance divided by L^2. To be precise, if we define global coordinates

$$Z_0 = \frac{1}{2z_0}(L^2 + z_0^2 + \vec{z}^2) \qquad \vec{Z} = L\frac{\vec{z}}{z_0} \qquad Z_{n+1} = \frac{1}{2z_0}(-L^2 + z_0^2 + \vec{z}^2) \,, \tag{2.152}$$

and similarly for W_M, then Euclidean AdS_{n+1} is the locus $\eta^{MN} Z_M Z_N = -L^2$, where $\eta^{MN} = \mathrm{diag}\{-1, 1, 1, \ldots, 1\}$, and $u_\infty = \eta^{MN}(Z_M - W_M)(Z_N - W_N)/L^2$.

To find the equivalence classes under the relation (2.154), note that

$$\left|\left(\frac{z_0}{w_0}+\frac{w_0}{z_0}-2,\frac{(z-w)^2}{z_0 w_0}\right)\right|_s = u_p \le 1\,, \tag{2.155}$$

which implies that $\frac{z_0}{w_0}+\frac{w_0}{z_0}-2$ is a p-adic integer. It follows that $\frac{w_0}{z_0}\in\mathbb{U}_p$. Next one can show using (2.155) that $\frac{z-w}{z_0}$ is also a p-adic integer, so $z-w\in z_0\mathbb{Z}_q$. In other words, for fixed (z_0,z), the set of all (w_0,w) with $u_p(z_0,z;w_0,w)\le 1$ is

$$B(z_0,z) = z_0\mathbb{U}_p \times (z+z_0\mathbb{Z}_q)\,. \tag{2.156}$$

In the natural measure on $p\mathrm{AdS}_{n+1}$, the volume of each block is the same:

$$\int_{B(z_0,z)}\frac{dw_0\,dw}{|w_0|_p^{n+1}} = \frac{1}{|z_0|^{n+1}}\left(\int_{z_0\mathbb{U}_p}dw_0\right)\left(\int_{z_0\mathbb{Z}_q}dw\right) = \frac{1}{\zeta_p(1)}\,, \tag{2.157}$$

where we have used the fact that $\mathbb{U}_p$ has measure $1-1/p = 1/\,\zeta_p(1)$.

We can label the blocks $B(z_0,z)$ uniquely by requiring $z_0=p^\omega$ for some $\omega\in\mathbb{Z}$ and $z\in S^\omega_{-\infty}\equiv\bigcup_{\mu<\omega}S^\omega_\mu$. The blocks $B(z_0,z)$ can now be regarded as the nodes of the tree T_q, and the distance function on T_q is defined by

$$p^{d(z_0,z;w_0,w)} = u_p(z_0,z;w_0,w) \qquad \text{provided } B(z_0,z)\neq B(w_0,w)\,, \tag{2.158}$$

together with the trivial definition $d(z_0,z;z_0,z)=0$. In the Archimedean place, the relation $u_\infty(z_0,\vec{z};w_0,\vec{w})\le 1$ means that $(z_0,\vec{z})$ and $(w_0,\vec{w})$ are essentially within an AdS radius of one another; thus (2.154) can be regarded as a p-adic analog of coarse-graining at the AdS curvature scale. However, there is no analog of the sets $B(z_0,z)$ in the Archimedean place, essentially because if we carried (2.154) over to the reals, the transitive property would fail. Less formally, we can't carve ordinary Euclidean AdS into blocks without points near the edges being very close to one another.

With the blocks $B(z_0,z)$ specified, we can go further and define a coarse topology on $p\mathrm{AdS}_{n+1}$ by saying that the closed sets are arbitrary unions of blocks.

Continuous functions with respect to this topology are precisely the ones which are constant on each block, which is to say well-defined as functions on T_q. If f is such a function, then we can calculate its integral as a sum over T_q:

$$\zeta_p(1) \int_{p\mathrm{AdS}_{n+1}} \frac{dz_0\, dz}{|z_0|_p^{n+1}} f(z_0, z) = \sum_{a \in T_q} f(a)\,, \tag{2.159}$$

where we have used (2.157).

It is natural to inquire whether we can coarse-grain $p\mathrm{AdS}_{n+1}$ differently. It is easy to see that if we try to form an equivalence relation by saying $(z_0, z) \sim (w_0, w)$ iff $u_p(z_0, z; w_0, w) \leq p^m$ for a positive integer m, then the transitive property fails, so we do not have a natural way to split $p\mathrm{AdS}_{n+1}$ into larger blocks than the ones defined in (2.156). On the other hand, for $m \in \mathbb{N} \equiv \{0, 1, 2, 3, \ldots\}$, we may define

$$(z_0, z) \sim_m (w_0, w) \qquad \text{iff} \qquad u_p(z_0, z; w_0, w) \leq p^{-2m}\,, \tag{2.160}$$

and then $\sim_m$ is an equivalence relation, and it coincides with $\sim$ when $m = 0$. (There is no point in considering $u_p(z_0, z; w_0, w) \leq p^{-2m-1}$, because u_p, if non-zero, must take the form p^σ where either $\sigma \in \mathbb{N}$ or $\sigma = -2m$ for $m \in \mathbb{N}$.) The equivalence classes $B(z_0, z)$ under $\sim$ are subdivided into smaller equivalence classes $B_m(z_0, z)$ under $\sim_m$: In other words, $\sim_m$ for $m > 0$ is a refinement of $\sim$. From the point of view of quantum gravity, such refinements are appealing because they allow us to use "ordinary" geometry down to a scale that we identify as the Planck scale, and length scales smaller than the Planck scale either don't exist or are qualitatively different. An interesting point of comparison is that tensor networks in AdS based on MERA generally cannot be made finer than the AdS scale [79].

To better understand the refinements described in the previous paragraph, let's examine how the block $B(1, 0)$ splits into smaller blocks $B_m(z_0, z)$. The

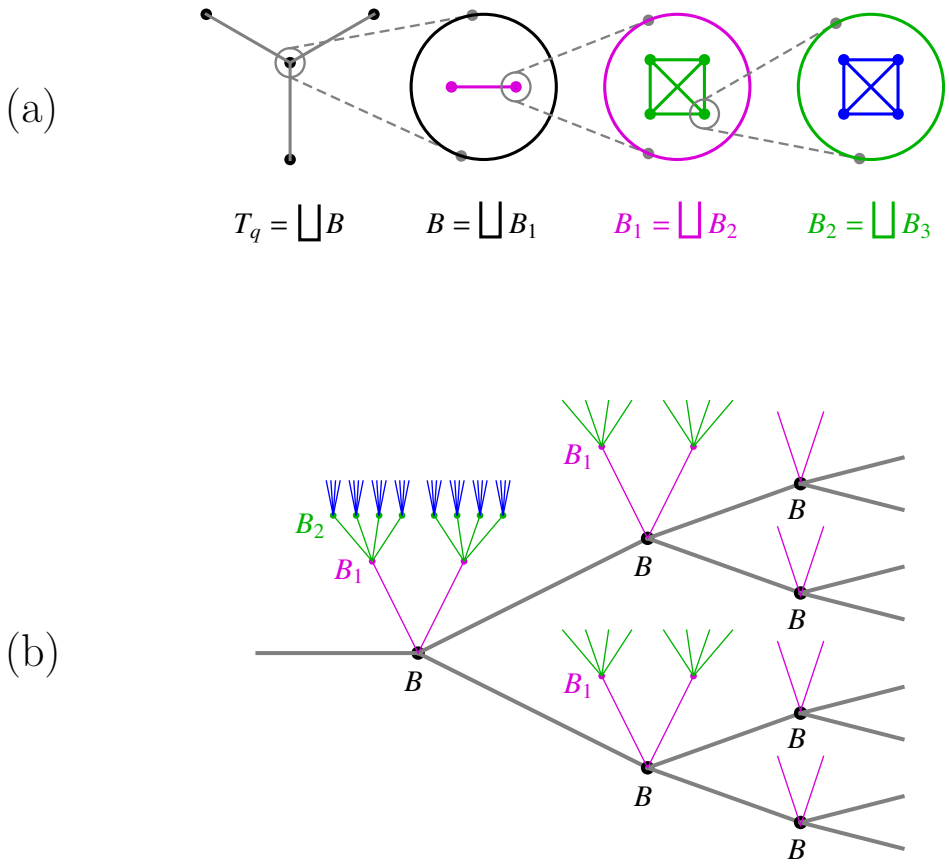

Figure 2.3: Successive refinements of the Bruhat–Tits tree. The example shown is for $q = p = 2$. (a) Successive refinements reveal more and more structure as we zoom in on any given bulk region. The first step is to write T_q as a disjoint union of blocks B as defined in (2.156). The next step is to write each block B as a disjoint union of blocks B_1 as defined in (2.162); then each block B_1 is written as a disjoint union of blocks B_2, and so forth. (b) Successive refinements of T_q lead to the enhanced tree T_{qp}, in which each vertex is a block B_m. The base tree T_q is shown in gray, and the height h measures how many steps away a point on T_{qp} is from the base tree.

first task is to parse the relationship $u_p(z_0, z; w_0, w) \leq p^{-2m}$ for points (z_0, z) and (w_0, w) in $B(1, 0)$. We have in particular $z_0, w_0 \in \mathbb{U}_p$, so

$$u_p = |(z_0 - w_0, z - w)|_s^2 \leq p^{-2m}\,, \tag{2.161}$$

The result (2.161) indicates that from the point of view of chordal distance, $B(1, 0)$ is like a patch of $\mathbb{Q}_q \times \mathbb{Q}_p$ equipped with the supremum norm; in other words, we don't see any sign of the curvature of $p\mathrm{AdS}_{n+1}$ once we look at length scales within a given block $B(z_0, z)$. From (2.161) we see immediately that the equivalence classes of $\sim_m$ inside $B(1, 0)$ are

$$B_m(z_0, z) = (z_0 + p^m\mathbb{Z}_p) \times (z + p^m\mathbb{Z}_q)\,. \tag{2.162}$$

These equivalence classes are uniquely labeled by (z_0, z) if we require

$$z_0 \in s_0^m \setminus s_1^m \qquad \text{and} \qquad z \in S_0^m\,. \tag{2.163}$$

The sets S_μ^ω were defined in (2.22), and by s_μ^ω we mean the analogous sets for $\mathbb{Q}_p$ instead of $\mathbb{Q}_q$. For $m > 0$, there are $p^{m(n+1)}(1-1/p)$ equivalence classes $B_m(z_0, z)$ inside $B(1, 0)$, and the volume of each one is $\int_{B_m(z_0,z)} \frac{dw_0 dw}{|w_0|_p^{n+1}} = p^{-m(n+1)}$. If $m = 1$, then (2.163) simplifies to $z_0 \in \mathbb{F}_p^\times = \{1, 2, \ldots, p-1\}$ and $z \in \mathbb{F}_q$. In this case, it is easy to see that $u_p = 1$ between any two points in distinct blocks $B_1(z_0, z)$ and $B_1(w_0, w)$, whereas (by definition) $u_p \leq p^{-2}$ between any two points in the same block. If we proceed next to $m = 2$, then each block $B_1(z_0, z)$ splits into p^{n+1} smaller blocks $B_2(w_0, w)$, and each pair of B_2 blocks within a given B_1 block is separated by a distance $u_p = p^{-2}$. A cartoon of these successive refinements is shown in figure 2.3a. Evidently, a sequence of topologies on $p\mathrm{AdS}_{n+1}$ can be defined, such that functions which are constant over all the blocks $B_m(z_0, z)$ are continuous with respect to the m^{th} topology. Without a Planck scale cutoff, the endpoint of the refinement process is the full geometry $p\mathrm{AdS}_{n+1}$. A simple way to think of a Planck scale cutoff is to stop refining after a finite number of steps.

The successive refinements of T_q into $p\mathrm{AdS}_{n+1}$ can be summarized by an enhanced tree structure, constructed as follows. From each node of the base tree T_q, we add $q(p-1)$ edges to indicate the splitting of $B(z_0, z)$ into blocks B_1. From the terminus of each of these edges, we add qp new edges to indicate the splitting of B_1 blocks into B_2 blocks. Continuing in this way, we wind up with a tree with uniform coordination number $qp+1$, which is to say T_{qp}: see figure 2.3b. We can identify each vertex on the enhanced tree with a block B_m, where the index m increases the further off of the base tree we go. Let the standard graph theoretic distance between two points a and b on T_{qp} be denoted $D(a, b)$, and let the distance from a point a on T_{qp} to the nearest point on the base tree T_q be denoted $h(a)$. Then if we define

$$\sigma(a, b) = D(a, b) - h(a) - h(b)\,, \tag{2.164}$$

it can be checked that the maximum value of the chordal distance u_p between a point in the block associated with a and a point in the block associated with b is $p^{\sigma(a,b)}$.

We would like to use $p\mathrm{AdS}_{n+1}$ and the geometry of chordal distance as jumping off points for the construction of bulk models that are more interesting than just a scalar with nearest neighbor interactions on T_q as in (2.19). Ideally we would like to have some notion of fluctuating bulk geometry. The absence of cycles in T_q makes it hard to see how to study gauge fields or Riemannian curvature. So it is interesting to observe that at each stage of refinement, the newly introduced blocks (for example, all the B_3 blocks inside a given B_2 block) form a complete graph in the sense that each is equidistant from all the others using the chordal distance function u_p. Can we take advantage of the cycles in these complete graphs to formulate some useful lattice notions of curvature? If we can, how does curvature fit in with the structure of the enhanced tree T_{qp}?

2.5.4 Wilson loops

Wilson loops are important observables in field theory. A natural question to ask is: What are the properties of p-adic Wilson loops? We give some preliminary indications in this section.

We begin by reviewing a simple case in the Archimedean place [80, 81]. The interquark potential energy $V(R)$ of a heavy quark-antiquark pair is given by the expectation value of the Wilson loop operator,

$$\langle W(\mathcal{C})\rangle \propto \mathrm{e}^{-V(R)\,T}\,, \tag{2.165}$$

where $\mathcal{C}$ is a long thin rectangular contour, of length T along the time direction, and length $R \ll T$ along the spatial direction. The calculations are all done in Euclidean signature, so the time direction is picked out essentially arbitrarily. According to the AdS/CFT prescription, the expectation value of a Wilson loop is given by the partition function for a string in AdS, whose edge at the boundary lies along $\mathcal{C}$. In particular, in the supergravity limit,

$$\langle W(\mathcal{C})\rangle \propto \mathrm{e}^{-(S_\Phi - \ell\Phi)} \tag{2.166}$$

where S_Φ is the action of the minimal surface in AdS of the string worldsheet ending on $\mathcal{C}$. The minimal action S_Φ and hence $V(R)$ suffer from UV divergences. We must subtract away from $V(R)$ the infinite energies of the free quark and the free antiquark to get a sensible finite answer. In other words, we must renormalize the minimal action S_Φ by subtracting from it the action of the worldsheets associated with the free quark and the free antiquark, both of which stretch all the way to infinity in AdS. This is what is meant by $\ell\Phi$ in (2.166). In conformal field theories, symmetry dictates that the potential energy take the form $V(R) \propto 1/R$. Indeed, an AdS calculation of the (regulated) minimal surface yields, via (2.165)

and (2.166)

$$V(R)\,T = -\frac{4\pi^2}{\Gamma_{\text{Euler}}(1/4)^4}\frac{L^2}{\alpha'}\frac{T}{R}\,, \tag{2.167}$$

where $1/2\pi\alpha'$ is the string tension. We include only the T-extensive contribution and ignore endpoint effects having to do with how we close the loop off at times $t = \pm T/2$. In (2.167), T serves as an infrared regulator imposed to avoid a divergent factor from integrating in the t direction.

Let's move on to discuss a simple analog of the long thin rectangular Wilson loop in the context of p-adic AdS/CFT. We restrict ourselves to a two-dimensional subspace of $\mathbb{Q}_{p^n}$, which itself is an n-dimensional vector space over $\mathbb{Q}_p$. Every point z in this two-dimensional subspace can be written as $z = t\,r^\ell + x\,r^k$ for fixed $\ell, k \in \{0, 1, \ldots\, n-1\}$, $\ell \neq k$, and $t, x \in \mathbb{Q}_p$. Here r is a primitive (p^n-1)-th root of unity. For the rest of this discussion we set $\ell = 0$ and $k = 1$ without loss of generality. Let the time direction be along the r^0 component, and let space be along r^1.

The p-adic analog of parallel lines in the t direction with spatial separation R is clear enough: each line is an affine map of $\mathbb{Q}_p$ to $\mathbb{Q}_q$, so that the quark line is all points of the form $t + x\,r$ with x fixed and t varying across $\mathbb{Q}_p$, while the antiquark line is $t + \tilde{x}\,r$, again with $\tilde{x}$ fixed and t varying across $\mathbb{Q}_p$. We anticipate the need for an infrared regulator, so we restrict the p-adic norm of the time coordinate: $|t|_p \leq |T|_p$, where we require

$$|T|_p \gg |R|_p \tag{2.168}$$

and $R = x - \tilde{x}$. For convenience we set

$$v_p(T) = \tau \qquad \text{and} \qquad v_p(R) = \rho\,. \tag{2.169}$$

Our results depend on T and R only through their norms, so we could set $T = p^\tau$ and $R = p^\rho$ without loss of generality. None of our calculations below depend on this choice.

Now we must specify what we mean in the discrete context of the Bruhat–Tits tree T_q by a string worldsheet whose edge is on one of the parallel lines. Consider the quark line for specificity. Any point $t + x\,r$ on the line is associated to a unique path through T_q from ∞ to $t + x\,r$. Adapting previous notation, let's denote this path as $(\infty : t + x\,r)$, with the convention that we exclude the endpoints at the boundary. The union of these paths is a subtree of T_q isomorphic to T_p. This subtree is what we want to regard as the string worldsheet. It is like a (Euclidean) AdS_2 subset of AdS_{n+1}. To bring in our infrared regulator, let's first assume that $|T|_p > |x|_p$. Then each path on T_q from ∞ to a point $t + x\,r$ with $|t|_p \leq |T|_p$ passes through the point $(p^\tau, 0)$ on the main trunk of T_q. We think of the infrared regulated path $((p^\tau, 0) : t + x\,r)$ as only that portion of the path starting at $(p^\tau, 0)$ and continuing upward to $t + x\,r$. We include $(p^\tau, 0)$, but not the boundary point $t + x\,r$, in the regulated path $((p^\tau, 0) : t + x\,r)$. The infrared regulated worldsheet is the union

$$M_x(T) \equiv \bigcup_{|t|_p \leq |T|_p} ((p^\tau, 0) : t + x\,r)\,. \tag{2.170}$$

The number of vertices of T_q in $M_x(T)$ is still infinite, but if we discard points sufficiently close to the boundary (i.e. impose an ultraviolet regulator) it becomes finite.

Next we need to describe in the context of T_q the string worldsheet with an edge on each of the parallel lines. To begin with, consider the x-direction only, and correspondingly the T_p subtree at $t = 0$. The common ancestor of x and $\tilde{x}$ on T_p is at bulk depth $z_0 = 1/|R|_p$. Moreover, there is a unique path leading from x to $\tilde{x}$ along T_p, and it goes through their common ancestor. Returning to T_q, we consider the string worldsheet with an edge on each of the parallel lines to be the union over t of all paths in T_q from $t + x\,r$ to $t + \tilde{x}\,r$:

$$M_{q\bar{q}}(T) \equiv \bigcup_{|t|_p \leq |T|_p} (t + x\,r : t + \tilde{x}\,r)\,, \tag{2.171}$$

where as before we exclude boundary points from the paths. Note that it is important that we consider only paths from $t + x\,r$ to $t + \tilde{x}\,r$ with the same value of t: If we allowed paths from $t + x\,r$ to $\tilde{t} + \tilde{x}\,r$ with $|t - \tilde{t}|_p > |R|_p$, then we would include points that go lower in T_q than the bulk depth $p^\rho = 1/|R|_p$. We caution that our prescription for forming the string worldsheet as a union of paths does not directly refer to minimal surfaces. Intuitively, the worldsheet (2.171) is the only discretized surface with no back-tracking with edges on the quark and antiquark lines. Closer consideration of how to describe more general string worldsheets in T_q is clearly merited.

The obvious p-adic analog of the Nambu–Goto action is the number of vertices on the string worldsheet. More precisely, we want to count each vertex on $M_{q\bar{q}}(T)$ with multiplicity 1, and at the same time count each vertex on $M_x(T) \sqcup M_{\tilde{x}}(T)$ with multiplicity -1. As shown in figure 2.4, this counting is made easier by the observation that $M_{q\bar{q}}(T)$ covers precisely the points in $M_x(T) \cup M_{\tilde{x}}(T)$ down to a depth $z_0 = p^\rho$, so points above this depth (that is, points with $|z_0|_p < p^{-\rho}$) can be ignored. Right at $z_0 = p^\rho$, where $M_{q\bar{q}}(T)$, $M_x(T)$, and $M_{\tilde{x}}(T)$ intersect, we should count points with net multiplicity -1 (which comes from 1 for $M_{q\bar{q}}(T)$ plus -1 for each of $M_x(T)$ and $M_{\tilde{x}}(T)$). Below this depth, continuing down to the infrared cutoff $z_0 = p^\tau$, we should count points with net multiplicity -2. At a depth $m \geq \tau$ (meaning closer to the boundary than the infrared cutoff), the number of points on $M_x(T)$ (or $M_{\tilde{x}}(T)$) is $p^{m-\tau}$. Thus the total count of points, including multiplicities as just described, is

$$S_{\text{reg}} = -p^{\rho-\tau} - 2\sum_{m=\tau}^{\rho-1} p^{m-\tau} = -\left|\frac{T}{R}\right|_p \frac{p + 1 - 2|R/T|_p}{p-1} \approx -\frac{\zeta_p(1)^2}{\zeta_p(2)}\left|\frac{T}{R}\right|_p , \quad (2.172)$$

where in the last term we have dropped a term which is suppressed by a relative factor of $|R/T|_p \ll 1$. The scaling of (2.172) with $|T|_p$ and $|R|_p$ is as expected for a conformal theory, so that the potential $V(R) \propto 1/|R|_p$. The coefficient

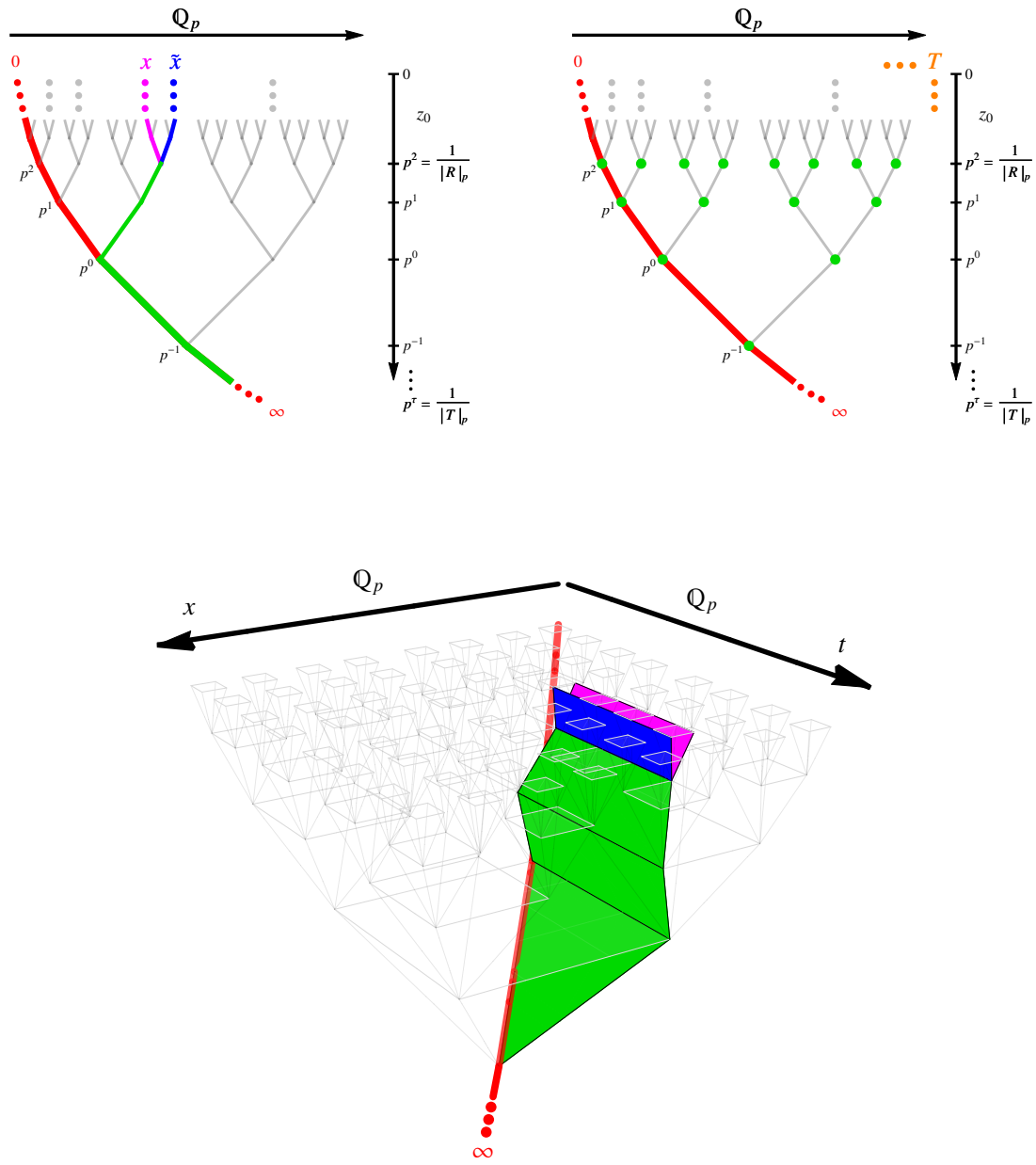

Figure 2.4: Two views of a Wilson loop in the Bruhat–Tits tree T_q for $q = 2^2$. Top: Constant-t and constant-x slices of a Wilson loop with length $|T|_p = p^{-\tau}$ and $|R|_p = p^{-2}$. Bottom: Segment of a Wilson loop in a perspective view. The green region in both views indicate the vertices that are in common for the Wilson lines of the free quark and antiquark. The purple region pertains to the quark, and the blue region pertains to the antiquark.

in (2.172) is negative, so that quarks and antiquarks in the dual theory attract, but it does not seem closely related to the prefactor in (2.167). Possibly a better understanding of more general Wilson loops could help shed light on this apparent mismatch.

2.6 Discussion

In p-adic AdS/CFT, the Bruhat–Tits tree plays the role of anti-de Sitter space, while the p-adic numbers replace the reals. In the simplest case, we eschew any extension of $\mathbb{Q}_p$, and then the relation between T_p and $\mathbb{Q}_p$ is like the relation between the upper half plane and the reals. In other words, unextended p-adic AdS/CFT is best compared to ordinary (Euclidean) $\mathrm{AdS}_2/\mathrm{CFT}_1$. Passing to the unramified extension $\mathbb{Q}_q$, where $q = p^n$, we have suggested that there is a natural comparison to Euclidean $\mathrm{AdS}_{n+1}/\mathrm{CFT}_n$. The obvious point in favor of this comparison is that $\mathbb{Q}_q$ is an n-dimensional vector space over $\mathbb{Q}_p$ with dimension n and a natural norm $|\cdot|_q$ with the property $|x|_q \geq 0$ with equality iff $x = 0$. Likewise, T_q can be thought of as having n dimensions in the directions parallel to the boundary; more technically, the edges rising up from a given vertex of T_q toward $\mathbb{Q}_q$ are enumerated by elements of $\mathbb{F}_q$, which is a vector space of dimension n over $\mathbb{F}_p$. On the other hand, the natural analog of the conformal group for $\mathbb{Q}_q$ is $\mathrm{PGL}(2, \mathbb{Q}_q)$, which seems closer to $\mathrm{SL}(2, \mathbb{R})$ than to $\mathrm{O}(n + 1, 1, \mathbb{R})$. Thus, field theories over $\mathbb{Q}_q$ are expected to be similar to n-dimensional Archimedean field theories, but they may possess simplifying features comparable to low-dimensional conformal field theories. Our main results, as summarized in section 2.5.1, reinforce these expectations.

2.6.1 Future directions

There are a number of potentially interesting directions for further work. To begin with, a more thorough analysis of the symmetries of p-adic field theories should be interesting. We started with the simplest possible lattice action invariant under the isometries of T_q, and from it we derived correlators with some version of p-adic conformal symmetry. We should ask, what exactly are the symmetries of these correlators? Is the symmetry group simply $\mathrm{PGL}(2, \mathbb{Q}_q)$? Or is there a larger symmetry algebra analogous to the Virasoro algebra? How much of the structure of correlators is fixed by symmetry considerations? For example, how much is the four-point function constrained by symmetry? We should also ask whether we can proceed beyond scalar fields on the Bruhat–Tits trees and correspondingly scalar operators in the field theory. If we start with more sophisticated lattice models on T_q, might we obtain correlators which can be expressed as products of multiplicative characters other than $|x|_p^s$?

Another interesting avenue to pursue is loop corrections. All our calculations have relied on treating the bulk theory as classical, meaning that we focus on the specific field configuration which extremizes the action. Adding in fluctuations perturbatively does not seem impossible, but the more interesting prospect is to pass to a fully statistical mechanical account of the bulk, where a "temperature" is dialed up from 0, where our classical account is justified, to arbitrary finite values. This may allow a closer connection with [54] as well as earlier works including [82, 83]. Ideally, it may help us understand deeper connections with fluctuating fields in Archimedean AdS/CFT. The real prize, of course, is to understand fluctuating geometry. We suspect it is necessary to go beyond the Bruhat–Tits tree in order to properly formulate questions about dynamical geometry. Perhaps the refinements of T_q introduced in (2.151)–(2.163) will be of help in this regard.

Finally, yet another direction to explore is the full range of possible extensions

of $\mathbb{Q}_p$. Some questions include: What is the most natural notion of dimension in a boundary theory formulated on a (partially) ramified extension of $\mathbb{Q}_p$? What sorts of correlators are sensitive to the particular extension we pick? How is information about the extension encoded in the tree structure and in natural bulk actions?

In the next chapter, we take a closer look at p-adic CFTs, the operator product expansion, conformal blocks, and the full four-point function.

Chapter 3

Efficient computation techniques on the Bruhat–Tits tree

This chapter is based on a lightly edited version of a paper with Steven S. Gubser [84]. We thank Bartek Czech, Eric Perlmutter, and Shivaji Sondhi for useful discussions.

3.1 Introduction and summary

In the previous chapter, we initiated the formulation of a non-Archimedean AdS/CFT correspondence, focussing on a toy model in the bulk - an interacting scalar field in a fixed classical geometry. We performed simple bulk calculations to obtain holographic correlators, namely the two-point function and the three- and four-point functions (limited to the contact diagram) of identical scalar operators. Like in the Archimedean case, the three-point function is entirely fixed by conformal invariance, upto an overall constant, and we found that this overall constant, which gives the OPE coefficient in the dual CFT once the normaliza-

tion of the two-point function is fixed, admitted an adelic expression,[1] when expressed in terms of local zeta functions. The p-adic four-point function had a simple closed form expression, and the coefficient of the log term also admitted an adelic form. In this chapter we will study the connection between the p-adic and Archimedean four-point functions more closely, and include this time the exchange diagrams arising from cubic bulk interaction vertices in the analysis.

Thanks to the tree-like geometry of the bulk, the computation of holographic correlators, done via evaluating Feynman diagrams on the tree, gets reduced to simple geometric sums. In principle, we should be able to evaluate *exactly* any Feynman diagram on the Bruhat–Tits tree (at least as long as backtracking is disallowed), although the complexity of the diagram might make the calculation computationally tedious. It is desirable to develop computational techniques which make the evaluation of Feynman diagrams, for example higher-point correlators between different operators or loop diagrams in the bulk, more straightforward. To this end, in this chapter we introduce various "propagator identities" on the Bruhat–Tits tree, some of which are inspired by analogous identities in the Archimedean setting, which help evaluate bulk diagrams without ever having to explicitly do any tedious bulk integrations (more precisely, tree summations). These identities can be proven once and for all, and the proofs involve straightforward tree summations. Our focus in this chapter will be on finding these identities, and then applying them to evaluate the complete four-point function of scalar operators. [2] These identities can easily be used to evaluate higher-point correlators and loop corrections to tree-level bulk Feynman diagrams as well, but

[1] More precisely, we found they had adelic forms up to an overall factor of 2.

[2] After the publication of work on which this chapter is based [84], related work appeared [85] where a direct computation of the p-adic exchange diagram was attempted, in the special case of identical external operators. The limited applicability of the brute-force calculations is in stark contrast with the leverage provided by the computational techniques introduced in [84] (and described in this chapter).

we won't have occasion to comment on that in this dissertation.

A key component of the methods presented here will be the equivalence between "geodesic bulk diagrams" and conformal blocks [86], often termed "geodesic Witten diagrams" since they are a simplification of the diagrammatic techniques introduced in [24]. In the Archimedean case, geodesic bulk diagrams are bulk exchange diagrams with the bulk points of integration restricted to the geodesics joining the boundary points, rather than the whole of AdS space. A geodesic bulk diagram so constructed turns out to be directly proportional to the four-point conformal blocks of the boundary CFT [86]. Due to the fact that all paths on the Bruhat–Tits tree are geodesics (provided backtracking is disallowed), we expect that if an analogous result were to be true in non-Archimedean AdS/CFT, it would be straightforward to prove. Indeed, we show that the proportionality between geodesic bulk diagrams and conformal blocks carries over to the p-adics effortlessly.

The computation of the four-point functions then proceeds as follows: we use various propagator identities to reduce the tree summation to geodesic bulk diagrams, following which we use the relation between geodesic bulk diagrams and conformal blocks to obtain the physical conformal block decomposition of the four-point function. Compared to the situation in Archimedean AdS/CFT, we find the p-adic contact and exchange diagrams in the direct and crossed channels have much simpler forms, and in fact we are able to obtain explicit closed-form expressions for them. These remarkable simplifications arise due to the fact that only the simplest double-trace operators appear in the conformal block decomposition of the diagrams — the ones with *no* derivatives; additionally no descendants contribute either. Despite the simplifications, one continues to find striking similarities between the results in $\mathbb{R}^n$ and $\mathbb{Q}_{p^n}$, and we emphasize these in this

chapter.[3]

To better understand the contrast between the Archimedean and non-Archimedean four-point functions, we highlight the key difference between operators in the Archimedean case and the non-Archimedean case, which are both real (or complex) valued functions, but have domains lying, respectively in the reals and the p-adics: a real (or complex) valued function which is supported on the p-adics does *not* admit local derivatives [87]. [4] (To write down the kinetic term in a p-adic CFT, we will use a non-local notion of derivative, called the Vladimirov derivative, defined in the next chapter.) The lack of local derivatives leads to much simpler operator product expansions (OPEs) in p-adic CFTs, first studied in [87] for two-dimensional CFTs. No descendants appear in the p-adic OPE; in fact in such a CFT a local stress-tensor is absent. [5] This is the reason why the p-adic conformal blocks are trivial, and the conformal block decomposition of the p-adic four-point function is significantly simpler.

In order to make contact with the standard results in $\mathbb{R}^n$, we restrict ourselves to a bulk scalar field on a fixed AdS background, since in this case the dual CFT

[3]We will often refer to the usual (Archimedean) AdS/CFT correspondence over the reals simply as $\mathbb{R}^n$, and refer to the non-Archimedean case over the p-adics simply as $\mathbb{Q}_{p^n}$.

[4]The theory of *p-adic* valued functions supported on the p-adics, referred to as p-adic analysis, is richer (see, for example, chapter 4 of [49]). However, it still is limited and different from *real* analysis in several aspects, the root cause being the lack of a mean-value theorem in the p-adics. The basic reason for that is while $\mathbb{R}$ is a connected metric space, the non-Archimedean p-adic field has a totally disconnected topology, which means for instance, that two open sets are either totally disjoint or one is fully contained inside the other. One can define intervals in $\mathbb{R}$ since it is an ordered field, and there is a well-defined notion of inequalities when comparing two elements in $\mathbb{R}$. This is not true in $\mathbb{Q}_p$.

It turns out p-adic valued functions which may be expressed as power series are simpler to deal with and a bit more like their real valued counterparts, but for a richer and more complete theory of p-adic analysis, one must study the sophisticated subject of *rigid analytic spaces* (see, for instance, [88]).

[5]Nevertheless, p-adic field theories share several common features with usual field theories, including renormalization group flows and the existence of a Wilson-Fisher fixed point which we study in the next chapter. At the fixed point, we will find in chapter 4 that anomalous dimensions admit universal expressions independent of the choice of space, whether p-adic or real.

in $\mathbb{R}^n$ lacks a stress tensor as well.[6] Like in chapter 2, the discrete bulk Euclidean action we will consider is

$$S[\phi] = \sum_{\langle ab \rangle} \frac{1}{2}(\phi_a - \phi_b)^2 + \sum_{a \in T_{p^n}} \left(\frac{1}{2} m_\Delta^2 \phi_a^2 + \frac{g_3}{3!}\phi_a^3 + \frac{g_4}{4!}\phi_a^4 \right), \tag{3.1}$$

which describes a single scalar field ϕ living on the vertices. This is the same action as the one written in (2.19), but with a slight change in notation. As before, the first sum in (3.1) runs over all edges, and the second sum runs over all the vertices of T_{p^n}, the Bruhat–Tits tree with coordination number $p^n + 1$. Here g_3 and g_4 are coupling constants, and the mass of the scalar is related to the scaling dimension of the dual operator, Δ via

$\mathbb{Q}_{p^n}$

$$m_\Delta^2 \equiv m_{\mathbb{Q}_{p^n},\Delta}^2 = \frac{-1}{\zeta(-\Delta)\zeta(\Delta - n)}\,. \tag{3.2}$$

The somewhat non-standard notation used in (3.2) and the rest of this chapter and the next is explained at the end of this section. It is worth noting here that the zeta function that appears in (3.2) is *not* the Riemann zeta function; instead, we reserve the symbol ζ to stand for the so-called local zeta functions introduced in the previous chapter, repeated once again in (3.4)-(3.5) with a slight notational change.

Thus far, we have lacked an explicit example of a dual pair of theories in the non-Archimedean AdS/CFT correspondence. The final goal in this chapter is to make progress along this direction by constructing a minimal bulk action which reproduces the two-, three- and four-point functions of a free-field theory. We will do that by introducing a nearest neighbor interaction in the bulk tree,

[6] In [32], in the context of p-adic AdS/CFT, a "stress-tensor" like operator dual to "graviton fluctuations" was considered. The bulk description consisted of a scalar field defined on the vertices of the Bruhat–Tits tree, with the "graviton" described as edge-length fluctuations. The operator dual to edge-length fluctuations shared some properties with the stress-tensor, such as the correct scaling dimension, but seemed to lack others, such as a notion of spin. In this dissertation, we avoid the unresolved question of the properties of a stress tensor in p-adic CFTs by restricting to a fixed bulk without dynamical gravity. For unrelated reasons, CFTs in $\mathbb{R}^n$ without a stress tensor were also recently considered in [89, 90, 91].

evaluating its contributions to the four-point correlator, and tuning the cubic and quartic bulk couplings to obtain the connected free-field correlators up to the four-point function. We will also make some comparisons of our construction with the Archimedean case.

We would now like to explain the non-standard notation used in this chapter and the next. Equations applicable only in $\mathbb{R}^n$ or $\mathbb{Q}_{p^n}$ will be marked to indicate so. For instance, the mass-scaling dimension relation between mass of a scalar field, and the scaling dimension of the dual operator in $\mathbb{Q}_{p^n}$ is given by (3.2), while in $\mathbb{R}^n$ it is the well known relation

$$\mathbb{R}^n \qquad m_\Delta^2 \equiv m^2_{\mathbb{R}^n,\Delta} = \Delta(\Delta - n)\,. \tag{3.3}$$

Throughout chapters 3 and 4, we will be expressing results in terms of the local zeta functions, defined to be

$$\mathbb{Q}_{p^n} \qquad \zeta(s) \equiv \zeta_{\mathbb{Q}_p}(s) = \frac{1}{1-p^{-s}} \tag{3.4}$$

and

$$\mathbb{R}^n \qquad \zeta(s) \equiv \zeta_{\mathbb{R}}(s) = \pi^{-s/2}\Gamma_{\text{Euler}}(s/2)\,, \tag{3.5}$$

in $\mathbb{Q}_{p^n}$ and $\mathbb{R}^n$, respectively.[7] The reason for defining the local zeta functions is that holographic correlators in $\mathbb{R}^n$ and $\mathbb{Q}_{p^n}$ have more or less a universal form as we already saw in chapter 2, when expressed in terms of these local zeta functions. Equations which hold both in $\mathbb{R}^n$ and $\mathbb{Q}_{p^n}$ will be left unmarked. For instance in $\mathbb{R}^n$ and $\mathbb{Q}_{p^n}$, it will be useful to define[8]

$$\beta^{(\Delta_1,\Delta_2)} \equiv \frac{\zeta(\Delta_1)\zeta(\Delta_2)}{\zeta(\Delta_1+\Delta_2)}\,. \tag{3.6}$$

[7]Here and in chapter 4, we avoid defining local zeta functions for $\mathbb{R}^n$ or $\mathbb{Q}_{p^n}$ and prefer to use only the local zeta functions defined in (3.4) and (3.5).

[8]In $\mathbb{R}^n$, $\beta^{(\Delta_1,\Delta_2)}$ reduces to the usual Euler Beta function, $\beta^{(\Delta_1,\Delta_2)}_{\mathbb{R}^n} = \text{B}_{\text{Euler}}(\Delta_1/2, \Delta_2/2)$.

From a purely CFT perspective, it will be shown in chapter 4 (in the context of the p-adic $O(N)$ model), that correlators and anomalous dimensions of various operators admit expressions expressible entirely in terms of suitably defined local Gamma and Beta functions, which are ultimately constructed out of the local zeta functions defined in (3.4)-(3.5). It is satisfying to see the same functions appear both from purely bulk calculations as well as purely boundary considerations, especially since in the context of p-adic AdS/CFT the bulk/boundary correspondence relates two seemingly disparate constructs: a bulk described by a discrete tree and a boundary described by the continuum of p-adic numbers. We will not have occasion to use the local Gamma and Beta functions in this chapter (though (3.6) is related); however, to prevent confusion we will always use Euler's Gamma and Beta functions as $\Gamma_{\text{Euler}}(z)$ and $\text{B}_{\text{Euler}}(z,w)$.

We also emphasize and clarify the terminology used in this chapter with reference to bulk exchange diagrams in various channels. Throughout the chapter, we will assume that the boundary operator insertion points $x_i \in \mathbb{Q}_{p^n}$ are in a configuration as depicted in figure 3.1, which corresponds to $u < v = 1$ (u and v are cross-ratios defined in (3.30)), and we have reserved the term 's-channel' to refer to that. (This admittedly confusing terminology has no connection with the textbook terminology for exchange of particles in an intermediate channel. Instead we refer to exchanges as, for example, the "exchange in the (12)(34) channel.") Note that this is not a simplification but in fact fully general on the Bruhat–Tits tree. Given any four boundary points, up to relabelling the x_i, they always arrange themselves in an 's-channel' configuration, with one exception. The exceptional case corresponds to $u = v = 1$, or equivalently when the bulk points c_1 and c_2 in figure 3.1 coincide. All our formulae derived in this chapter are applicable when $u = v = 1$, which can be thought of as a degeneration of the s-, t-, and u-channel boundary configurations, where for example, the 't-channel'

configuration is obtained after switching x_2 and x_3 in figure 3.1.[9] It is worth emphasizing that $u = v = 1$ is the *only* case which admits a pairwise overlap between the s-, t- and u-channels [87].

Finally the normalization of bulk-to-boundary propagator and the two-point function differs slightly from the one used in chapter 2 — see footnotes 12 and 23 in this chapter.

The organisation of the rest of the chapter is as follows. In section 3.2 we establish the relation between p-adic conformal blocks and geodesic bulk diagrams on the Bruhat–Tits tree, and in section 3.3 we use results from section 3.2 as well as some bulk propagator identities to evaluate the full four-point function of scalar operators (including contact interactions as well as exchange diagrams in all channels). In section 3.4 we describe a minimal bulk construction which yields the two-, three-, and four-point functions of a free theory on the boundary. We end with a summary and discussion of some open questions in section 3.5. In the appendices we list some additional propagator identities on the Bruhat–Tits tree, illustrate crossing symmetry in the p-adics, and explore the connection between nearest neighbor interactions and derivative couplings.

3.2 Conformal blocks and geodesic bulk diagrams

3.2.1 The p-adic OPE and the three-point function

The OPE between two (scalar) operators in a CFT takes the general form

$$\mathcal{O}_1(x_1)\mathcal{O}_2(x_2) = \sum_r \widetilde{C}_{12r}|x_{12}|^{-\Delta_1-\Delta_2+\Delta_r}\mathcal{O}_r(x_2)\,, \tag{3.7}$$

[9] Curiously, this degeneration is impossible when $p^n = 2$, since the Bruhat–Tits tree T_2 has coordination number 3, while we need a coordination number of at least 4 to realize $u = v = 1$. This is one of the many reasons, which are all related to the fact that 2 is an even prime, why 2-adic conformal field theories may be quite exotic.

where the sum is over all operators in the CFT. The operator $\mathcal{O}_r$ has scaling dimension Δ_r, and $\widetilde{C}_{ijk}$s are the OPE coefficients. In a p-adic CFT, descendants do not appear in the OPE, and the index r runs only over the 'primaries' [87]. A scalar 'primary' operator $\mathcal{O}$ with scaling dimension Δ transforms under p-adic conformal transformations,

$$\mathbb{Q}_{p^n} \qquad z \to z' = \frac{az+b}{cz+d}\,, \quad \begin{pmatrix} a & b \\ c & d \end{pmatrix} \in \mathrm{PGL}(2,\mathbb{Q}_{p^n}) \tag{3.8}$$

as

$$\mathbb{Q}_{p^n} \qquad \mathcal{O}'(z') = \left|\frac{ad-bc}{(cz+d)^2}\right|^{-\Delta} \mathcal{O}(z)\,, \tag{3.9}$$

where $|\cdot|$ represents the p-adic norm. This serves as the defining property of scalar 'primary' operators in p-adic CFTs [87]. Moreover, we postulate orthonormality

$$\langle \mathcal{O}_i(x_1)\mathcal{O}_j(x_2)\rangle = \frac{\delta_{ij}}{|x_{12}|^{2\Delta_j}}\,. \tag{3.10}$$

First consider a theory of bulk scalars of generic masses with cubic couplings of the form $\phi_i\phi_j\phi_k$ in a fixed AdS background. The p-adic OPE of two non-degenerate operators takes the form in (3.7) where the sum runs over all operators, including multi-trace. Inserting a single-trace operator $\mathcal{O}_3$ at x_3 of dimension $\Delta_3 \neq \Delta_1+\Delta_2$ such that $|x_{12}| < |x_{13}|, |x_{23}|$, the three-point function of three single-trace operators following from the OPE is

$$\begin{aligned} \mathbb{Q}_{p^n} \qquad \langle \mathcal{O}_1(x_1)\mathcal{O}_2(x_2)\mathcal{O}_3(x_3)\rangle &= \sum_r \widetilde{C}_{12r}|x_{12}|^{-\Delta_1-\Delta_2+\Delta_r}\langle \mathcal{O}_r(x_2)\mathcal{O}_3(x_3)\rangle \\ &= \widetilde{C}_{123}|x_{12}|^{-\Delta_1-\Delta_2+\Delta_3}|x_{23}|^{-2\Delta_3}\,, \end{aligned} \tag{3.11}$$

where we used the orthonormality property (3.10) and assumed that the cubic coupling $\phi_1\phi_2\phi_3$ is present. Since p-adic conformal invariance fixes the form of the three-point function up to an overall constant $\widetilde{f}_{ijk}$ [87], we may set (3.11) to

$$\langle \mathcal{O}_1(x_1)\mathcal{O}_2(x_2)\mathcal{O}_3(x_3)\rangle = \frac{\widetilde{f}_{123}}{|x_{12}|^{\Delta_1+\Delta_2-\Delta_3}|x_{23}|^{\Delta_2+\Delta_3-\Delta_1}|x_{13}|^{\Delta_3+\Delta_1-\Delta_2}}\,. \tag{3.12}$$

Ultrametricity of the p-adic norm implies $|x_{13}| = |x_{23}|$.[10] This immediately yields at leading order (i.e. tree-level),

$\mathbb{Q}_{p^n}$ $$\widetilde{C}_{123} = \widetilde{f}_{123}\,. \tag{3.13}$$

The OPE coefficient can be determined by working out the three-point function holographically. For operators with generic dimensions $\Delta_1, \Delta_2, \Delta_3$, which are bulk duals to ϕ_1, ϕ_2, ϕ_3 appearing in a cubic vertex,[11] the standard prescription in $\mathbb{R}^n$ to compute the tree-level contribution to the three-point function is to evaluate the integral[12]

$\mathbb{R}^n$ $$\langle \mathcal{O}_1(\vec{x}_1)\mathcal{O}_2(\vec{x}_2)\mathcal{O}_3(\vec{x}_3)\rangle = \mathcal{N}_3 \int \frac{d^{n+1}y}{y_0^{n+1}} \left(\prod_i^3 \hat{K}_{\Delta_i}(y_0, \vec{y}-\vec{x}_i)\right), \tag{3.14}$$

where $\hat{K}_\Delta$ is the unnormalized bulk-to-boundary propagator

$\mathbb{R}^n$ $$\hat{K}_\Delta(y_0, \vec{y}-\vec{x}) = \frac{y_0^\Delta}{(y_0^2 + (\vec{y}-\vec{x})^2)^\Delta}\,, \tag{3.15}$$

and

$$\mathcal{N}_k \equiv -g_k \left(\prod_i^k \sqrt{\widetilde{c}_{\Delta_i}}\right)\,, \tag{3.16}$$

with

$\mathbb{R}^n$ $$\widetilde{c}_\Delta \equiv c_\Delta/(2\Delta - n)\,, \tag{3.17}$$

and

$$c_\Delta \equiv \zeta(2\Delta)/\zeta(2\Delta - n)\,. \tag{3.18}$$

[10]The proof proceeds as follows. Rewrite $|x_{13}| = |x_{12} + x_{23}|$. By assumption, $|x_{12}| < |x_{23}|$. Then the desired relation follows directly from the general property of the p-adic norm that $|x + y| = |x|$ if $|x| > |y|$.

[11]In the special case of non-generic scaling dimensions with $\Delta_i + \Delta_j - \Delta_k = 0$, anomalous dimensions become important at tree-level. We will not address this case here.

[12]The normalization differs slightly from the one used in chapter 2, due to the different choice of normalization for the two-point function. (See also footnote 23.)

In $\mathbb{Q}_{p^n}$, as discussed in chapter 2, integration over the bulk point y gets replaced by a sum over all vertices a of the Bruhat–Tits tree, giving

$$\mathbb{Q}_{p^n} \qquad \langle \mathcal{O}_1(x_1)\mathcal{O}_2(x_2)\mathcal{O}_3(x_3)\rangle = \mathcal{N}_3 \sum_{a\in T_{p^n}} \left(\prod_i^3 \hat{K}_{\Delta_i}(a,x_i)\right), \tag{3.19}$$

where the unnormalized bulk-to-boundary propagator $\hat{K}_\Delta$ is given by

$$\mathbb{Q}_{p^n} \qquad \hat{K}_\Delta(a,x) = \hat{K}_\Delta(y_0, y-x) = \frac{|y_0|^\Delta}{|y_0, y-x|_s^{2\Delta}}, \tag{3.20}$$

$\mathcal{N}_3$ is as in (3.16), $\widetilde{c}_\Delta$ is defined to be

$$\mathbb{Q}_{p^n} \qquad \widetilde{c}_\Delta \equiv \frac{c_\Delta}{p^\Delta/\zeta(2\Delta-n)}\,, \tag{3.21}$$

and c_Δ is given by (3.18). In the first equality in (3.20), the bulk vertex a is re-expressed in terms of the boundary coordinate $y \in \mathbb{Q}_{p^n}$ and the bulk depth coordinate $y_0 \in p^{\mathbb{Z}}$ which, as we explained in chapter 2, together specify a. The notation $|z,w|_s$ stands for supremum norm, $|z,w|_s \equiv \sup\{|z|,|w|\}$.[13]

In $\mathbb{R}^n$, evaluating the three-point function given in (3.14), leads to (3.12) with [77]

$$\mathbb{R}^n \qquad \widetilde{f}_{123} = \frac{\mathcal{N}_3}{2} f_{123}\,, \tag{3.22}$$

where

$$f_{ijk} \equiv \zeta(\Delta_i+\Delta_j+\Delta_k-n)\frac{\zeta(\Delta_i+\Delta_{jk})\zeta(\Delta_j+\Delta_{ki})\zeta(\Delta_k+\Delta_{ij})}{\zeta(2\Delta_i)\zeta(2\Delta_j)\zeta(2\Delta_k)}\,. \tag{3.23}$$

Here $\Delta_{ij} = \Delta_i - \Delta_j$ and $\zeta(s)$ is defined in (3.5). By comparison in p-adic AdS/CFT, to evaluate (3.19) a simple generalization of the computation of the holographic three-point amplitude presented in chapter 2 leads to (3.12) with

$$\mathbb{Q}_{p^n} \qquad \widetilde{f}_{123} = \mathcal{N}_3\, f_{123}\,, \tag{3.24}$$

[13]For brevity, from now on we will suppress the vector symbol on boundary coordinates in $\mathbb{R}^n$, and analogous to the p-adics, refer to bulk coordinates with lower-case Latin alphabets such as a, b, c, so that for example, $a = (y_0, \vec{y})$. Boundary coordinates will usually be denoted using letters from the other end of the alphabet, for example x, y, z.

where f_{123} is again given by (3.23), and $\zeta(s)$ is defined in (3.4).

While the equalities in (3.22) and (3.24) are sufficient to show the striking similarity between the form of the structure constants in $\mathbb{R}^n$ and $\mathbb{Q}_{p^n}$, an alternate form for the structure constants will be more instructive when we later compare the scalar four-point functions in $\mathbb{R}^n$ and $\mathbb{Q}_{p^n}$. For $n = 2$ in $\mathbb{R}^n$,

$$\mathbb{R}^n \qquad \widetilde{f}_{123} \overset{(n=2)}{=} \frac{-\mathcal{N}_3}{\widetilde{c}_{\Delta_1+\Delta_2}} \beta^{(\Delta_3+\Delta_{12},\Delta_3-\Delta_{12})} \sum_{M=0}^{\infty} \frac{a_M^{(\Delta_1,\Delta_2)}}{m^2_{\Delta_3} - m^2_{\Delta_1+\Delta_2+2M}}\,, \tag{3.25}$$

where $\widetilde{c}_\Delta$ is defined in (3.17), $\beta^{(s,t)}$ is defined in (3.6), the mass squared in $\mathbb{R}^n$ is given by (3.3), and

$$\mathbb{R}^n \qquad a_M^{(\Delta_1,\Delta_2)} \equiv \frac{1}{\beta^{(2\Delta_1+2M,2\Delta_2+2M)}} \frac{(-1)^M}{M!} \frac{(\Delta_1)_M (\Delta_2)_M}{(\Delta_1+\Delta_2+M-n/2)_M}\,, \tag{3.26}$$

where $(\Delta)_M \equiv \Gamma_{\text{Euler}}(\Delta+M)/\Gamma_{\text{Euler}}(\Delta)$ is the Pochhammer symbol. On the other hand, in $\mathbb{Q}_{p^n}$ for general n,

$$\mathbb{Q}_{p^n} \qquad \widetilde{f}_{123} = \frac{-\mathcal{N}_3}{\widetilde{c}_{\Delta_1+\Delta_2}} \beta^{(\Delta_3+\Delta_{12},\Delta_3-\Delta_{12})} \frac{a^{(\Delta_1,\Delta_2)}}{m^2_{\Delta_3} - m^2_{\Delta_1+\Delta_2}}\,. \tag{3.27}$$

Here $\widetilde{c}_\Delta$ is defined in (3.21) and $\beta^{(s,t)}$ is defined in (3.6). The p-adic mass squared is given by (3.2), and

$$\mathbb{Q}_{p^n} \qquad a^{(\Delta_1,\Delta_2)} \equiv \frac{1}{\beta^{(2\Delta_1,2\Delta_2)}}\,. \tag{3.28}$$

Although the equality in (3.25) holds only for $n = 2$, the comparison between (3.25) and (3.27) proves useful in section 3.3, when we compare the four-point functions in $\mathbb{R}^n$ and $\mathbb{Q}_{p^n}$ for any n. The absence of an infinite sum in (3.27) along the lines of (3.25) turns out to be directly related to the absence of derivatives in the OPE in p-adic CFTs. We will return to this point in section 3.3. It is worth making the trivial observation that at $M = 0$, $a_M^{(\Delta_1,\Delta_2)}$ in (3.26) reduces to the simple form

$$\mathbb{R}^n \qquad a_0^{(\Delta_1,\Delta_2)} = \frac{1}{\beta^{(2\Delta_1,2\Delta_2)}}, \tag{3.29}$$

which is to be compared with the definition (3.28) in $\mathbb{Q}_{p^n}$.

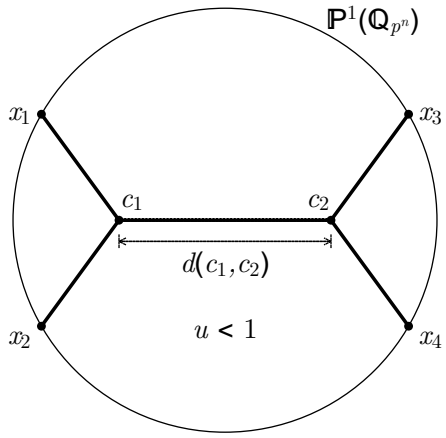

Figure 3.1: Boundary points x_i in the s-channel configuration. Solid lines are geodesics on the Bruhat–Tits tree, tracing the path joining the four points together. Bulk points c_1, c_2 are uniquely fixed once x_i are specified. The conformal cross-ratio in (3.30) is given by $u = p^{-d(c_1,c_2)}$ where $d(c_1, c_2)$ is the graph distance between points c_1 and c_2. In the s-channel configuration, $u < 1$.

3.2.2 Four-point contact diagram

For four boundary points x_1, x_2, x_3 and x_4, the conformal cross-ratios u and v are defined to be

$$\mathbb{Q}_{p^n} \qquad u \equiv \left|\frac{x_{12}x_{34}}{x_{13}x_{24}}\right| \qquad v \equiv \left|\frac{x_{14}x_{23}}{x_{13}x_{24}}\right| . \tag{3.30}$$

In this chapter, the points of insertion of external scalar operators will always be in an 's-channel' configuration on the boundary (see figure 3.1). The defining property of 's-channel' is that the cross-ratio $u < 1$. A striking consequence of ultrametricity is that, $u < 1 \Rightarrow v = 1$. To prove this, observe that

$$\mathbb{Q}_{p^n} \qquad \frac{x_{14}x_{23}}{x_{13}x_{24}} = 1 - \frac{x_{12}x_{34}}{x_{13}x_{24}} . \tag{3.31}$$

The claim then follows directly from an application of the ultrametric property of p-adic norms described in footnote 10.

We define the p-adic four-point contact amplitude to be the sum

$$\mathbb{Q}_{p^n} \qquad \mathcal{D}(x_i) \equiv \frac{1}{W_0(x_i)} \sum_{a \in T_{p^n}} \left(\prod_i^4 \hat{K}_{\Delta_i}(a, x_i) \right) , \tag{3.32}$$

where

$$\mathbb{Q}_{p^n} \qquad W_\Delta(x_i) \equiv \hat{K}_{\Delta_1}(c_1,x_1)\hat{K}_{\Delta_2}(c_1,x_2)\hat{G}_\Delta(c_1,c_2)\hat{K}_{\Delta_3}(c_2,x_3)\hat{K}_{\Delta_4}(c_2,x_4)\,, \tag{3.33}$$

and $\hat{G}_\Delta$ is the unnormalized bulk-to-bulk propagator computed in chapter 2, given by

$$\mathbb{Q}_{p^n} \qquad \hat{G}_\Delta(c_1,c_2) = p^{-\Delta d(c_1,c_2)} = u^\Delta\,, \tag{3.34}$$

where c_1 and c_2 are the unique points of intersection of the geodesics joining together the boundary points x_i (see figure 3.1), and u is the cross-ratio defined in (3.30). The product in (3.33) evaluates to (see chapter 2 for similar computations)

$$\mathbb{Q}_{p^n} \qquad W_\Delta(x_i) = u^\Delta\, W_0(x_i), \tag{3.35}$$

where

$$\mathbb{Q}_{p^n} \qquad W_0 = \frac{1}{|x_{12}x_{34}|^{\sigma/2}} \prod_{1\le i<j\le 4} \frac{1}{|x_{ij}|^{\Delta_i+\Delta_j-\sigma/2}}, \tag{3.36}$$

with $\sigma \equiv \sum_{i=1}^4 \Delta_i$. It is clear that $W_0(x_i)$ carries the trivial coordinate dependence of the four-point function. An alternate representation for W_0 is

$$\mathbb{Q}_{p^n} \qquad W_0 = \left|\frac{x_{24}}{x_{14}}\right|^{\Delta_{12}} \left|\frac{x_{14}}{x_{13}}\right|^{\Delta_{34}} \frac{v^{(\Delta_{12}-\Delta_{34})/2}}{|x_{12}|^{\Delta_1+\Delta_2}|x_{34}|^{\Delta_3+\Delta_4}}, \tag{3.37}$$

where we can freely set $v = 1$ in the 's-channel'.

The sum over Bruhat–Tits tree in (3.32) was computed in chapter 2 in the special case of identical Δ_i. Generalizing to non-identical Δ_i, we obtain[14]

$$\mathbb{Q}_{p^n} \qquad \mathcal{D}(x_i) = u^{\Delta_A} f_{34A} + u^{\Delta_B} f_{12B}\,, \tag{3.38}$$

[14]For convergence of the sum in (3.32), we require:

$$\sum_{i=1}^4 \Delta_i > n \qquad \Delta_2+\Delta_3+\Delta_4 > \Delta_1 \quad \text{and other permutations.}$$

The computation proceeds straightforwardly using the tree-summation methods described in chapter 2. Later in section 3.3.2, we will provide an alternate derivation of (3.38).

where

$$\Delta_A = \Delta_1 + \Delta_2 \qquad \Delta_B = \Delta_3 + \Delta_4\,, \tag{3.39}$$

and the f_{ijk}s are given by (3.23). We note that $\mathcal{D}(x_i)$ depends on the coordinates only through the cross-ratio u, and from here on we will simply write it as $\mathcal{D}(u)$. The tree-level four-point function is thus given by

$\mathbb{Q}_{p^n}$
$$\langle \mathcal{O}_1(x_1)\mathcal{O}_2(x_2)\mathcal{O}_3(x_3)\mathcal{O}_4(x_4)\rangle = \mathcal{N}_4 W_0(x_i)\mathcal{D}(u), \tag{3.40}$$

assuming no bulk cubic couplings are present, with $\mathcal{N}_4$ given by (3.16). In $\mathbb{R}^n$, conformal invariance constrains the four-point function of scalar operators to be of the form

$\mathbb{R}^n$
$$\langle \mathcal{O}_1(x_1)\mathcal{O}_2(x_2)\mathcal{O}_3(x_3)\mathcal{O}_4(x_4)\rangle = W_0(x_i) g(u,v), \tag{3.41}$$

where $W_0(x_i)$ is given by

$\mathbb{R}^n$
$$W_0 \equiv \left(\frac{|x_{24}|}{|x_{14}|}\right)^{\Delta_{12}} \left(\frac{|x_{14}|}{|x_{13}|}\right)^{\Delta_{34}} \frac{1}{|x_{12}|^{\Delta_1+\Delta_2}|x_{34}|^{\Delta_3+\Delta_4}}, \tag{3.42}$$

and $g(u,v)$ is an arbitrary function of cross-ratios u and v, defined to be

$\mathbb{R}^n$
$$u \equiv \frac{|x_{12}||x_{34}|}{|x_{13}||x_{24}|} \qquad v \equiv \frac{|x_{14}||x_{23}|}{|x_{13}||x_{24}|}\,, \tag{3.43}$$

where $|\cdot|$ are L^2-norms in $\mathbb{R}^n$. As noted above (3.31), in the 's-channel' in $\mathbb{Q}_{p^n}$ one of the cross-ratios is trivial. So we see that up to an overall normalization factor, $\mathcal{D}(u)$ is the p-adic analog of $g(u,v)$. From here on we will not concern ourselves with the four-point function $\langle \mathcal{O}\ldots\mathcal{O}\rangle$, but study directly the amplitude $\mathcal{D}(u)$, which is stripped off of the trivial kinematic factors and contains only the dynamical information of the theory.

3.2.3 p-adic conformal blocks

In analogy with the decomposition of $g(u,v)$ into conformal blocks in $\mathbb{R}^n$, the amplitude $\mathcal{D}(u)$ may also be decomposed into (scalar) conformal blocks $\mathcal{G}_\Delta(u)$,

$\mathbb{Q}_{p^n}$
$$\mathcal{D}(u) = \sum_r C_{12r} C_{34r}\, \mathcal{G}_{\Delta_r}(u)\,. \tag{3.44}$$

Comparing with (3.38), we see the p-adic conformal blocks are simply given by

$\mathbb{Q}_{p^n}$
$$\mathcal{G}_\Delta(u) = u^\Delta\,. \tag{3.45}$$

We can now also identify the kinematic factor $W_\Delta(x_i)$ in (3.35) with the scalar conformal partial wave, since

$\mathbb{Q}_{p^n}$
$$W_\Delta(x_i) = W_0(x_i)\mathcal{G}_\Delta(u)\,. \tag{3.46}$$

Incidentally in $\mathbb{R}^n$, the conformal partial wave takes the form

$\mathbb{R}^n$
$$W_\Delta(x_i) \equiv W_0(x_i)\mathcal{G}_\Delta(u,v)\,, \tag{3.47}$$

where $\mathcal{G}(u,v)$ is the scalar conformal block.[15]

To arrive at (3.44) starting from the OPE, consider a bulk theory of four scalar fields ϕ_i with a quartic interaction of the form $\phi_1\phi_2\phi_3\phi_4$ and no cubic coupling. The OPEs to consider are

$$\begin{aligned}\mathcal{O}_1(x_1)\mathcal{O}_2(x_2) &= \sum_r \widetilde{C}_{12r}|x_{12}|^{-\Delta_1-\Delta_2+\Delta_r}\mathcal{O}_r(x_2)\\ \mathcal{O}_3(x_3)\mathcal{O}_4(x_4) &= \sum_r \widetilde{C}_{34r}|x_{34}|^{-\Delta_3-\Delta_4+\Delta_r}\mathcal{O}_r(x_4)\,.\end{aligned} \tag{3.49}$$

[15]The contrast between the p-adic conformal blocks (3.45) and scalar conformal blocks in $\mathbb{R}^n$ is striking. In $\mathbb{R}^n$ the conformal block admits a double power series expansion in u^2 and $(1-v^2)$,

$\mathbb{R}^n$
$$\mathcal{G}_\Delta(u,v) = u^\Delta \sum_{m,n=0}^{\infty} a_{mn} u^{2m}(1-v^2)^n\,, \tag{3.48}$$

for some (known) coefficients a_{mn} [92].

For the OPEs to make sense, we must have

$$|x_{12}|, |x_{34}| < |x_{13}|, |x_{24}|, |x_{14}|, |x_{23}|\,. \tag{3.50}$$

These requirements are consistent with the s-channel configuration shown in figure 3.1. In fact the conditions (3.50) are stronger than just requiring $u < 1$, and due to ultrametricity, they lead to the following equalities:

$$\mathbb{Q}_{p^n} \qquad |x_{13}| = |x_{24}| = |x_{14}| = |x_{23}|\,, \tag{3.51}$$

which are consistent with but stronger than $v = 1$. Then using (3.10) we obtain

$$\langle \mathcal{O}_1(x_1)\mathcal{O}_2(x_2)\mathcal{O}_3(x_3)\mathcal{O}_4(x_4)\rangle \sum_r \widetilde{C}_{12r}\widetilde{C}_{34r}|x_{12}|^{-\Delta_1-\Delta_2+\Delta_r}|x_{34}|^{-\Delta_3-\Delta_4+\Delta_r}|x_{24}|^{-2\Delta_r}. \tag{3.52}$$

Recalling the properties of the p-adic OPE from section 3.2.1, and exploiting the fact that there are no bulk cubic couplings but only the quartic coupling $\phi_1\phi_2\phi_3\phi_4$, we conclude that at tree-level, the index r in (3.49) runs over only the double-trace operators $\mathcal{O}_B \equiv \mathcal{O}_3\mathcal{O}_4$ in the first line, and $\mathcal{O}_A \equiv \mathcal{O}_1\mathcal{O}_2$ in the second line of (3.49), with Δ_A and Δ_B given by (3.39) to leading order. Then using (3.40) and various equalities from (3.51), it is easy to show that (3.52) reproduces (3.38) provided we make the identification

$$\mathbb{Q}_{p^n} \qquad \widetilde{C}_{12r}\widetilde{C}_{34r} = \mathcal{N}_4 C_{12r}C_{34r} \qquad r = A, B \tag{3.53}$$

with

$$\mathbb{Q}_{p^n} \qquad C_{12A}C_{34A} = f_{34A} \qquad C_{12B}C_{34B} = f_{12B}\,, \tag{3.54}$$

where f_{ijk}s are given in (3.23). Crossing symmetry imposes the p-adic OPE coefficients $\widetilde{C}_{ijk}$ to satisfy associativity:[87]

$$\mathbb{Q}_{p^n} \qquad \sum_r \widetilde{C}_{ijr}\widetilde{C}_{k\ell r} = \sum_r \widetilde{C}_{i\ell r}\widetilde{C}_{jkr} = \sum_r \widetilde{C}_{ikr}\widetilde{C}_{j\ell r}\,. \tag{3.55}$$

The coefficients given in (3.53)-(3.54) satisfy (3.55) at leading order in the coupling. The associativity constraints with $\{i, j, k, \ell\}$ being some permutation of $\{1, 2, 3, 4\}$ leave some freedom to rescale the C_{ijk} while maintaining (3.54).[16]

3.2.4 Geodesic bulk diagrams

Following [86], we define the geodesic bulk diagram $\mathcal{W}_\Delta^S$ to be

$$\mathbb{Q}_{p^n} \qquad \mathcal{W}_\Delta^S \equiv \sum_{a\in\gamma_{12}} \sum_{b\in\gamma_{34}} \Big(\hat{K}_{\Delta_1}(x_1, a)\hat{K}_{\Delta_2}(x_2, a)\hat{G}_\Delta(a, b)\hat{K}_{\Delta_3}(b, x_3)\hat{K}_{\Delta_4}(b, x_4) \Big) , \tag{3.56}$$

where the bulk point a (b) is summed over the unique bulk geodesic γ_{12} (γ_{34}) on the Bruhat–Tits tree joining boundary points x_1 and x_2 (x_3 and x_4). The label S is unrelated to the 's-channel' configuration of the boundary points x_i, but indicates that the bulk points a and b are integrated along γ_{12} and γ_{34}, respectively. Later in section 3.3.4 we will have occasion to define $\mathcal{W}_\Delta^T$ and $\mathcal{W}_\Delta^U$. Figure 3.2 shows the *subway* diagram, i.e. a Feynman diagram on the Bruhat–Tits tree, for the geodesic bulk diagram $\mathcal{W}_\Delta^S$. Summing over a and b as indicated in (3.56) leads immediately to (see appendix 3.D for details)

$$\mathbb{Q}_{p^n} \qquad \frac{\mathcal{W}_\Delta^S}{W_\Delta} = \beta^{(\Delta+\Delta_{12},\Delta-\Delta_{12})}\beta^{(\Delta+\Delta_{34},\Delta-\Delta_{34})}. \tag{3.57}$$

The result (3.57) is to be compared with results of [86], where it is shown that that the Archimedean geodesic bulk diagram, $\mathcal{W}_\Delta^S$ is related to the conformal partial wave W_Δ via

$$\mathbb{R}^n \qquad \frac{\mathcal{W}_\Delta^S}{W_\Delta} = \frac{1}{4}\beta^{(\Delta+\Delta_{12},\Delta-\Delta_{12})}\beta^{(\Delta+\Delta_{34},\Delta-\Delta_{34})}, \tag{3.58}$$

[16] The aforementioned associativity boils down to verifying the unobvious identity

$$f_{34A} + f_{12B} = f_{24C} + f_{13D} = f_{23E} + f_{14F} ,$$

where the f_{ijk}s are given in (3.23), Δ_A, Δ_B are given in (3.39) and $\Delta_C = \Delta_1 + \Delta_3, \Delta_D = \Delta_2 + \Delta_4, \Delta_E = \Delta_1 + \Delta_4$ and $\Delta_F = \Delta_2 + \Delta_3$.

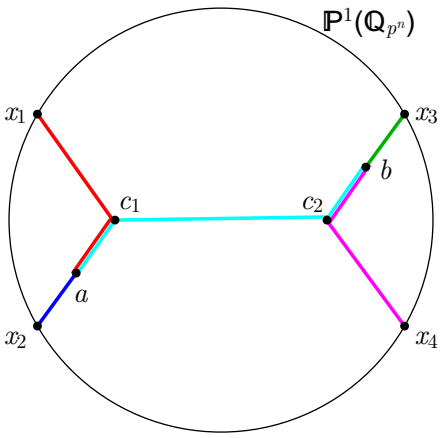

Figure 3.2: A geodesic subway diagram. Bulk point a runs along the geodesic joining x_1 with x_2, and b runs along the geodesic joining x_3 with x_4. Colors differentiate the individual propagators in (3.56).

and $\beta^{(s,t)}$ is defined in (3.6).[17] Remarkably, comparing (3.58) with (3.57), we see that the proportionality factors in $\mathbb{R}^n$ and $\mathbb{Q}_{p^n}$ have an (almost) identical form.

A special case of interest corresponds to setting all external dimensions equal to the dimension of the exchanged scalar. In this case, the tree-sum in (3.56) simplifies to (where now all $\Delta_i = \Delta$)

$\mathbb{Q}_{p^n}$
$$\mathcal{W}^S_\Delta = W_0(x_i) \times \sum_{a\in\gamma_{12}} \sum_{b\in\gamma_{34}} \hat{G}_\Delta(a,b), \tag{3.59}$$

On the other hand, setting all dimensions equal in (3.57) yields

$\mathbb{Q}_{p^n}$
$$\frac{\mathcal{W}^S_\Delta}{W_\Delta} = \left(\beta^{(\Delta,\Delta)}\right)^2 . \tag{3.60}$$

From (3.59), (3.60) and (3.46), it follows

$\mathbb{Q}_{p^n}$
$$\left(\beta^{(\Delta,\Delta)}\right)^2 \mathcal{G}_\Delta(u) = \sum_{a\in\gamma_{12}} \sum_{b\in\gamma_{34}} \hat{G}_\Delta(a,b)\,. \tag{3.61}$$

[17] Our notation differs slightly from the one used in [86]. In [86],

$$\beta_{\Delta ij} \equiv \frac{1}{2}\beta^{(\Delta+\Delta_{ij},\Delta-\Delta_{ij})}_{\mathbb{R}^n} = \frac{1}{2}\frac{\zeta_{\mathbb{R}}(s)\zeta_{\mathbb{R}}(t)}{\zeta_{\mathbb{R}}(s+t)}\,,$$

so that $\mathcal{W}^S_\Delta = \beta_{\Delta 12}\beta_{\Delta 34} W_\Delta$ (c.f. (3.3) of [86]). The difference in notation is the origin of the explicit factor of $1/4$ in (3.58).

For comparison, the Archimedean analog of (3.61) is [86, 93]

$$\mathbb{R}^n \qquad \frac{1}{4}\left(\beta^{(\Delta,\Delta)}\right)^2 \mathcal{G}_\Delta(u,v) = \int_{a\in\gamma_{12}} \int_{b\in\gamma_{34}} \hat{G}_\Delta(a,b)\,, \tag{3.62}$$

where $\hat{G}(a,b)$ is the unnormalized scalar bulk-to-bulk propagator in $\mathbb{R}^n$, and $\mathcal{G}_\Delta(u,v)$ is the scalar conformal block.

3.3 Four-point contact and exchange diagrams

In this section we introduce some p-adic propagator identities which greatly reduce the complexity of performing bulk integrations (more precisely, tree summations) encountered while evaluating various four-point amplitudes. The Archimedean analogs of these identities [86] proved to be of great use in $\mathbb{R}^n$ for the evaluation of bulk integrals in the scalar four-point contact and exchange diagrams, and we show below how this carries over to $\mathbb{Q}_{p^n}$.

3.3.1 Two AdS propagator identities

An identity which will be especially useful for decomposing bulk diagrams into geodesic bulk diagrams (and as a consequence of (3.57) and (3.46) into a conformal block decomposition) is

$$\mathbb{Q}_{p^n} \qquad \hat{K}_{\Delta_1}(b,x_1)\hat{K}_{\Delta_2}(b,x_2) = a^{(\Delta_1,\Delta_2)} \sum_{a\in\gamma_{12}} \hat{K}_{\Delta_1}(a,x_1)\hat{K}_{\Delta_2}(a,x_2)\hat{G}_{\Delta_1+\Delta_2}(a,b) \tag{3.63}$$

where $a^{(s,t)}$ is given by (3.28), and the bulk point a is restricted to lie along γ_{12}, which is the unique bulk geodesic joining x_1 to x_2. This identity can be verified straightforwardly by explicit evaluation, but it's helpful to think about it geometrically as well. On the Bruhat–Tits tree, the paths from x_1 and x_2 to b can be divided into two sub-paths each: the first which lies along the geodesic

joining x_1 and x_2, and the second which lies off of that geodesic, and which is in fact common to both the paths from x_1 and x_2 to b. The r.h.s. of (3.63) can similarly be seen to decompose into subpaths: the bulk-to-boundary propagators are restricted to lie along the geodesic joining x_1 and x_2, while the bulk-to-bulk propagator travels partially along the geodesic, and partially along the common subpath mentioned above. The overall factor accounts for the over-counting of paths on the r.h.s. The corresponding identity in $\mathbb{R}^n$ is [86][18]

$$\mathbb{R}^n \quad \hat{K}_{\Delta_1}(b,x_1)\hat{K}_{\Delta_2}(b,x_2) = 2\sum_{M=0}^{\infty} a_M^{(\Delta_1,\Delta_2)} \int_{a\in\gamma_{12}} \hat{K}_{\Delta_1}(a,x_1)\hat{K}_{\Delta_2}(a,x_2)\hat{G}_{\Delta_1+\Delta_2+2M}(a,b) \tag{3.64}$$

where $a_M^{(s,t)}$ is given by (3.26). The crucial difference between (3.63) and (3.64) is the infinite sum over M that has collapsed to the leading $M = 0$ term in (3.63). The bulk-to-bulk propagators appearing in the identity represent a scalar of scaling dimension Δ with $\Delta = \Delta_1 + \Delta_2$ in $\mathbb{Q}_{p^n}$, while in $\mathbb{R}^n$ one must perform a (weighted) sum over all scalars with $\Delta = \Delta_1 + \Delta_2 + 2M$ for all integral $M \geq 0$.

Another identity, which is extremely useful for replacing certain integrations over all of AdS with unintegrated expressions, takes the following form:

$$\mathbb{Q}_{p^n} \qquad \sum_{c\in T_{p^n}} \hat{G}_{\Delta_1}(a,c)\hat{G}_{\Delta_2}(b,c) = \frac{-\hat{G}_{\Delta_1}(a,b)/\widetilde{c}_{\Delta_2} + \hat{G}_{\Delta_2}(a,b)/\widetilde{c}_{\Delta_1}}{m_{\Delta_1}^2 - m_{\Delta_2}^2}\,, \tag{3.65}$$

where we remind the reader that m_Δ is the p-adic mass given by (3.2), and $\widetilde{c}_\Delta$ is given in (3.21). It is worth rewriting this identity in terms of the normalized bulk-to-bulk propagators of chapter 2,[19]

$$\mathbb{Q}_{p^n} \qquad G_\Delta(a,b) = \widetilde{c}_\Delta \hat{G}_\Delta(a,b)\,, \tag{3.66}$$

[18]There is an overall explicit factor of 2 as compared with (4.1) of [86] due to a small difference in notation — see footnote 17.

[19]Likewise in $\mathbb{R}^n$, $\widetilde{c}_\Delta$ given in (3.17) is the usual normalization constant of the bulk-to-bulk propagator. See, for example, equations (6.12) and (8.29) of [94], and (2.141) of chapter 2.

in which case it becomes

$$\mathbb{Q}_{p^n} \qquad \sum_{c\in T_{p^n}} G_{\Delta_1}(a,c)G_{\Delta_2}(b,c) = \frac{G_{\Delta_2}(a,b) - G_{\Delta_1}(a,b)}{m^2_{\Delta_1} - m^2_{\Delta_2}}\,. \tag{3.67}$$

The corresponding identity satisfied by the unnormalized bulk-to-bulk propagators in $\mathbb{R}^n$ takes the form [86]

$$\mathbb{R}^n \qquad \int_c \hat{G}_{\Delta_1}(a,c)\hat{G}_{\Delta_2}(b,c) = \frac{\hat{G}_{\Delta_1}(a,b) - \hat{G}_{\Delta_2}(a,b)}{m^2_{\Delta_1} - m^2_{\Delta_2}}\,, \tag{3.68}$$

where the Archimedean mass is given by (3.3). We list some more propagator identities in appendix 3.A, which we will not have occasion to use in this thesis, but which may prove useful in evaluating higher-point correlators and bulk loop diagrams.

Curiously, despite having very different expressions, the masses in $\mathbb{Q}_{p^n}$ and $\mathbb{R}^n$ subtract in a surprisingly similar manner. From the expression for the p-adic mass in (3.2), it follows

$$\mathbb{Q}_{p^n} \qquad m^2_{\Delta_A} - m^2_{\Delta_B} = \frac{-p^{\Delta_B}}{\zeta(\Delta_B - \Delta_A)\zeta(\Delta_A + \Delta_B - n)}\,. \tag{3.69}$$

This is to be compared with the Archimedean place, where

$$\mathbb{R}^n \qquad m^2_{\Delta_A} - m^2_{\Delta_B} = (\Delta_A - \Delta_B)(\Delta_A + \Delta_B - n)\,. \tag{3.70}$$

This observation will prove useful later when we discuss and compare the the logarithmic singularity structure of the four-point function in $\mathbb{R}^n$ and $\mathbb{Q}_{p^n}$.

3.3.2 Four-point contact diagram, again

We will now use (3.63) and (3.65) to rederive (3.38). Starting with (3.32) with the x_i arranged in the s-channel configuration shown in figure 3.1, and applying

identity (3.63) to the pairs $\hat{K}_{\Delta_1}\hat{K}_{\Delta_2}$ and $\hat{K}_{\Delta_3}\hat{K}_{\Delta_4}$, we obtain

$$\begin{aligned}\mathcal{D}W_0 = a^{(\Delta_1,\Delta_2)}a^{(\Delta_3,\Delta_4)} \sum_{a\in T_{p^n}} \sum_{b_1\in\gamma_{12}} \sum_{b_2\in\gamma_{34}} \\ \times \hat{K}_{\Delta_1}(b_1,x_1)\hat{K}_{\Delta_1}(b_1,x_2)\hat{G}_{\Delta_1+\Delta_2}(b_1,a) \\ \times \hat{K}_{\Delta_3}(b_2,x_3)\hat{K}_{\Delta_4}(b_2,x_4)\hat{G}_{\Delta_3+\Delta_4}(b_2,a)\,.\end{aligned} \qquad \mathbb{Q}_{p^n} \tag{3.71}$$

While it may seem we have made our lives harder by introducing two additional summations over geodesics within the Bruhat–Tits tree, the effect is in fact the opposite: Thanks to the identities of sections 3.2.4 and 3.3.1, we never have to explicitly evaluate *any* of these integrals. We first eliminate the sum over the bulk point a by recognising it takes exactly the form of identity (3.65). This results in two terms with the propagator content schematically of the form $\sim \sum_\gamma \sum_\gamma \hat{K}\hat{K}\hat{G}_\Delta\hat{K}\hat{K}$, with $\Delta = \Delta_1 + \Delta_2$ in one term, and $\Delta = \Delta_3 + \Delta_4$ in the other. This combination is exactly the same as (3.56), which is the definition of a geodesic bulk diagram. Substituting the geodesic bulk diagram with conformal partial waves using (3.57), we arrive at

$$\mathcal{D}(u) = P_1^{(12)}\mathcal{G}_{\Delta_A}(u) + P_1^{(34)}\mathcal{G}_{\Delta_B}(u)\,, \qquad \mathbb{Q}_{p^n} \tag{3.72}$$

with the squared OPE coefficients

$$\begin{aligned}P_1^{(12)} &= \frac{-1}{\widetilde{c}_{\Delta_B}}\left(\beta^{(2\Delta_1,2\Delta_2)}a^{(\Delta_1,\Delta_2)}\right)\left(\beta^{(\Delta_A+\Delta_{34},\Delta_A-\Delta_{34})}\frac{a^{(\Delta_3,\Delta_4)}}{m^2_{\Delta_A}-m^2_{\Delta_B}}\right) \\ P_1^{(34)} &= \frac{-1}{\widetilde{c}_{\Delta_A}}\left(\beta^{(2\Delta_3,2\Delta_4)}a^{(\Delta_3,\Delta_4)}\right)\left(\beta^{(\Delta_B+\Delta_{12},\Delta_B-\Delta_{12})}\frac{a^{(\Delta_1,\Delta_2)}}{m^2_{\Delta_B}-m^2_{\Delta_A}}\right).\end{aligned} \qquad \mathbb{Q}_{p^n} \tag{3.73}$$

It is straightforward to check that (3.72) with the coefficients given in (3.73) agrees precisely with (3.38). That the expression for the p-adic four-point amplitude in (3.38) has an equivalent representation featuring p-adic mass singularities as shown in (3.72)-(3.73) is highly non-trivial but physical. We comment more on this at the end of section 3.3.4.

A calculation in $\mathbb{R}^n$, similar to the one described for $\mathbb{Q}_{p^n}$ using the propagator identities, results in an expression for the contact diagram similar to (3.73), but with an important difference. We quote the result computed in [86]:

$$\mathbb{R}^n \quad g(u,v) = \sum_{M=0}^{\infty} P_1^{(12)}(M)\mathcal{G}_{\Delta_A+2M}(u,v) + \sum_{N=0}^{\infty} P_1^{(34)}(N)\mathcal{G}_{\Delta_B+2N}(u,v)\,, \tag{3.74}$$

where the squared OPE coefficients are given by

$$\begin{aligned}
\mathbb{R}^n \qquad P_1^{(12)}(M) &= \left(\beta^{(2\Delta_1+2M,2\Delta_2+2M)} a_M^{(\Delta_1,\Delta_2)}\right) \\
&\quad \times \left(\beta^{(\Delta_A+\Delta_{34}+2M,\Delta_A-\Delta_{34}+2M)} \sum_{N=0}^{\infty} \frac{a_N^{(\Delta_3,\Delta_4)}}{m^2_{\Delta_A+2M} - m^2_{\Delta_B+2N}}\right) \\
P_1^{(34)}(N) &= \left(\beta^{(2\Delta_3+2N,2\Delta_4+2N)} a_N^{(\Delta_3,\Delta_4)}\right) \\
&\quad \times \left(\beta^{(\Delta_B+\Delta_{12}+2N,\Delta_B-\Delta_{12}+2N)} \sum_{M=0}^{\infty} \frac{a_M^{(\Delta_1,\Delta_2)}}{m^2_{\Delta_B+2N} - m^2_{\Delta_A+2M}}\right).
\end{aligned} \tag{3.75}$$

It can be seen in the conformal block decomposition of the four-point contact diagram in (3.74) that double-trace operators, schematically of the form $\mathcal{O}_i\partial^{2N}\mathcal{O}_j$ with scaling dimension $\Delta_i + \Delta_j + 2N$ at leading order, run in the intermediate channel. In $\mathbb{Q}_{p^n}$, looking at (3.72), we conclude that only double-trace operators *without* derivatives appear in the intermediate channel. (Essentially, in (3.72)-(3.73), the infinite sums over M and N in (3.74)-(3.75) have collapsed to the $M = N = 0$ term.) This is consistent with the general expectation that local derivatives of operators do not appear in p-adic CFTs. This expectation stems in turn from the understanding that the ultrametric analog of a smooth function from reals to reals is a piecewise constant function from an ultrametric field to the reals.

3.3.3 Exchange diagram in the direct channel

In the rest of this section, we will use the previously stated propagator identities to evaluate four-point exchange diagrams. First we compute the diagram associated

with the exchange of a scalar of dimension Δ in the (12)(34) channel, which we will express in terms of a conformal block decomposition in the direct channel. Explicitly, we wish to evaluate

$$\mathcal{D}^S_\Delta(x_i) \equiv \frac{1}{W_0}\sum_{a_1,a_2\in T_{p^n}} \hat{K}_{\Delta_1}(a_1,x_1)\hat{K}_{\Delta_2}(a_1,x_2) \times \hat{G}_\Delta(a_1,a_2)\hat{K}_{\Delta_3}(a_2,x_3)\hat{K}_{\Delta_4}(a_2,x_4). \tag{3.76}$$

$\mathbb{Q}_{p^n}$

Applying the propagator identity (3.63) on the $\hat{K}_{\Delta_1}\hat{K}_{\Delta_2}$ and $\hat{K}_{\Delta_3}\hat{K}_{\Delta_4}$ legs leaves us with an expression involving the following double integration on the tree

$$\sum_{a_1,a_2\in T_{p^n}} \hat{G}_{\Delta_A}(b_1,a_1)\hat{G}_\Delta(a_1,a_2)\hat{G}_{\Delta_B}(a_2,b_2), \tag{3.77}$$

$\mathbb{Q}_{p^n}$

where $b_1 \in \gamma_{12}$ and $b_2 \in \gamma_{34}$. This can be immediately reduced to a combination of unintegrated bulk-to-bulk propagators by applying the identity (3.65) twice. Altogether, we wind up with

$$\begin{aligned}\mathcal{D}^S_\Delta = &\frac{a^{(\Delta_1,\Delta_2)}a^{(\Delta_3,\Delta_4)}}{W_0\widetilde{c}_\Delta\widetilde{c}_{\Delta_A}\widetilde{c}_{\Delta_B}}\sum_{b_1\in\gamma_{12}}\sum_{b_2\in\gamma_{34}}\Bigg[\hat{K}_{\Delta_1}(b_1,x_1)\hat{K}_{\Delta_2}(b_1,x_2)\hat{K}_{\Delta_3}(b_2,x_3)\hat{K}_{\Delta_4}(b_2,x_4)\\ &\times\Bigg(\frac{\widetilde{c}_\Delta\hat{G}_\Delta(b_1,b_2)}{(m^2_\Delta-m^2_{\Delta_A})(m^2_\Delta-m^2_{\Delta_B})}+\frac{\widetilde{c}_{\Delta_A}\hat{G}_{\Delta_A}(b_1,b_2)}{(m^2_{\Delta_A}-m^2_\Delta)(m^2_{\Delta_A}-m^2_{\Delta_B})}\\ &+\frac{\widetilde{c}_{\Delta_B}\hat{G}_{\Delta_B}(b_1,b_2)}{(m^2_{\Delta_B}-m^2_\Delta)(m^2_{\Delta_B}-m^2_{\Delta_A})}\Bigg)\Bigg].\end{aligned} \tag{3.78}$$

$\mathbb{Q}_{p^n}$

Recognizing the integral over points b_1, b_2 as the geodesic bulk diagram defined in (3.56), and using (3.57) and (3.46) to express in terms of conformal blocks, we obtain

$$\mathcal{D}^S_\Delta(u) = C_{12\Delta}C_{34\Delta}\,\mathcal{G}_\Delta(u) + P_1^{(12)}\mathcal{G}_{\Delta_A}(u) + P_1^{(34)}\mathcal{G}_{\Delta_B}(u) \tag{3.79}$$

$\mathbb{Q}_{p^n}$

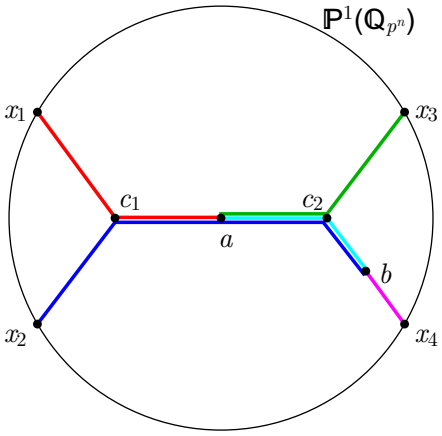

Figure 3.3: Geodesic subway diagram $\mathcal{W}_\Delta^T$, with exchange of a scalar in the (13)(24) channel. The bulk point a runs along the geodesic joining x_1 with x_3, and b runs along the geodesic joining x_2 with x_4, while a scalar of dimension Δ is exchanged between a and b. Colors differentiate the individual propagators found in $\mathcal{W}_\Delta^T$ in (3.81).

where

$$\begin{aligned} C_{12\Delta}C_{34\Delta} &= \frac{1}{\widetilde{c}_{\Delta_A}\widetilde{c}_{\Delta_B}}\left(\beta^{(\Delta+\Delta_{12},\Delta-\Delta_{12})}\frac{a^{(\Delta_1,\Delta_2)}}{m_\Delta^2-m_{\Delta_A}^2}\right)\left(\beta^{(\Delta+\Delta_{34},\Delta-\Delta_{34})}\frac{a^{(\Delta_3,\Delta_4)}}{m_\Delta^2-m_{\Delta_B}^2}\right) \\ \mathbb{Q}_{p^n} \qquad P_1^{(12)} &= \frac{1}{\widetilde{c}_{\Delta}\widetilde{c}_{\Delta_B}}\left(\beta^{(2\Delta_1,2\Delta_2)}\frac{a^{(\Delta_1,\Delta_2)}}{m_{\Delta_A}^2-m_\Delta^2}\right)\left(\beta^{(\Delta_A+\Delta_{34},\Delta_A-\Delta_{34})}\frac{a^{(\Delta_3,\Delta_4)}}{m_{\Delta_A}^2-m_{\Delta_B}^2}\right) \\ P_1^{(34)} &= \frac{1}{\widetilde{c}_{\Delta}\widetilde{c}_{\Delta_A}}\left(\beta^{(2\Delta_3,2\Delta_4)}\frac{a^{(\Delta_3,\Delta_4)}}{m_{\Delta_B}^2-m_\Delta^2}\right)\left(\beta^{(\Delta_B+\Delta_{12},\Delta_B-\Delta_{12})}\frac{a^{(\Delta_1,\Delta_2)}}{m_{\Delta_B}^2-m_{\Delta_A}^2}\right). \end{aligned} \tag{3.80}$$

This is the p-adic analog of equations (4.16)–(4.17) in [86]. The similarities between the p-adic and Archimedean OPE coefficients (squared) are remarkable. In the conformal block decomposition in the direct channel, in addition to the double-trace exchanges (albeit without derivatives just like in the case of the contact diagram), we find as expected, a term representing the single-trace exchange of a scalar of dimension Δ.

3.3.4 Exchange diagrams in the crossed channel

In section 3.2.4, we computed the geodesic bulk diagram for boundary points x_i in an 's-channel' configuration (i.e. $u < 1$) with a scalar of dimension Δ exchanged in the (12)(34) channel (see figure 3.2). Equation (3.57) then states that up to an overall factor, the geodesic bulk diagram is simply the conformal partial wave $W_\Delta(x_i)$. Let's now consider two closely related geodesic bulk diagrams which will prove useful for computing exchange diagrams in the crossed channels. In these geodesic diagrams the boundary points x_i remain in the 's-channel' configuration shown in figure 3.1 with $u < 1$, but a scalar of dimension Δ is exchanged in the (13)(24) channel, or the (14)(23) channel. Explicitly, we define these geodesic bulk diagrams to be (see figure 3.3)

$$\mathbb{Q}_{p^n} \qquad \begin{aligned} \mathcal{W}^T_\Delta(x_i) &\equiv \sum_{\substack{a\in\gamma_{13}\\ b\in\gamma_{24}}} \hat{K}_{\Delta_1}(x_1,a)\hat{K}_{\Delta_3}(x_3,a)\hat{G}_\Delta(a,b)\hat{K}_{\Delta_2}(x_2,b)\hat{K}_{\Delta_4}(x_4,b) \\ \mathcal{W}^U_\Delta(x_i) &\equiv \sum_{\substack{a\in\gamma_{14}\\ b\in\gamma_{23}}} \hat{K}_{\Delta_1}(x_1,a)\hat{K}_{\Delta_4}(x_4,a)\hat{G}_\Delta(a,b)\hat{K}_{\Delta_2}(x_2,b)\hat{K}_{\Delta_3}(x_3,b)\,. \end{aligned} \tag{3.81}$$

A direct computation on the Bruhat–Tits tree, detailed in appendix 3.D, reveals the following decomposition of a geodesic bulk diagram in the crossed-channel,

$$\mathbb{Q}_{p^n} \qquad \begin{aligned} \mathcal{W}^T_\Delta &= \beta^{(\Delta+\Delta_{13},\Delta-\Delta_{13})}\beta^{(-\Delta_{13}-\Delta_{24},\Delta+\Delta_{24})}W_{\Delta_A} \\ &\quad + \beta^{(\Delta+\Delta_{13},\Delta-\Delta_{13})}\beta^{(\Delta_{13}+\Delta_{24},\Delta-\Delta_{24})}W_{\Delta_B} \\ &= \beta^{(\Delta+\Delta_{24},\Delta-\Delta_{24})}\beta^{(-\Delta_{13}-\Delta_{24},\Delta+\Delta_{13})}W_{\Delta_A} \\ &\quad + \beta^{(\Delta+\Delta_{24},\Delta-\Delta_{24})}\beta^{(\Delta_{13}+\Delta_{24},\Delta-\Delta_{13})}W_{\Delta_B}. \end{aligned} \tag{3.82}$$

The corresponding identity for a geodesic diagram with exchange in the (14)(23) channel, $\mathcal{W}^U_\Delta$, is obtained simply by switching $\Delta_3 \leftrightarrow \Delta_4$ in (3.82).

A non-trivial consistency check on (3.82) can be obtained by starting from the defining expression (3.32) for the contact diagram, then using (3.63) on the

$\hat{K}_{\Delta_1}\hat{K}_{\Delta_3}$ and $\hat{K}_{\Delta_2}\hat{K}_{\Delta_4}$ legs, then applying (3.65) once, and finally employing (3.82) to obtain (3.38). This slightly round-about method is easily seen to agree with the simpler calculation outlined in section 3.3.2.

We can now use the identity (3.82) to evaluate the four-point exchange diagram where a scalar of dimension Δ is exchanged in the (13)(24) channel (we remind the reader that the boundary points x_i will always be in the 's-channel' configuration shown in figure 3.3, i.e. $u < 1$):

$$\mathbb{Q}_{p^n} \quad \mathcal{D}^T_\Delta(x_i) \equiv \frac{1}{W_0} \sum_{a_1,a_2 \in T_{p^n}} \hat{K}_{\Delta_1}(a_1,x_1)\hat{K}_{\Delta_3}(a_1,x_3)\hat{G}_\Delta(a_1,a_2)\hat{K}_{\Delta_2}(a_2,x_2)\hat{K}_{\Delta_4}(a_2,x_4). \tag{3.83}$$

We will express the final result in terms of a conformal block decomposition in the crossed channel. The computation proceeds along lines similar to the one for $\mathcal{D}^S_\Delta$ sketched in section 3.3.3, and is described in appendix 3.D. The final result is

$$\mathbb{Q}_{p^n} \qquad \mathcal{D}^T_\Delta(u) = P_1^{(12)}\mathcal{G}_{\Delta_A}(u) + P_1^{(34)}\mathcal{G}_{\Delta_B}(u), \tag{3.84}$$

where

$$\begin{aligned} P_1^{(12)} &= \frac{1}{\widetilde{c}_{\Delta_C}\widetilde{c}_{\Delta_D}} \left(\beta^{(\Delta+\Delta_{13},\Delta-\Delta_{13})} \frac{a^{(\Delta_1,\Delta_3)}}{m^2_\Delta - m^2_{\Delta_C}}\right)\left(\beta^{(-\Delta_{13}-\Delta_{24},\Delta+\Delta_{24})} \frac{a^{(\Delta_2,\Delta_4)}}{m^2_\Delta - m^2_{\Delta_D}}\right) \\ \mathbb{Q}_{p^n} \qquad &+ \frac{1}{\widetilde{c}_{\Delta}\widetilde{c}_{\Delta_D}} \left(\beta^{(2\Delta_1,2\Delta_3)} \frac{a^{(\Delta_1,\Delta_3)}}{m^2_{\Delta_C} - m^2_\Delta}\right)\left(\beta^{(-\Delta_{13}-\Delta_{24},\Delta_C+\Delta_{24})} \frac{a^{(\Delta_2,\Delta_4)}}{m^2_{\Delta_C} - m^2_{\Delta_D}}\right) \\ &+ \frac{1}{\widetilde{c}_{\Delta}\widetilde{c}_{\Delta_C}} \left(\beta^{(2\Delta_2,2\Delta_4)} \frac{a^{(\Delta_2,\Delta_4)}}{m^2_{\Delta_D} - m^2_\Delta}\right)\left(\beta^{(-\Delta_{13}-\Delta_{24},\Delta_D+\Delta_{13})} \frac{a^{(\Delta_1,\Delta_3)}}{m^2_{\Delta_D} - m^2_{\Delta_C}}\right), \end{aligned} \tag{3.85}$$

and

$$P_1^{(34)} = \frac{1}{\widetilde{c}_{\Delta_C}\widetilde{c}_{\Delta_D}}\left(\beta^{(\Delta+\Delta_{13},\Delta-\Delta_{13})}\frac{a^{(\Delta_1,\Delta_3)}}{m_\Delta^2-m_{\Delta_C}^2}\right)\left(\beta^{(\Delta_{13}+\Delta_{24},\Delta-\Delta_{24})}\frac{a^{(\Delta_2,\Delta_4)}}{m_\Delta^2-m_{\Delta_D}^2}\right)$$

$\mathbb{Q}_{p^n}$

$$+\frac{1}{\widetilde{c}_{\Delta}\widetilde{c}_{\Delta_D}}\left(\beta^{(2\Delta_1,2\Delta_3)}\frac{a^{(\Delta_1,\Delta_3)}}{m_{\Delta_C}^2-m_\Delta^2}\right)\left(\beta^{(\Delta_{13}+\Delta_{24},\Delta_C-\Delta_{24})}\frac{a^{(\Delta_2,\Delta_4)}}{m_{\Delta_C}^2-m_{\Delta_D}^2}\right)$$

$$+\frac{1}{\widetilde{c}_{\Delta}\widetilde{c}_{\Delta_C}}\left(\beta^{(2\Delta_2,2\Delta_4)}\frac{a^{(\Delta_2,\Delta_4)}}{m_{\Delta_D}^2-m_\Delta^2}\right)\left(\beta^{(\Delta_{13}+\Delta_{24},\Delta_D-\Delta_{13})}\frac{a^{(\Delta_1,\Delta_3)}}{m_{\Delta_D}^2-m_{\Delta_C}^2}\right). \tag{3.86}$$

Here we have defined

$$\Delta_C = \Delta_1+\Delta_3 \qquad \Delta_D = \Delta_2+\Delta_4\,. \tag{3.87}$$

From a diagrammatic point of view in the bulk it appears that $\mathcal{G}_\delta(u)$ for various other values of δ, like $\Delta_1+\Delta_4+\Delta$ or $\Delta_2+\Delta_3+\Delta$, might appear in the intermediate steps while computing (3.83). But miraculously these contributions wind up canceling in the final result, and as expected for exchange diagrams expressed in the conformal block decomposition in a crossed-channel, only double-trace exchanges appear. (See appendix 3.B for an explanation of this point and related comments on crossing symmetry.) The exchange diagram $\mathcal{D}_\Delta^U$, where a scalar of dimension Δ is exchanged in the (14)(23) channel is obtained from (3.84) simply by switching $\Delta_3 \leftrightarrow \Delta_4$.

It is worth pointing out that in $\mathbb{R}^n$, anomalous dimensions appear in the tree-level four-point contact amplitude in the form of logarithmic singularities when the integrality condition, $\Delta_A-\Delta_B \in 2\mathbb{Z}$ is met, or equivalently when the algebraic condition $m^2_{\Delta_A+2M} = m^2_{\Delta_B+2N}$ is satisfied in (3.75) for integral $M, N \geq 0$ [95, 86]. Instead in $\mathbb{Q}_{p^n}$, we find logarithmic singularities arise only when $\Delta_A - \Delta_B = 0$, or equivalently when $m^2_{\Delta_A} = m^2_{\Delta_B}$.[20] This is intriguingly reminiscent of the

[20]If alternate quantization is allowed, it is clear from (3.69)-(3.70) that the condition $m^2_{\Delta_A+2M} = m^2_{\Delta_B+2N}$ has in addition to $\Delta_A - \Delta_B \in 2\mathbb{Z}$, a second solution, $\Delta_A + \Delta_B - n = 2\ell$ where ℓ is a non-positive integer. (In the p-adics, $M = N = 0$, so the conditions are more

existence of an infinite sequence of poles in the anomalous dimension of composite operators in CFTs in $\mathbb{R}^n$ as opposed to just one pole in p-adic CFTs, at least in the context of the $O(N)$ model (see chapter 4). Analogously for the exchange diagrams, logarithmic singularities arise in the exchange amplitude (3.79)-(3.80) when any of $m^2_\Delta, m^2_{\Delta_A}, m^2_{\Delta_B}$ coincide, and in (3.84)-(3.86) simply when any of $m^2_\Delta, m^2_{\Delta_C}, m^2_{\Delta_D}$ coincide.

3.4 Towards a bulk dual of free field theory

So far in this chapter, we have presented, in the context of p-adic AdS/CFT, the holographic computation of the four-point contact and exchange diagrams for scalar composite operators of general dimensions. In this section we would like to construct a minimal bulk theory that reproduces the correlators of a free p-adic field theory, featuring an operator $\mathcal{O}$ of dimension Δ.

In the minimal construction, we would include only one bulk field, namely a scalar ϕ with mass squared m^2_Δ as defined in (3.2), and with only cubic interactions. It turns out this is not enough to give a four-point function that agrees with a free p-adic field theory. As a next-to-minimal construction, we could consider adding quartic interactions for ϕ. This is still not enough to reproduce the four-point function of a free boundary theory. As we will explain, a strategy which *does* work (at least as far as the four-point function) is to include also quartic

restrictive: $\Delta_A - \Delta_B = 0$ or $\Delta_A + \Delta_B - n = 0$.) For $n > 4$, the second solution is disallowed since it violates the unitarity bound, which restricts $\Delta_A, \Delta_B \geq n - 2$. For the second solution to exist in $n = 4$, Δ_A and Δ_B must saturate the unitarity bound, so $\Delta_A = \Delta_B = 2$ and $\Delta_A - \Delta_B \in 2\mathbb{Z}$ is satisfied. However, for $n \leq 3$ there exist pairs of scaling dimensions satisfying the unitarity bound, such that $\Delta_A + \Delta_B = n$ but $\Delta_A - \Delta_B \notin 2\mathbb{Z}$. Such exceptional choices would seem to hint at the appearance of a new kind of logarithmic singularity with an origin different from the usual integrality condition $\Delta_A - \Delta_B \in 2\mathbb{Z}$. In the p-adics, the convergence conditions listed in footnote 14 portend the appearance of severe singularities in the four-point contact amplitude if $\Delta_A + \Delta_B \leq n$. So for example, (3.38) or equivalently (3.72)-(3.73) is altogether not to be trusted when $\Delta_A + \Delta_B - n \leq 0$, and we cannot reasonably inquire about singularities at special values. Might a similar argument in $\mathbb{R}^n$ prevent the appearance of these exceptional singularities?

interactions for ϕ which act across a link: that is, nearest neighbor interactions. An efficient way to package all the constructions we have in mind is to introduce an additional bulk scalar $\tilde{\phi}$ whose scaling dimension $\widetilde{\Delta}$ we will eventually take to be large, and to allow only cubic on-site interactions of the form ϕ^3 and $\tilde{\phi}\phi^2$. The action for such a ϕ-$\tilde{\phi}$ theory takes the form

$\mathbb{Q}_{p^n}$
$$S[\phi,\tilde{\phi}] = \sum_{\langle ab\rangle}\frac{1}{2}(\phi_a-\phi_b)^2 + \sum_{\langle ab\rangle}\frac{1}{2}(\tilde{\phi}_a-\tilde{\phi}_b)^2 + \sum_{a\in T_{p^n}}\left(\frac{1}{2}m_\Delta^2\phi_a^2+\frac{1}{2}m_{\widetilde{\Delta}}^2\tilde{\phi}_a^2 + \frac{g_3}{3!}\phi_a^3+\frac{\widetilde{g}_3}{2}\phi_a^2\tilde{\phi}_a\right). \tag{3.88}$$

In the strict limit of large $m_{\widetilde{\Delta}}$, any diagram where $\tilde{\phi}$ propagates even a single step becomes negligible.

Specialising in (3.79) and (3.84) to the case of all four $\Delta_i = \Delta$ with the dimension of the exchanged scalar relabelled $\widetilde{\Delta}$, we get, after summing up the exchange contributions from all channels,

$\mathbb{Q}_{p^n}$
$$\mathcal{D}_{\widetilde{\Delta}}^{(\text{exchange})} \equiv \mathcal{D}_{\widetilde{\Delta}}^{S}+\mathcal{D}_{\widetilde{\Delta}}^{T}+\mathcal{D}_{\widetilde{\Delta}}^{U} = F_1 u^{\widetilde{\Delta}} + F_2 u^{2\Delta} + F_3 u^{2\Delta}\frac{\log u}{\log p}\,, \tag{3.89}$$

where the constants F_i depend on n, p, Δ and $\widetilde{\Delta}$ but not on u. The F_i can be evaluated immediately from (3.79)-(3.80) and (3.84)-(3.86), but the explicit form is complicated enough as to be unenlightening at this stage. In (3.89) we are not assuming large $m_{\widetilde{\Delta}}$. The first term in (3.89) indicates, heuristically, that an operator of dimension $\widetilde{\Delta}$ can participate in the connected four-point function of an operator $\mathcal{O}$ of dimension Δ, while the second two terms are evidence that one or more operators with dimensions close to 2Δ participate.

We now show explicitly that integrating out $\tilde{\phi}$ results in the contact diagram. If we set

$\mathbb{Q}_{p^n}$
$$y = p^{-\widetilde{\Delta}}\,, \tag{3.90}$$

then we find

$$\mathbb{Q}_{p^n} \qquad F_1 = O(y^2) \qquad F_2 = O(1) \qquad F_3 = O(1)\,. \tag{3.91}$$

Setting $y = 0$ is the same as $\widetilde{\Delta} \to \infty$, and because of (3.91) it gives a finite limit:

$$\begin{aligned} \mathbb{Q}_{p^n} \qquad \mathcal{D}^{(\text{contact})} &\equiv \lim_{\widetilde{\Delta}\to\infty} \mathcal{D}^{(\text{exchange})}_{\widetilde{\Delta}} = \mathcal{D}^{(\text{exchange})}_{\widetilde{\Delta}}\Big|_{y=0} \\ &= \frac{3(1+4p^{2\Delta}+p^{4\Delta}+d(-1+p^{4\Delta}))}{-p^n+p^{4\Delta}} u^{2\Delta}\,, \end{aligned} \tag{3.92}$$

where $d \equiv -\log u/\log p$. A useful check is to note that $\mathcal{D}^{(\text{contact})} = 3\mathcal{D}|_{\Delta_i=\Delta}$, where $\mathcal{D}$ is the four-point contact amplitude given in (3.72).[21]

If instead of setting $y = 0$ we pick out the $O(y)$ term of $\mathcal{D}^{(\text{exchange})}_{\widetilde{\Delta}}$ at large $\widetilde{\Delta}$ (meaning small y), it means we are focusing on nearest neighbor interactions, i.e. an interaction which takes place when two bulk points are precisely one step apart. Thus we define

$$\mathbb{Q}_{p^n} \qquad \mathcal{D}^{(\text{nearest})} \equiv \frac{d\mathcal{D}^{(\text{exchange})}_{\widetilde{\Delta}}}{dy}\bigg|_{y=0} = (p^{2\Delta}+p^{n-2\Delta})\mathcal{D}^{(\text{contact})} - u^{2\Delta}\left(\frac{3}{\widetilde{c}_{2\Delta}}+\frac{2d}{\widetilde{c}^2_{\Delta}}\right), \tag{3.93}$$

where $\widetilde{c}_\Delta$ is given by (3.21).

To gain more intuition on the nearest neighbor interaction, it helps to arrive at (3.93) from a different starting point. Define the nearest neighbor exchange amplitudes,

$$\begin{aligned} \mathcal{F}_S &\equiv \frac{1}{W_0}\sum_{a\in T_{p^n}}\sum_{b\sim a}\hat{K}_\Delta(x_1,a)\hat{K}_\Delta(x_2,a)\hat{K}_\Delta(x_3,b)\hat{K}_\Delta(x_4,b) \\ \mathcal{F}_T &\equiv \frac{1}{W_0}\sum_{a\in T_{p^n}}\sum_{b\sim a}\hat{K}_\Delta(x_1,a)\hat{K}_\Delta(x_2,b)\hat{K}_\Delta(x_3,a)\hat{K}_\Delta(x_4,b) \\ \mathcal{F}_U &\equiv \frac{1}{W_0}\sum_{a\in T_{p^n}}\sum_{b\sim a}\hat{K}_\Delta(x_1,a)\hat{K}_\Delta(x_2,b)\hat{K}_\Delta(x_3,b)\hat{K}_\Delta(x_4,a). \end{aligned} \tag{3.94}$$

[21] Moreover, $\mathcal{D}^{(\text{contact})} = 3D_p/W_0$, where D_p is the four-point contact amplitude evaluated in (2.130) of chapter 2.

Here $\sum_{b\sim a}$ represents summing over all nearest neighbors of a, with a held fixed. Thus, nearest neighbor interactions are manifest in the amplitudes (3.94). In fact, one can easily check that $\mathcal{D}^{(\text{nearest})} = \mathcal{F}_S + \mathcal{F}_T + \mathcal{F}_U$. This was expected precisely because $\mathcal{D}^{(\text{nearest})}$ represents a nearest neighbor interaction where two pairs of propagators meet one edge apart, and summing the amplitudes in (3.94) accounts for all the possible ways that may happen. We briefly discuss the connection between nearest neighbor interactions and derivative couplings in appendix 3.C.

Now we observe that including both contact and nearest neighbor interactions allows us to form a four-point function where we can control F_2 and F_3, where F_1, F_2 and F_3 are the coefficients of $u^\Delta, u^{2\Delta}$ and $u^{2\Delta}\log_p u$, respectively. In particular, we can cancel off F_3 and control the ratio F_2/F_1. The interesting case to consider is the amplitude

$$\begin{aligned}\mathcal{D}^{(\text{combined})} &\equiv -\frac{(1+p^\Delta)^2(-p^n+p^{4\Delta})}{2(p^n-p^{3\Delta})^2}\mathcal{D}^{(\text{contact})} \\ &\quad + \mathcal{D}_\Delta^{(\text{exchange})} - \frac{p^{2\Delta}(-1+p^{2\Delta})}{2(p^n-p^{3\Delta})^2}\mathcal{D}^{(\text{nearest})} \\ &= \frac{f_{\Delta\Delta\Delta}^2}{2}\left(2u^\Delta + u^{2\Delta}\right),\end{aligned} \tag{3.95}$$

$\mathbb{Q}_{p^n}$

where the structure constant $f_{\Delta\Delta\Delta}$ is given by (3.23). The coefficients of $\mathcal{D}^{(\text{contact})}$ and $\mathcal{D}^{(\text{nearest})}$ in (3.95) were chosen carefully so that the u-dependence of $\mathcal{D}^{(\text{combined})}$ would be exactly the $2u^\Delta + u^{2\Delta}$ behavior expected in case the operator $\mathcal{O} = \vec{\Phi}^2$ where $\vec{\Phi}$ is a free field on the boundary.[22]

Having found in (3.95) a combination of bulk amplitudes suggestive of a free

[22]To see this, note that

$$u^\Delta W_0(x_i) = \frac{1}{|x_{12}x_{24}x_{34}x_{13}|^\Delta} = \frac{1}{|x_{12}x_{23}x_{34}x_{41}|^\Delta}$$

$$u^{2\Delta} W_0(x_i) = \frac{1}{|x_{13}x_{24}|^{2\Delta}} = \frac{1}{|x_{13}x_{23}x_{24}x_{14}|^\Delta},$$

where in the second and fourth equalities we used $|x_{14}x_{23}| = |x_{13}x_{24}|$ (which is simply a rephrasing of $v = 1$). These account for the three possible Wick contractions we expect to see in the connected four-point function of a free theory.

field dual, we should next inquire what bulk action leads to (3.95). It is awkward to use (3.88) because to get $\mathcal{D}^{(\text{nearest})}$ from it we require the derivative operation (3.93) in the $\widetilde{\Delta} \to \infty$ limit. Let us therefore start instead from the action

$$\mathbb{Q}_{p^n} \quad S[\phi] = \sum_{\langle ab \rangle} \frac{1}{2}(\phi_a - \phi_b)^2 + \sum_{a \in T_{p^n}} \left(\frac{1}{2} m_\Delta^2 \phi_a^2 + \frac{g_3}{3!}\phi_a^3 + \frac{g_4}{4!}\phi_a^4 \right) + \frac{\widetilde{g}_4}{8} \sum_{a \in T_{p^n}} \sum_{b \sim a} \phi_a^2 \phi_b^2 \,, \tag{3.96}$$

which is precisely (3.1) augmented by a nearest neighbor interaction. Straightforward diagrammatic considerations lead us from (3.96) to

$$\begin{aligned} &\mathbb{Q}_{p^n} \qquad \frac{1}{W_0}\langle \mathcal{O}(x_1)\mathcal{O}(x_2)\mathcal{O}(x_3)\mathcal{O}(x_4)\rangle \\ &\qquad\qquad = -g_4 \widetilde{c}_\Delta^2 \frac{\mathcal{D}^{(\text{contact})}}{3} + g_3^2 \widetilde{c}_\Delta^3 \mathcal{D}^{(\text{exchange})} - \widetilde{g}_4 \widetilde{c}_\Delta^2 \mathcal{D}^{(\text{nearest})} \,. \end{aligned} \tag{3.97}$$

The factors of $\widetilde{c}_\Delta$ arise because each external leg picks up a factor of $\sqrt{\widetilde{c}_\Delta}$ (c.f. the discussion around (3.14)-(3.21)) and an extra factor of $\widetilde{c}_\Delta$ comes from the bulk-to-bulk propagator, as in (3.66). The factor of $1/3$ in the first term comes from the relation $\mathcal{D}^{(\text{contact})} = 3\mathcal{D}|_{\Delta_i = \Delta}$. Choosing the couplings to be

$$\mathbb{Q}_{p^n} \qquad g_4 = \frac{3g_3^2}{2} \frac{m_{3\Delta}^2 - m_\Delta^2}{\left(m_{2\Delta}^2 - m_\Delta^2\right)^2} \qquad \widetilde{g}_4 = \frac{g_3^2}{2} \frac{\left(\beta^{(\Delta,-4\Delta)}\beta^{(\Delta,3\Delta)}\right)^{-1}}{\left(m_{2\Delta}^2 - m_\Delta^2\right)^2} \,, \tag{3.98}$$

we arrive at the connected four-point function of a free theory,

$$\mathbb{Q}_{p^n} \qquad \langle \mathcal{O}(x_1)\mathcal{O}(x_2)\mathcal{O}(x_3)\mathcal{O}(x_4)\rangle = \frac{g_3^2}{2}\widetilde{c}_\Delta^3 f_{\Delta\Delta\Delta}^2 (2u^\Delta + u^{2\Delta}) W_0 \,. \tag{3.99}$$

Now, from the boundary perspective, $\mathcal{O} = \vec{\Phi}^2$ where $\vec{\Phi}$ is a free-field on the boundary, with the propagator

$$\mathbb{Q}_{p^n} \qquad \langle \Phi^I(x_1)\Phi^J(x_2)\rangle = \frac{C\delta^{IJ}}{|x_{12}|^{2\Delta_\Phi}} \,, \tag{3.100}$$

for some constant C, and $I, J = 1, \ldots, N$. We set $C = 1/\sqrt{2N}$. It then follows that the two- and three-point functions of the composite operator $\mathcal{O}$ are (up to contact terms)

$$\mathbb{Q}_{p^n} \qquad \langle \mathcal{O}(x_1)\mathcal{O}(x_2)\rangle = \langle \Phi^I(x_1)\Phi^I(x_1)\Phi^J(x_2)\Phi^J(x_2)\rangle = \frac{1}{|x_{12}|^{4\Delta_\Phi}} \tag{3.101}$$

and

$$\mathbb{Q}_{p^n} \qquad \langle \mathcal{O}(x_1)\mathcal{O}(x_2)\mathcal{O}(x_3)\rangle = \frac{2\sqrt{2}}{\sqrt{N}} \frac{1}{|x_{12}x_{23}x_{31}|^{2\Delta_\Phi}}\,, \tag{3.102}$$

where $2\sqrt{2}/\sqrt{N} = 8C^3N$, with the factor of 8 coming from the possible Wick contractions. On the other hand, the holographically obtained two- and three-point functions are[23]

$$\mathbb{Q}_{p^n} \qquad \begin{aligned} \langle \mathcal{O}(x_1)\mathcal{O}(x_2)\rangle &= \frac{1}{|x_{12}|^{2\Delta}} \\ \langle \mathcal{O}(x_1)\mathcal{O}(x_2)\mathcal{O}(x_3)\rangle &= \frac{-g_3 \widetilde{c}_\Delta^{3/2} f_{\Delta\Delta\Delta}}{|x_{12}x_{23}x_{31}|^{\Delta}}\,. \end{aligned} \tag{3.103}$$

Equating (3.101)-(3.102) with the holographic correlators in (3.103) we conclude $\Delta = 2\Delta_\Phi$, with

$$\mathbb{Q}_{p^n} \qquad g_3 = \frac{-1}{\sqrt{N}} \frac{2\sqrt{2}}{\widetilde{c}_\Delta^{3/2} f_{\Delta\Delta\Delta}}\,. \tag{3.104}$$

In a free p-adic CFT, $\Delta_\Phi = (n-s)/2$ where s is a (continuous) free parameter and is usually restricted to be in the range $n/2 < s < n$ (these points will be explained in chapter 4). Using (3.104), referring to (3.23) for the explicit form of $f_{\Delta\Delta\Delta}$, and setting $\Delta = 2\Delta_\Phi$, we see that g_3 vanishes at $n = 3s/2$, while g_4 and $\widetilde{g}_4$ in (3.98) stay finite and non-vanishing there. It is interesting to compare this with the situation in the Archimedean case, where we usually set $s = 2$ and the cubic scalar coupling vanishes at $n = 3$ [96, 97].[24]

Continuing on to the connected free-field four-point function, up to contact

[23] The three-point function in (3.103) comes from (3.19). The calculation of the two-point function is slightly subtle and is discussed in detail in chapter 2. To translate from chapter 2 to our current conventions, set $\eta_p = 1$ and $\mathcal{O}_{\text{here}} = \sqrt{\widetilde{c}_\Delta}/c_\Delta \mathcal{O}_{\text{there}}$ where c_Δ, $\widetilde{c}_\Delta$ are given in (3.18) and (3.21) respectively. This rescaling leads directly to $\langle \mathcal{O}_{\text{here}}(x_1)\mathcal{O}_{\text{here}}(x_2)\rangle = 1/|x_{12}|^{2\Delta}$.

[24] Curiously, the p-adic couplings g_3, g_4 and $\widetilde{g}_4$ vanish simultaneously for $n = s$. Could this be related to higher spin theories at $n = s = 2$ (i.e. AdS_3) in the Archimedean case, which are known to have special properties [98, 99, 100]?

terms, it is

$$\mathbb{Q}_{p^n} \qquad \begin{aligned} &\langle \mathcal{O}(x_1)\mathcal{O}(x_2)\mathcal{O}(x_3)\mathcal{O}(x_4)\rangle \\ &= \frac{4}{N}\left(\frac{1}{|x_{12}x_{23}x_{34}x_{41}|^{2\Delta_\Phi}} + \frac{1}{|x_{12}x_{24}x_{43}x_{31}|^{2\Delta_\Phi}} + \frac{1}{|x_{13}x_{32}x_{24}x_{41}|^{2\Delta_\Phi}}\right), \end{aligned} \tag{3.105}$$

where $4/N = 16C^4N$ with the factor of 16 coming from the possible Wick contractions. Holographically, we found the four-point function to be given by (3.99). Since g_3 has already been fixed, a non-trivial consistency check is to verify that (3.104) is consistent with

$$\mathbb{Q}_{p^n} \qquad \frac{4}{N} = \frac{g_3^2}{2}\widetilde{c}_\Delta^3 f_{\Delta\Delta\Delta}^2\,, \tag{3.106}$$

and we find that it is.

In $\mathbb{R}^n$, the coupling constant for a spin-ℓ_1–spin-ℓ_2–spin-ℓ_3 cubic vertex in the minimal bosonic higher spin theory conjecturally dual to the free $O(N)$ model in n dimensions is (c.f. (2.14) of [101] for the scalar–scalar–spin-ℓ coupling, or more generally (1.12) of [102])

$$\mathbb{R}^n \qquad g_3^{(\ell_1,\ell_2,\ell_3)} = \frac{\pi^{\frac{n-3}{4}} 2^{\frac{1}{2}(3n+\ell_1+\ell_2+\ell_3-1)}}{\sqrt{N}\,\Gamma_{\text{Euler}}(n+\ell_1+\ell_2+\ell_3-3)} \prod_{i=1}^{3} \sqrt{\frac{\Gamma_{\text{Euler}}(\ell_i+\frac{n-1}{2})}{\Gamma_{\text{Euler}}(\ell_i+1)}}\,, \tag{3.107}$$

which at $\ell_i = 0$ for all i reduces to the scalar–scalar–scalar coupling constant

$$\mathbb{R}^n \qquad g_3^{(0,0,0)} = \frac{1}{\sqrt{N}} \frac{2\sqrt{2}}{\widetilde{c}_\Delta^{3/2} f_{\Delta\Delta\Delta}}\,, \tag{3.108}$$

where $\widetilde{c}_\Delta$ is given by (3.17), $f_{\Delta\Delta\Delta}$ by (3.23), and $\Delta = n-2$. Equation (3.108) is to be compared with the p-adic result in (3.104). The authors of [101] determine the full quartic scalar coupling in the bulk dual to the free $O(N)$ model by choosing an ansatz for the contact interaction schematically of the form

$$\mathbb{R}^n \quad \mathcal{V} = \sum_{m,\ell=0}^{\infty} \lambda_{m,\ell}(\phi(x)\nabla_{\mu_1}\ldots\nabla_{\mu_\ell}\phi(x)+\cdots)\,\Box^m(\phi(x)\nabla^{\mu_1}\ldots\nabla^{\mu_\ell}\phi(x)+\cdots)\,, \tag{3.109}$$

which together with contributions from exchange diagrams [103], must reproduce the full connected four-point function of the free-theory. This leads to a generating function for the constants $\lambda_{m,\ell}$ [101].

In the minimal construction presented in this chapter, we have avoided a discussion of higher spin operators in the boundary theory since local currents in p-adic field theories are still not properly understood. Analogously, an understanding of gauge fields on the Bruhat–Tits tree remains elusive so far. With this caveat in mind, we may summarise the findings of this section in the form of a bulk quartic coupling on the Bruhat–Tits tree

$$\mathbb{Q}_{p^n} \qquad \mathcal{V} = \sum_{m=0}^{1} \lambda_m \phi_a^2 \, \Box^m \, \phi_a^2 \,, \tag{3.110}$$

which, together with exchange diagrams coming from the cubic coupling reproduces the $O(1/N)$ four-point function of the free p-adic $O(N)$ model. Here $\Box$ is the Laplacian on the tree, defined by

$$\mathbb{Q}_{p^n} \qquad \Box \, \phi_a \equiv \sum_{b \sim a} (\phi_a - \phi_b) \,, \tag{3.111}$$

where the sum $\sum_{b\sim a}$ is over the nearest neighbors b of a, and the coefficients λ_m are related to $g_4, \widetilde{g}_4$ given in (3.98) via

$$\mathbb{Q}_{p^n} \qquad \lambda_0 = \frac{g_4}{4!} + \frac{\widetilde{g}_4}{8}(p^n + 1) \qquad \lambda_1 = -\frac{\widetilde{g}_4}{8} \,. \tag{3.112}$$

In this section we were guided by Occam's razor to find the simplest action which produces the desired correlators of a free field theory, up to the four-point function. A reasonable expectation is that if we allow more interaction terms (for example, next-to-nearest neighbor quartic interactions), the bulk theory will no longer be entirely constrained by its correlators up to four-point functions. Indeed, it is possible that the introduction of gauge degrees of freedom, or considerations of higher-point correlators, will suggest the existence of additional interaction vertices. It would be interesting to find symmetry principles which fully dictate the form of the bulk dual of the free p-adic $O(N)$ model.

3.5 Discussion

Despite appearances, non-Archimedean AdS/CFT is not disconnected from the usual Archimedean AdS/CFT correspondence; this becomes strikingly transparent when all quantities are expressed in terms of the right functions, namely the local zeta functions defined in (3.4)-(3.5) (and related physical quantities such as the mass). Building on chapter 2, we have shown in this chapter explicit evidence in line with this point of view, via the holographic computation of the structure constants as well as the complete four-point function of scalar operators – *i.e.* the four-point contact and exchange diagrams. We showed that the conformal block decomposition essentially truncates at the leading term, and the coefficients of the leading terms admit an adelic structure. Logarithmic singularities occur in the tree-level four-point function when there are multiple operators (single trace or double trace) with identical scaling dimensions, just like in the Archimedean case. In fact, just like in the Archimedean case [86], we wrote down algebraic conditions when these singularities occur. These conditions are the same as the Archimedean conditions, except there are finitely many of them, rather than infinitely many in the Archimedean case. This can be attributed to the presence of a single pole in the p-adic zeta function, as opposed to infinitely many poles in the Archimedean zeta function. We will see this more explicitly in the next chapter, when we compute anomalous dimensions of operators purely from the CFT perspective.

A related source of considerable simplifications in p-adic field theories is the absence of derivatives in the p-adic OPE and hence in the conformal block decomposition of the p-adic four-point function. In fact, the p-adic conformal blocks themselves are significantly simpler than their Archimedean counterparts. Thus subleading (derivative) terms in the conformal block decomposition are absent,

which allows the four-point function to be expressible in closed form. We believe that further insight into how p-adic and Archimedean field theories are to be compared may be gained by studying the integral representation of the p-adic OPE, which does not rely on a derivative expansion even in $\mathbb{R}^n$. Additionally, the simple structure of the OPE, and the remarkable similarity with the geodesic bulk diagram story in the Archimedean place, leads naturally to the expectation that a p-adic analog of kinematic space technology [93] exists. It would be interesting to explore this connection further.

Since the absence of derivatives leads to remarkable simplifications in calculations, we anticipate the computation of higher-point correlators as well as the evaluation of loop corrections in AdS to be considerably easier than in $\mathbb{R}^n$. It will be interesting to compute loop corrections and compare with recent results in $\mathbb{R}^n$ [90]. It will also be interesting to compute diagrams which have remained out of reach so far on the Archimedean side, since the p-adic results may potentially shed some light into computations in $\mathbb{R}^n$. To this end we have presented in appendix 3.A some propagator identities which we expect to be of use in direct computations of certain diagrams.

Crossing symmetry and Mellin space methods were found to be especially useful in computing loop diagrams in $\mathbb{R}^n$ [90]. In p-adic CFTs, crossing symmetry is not as constraining as in $\mathbb{R}^n$; it merely restricts the OPE coefficients to obey the associativity property of a commutative algebra. Once the OPE coefficients have been chosen to obey the associativity property (3.55), there are no further constraints to impose on the scaling dimensions of operators. (We show an explicit example of the triviality of crossing symmetry in the p-adics in appendix 3.B.) On the other hand, application of Mellin space methods in the context of p-adic AdS/CFT do lead to further significant simplifications. However, we leave further comment on this to future work. Recent progress along the lines of [104]

would also be interesting to realize in the p-adic setting.

So far we have restricted ourselves to correlators of external operators without spin. It would be very interesting to include spin degrees of freedom both in the bulk and on the boundary. This will likely involve the use of more general multiplicative characters of the multiplicative group $\mathbb{Q}_{p^n}^{\times}$, along the lines mentioned in [59, 105]. Comparisons with recent work on geodesic bulk diagrams for operators with spin [86, 106, 107, 108, 109] as well as other alternative approaches to conformal block decomposition, such as the one in [110], would also be very interesting.

A difficulty in the study of p-adic AdS/CFT has been the absence of a clean dual pair, where on the bulk side we have a classical theory on the Bruhat–Tits tree and on the boundary side we have a large N field theory which can be formulated independently of any holographic considerations. Our calculations in section 3.4 bring us a step closer to exhibiting such a pair, as we summarize in the next two paragraphs.

On the field theory side, we have the free $O(N)$ model, which admits a lagrangian treatment and has deformations that lead to a Wilson-Fisher fixed point (this will be discussed in detail in chapter 4). On the bulk side, we have the theory (3.96) with couplings chosen as in (3.98) and (3.104). Though this theory seems contrived, it has the virtue of matching the two-, three-, and four-point functions of the operator $\mathcal{O} = \vec{\Phi}^2$. We should ask, what part of this matching was forced, or guaranteed, and what part is non-trivial? The functional form of the two-point and three-point functions are fixed by conformal invariance, so that is an example of a guaranteed match once we choose the mass m_Δ^2 correctly in the bulk action (3.96). The dependence of the four-point function on u is *not* fixed by conformal invariance, but by including on-site cubic, on-site quartic, and nearest neighbor quartic interactions in (3.96), we are giving ourselves just enough parameters to

force an agreement in the functional form of the four-point function between the field theory and the bulk theory. This agreement of the functional form of the four-point function is guaranteed once we impose the relations (3.98).

With functional forms matching perfectly between the field theory and the bulk, there remains the question of whether normalizations match. At the level of our analysis, the normalization of the two-point function is another forced match, based essentially on choosing the normalization of the operator $\mathcal{O}$. Even the normalization of the three-point function is a forced match, because we have one last free parameter in the bulk theory to adjust, namely the cubic coupling g_3. The choice made in (3.104) guarantees a match in the normalization of the three-point function. But there is one more calculation to do, namely the normalization of the four-point function! The condition (3.106) providing for a precise match in the four-point normalization is non-trivial because all quantities involved in it have been fixed by previous considerations as just described. Thus, finding that (3.106) holds is the first non-trivial match we have found between explicit field theory calculations and bulk calculations in p-adic AdS/CFT.

Of course, we hope for much more. In particular, because the setup is so similar to the correspondence [39] between the Archimedean $O(N)$ model and Vasiliev theory in AdS_4 [111, 112], we naturally hope to find some way to reformulate Vasiliev theory on a discrete geometry such as the Bruhat–Tits tree. And we expect to see that the interacting Wilson-Fisher fixed point can be treated holographically just by changing boundary conditions on the bulk field ϕ, as in the Archimedean case. As a step in this direction, we describe the p-adic CFT at the interacting Wilson-Fisher fixed point in the next chapter.

Appendices

3.A Some more propagator identities

In this appendix we list (without proof) some additional propagator identities on the Bruhat–Tits tree which could prove useful in evaluating higher-point correlators and higher loop bulk integrals. Moreover, it is likely they will be useful in obtaining by analogy with $\mathbb{Q}_{p^n}$ the corresponding, as yet unknown, propagator identities in $\mathbb{R}^n$, which could in turn potentially simplify the evaluation of loop diagrams and higher-point functions in $\mathbb{R}^n$.

3.A.1 Identities involving two propagators

Two identities, similar in spirit to (3.67), are:

$$\mathbb{Q}_{p^n} \qquad \sum_{c\in T_{p^n}} \hat{K}_{\Delta_1}(x_1,c)\hat{K}_{\Delta_2}(x_2,c) = \frac{\hat{K}_{\Delta_1}(x_1,o)\hat{K}_{\Delta_2}(x_2,o)}{m^2_{\Delta_1+\Delta_2}\zeta(\Delta_1+\Delta_2)}\,, \tag{3.113}$$

where o is any fixed bulk point lying on the geodesic between x_1 and x_2, and

$$\mathbb{Q}_{p^n} \qquad \sum_{c\in T_{p^n}} G_{\Delta_1}(a_1,c)\hat{K}_{\Delta_2}(x_2,c) = \frac{\hat{K}_{\Delta_2}(x_2,a_1)}{m^2_{\Delta_1}-m^2_{\Delta_2}}\,. \tag{3.114}$$

3.A.2 Identities involving three propagators

We begin by recalling the three-point amplitude

$$\mathbb{Q}_{p^n} \quad \sum_{c\in T_{p^n}} \hat{K}_{\Delta_1}(x_1,c)\hat{K}_{\Delta_2}(x_2,c)\hat{K}_{\Delta_3}(x_3,c) = \hat{K}_{\Delta_1}(x_1,o)\hat{K}_{\Delta_2}(x_2,o)\hat{K}_{\Delta_3}(x_3,o)\, f_{123}\,, \tag{3.115}$$

where o is the unique point of intersection of the geodesics connecting the (boundary) points x_1, x_2, x_3, and f_{123} is a constant given in (3.24).

A few identities which may be useful in evaluating loop diagrams involve, similar to (3.115), a reduction of the integration over a bulk point of a product of three propagators, to a combination of unintegrated propagators. We list here

the identities:

$$\mathbb{Q}_{p^n} \quad \begin{aligned} &\sum_{c\in T_{p^n}} G_{\Delta_1}(a_1,c)\hat{K}_{\Delta_2}(x_2,c)\hat{K}_{\Delta_3}(x_3,c) \\ &= G_{\Delta_1}(a_1,o)\hat{K}_{\Delta_2}(x_2,o)\hat{K}_{\Delta_3}(x_3,o)\, f_{123} - \frac{\hat{K}_{\Delta_2}(x_2,a_1)\hat{K}_{\Delta_3}(x_3,a_1)}{m^2_{\Delta_2+\Delta_3}-m^2_{\Delta_1}}\,, \end{aligned} \tag{3.116}$$

where o is now the bulk point of intersection of geodesics connecting a_1, x_2, x_3. In addition,

$$\mathbb{Q}_{p^n} \quad \begin{aligned} &\sum_{c\in T_{p^n}} G_{\Delta_1}(a_1,c)G_{\Delta_2}(a_2,c)\hat{K}_{\Delta_3}(x_3,c) \\ &= G_{\Delta_1}(a_1,o)G_{\Delta_2}(a_2,o)\hat{K}_{\Delta_3}(x_3,o)\, f_{123} \\ &\quad - \frac{G_{\Delta_2}(a_2,a_1)\hat{K}_{\Delta_3}(x_3,a_1)}{m^2_{\Delta_2+\Delta_3}-m^2_{\Delta_1}} - \frac{G_{\Delta_1}(a_1,a_2)\hat{K}_{\Delta_3}(x_3,a_2)}{m^2_{\Delta_1+\Delta_3}-m^2_{\Delta_2}}\,, \end{aligned} \tag{3.117}$$

and

$$\mathbb{Q}_{p^n} \quad \begin{aligned} &\sum_{c\in T_{p^n}} G_{\Delta_1}(a_1,c)G_{\Delta_2}(a_2,c)G_{\Delta_3}(a_3,c) \\ &= G_{\Delta_1}(a_1,o)G_{\Delta_2}(a_2,o)G_{\Delta_3}(a_3,o)\, f_{123} - \frac{G_{\Delta_2}(a_2,a_1)G_{\Delta_3}(a_3,a_1)}{m^2_{\Delta_2+\Delta_3}-m^2_{\Delta_1}} \\ &\quad - \frac{G_{\Delta_1}(a_1,a_2)G_{\Delta_3}(a_3,a_2)}{m^2_{\Delta_1+\Delta_3}-m^2_{\Delta_2}} - \frac{G_{\Delta_1}(a_1,a_3)G_{\Delta_2}(a_2,a_3)}{m^2_{\Delta_1+\Delta_2}-m^2_{\Delta_3}}\,. \end{aligned} \tag{3.118}$$

As a check, when $a_1 = a_2$ (in which case the point of intersection $o = a_1 = a_2$), we recover from (3.118) the two propagator identity (3.67),

$$\mathbb{Q}_{p^n} \quad \sum_{c\in T_{p^n}} G_{\Delta_1+\Delta_2}(a_1,c)G_{\Delta_3}(a_3,c) = \frac{G_{\Delta_1+\Delta_2}(a_1,a_3)-G_{\Delta_3}(a_1,a_3)}{m^2_{\Delta_3}-m^2_{\Delta_1+\Delta_2}}\,. \tag{3.119}$$

3.B Crossing symmetry of the four-point function

In this appendix, we demonstrate how crossing symmetry of the p-adic four-point function works with an explicit example (see [87] for a more general argument).

Let us consider an exchange diagram where the boundary configuration is in the 's-channel' (more accurately, we'd like to allow $u \leq v = 1$), and a scalar of dimension Δ is exchanged in the (13)(24) channel. This is precisely the diagram defined in (3.83), whose conformal block decomposition in the crossed channel is given in (3.84)-(3.86). As expected it involves just the conformal blocks of double-trace operators. If we wanted the conformal block decomposition of (3.83) in the direct channel (for which the boundary points x_i must be able to admit a 't-channel' configuration as well), we need only adapt the result in (3.79)-(3.80) by making the replacements $\Delta_2 \leftrightarrow \Delta_3$ and $x_2 \leftrightarrow x_3$. (This prescription is obvious upon comparing (3.76) with (3.83).) This leads to

$\mathbb{Q}_{p^n}$
$$\mathcal{D}^T_\Delta = C_{13\Delta}C_{24\Delta}\mathcal{G}_\Delta(u') + P_1(13)\mathcal{G}_{\Delta_C}(u') + P_1(24)\mathcal{G}_{\Delta_D}(u') \tag{3.120}$$

where the OPE coefficients-squared are obtained by making the replacements in (3.79)-(3.80) as described above, Δ_C, Δ_D are defined in (3.87) and

$\mathbb{Q}_{p^n}$
$$u' = \left|\frac{x_{13}x_{24}}{x_{12}x_{34}}\right| = \frac{1}{u}\,. \tag{3.121}$$

As expected in the direct channel, in addition to the double-trace operators, the single-trace operator exchanged in the intermediate channel appears in the conformal block decomposition. Now crossing symmetry requires that the expressions in the direct and crossed channels agree. The crucial point is that we required the boundary points x_i to admit both an 's-channel' as well a 't-channel' configuration. As we remarked at the end of section 3.1, this forces $u = 1/u' = 1$ (and v remains fixed at $v = 1$). Plugging this in the expressions and comparing (3.84)-(3.86) with (3.120), we find they agree exactly as required by crossing symmetry.

3.C Cubic derivative interactions

In this appendix we briefly discuss bulk cubic couplings with derivatives. We have shown in section 3.2.1 that a $\phi_1\phi_2\phi_3$ bulk coupling results in a three-point amplitude for the dual operator given by

$$\mathbb{Q}_{p^n} \qquad \mathcal{A} \equiv \frac{1}{V(x_i)} \sum_{a \in T_{p^n}} \prod_i^3 \hat{K}_{\Delta_i}(x_i, a) = f_{123}\,, \tag{3.122}$$

where f_{ijk} is given in (3.23) and

$$V(x_i) = \frac{1}{|x_{12}|^{\Delta_1+\Delta_2-\Delta_3}|x_{23}|^{\Delta_2+\Delta_3-\Delta_1}|x_{13}|^{\Delta_3+\Delta_1-\Delta_2}}. \tag{3.123}$$

The corresponding amplitude in $\mathbb{R}^n$ is [77]

$$\mathbb{R}^n \qquad \mathcal{A} \equiv \frac{1}{V(x_i)} \int \frac{d^{n+1}y}{y_0^{n+1}} \prod_i^3 \hat{K}_{\Delta_i}(y_0, \vec{y} - \vec{x}_i) = \frac{1}{2} f_{123}\,. \tag{3.124}$$

We now describe what a derivative cubic coupling, schematically of the form $\phi(\nabla\phi)^2$, looks like on the Bruhat–Tits tree. Mimicking $\mathbb{R}^n$, where such a coupling arises from a $\phi_1 g^{\mu\nu}\partial_\mu\phi_2\partial_\nu\phi_3$ interaction vertex, we posit an obvious candidate vertex on the Bruhat–Tits tree,

$$\mathbb{Q}_{p^n} \qquad S \supset \sum_{\langle ab \rangle} \phi_{1a}\left(\phi_{2a} - \phi_{2b}\right)\left(\phi_{3a} - \phi_{3b}\right), \tag{3.125}$$

where ϕ_i has scaling dimension Δ_i and a, b label vertices on the tree. The symbol $\sum_{\langle ab \rangle}$ stands for summing over all pairs of nearest neighbors. It is apparent from the structure of (3.125) that it involves nearest-neighbor interactions of the form $\phi_a\phi_a\phi_b$, where a and b are adjacent vertices on the tree. Thus introducing derivative bulk couplings is tantamount to introducing nearest-neighbor interactions on the tree. (More generally, for higher derivative couplings, one should introduce $(\text{next})^k$-to-nearest neighbor interactions on the tree.) Computing the amplitude

arising from (3.125), we obtain

$$\mathbb{Q}_{p^n} \qquad \begin{aligned} \mathcal{A}_\partial &\equiv \frac{1}{V}\sum_{\langle ab\rangle} \hat{K}_{\Delta_1}(x_1,a)(\hat{K}_{\Delta_2}(x_2,a)-\hat{K}_{\Delta_2}(x_2,b))(\hat{K}_{\Delta_3}(x_3,a)-\hat{K}_{\Delta_3}(x_3,b)) \\ &= \frac{1}{2}\left(m_{\Delta_1}^2 - m_{\Delta_2}^2 - m_{\Delta_3}^2\right)\mathcal{A}\,, \end{aligned} \tag{3.126}$$

where $\mathcal{A}$ is given by (3.122). The final expression in (3.126) follows from a straightforward computation on the Bruhat–Tits tree. The corresponding amplitude in $\mathbb{R}^n$ is [77]

$$\mathbb{R}^n \qquad \begin{aligned} \mathcal{A}_\partial &\equiv \frac{1}{V}\int \frac{d^{n+1}y}{y_0^{n+1}}\,\hat{K}_{\Delta_1}(y_0,\vec{y}-\vec{x}_1)\partial_\mu \hat{K}_{\Delta_2}(y_0,\vec{y}-\vec{x}_2) y_0^2 \partial^\mu \hat{K}_{\Delta_3}(y_0,\vec{y}-\vec{x}_3) \\ &= \frac{1}{2}\left(m_{\Delta_1}^2 - m_{\Delta_2}^2 - m_{\Delta_3}^2\right)\mathcal{A}\,, \end{aligned} \tag{3.127}$$

where $\mathcal{A}$ is given by (3.124). The identical form of the amplitudes in (3.126) and (3.127) supports the claim that (3.125) is indeed a derivative coupling on the tree.

3.D Direct computation of geodesic bulk diagrams

Using variants of (3.63) and (3.65) repeatedly, we can convert the four-point amplitudes (such as those in (3.32), (3.76) and (3.83)) into a sum of several terms of the form given in (3.56) and (3.81), repeated below for convenience:

$$\begin{aligned} \mathcal{W}_\Delta^S &= \sum_{\substack{b_1\in\gamma_{12}\\ b_2\in\gamma_{34}}} (x_1b_1)^{\Delta_1}(x_2b_1)^{\Delta_2}(b_1b_2)^{\Delta}(x_3b_2)^{\Delta_3}(x_4b_2)^{\Delta_4} \\ \mathcal{W}_\Delta^T &= \sum_{\substack{b_1\in\gamma_{13}\\ b_2\in\gamma_{24}}} (x_1b_1)^{\Delta_1}(x_3b_1)^{\Delta_3}(b_1b_2)^{\Delta}(x_2b_2)^{\Delta_2}(x_4b_2)^{\Delta_4} \\ \mathcal{W}_\Delta^U &= \sum_{\substack{b_1\in\gamma_{14}\\ b_2\in\gamma_{23}}} (x_1b_1)^{\Delta_1}(x_4b_1)^{\Delta_4}(b_1b_2)^{\Delta}(x_2b_2)^{\Delta_2}(x_3b_2)^{\Delta_3}\,. \end{aligned} \tag{3.128}$$

(One such computation was detailed in section 3.3.3.) Here we write $(ab)^\Delta$ instead of $\hat{G}_\Delta(b,a)$ or $\hat{K}_\Delta(b,a)$ for brevity. The symbol γ_{ij} denotes a geodesic joining boundary points x_i and x_j. From here on we will denote geodesic paths by $(x_i : x_j)$. If paths from boundary points x_1, x_2, and x_3 meet at a bulk point c, then we have

$$\mathbb{Q}_{p^n} \qquad (x_1 c)^\Delta = \left| \frac{x_{23}}{x_{12} x_{13}} \right|^\Delta . \tag{3.129}$$

We restrict attention to configurations of the x_i such that $u \leq 1$ and $v = 1$, where u and v are defined in (3.30). We can do this without loss of generality because upto relabelling of x_i, we can always arrange $u \leq 1$ and $v = 1$. In these sorts of configurations, paths from x_1 and x_2 converge at a bulk point c_1, which connects to a bulk point c_2 where paths from x_3 and x_4 converge (see, for example, figure 3.1). An important identity is

$$\mathbb{Q}_{p^n} \qquad u = \left| \frac{x_{12} x_{34}}{x_{13} x_{24}} \right| = (c_1 c_2) = p^{-d(c_1, c_2)} . \tag{3.130}$$

If $u = 1$ then c_1 and c_2 coincide.

In the main text, we noted without proof that the sums in (3.128), which are referred to as geodesic bulk diagrams, are related to p-adic conformal blocks via the identities in (3.57) and (3.82). The goal of this appendix is to prove these identities by direct computation.

We can conveniently factor out most of the x_i dependence from any of the geodesic bulk diagrams we consider by dividing out by the trivial conformal partial wave $W_0(x_i)$, given in (3.36). A more convenient form for W_0 follows from (3.33),

$$\mathbb{Q}_{p^n} \qquad W_0(x_i) = (x_1 c_1)^{\Delta_1} (x_2 c_1)^{\Delta_2} (x_3 c_2)^{\Delta_3} (x_4 c_2)^{\Delta_4} . \tag{3.131}$$

Then for any of the geodesic bulk diagrams $\mathcal{W}$ we consider, $\mathcal{W}/W_0(x_i)$ is a func-

tion of the x_i only through dependence on the cross-ratio u. An easy case is

$$\mathbb{Q}_{p^n} \quad \frac{\mathcal{W}_\Delta^S}{W_0} = \left[\sum_{b_1 \in (x_1 : c_1]} \frac{(x_1 b_1)^{\Delta_1} (x_2 b_1)^{\Delta_2} (b_1 c_1)^{\Delta}}{(x_1 c_1)^{\Delta_1} (x_2 c_1)^{\Delta_2}} + \sum_{b_1 \in (c_1 : x_2)} \frac{(x_1 b_1)^{\Delta_1} (x_2 b_1)^{\Delta_2} (b_1 c_1)^{\Delta}}{(x_1 c_1)^{\Delta_1} (x_2 c_1)^{\Delta_2}} \right] u^\Delta \times \left[\sum_{b_2 \in (x_3 : c_2]} \frac{(x_3 b_2)^{\Delta_3} (x_4 b_2)^{\Delta_4} (b_2 c_2)^{\Delta}}{(x_3 c_2)^{\Delta_3} (x_4 c_2)^{\Delta_4}} + \sum_{b_2 \in (c_2 : x_4)} \frac{(x_3 b_2)^{\Delta_3} (x_4 b_2)^{\Delta_4} (b_2 c_2)^{\Delta}}{(x_3 c_2)^{\Delta_3} (x_4 c_2)^{\Delta_4}} \right]. \tag{3.132}$$

What makes this case relatively easy is that b_1 and b_2 cannot belong to $(c_1 : c_2)$, because the paths $(x_1 : x_2)$ and $(x_3 : x_4)$ do not have any points in common with $(c_1 : c_2)$. In the first sum inside square brackets in (3.132), we have $(x_1 c_1) = (x_1 b_1)(b_1 c_1)$ and $(x_2 b_1) = (x_1 c_1)(b_1 c_1)$. In subsequent sums, similar equalities apply, and using them we simplify (3.132) to

$$\mathbb{Q}_{p^n} \quad \begin{aligned} \frac{\mathcal{W}_\Delta^S}{W_0} &= u^\Delta \left[\sum_{b_1 \in (x_1 : c_1]} (b_1 c_1)^{\Delta - \Delta_{12}} + \sum_{b_1 \in (c_1 : x_2)} (b_1 c_1)^{\Delta + \Delta_{12}} \right] \\ &\quad \times \left[\sum_{b_2 \in (x_3 : c_2]} (b_2 c_2)^{\Delta - \Delta_{34}} + \sum_{b_2 \in (c_2 : x_4)} (b_2 c_2)^{\Delta + \Delta_{34}} \right] \\ &= \beta^{(\Delta + \Delta_{12}, \Delta - \Delta_{12})} \beta^{(\Delta + \Delta_{34}, \Delta - \Delta_{34})}, \end{aligned} \tag{3.133}$$

where $\beta^{(s,t)}$ is defined in (3.6). This proves (3.57). A graphical method of obtaining (3.133) is shown in figure 3.4. It is worth noting that the sums in (3.133) converge iff the four quantities $\Delta \pm \Delta_{12}$ and $\Delta \pm \Delta_{34}$ are all positive. If any one of them goes to 0, then we have a logarithmic divergence.

$\mathcal{W}_\Delta^T$ is more complicated than $\mathcal{W}_\Delta^S$ because the paths $(x_1 : x_3)$ and $(x_2 : x_4)$ are longer than $(x_1 : x_2)$ and $(x_3 : x_4)$, and there are more distinct ways to position

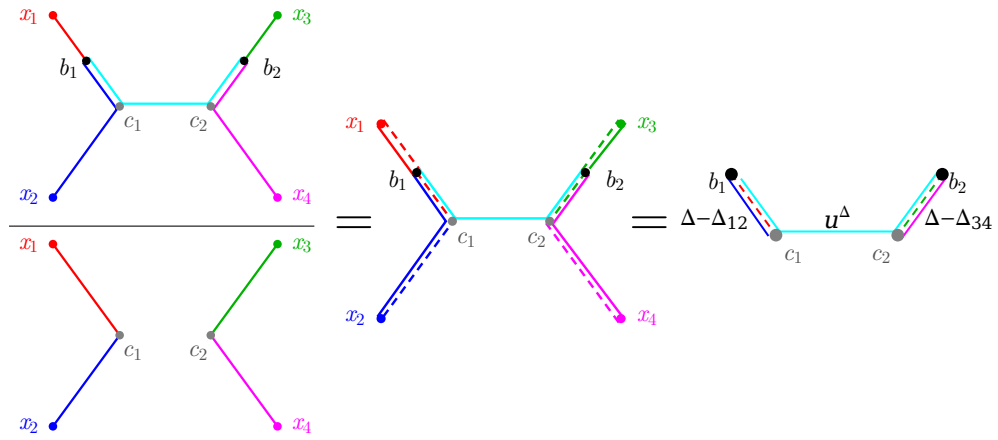

Figure 3.4: A graphical method of representing terms in (3.132)-(3.133). Here and in figure 3.5, a solid line means that the amplitude should include a factor of the propagator between the endpoints of that line, whereas a dashed line means that we are dividing by that propagator. When a combination of solid and dashed lines is labeled with a power δ, like $\Delta - \Delta_{12}$, it means that each step along this combinations of lines is weighted by a factor of $p^{-\delta}$. To improve readability we use u^{δ} instead of δ to label combined lines between c_1 and c_2.

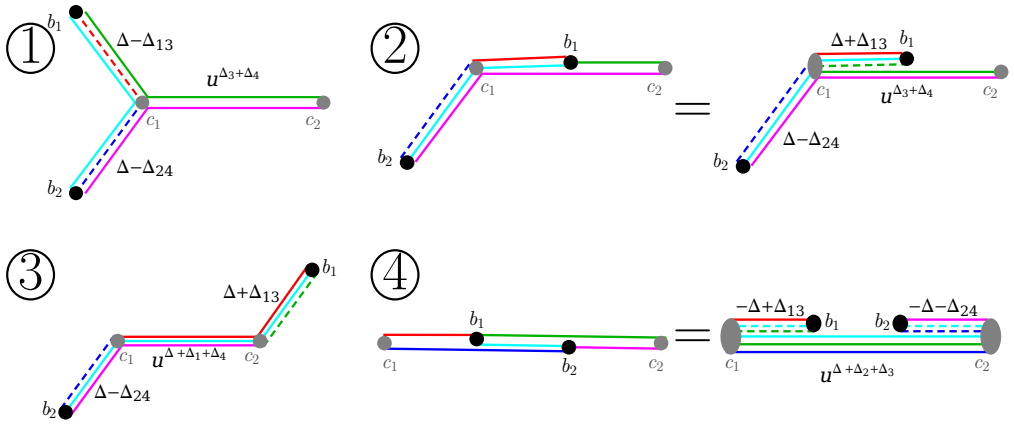

Figure 3.5: Subway diagrams leading to summands in (3.134).

b_1 and b_2 along these paths. The full list of possibilities can be enumerated as follows:

#	$b_1 \in$	$b_2 \in$	summand
1:	$(x_1 : c_1)$	$(x_2 : c_1)$	$u^{\Delta_B}(b_1c_1)^{\Delta-\Delta_{13}}(b_2c_1)^{\Delta-\Delta_{24}}$
$\tilde{1}$:	$(x_3 : c_2)$	$(x_4 : c_2)$	$u^{\Delta_A}(b_1c_2)^{\Delta-\Delta_{13}}(b_2c_2)^{\Delta+\Delta_{24}}$
2:	$[c_1 : c_2]$	$(x_2 : c_1)$	$u^{\Delta_B}(b_1c_1)^{\Delta+\Delta_{13}}(b_2c_1)^{\Delta-\Delta_{24}}$
$\tilde{2}$:	$[c_1 : c_2]$	$(x_4 : c_2)$	$u^{\Delta_A}(b_1c_2)^{\Delta-\Delta_{13}}(b_2c_2)^{\Delta+\Delta_{24}}$
$\underline{2}$:	$(x_1 : c_1)$	$[c_1 : c_2]$	$u^{\Delta_B}(b_1c_1)^{\Delta+\Delta_{24}}(b_2c_1)^{\Delta-\Delta_{13}}$
$\tilde{\underline{2}}$:	$(x_3 : c_2)$	$[c_1 : c_2]$	$u^{\Delta_A}(b_1c_2)^{\Delta-\Delta_{24}}(b_2c_2)^{\Delta+\Delta_{13}}$
3:	$(x_3 : c_2)$	$(x_2 : c_1)$	$u^{\Delta+\Delta_E}(b_1c_2)^{\Delta+\Delta_{13}}(b_2c_2)^{\Delta-\Delta_{24}}$
$\tilde{3}$:	$(x_2 : c_1)$	$(x_4 : c_2)$	$u^{\Delta+\Delta_F}(b_1c_1)^{\Delta-\Delta_{13}}(b_2c_1)^{\Delta+\Delta_{24}}$
4:	$[c_1 : c_2]$	$[b_1 : c_2]$	$u^{\Delta+\Delta_F}(b_1c_1)^{-\Delta+\Delta_{13}}(b_2c_2)^{-\Delta-\Delta_{24}}$
$\tilde{4}$:	$(c_1 : c_2]$	$[c_1 : b_1)$	$u^{\Delta+\Delta_E}(b_1c_2)^{-\Delta-\Delta_{13}}(b_2c_1)^{-\Delta+\Delta_{24}}$

(3.134)

where $\Delta_A, \Delta_B, \Delta_E$ and Δ_F are defined in footnote 16. The summands can be written down by inspection of the relevant subway diagrams, a representative sampling of which is shown in figure 3.5.

Of the ten rows of (3.134), only the following five need to be computed explicitly:

$$\begin{aligned} V_1 &\equiv u^{\Delta_B} \sum_{\substack{b_1 \in (x_1:c_1) \\ b_2 \in (x_2:c_1)}} (b_1c_1)^{\Delta-\Delta_{13}}(b_2c_1)^{\Delta-\Delta_{24}} \\ &= u^{\Delta_B} \left[\sum_{m_1=1}^{\infty} p^{-m_1(\Delta-\Delta_{13})}\right] \left[\sum_{m_2=1}^{\infty} p^{-m_2(\Delta-\Delta_{24})}\right] \end{aligned} \tag{3.135}$$

$$\begin{aligned} V_2 &\equiv u^{\Delta_B} \sum_{\substack{b_1 \in [c_1:c_2] \\ b_2 \in (x_2:c_1)}} (b_1c_1)^{\Delta+\Delta_{13}}(b_2c_1)^{\Delta-\Delta_{24}} \\ &= u^{\Delta_B} \left[\sum_{m_1=0}^{d} p^{-m_1(\Delta+\Delta_{13})}\right] \left[\sum_{m_2=1}^{\infty} p^{-m_2(\Delta-\Delta_{24})}\right] \end{aligned} \tag{3.136}$$

$$
\begin{aligned}
V_3 &\equiv u^{\Delta+\Delta_E} \sum_{\substack{b_1\in(x_3:c_2)\\ b_2\in(x_2:c_1)}} (b_1c_2)^{\Delta+\Delta_{13}}(b_2c_2)^{\Delta-\Delta_{24}} \\
&= u^{\Delta+\Delta_E}\left[\sum_{m_1=1}^{\infty} p^{-m_1(\Delta+\Delta_{13})}\right]\left[\sum_{m_2=1}^{\infty} p^{-m_2(\Delta-\Delta_{24})}\right]
\end{aligned}
\tag{3.137}
$$

$$
\begin{aligned}
V_4 &\equiv u^{\Delta+\Delta_F} \sum_{\substack{b_1\in[c_1:c_2]\\ b_2\in[b_1:c_2]}} (b_1c_1)^{-\Delta+\Delta_{13}}(b_2c_2)^{-\Delta-\Delta_{24}} \\
&= u^{\Delta+\Delta_F} \sum_{m_1=0}^{d} p^{-m_1(-\Delta+\Delta_{13})} \sum_{m_2=0}^{d-m_1} p^{-m_2(-\Delta-\Delta_{24})}
\end{aligned}
\tag{3.138}
$$

$$
\begin{aligned}
V_{\tilde{4}} &\equiv u^{\Delta+\Delta_E} \sum_{\substack{b_1\in(c_1:c_2]\\ b_2\in[c_1:b_1)}} (b_1c_2)^{-\Delta-\Delta_{13}}(b_2c_1)^{-\Delta+\Delta_{24}} \\
&= u^{\Delta+\Delta_E} \sum_{m_1=0}^{d-1} p^{-m_1(-\Delta-\Delta_{13})} \sum_{m_2=0}^{d-1-m_1} p^{-m_2(-\Delta+\Delta_{24})}\,,
\end{aligned}
\tag{3.139}
$$

where $d = d(c_1, c_2) = -\log_p u$. Using obvious relations like

$$
\sum_{m=0}^{\infty} p^{-ma} = \zeta(a) \qquad \sum_{m=1}^{\infty} p^{-ma} = -\zeta(-a)
$$

$\mathbb{Q}_{p^n}$

$$
\sum_{m=0}^{d} p^{-ma} = \zeta(a) + u^a\zeta(-a) \tag{3.140}
$$

$$
\zeta(a)\zeta(b) + \zeta(a+b)\zeta(-b) - \zeta(a+b)\zeta(a) = 0\,,
$$

we can simplify (3.135)-(3.139) to

$$\begin{aligned}
V_1 &= u^{\Delta_3+\Delta_4}\zeta(-\Delta+\Delta_{13})\zeta(-\Delta+\Delta_{24}) \\
V_2 &= -u^{\Delta_3+\Delta_4}\zeta(\Delta+\Delta_{13})\zeta(-\Delta+\Delta_{24}) \\
&\quad - u^{\Delta+\Delta_1+\Delta_4}\zeta(-\Delta-\Delta_{13})\zeta(-\Delta+\Delta_{24}) \\
V_3 &= u^{\Delta+\Delta_1+\Delta_4}\zeta(-\Delta-\Delta_{13})\zeta(-\Delta+\Delta_{24}) \\
V_4 &= u^{\Delta_1+\Delta_2}\zeta(\Delta-\Delta_{13})\zeta(-\Delta_{13}-\Delta_{24}) \\
&\quad + u^{\Delta_3+\Delta_4}\zeta(\Delta+\Delta_{24})\zeta(\Delta_{13}+\Delta_{24}) \\
&\quad + u^{\Delta+\Delta_2+\Delta_3}\zeta(-\Delta+\Delta_{13})\zeta(-\Delta-\Delta_{24}) \\
V_{\tilde{4}} &= -u^{\Delta_1+\Delta_2}\zeta(-\Delta+\Delta_{24})\zeta(-\Delta_{13}-\Delta_{24}) \\
&\quad - u^{\Delta_3+\Delta_4}\zeta(-\Delta-\Delta_{13})\zeta(\Delta_{13}+\Delta_{24}) \\
&\quad + u^{\Delta+\Delta_1+\Delta_4}\zeta(-\Delta-\Delta_{13})\zeta(-\Delta+\Delta_{24})\,.
\end{aligned} \tag{3.141}$$

$\mathbb{Q}_{p^n}$

To obtain the remaining five amplitudes explicitly, we can either swap $1 \leftrightarrow 3$ and $2 \leftrightarrow 4$ (e.g. to go from 2 to $\tilde{2}$) or $1 \leftrightarrow 2$ and $3 \leftrightarrow 4$ (to go from 2 to $\underline{2}$). In summary,

$$\begin{aligned}
V_{\tilde{1}} &= u^{\Delta_1+\Delta_2}\zeta(-\Delta-\Delta_{13})\zeta(-\Delta-\Delta_{24}) \\
V_{\tilde{2}} &= -u^{\Delta_1+\Delta_2}\zeta(\Delta-\Delta_{13})\zeta(-\Delta-\Delta_{24}) \\
&\quad - u^{\Delta+\Delta_2+\Delta_3}\zeta(-\Delta+\Delta_{13})\zeta(-\Delta-\Delta_{24}) \\
V_{\underline{2}} &= -u^{\Delta_3+\Delta_4}\zeta(-\Delta+\Delta_{13})\zeta(\Delta+\Delta_{24}) \\
&\quad - u^{\Delta+\Delta_2+\Delta_3}\zeta(-\Delta+\Delta_{13})\zeta(-\Delta-\Delta_{24}) \\
V_{\underline{\tilde{2}}} &= -u^{\Delta_1+\Delta_2}\zeta(-\Delta-\Delta_{13})\zeta(\Delta-\Delta_{24}) \\
&\quad - u^{\Delta+\Delta_1+\Delta_4}\zeta(-\Delta-\Delta_{13})\zeta(-\Delta+\Delta_{24}) \\
V_{\tilde{3}} &= u^{\Delta+\Delta_2+\Delta_3}\zeta(-\Delta+\Delta_{13})\zeta(\Delta-\Delta_{24})\,.
\end{aligned} \tag{3.142}$$

$\mathbb{Q}_{p^n}$

Our eventual goal is to add all ten V_a together. As a step in that direction, let's call $u^{\Delta_1+\Delta_2}$ and $u^{\Delta_3+\Delta_4}$ "compliant" powers of u, whereas any power of u involving Δ is "non-compliant." Then we notice that non-compliant powers cancel in the following partial sums:

$$\begin{aligned}
V_2 + V_3 &= -u^{\Delta_3+\Delta_4}\zeta(\Delta+\Delta_{13})\zeta(-\Delta+\Delta_{24}) \\
V_{\bar{2}} + V_{\bar{3}} &= -u^{\Delta_1+\Delta_2}\zeta(\Delta-\Delta_{13})\zeta(-\Delta-\Delta_{24}) \\
V_{\underline{2}} + V_4 &= u^{\Delta_1+\Delta_2}\zeta(\Delta-\Delta_{13})\zeta(-\Delta_{13}-\Delta_{24}) \\
&\quad + u^{\Delta_3+\Delta_4}\zeta(\Delta-\Delta_{13})\zeta(\Delta_{13}+\Delta_{24}) \\
V_{\underline{\bar{2}}} + V_{\bar{4}} &= -u^{\Delta_1+\Delta_2}\zeta(-\Delta-\Delta_{13})\zeta(-\Delta_{13}-\Delta_{24}) \\
&\quad - u^{\Delta_3+\Delta_4}\zeta(-\Delta-\Delta_{13})\zeta(\Delta_{13}+\Delta_{24})\,.
\end{aligned} \tag{3.143}$$

$\mathbb{Q}_{p^n}$

Finally, we can assemble the full exchange amplitude in the (13)(24)-channel

$$\begin{aligned}
\frac{\mathcal{W}_\Delta^T}{W_0} &= V_1 + V_2 + V_3 + V_{\bar{1}} + V_{\bar{2}} + V_{\bar{3}} + V_{\underline{2}} + V_4 + V_{\underline{\bar{2}}} + V_{\bar{4}} \\
&= \beta^{(\Delta+\Delta_{13},\Delta-\Delta_{13})}\beta^{(-\Delta_{13}-\Delta_{24},\Delta+\Delta_{24})}u^{\Delta_1+\Delta_2} \\
&\quad + \beta^{(\Delta+\Delta_{13},\Delta-\Delta_{13})}\beta^{(\Delta_{13}+\Delta_{24},\Delta-\Delta_{24})}u^{\Delta_3+\Delta_4}.
\end{aligned} \tag{3.144}$$

$\mathbb{Q}_{p^n}$

This proves (3.82). Despite appearances, $\mathcal{W}_\Delta^T$ is symmetric under $1 \leftrightarrow 3$, $2 \leftrightarrow 4$ as well as $1 \leftrightarrow 2$, $3 \leftrightarrow 4$. The amplitude with the exchange in the (14)(23)-channel is obtained by swapping $3 \leftrightarrow 4$ in $\mathcal{W}_\Delta^T$:

$$\begin{aligned}
\frac{\mathcal{W}_\Delta^U}{W_0} &= \beta^{(\Delta+\Delta_{14},\Delta-\Delta_{14})}\beta^{(-\Delta_{14}-\Delta_{23},\Delta+\Delta_{23})}u^{\Delta_1+\Delta_2} \\
&\quad + \beta^{(\Delta+\Delta_{14},\Delta-\Delta_{14})}\beta^{(\Delta_{14}+\Delta_{23},\Delta-\Delta_{23})}u^{\Delta_3+\Delta_4}.
\end{aligned} \tag{3.145}$$

$\mathbb{Q}_{p^n}$

Chapter 4

p-adic field theories

This chapter is based on a lightly edited version of a paper with Steven S. Gubser, Christian Jepsen and Brian Trundy [105]. We thank Przemek Witaszczyk for collaborations on the early stages of this project. We have benefited from discussions with Curt Callan, David Huse, Shivaji Sondhi, Bogdan Stoica, and Grigory Tarnopolsky.

4.1 Introduction and summary

Having studied bulk theories on the Bruhat–Tits tree in the previous two chapters, we now turn to p-adic field theories. Our primary focus will be on the ϕ^4 $O(N)$ vector model defined on a p-adic spacetime (which we'll simply refer to as the p-adic $O(N)$ model).

The precursor to p-adic field theories was the Dyson hierarchical model [113]. It describes a discrete lattice model of spin variables interacting via long-range power law interactions. These interactions have a hierarchical structure — with the spin variables grouped in pairs, and then the pairs paired themselves, and so on — reminiscent of the tree structure of the Bruhat–Tits tree for $p = 2$. In

the continuum limit, this gives rise to a ϕ^4 scalar field theory on $\mathbb{Q}_2$, whereas if p spins are grouped together at each step one obtains in an appropriate limit a field theory over $\mathbb{Q}_p$ [114]. The spin variables defined on lattice sites become a real valued field defined on the p-adic numbers. One can similarly treat theories where $\mathbb{Q}_p$ is replaced by a field extension $\mathbb{Q}_{p^n}$, which in part means working with a vector space $\mathbb{Q}_p^n$. [1]

Around the time when the hierarchical model was first introduced, early work on the renormalization group flow in continuum field theories [115, 116, 117] built on Kadanoff's spin-blocking methods [118], to obtain finite-step recursion relations which served as an approximation to the flow in continuum systems. In fact it was noted in Wilson's earlier works that the recursion relations become exact when used on the Dyson hierarchical model, while when applied to ordinary ϕ^4 field theory on $\mathbb{R}^n$ they can be used to extract scaling dimensions at the Wilson-Fisher fixed point that are correct through order ϵ, where $\epsilon = 4 - n$. Subsequent work, including [119, 120] and reviewed in [121], established rigorous results on the solvability and fixed points of the renormalization group for hierarchical models as realized by the finite-step recursion relations.

Renormalization in the continuum limit, corresponding to a p-adic ϕ^4 theory, was studied in [114], and its $O(N)$ generalization was explored in [122, 123, 124] at the Wilson-Fisher fixed point in an (appropriate analog of the) ϵ-expansion, leading to expressions for the critical exponents. We review this in section 4.2 where we carry out standard diagrammatic perturbation theory in a small parameter, similar to $\epsilon = 4 - n$ in the Archimedean case.[2] Starting with the action

[1] The spirit of this construction does not seem to require that $q = p^n$ is a power of a prime. However, if it is not, "$\mathbb{Q}_q$" is not a field, nor even an integral domain, and it is harder to understand either the q-adic norm which enters into correlators or the q-adic conformal symmetry that arises near a critical point. We therefore leave the interesting point of general composite q to future work.

[2] Although we do not pursue holographic calculations in the current work, it is natural to hope that the p-adic $O(N)$ model for large N is dual to some appropriate modification of

given in (4.5)-(4.6) defined over $\mathbb{Q}_{p^n}$, we implement Wilsonian renormalization for the two- and four-point functions to one loop order, by integrating out hard momenta shells, one shell at a time. The momentum shell integration is very simply and naturally realized in $\mathbb{Q}_{p^n}$, owing to the ultrametric nature of momentum space. Ultrametricity leads to a significantly simpler renormalization group flow, with *no* wave-function renormalization and *no* generation of new derivative couplings! We exhibit the discrete transformations that implement the Wilsonian renormalization group, and use them to analyze the Wilson-Fisher fixed point in an ϵ-expansion, where $\epsilon = 2s - n$ is the dimension of the relevant coupling in the Gaussian theory, and s is the spectral parameter appearing in the kinetic term.

A key feature of ultrametric theories is that their kinetic terms are non-local. In momentum space, they are expressed as $\int dk\, \frac{1}{2}\phi(-k)|k|^s\phi(k)$, where the spectral parameter s is a real number which we must usually choose between 0 and n. This makes ultrametric theories similar to bilocal field theories on $\mathbb{R}^n$ as studied in [126, 127] and more recently, for example, in [128, 91]. In these bilocal theories, similar kinetic terms are considered, with $|k|^s$ as their momentum space kernel. A special feature of field theories on $\mathbb{R}^n$ is that when s is a positive even integer, the kinetic term becomes local in position space. In section 4.3, we mostly focus on the case $s = 2$ when we examine field theories on $\mathbb{R}^n$. In section 4.4, we argue that $s = 4$ and higher even integers are also interesting: these values give rise to higher derivative $O(N)$ models, and they seem to be free of pathologies as long as they are regarded as Euclidean path integral field theories. Indeed, we seem to recover a four-dimensional non-linear sigma-model originally proposed in the seventies [129]. The four derivative theories have also been considered in the condensed matter literature [130], where they have been used to investigate spatially modulated phases [131] along the lines of the Landau-Brazovskii model

Vasiliev theory defined on the Bruhat-Tits tree, along the lines of [39, 125, 47, 59, 32]. See also section 3.4 of chapter 3.

[132]. Commonly called Lifshitz points, these four derivative theories have connections with the next-to-nearest neighbor Ising model, as reviewed in [133].[3] We will recall the basics of these approaches in section 4.4.

In section 4.3, we adapt methods of [134, 135] to the p-adics to obtain self-consistent results for the critical exponents of the non-Gaussian fixed point that are exact in ϵ and valid through the first non-trivial order in large N. Let us briefly summarise the results here. We start with the action

$$S = \int dx \, \left[\frac{1}{2} \phi^i(x) D^s \phi^i(x) + \frac{\lambda}{4!} \left(\phi^i(x) \phi^i(x) \right)^2 \right] \tag{4.1}$$

for Euclidean quantum field theory defined over some n-dimensional vector space V, where V can be either $\mathbb{R}^n$ or the vector space associated with $\mathbb{Q}_{p^n}$. The integration measure is over this n-dimensional vector space V. D^s is an s-th order derivative operator, which in Fourier space is implemented by multiplying ϕ by $|k|^s$. As alluded to above, this a bilocal term in position space for generic values of s. The kinetic terms becomes a local term for positive integral values of s when $V = \mathbb{R}^n$. (For instance, for $s = 2$, the kinetic term in (4.1) reduces to the familiar $\phi^i \Box \phi^i$.) The sums over i run from 1 to N, which we take to be large. It is reasonable to suppose that in fairly generic circumstances, the theory (4.1) flows to a Wilson-Fisher fixed point — assuming we appropriately tune away relevant operators, in particular the mass deformation. We employ the large-N methods with a Hubbard-Stratonovich field σ, whose equation of motion sets $\sigma = \phi^i \phi^i$ up to a factor. Working to the leading non-trivial order in N, we obtain the anomalous dimensions

$$\begin{aligned} \gamma_\phi &\equiv \Delta_\phi - \frac{n-s}{2} = \operatorname*{Res}_\delta g_\phi(\delta) + \mathcal{O}(1/N^2) \\ \gamma_\sigma &\equiv \Delta_\sigma - s = \operatorname*{Res}_\delta g_\sigma(\delta) + \mathcal{O}(1/N^2) \,, \end{aligned} \tag{4.2}$$

[3] The main focus of many of the condensed matter applications is anisotropic models, in which one direction is singled out and may exhibit different scaling behavior. In this chapter, we are instead interested in the isotropic case.

where $\mathrm{Res}_\delta\, g(\delta)$ means the residue of a meromorphic function $g(\delta)$ at $\delta = 0$. The meromorphic functions are found to be

$$g_\phi(\delta) = \frac{1}{N}\frac{\mathrm{B}(n-s,-s+\delta)}{\mathrm{B}(n-s,n-s)}$$
$$g_\sigma(\delta) = -\frac{2}{N}\frac{\mathrm{B}(n-s,-s+\delta)}{\mathrm{B}(n-s,n-s)} + \frac{1}{N}\left(-1+2\frac{\mathrm{B}(n-s,n-2s)}{\mathrm{B}(n-s,n-s)}\right)\frac{\mathrm{B}(\delta,\delta)}{\mathrm{B}(n-s,n-s)}\,, \tag{4.3}$$

where B is a variant of the Euler Beta function which will be defined in (4.4). An important point is that $g_\phi(\delta)$ has no pole at $\delta = 0$ for $\mathbb{Q}_{p^n}$, and so $\gamma_\phi = 0$ in this case. For $\mathbb{R}^n$, $g_\phi(\delta)$ does have a pole, and one easily recovers standard results [134, 135] for γ_ϕ upon setting $s = 2$. On the other hand, $g_\sigma(\delta)$ generically has a pole both for $\mathbb{R}^n$ and for $\mathbb{Q}_{p^n}$. We have checked that its residue gives γ_σ in accord with the standard results for the case of $\mathbb{R}^n$, and in accord with results from the Wilsonian approach of section 4.2 for $\mathbb{Q}_{p^n}$. In section 4.4, we also check our results against the literature on higher derivative theories corresponding to $s = 4$.

A reminder about the non-standard notation introduced in the previous chapter: $\zeta(t)$ in this chapter will not be the usual Riemann zeta function, nor will $\Gamma(t)$ and $\mathrm{B}(t_1,t_2)$ refer to usual Gamma or Beta functions. Instead $\zeta(t)$ is the "local" zeta function defined either for $\mathbb{R}$ or for $\mathbb{Q}_p$, while $\Gamma(t)$ and $\mathrm{B}(t_1,t_2)$ are defined in reference either to $\mathbb{R}^n$ or the unramified extension $\mathbb{Q}_{p^n}$ of the p-adic numbers of degree n. All these functions take complex arguments and are meromorphic. The point of defining ζ, Γ, and B anew every time we pass to a new field or vector space is that physical quantities like scaling dimensions tend to have a universal form when expressed in terms of the appropriate functions. Even well-known results in $\mathbb{R}^n$ assume pleasingly simple forms in terms of suitably defined $\Gamma_{\mathbb{R}^n}(t)$ and $\mathrm{B}_{\mathbb{R}^n}(t_1,t_2)$.

Formulas applicable only to $\mathbb{R}^n$ or only to $\mathbb{Q}_{p^n}$ will be suitably marked. For

example, the local zeta functions are defined in (3.4)-(3.5) in the previous chapter. Note that the volume of S^{n-1} is $2/\zeta_{\mathbb{R}}(n)$, whereas $1/\zeta_{\mathbb{Q}_p}(n)$ is the volume of the set of units in $\mathbb{Q}_{p^n}$, which is the set of elements $\xi \in \mathbb{Q}_{p^n}$ with $|\xi| = 1$. It is tempting to define $\zeta_{\mathbb{R}^n}(t) \equiv \zeta_{\mathbb{R}}(nt)$ and $\zeta_{\mathbb{Q}_{p^n}}(t) \equiv \zeta_{\mathbb{Q}_p}(nt)$, along the lines of [136, 67], but for our current purposes it is clearer not to do so, and instead always to construe $\zeta(t)$ as $\zeta_{\mathbb{R}}(t)$ or $\zeta_{\mathbb{Q}_p}(t)$, as defined in (3.4)-(3.5).

Formulas which apply equally to $\mathbb{R}^n$ and $\mathbb{Q}_{p^n}$ will be left unmarked, just like in chapter 3. For example,[4]

$$\Gamma(t) \equiv \frac{\zeta(t)}{\zeta(n-t)} \qquad\qquad \mathrm{B}(t_1, t_2) \equiv \frac{\Gamma(t_1)\Gamma(t_2)}{\Gamma(t_1+t_2)}\,. \tag{4.4}$$

In the same spirit as Γ and B implicitly refer either to $\mathbb{R}^n$ or to $\mathbb{Q}_{p^n}$, we also use $|x|$ to denote the absolute value in either $\mathbb{R}^n$ or $\mathbb{Q}_{p^n}$. In the former case, $|x| = \sqrt{\sum_{i=1}^n x_i^2}$, which is an Archimedean norm. In the latter case, $|x|$ is ultrametric and takes values which are integer powers of p; formally, $|x|$ is defined as the p-adic norm of the field norm of x with respect to the extension relation $\mathbb{Q}_{p^n} : \mathbb{Q}_p$.

4.2 p-adic Wilsonian renormalization

Let ϕ^i be a map from $\mathbb{Q}_{p^n}$ to $\mathbb{R}^N$, where n and N are positive integers and p is a prime number. (If $n = 1$ then the domain of ϕ^i is the p-adic numbers themselves). Our reason for focusing on the unramified extension $\mathbb{Q}_{p^n}$ is that it is an n-dimensional vector space over $\mathbb{Q}_p$ with a natural ultrametric norm taking the same values as the norm on $\mathbb{Q}_p$, similar to the way $\mathbb{R}^n$ is an n-dimensional vector space over $\mathbb{R}$ with a natural Archimedean norm (namely the usual L^2 norm). It is likely that the discussion to follow could be generalized to somewhat more general ultrametric spaces, but we do not pursue this.

[4]Gamma-functions defined this way satisfy the functional equation $\Gamma(t)\Gamma(n-t) = 1$. This results in the following useful identity for the Beta function: $\mathrm{B}(t_1, t_2) = \mathrm{B}(t_1, n - t_1 - t_2) = \mathrm{B}(t_2, n - t_1 - t_2)$.

4.2.1 Action

Following [114], we consider the action

$\mathbb{Q}_{p^n}$
$$S = \int dk\, \frac{1}{2}\phi^i(-k)(|k|^s + r)\phi^i(k) + \int dk_1 dk_2 dk_3 dk_4\, \delta(k_1+k_2+k_3+k_4)\frac{\lambda}{4!}T_{i_1i_2i_3i_4}\phi^{i_1}(k_1)\phi^{i_2}(k_2)\phi^{i_3}(k_3)\phi^{i_3}(k_4)\,, \tag{4.5}$$

where summation over repeated indices is implied, and following [137] we set

$\mathbb{Q}_{p^n}$
$$T_{i_1i_2i_3i_4} = \frac{1}{3}(\delta_{i_1i_2}\delta_{i_3i_4} + \delta_{i_1i_3}\delta_{i_2i_4} + \delta_{i_1i_4}\delta_{i_2i_3})\,. \tag{4.6}$$

Fourier transforms are defined by

$\mathbb{Q}_{p^n}$
$$\phi^i(x) = \int dk\, \chi(kx)\phi^i(k)\,, \tag{4.7}$$

where $\chi(\xi) = e^{2\pi i\{\xi\}}$ is an additive character on $\mathbb{Q}_{p^n}$. All integrals in (4.5) and (4.7) are by default over all of $\mathbb{Q}_{p^n}$; however, we may impose a hard momentum cutoff $|k| \leq \Lambda$ where Λ is an integer power of p and $|k|$ is the standard norm on $\mathbb{Q}_{p^n}$, whose values are integer powers of p.

The $O(N)$ model on $\mathbb{Q}_{p^n}$ comes with three real parameters, r (a mass-squared parameter), λ, and a spectral parameter s which tells us in the free theory that the dimension of ϕ is $\frac{n-s}{2}$. Unlike in ordinary local field theories on $\mathbb{R}^n$, s is an adjustable parameter in a p-adic context.

4.2.2 One-loop amplitudes

To renormalize ϕ^4 theory we typically need to handle divergences in the two-point and four-point functions. To one loop order, these Green's functions take

the following forms:

$$\mathbb{Q}_{p^n} \qquad \begin{aligned} G^{(2)}_{ij}(k) &= \frac{\delta_{ij}}{|k|^s + r} + \frac{\delta_{ij}}{(|k|^s + r)^2}\frac{1}{2}(-\lambda)\frac{N+2}{3} I_2 = \frac{\delta_{ij}}{|k|^s + r + \lambda\frac{N+2}{6} I_2} \\ G^{(4)}_{i_1 i_2 i_3 i_4}(k_i) &= -\lambda T_{i_1 i_2 i_3 i_4} + \frac{1}{2}(-\lambda)^2 \frac{N+8}{9}(I_4^{(s)} + I_4^{(t)} + I_4^{(u)}) T_{i_1 i_2 i_3 i_4}\,, \end{aligned} \tag{4.8}$$

In (4.8) and below, we omit the momentum-conserving delta functions from the Green's functions. The loop integrals are

$$\mathbb{Q}_{p^n} \qquad I_2 = \int \frac{d\ell}{|\ell|^s + r} \qquad\qquad I_4^{(S)} = \int \frac{d\ell}{(|\ell|^s + r)(|\ell + k_1 + k_2|^s + r)}\,. \tag{4.9}$$

$I_4^{(T)}$ and $I_4^{(U)}$ are defined like $I_4^{(S)}$, but with $k_1 + k_2$ replaced by $k_1 + k_3$ for $I_4^{(T)}$ and by $k_1 + k_4$ for $I_4^{(U)}$. A diagrammatic account of the formulas (4.8) is summarized in figure 4.1. The standard challenge of perturbative renormalization group analysis is to tame divergences at large $|\ell|$ (the ultraviolet) arising in the integrals (4.9).

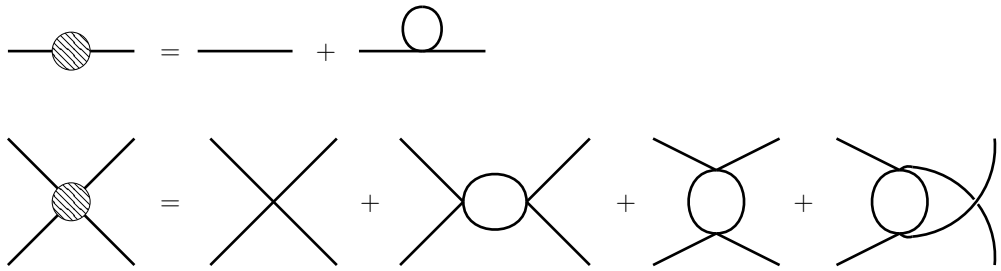

Figure 4.1: Diagrammatic representation of the two- and four-point functions to one loop order.

4.2.3 Wilsonian renormalization

In a Wilsonian approach, we integrate out a shell of hard momenta, so we want the internal momenta, denoted ℓ in (4.8)-(4.9), to be hard, while the external momenta k_i are soft. A key property of $\mathbb{Q}_{p^n}$ is that it organizes into momentum shells whose magnitudes are integer powers of p, and we can integrate out one such

momentum shell at a time. Momentum shell integration is easy to do because the integrands are constant over each momentum shell. Explicitly,

$$\mathbb{Q}_{p^n} \qquad \begin{aligned} I_2 &= \int_{|\ell|=\Lambda} \frac{d\ell}{\Lambda^s + r} = \frac{1}{\zeta(n)} \frac{\Lambda^n}{\Lambda^s + r} \\ I_4 &= \int_{|\ell|=\Lambda} \frac{d\ell}{(\Lambda^s + r)^2} = \frac{1}{\zeta(n)} \frac{\Lambda^n}{(\Lambda^s + r)^2} \,. \end{aligned} \tag{4.10}$$

The result for I_4 is the same for all three channels (so we dropped the channel label), and it relies on the fact that $|\ell + k| = |\ell|$ when ℓ is hard and k is soft. This equality is an exact statement which follows directly from $|k| < |\ell|$ together with the ultrametric property of the norm on $\mathbb{Q}_{p^n}$. The situation contrasts strongly with the Archimedean case, where we have the weaker condition $|\ell + k| \approx |\ell|$ when $|k| \ll |\ell|$.

To extract the recursion relations that define the renormalization group for the p-adic $O(N)$ model, we require that $G^{(2)}_{ij}(k)$ as computed in (4.8) through one-loop order, with the loop momentum required to satisfy $|\ell| = \Lambda$, should coincide with the tree level Green's function $G^{(2)}_{\text{soft},ij}(k) = \frac{\delta_{ij}}{|k|^s + r_{\text{soft}}}$ of an effective soft theory with a hard momentum cutoff at Λ/p instead of Λ. Likewise, we seek to have $G^{(4)}_{i_1 i_2 i_3 i_4}$ as computed in (4.8) coincide with the tree-level $G^{(4)}_{\text{soft},i_1 i_2 i_3 i_4} = -\lambda_{\text{soft}} T_{i_1 i_2 i_3 i_4}$, and this is possible because $G^{(4)}_{i_1 i_2 i_3 i_4}$ has no momentum dependence (beyond the momentum-conserving delta function which we have suppressed). Altogether, we find

$$\mathbb{Q}_{p^n} \qquad \begin{aligned} r_{\text{soft}} &= r + \lambda \frac{N+2}{6} \frac{1}{\zeta(n)} \frac{\Lambda^n}{\Lambda^s + r} \\ \lambda_{\text{soft}} &= \lambda - \lambda^2 \frac{N+8}{6} \frac{1}{\zeta(n)} \frac{\Lambda^n}{(\Lambda^s + r)^2} \,. \end{aligned} \tag{4.11}$$

The relations (4.11) are more simply expressed in terms of analogs of "dimen-

sionless couplings"

$$\mathbb{Q}_{p^n} \qquad \begin{aligned} \bar{r} &= \frac{r}{\Lambda^{[r]}} & \bar{r}_{\rm soft} &= \frac{r_{\rm soft}}{(\Lambda/p)^{[r]}} \\ \bar{\lambda} &= \frac{\lambda}{\Lambda^{[\lambda]}} & \bar{\lambda}_{\rm soft} &= \frac{\lambda_{\rm soft}}{(\Lambda/p)^{[\lambda]}}\,, \end{aligned} \tag{4.12}$$

where

$$\mathbb{Q}_{p^n} \qquad [r] = s \qquad [\lambda] = \epsilon \equiv 2s - n\,. \tag{4.13}$$

In general, $[X]$ is the dimension of a quantity X for the Gaussian fixed point at $\lambda = 0$. Thus for example $[|k|] = 1$, $[dk] = n$, $[|x|] = -1$, and $[\phi(x)] = \frac{n-s}{2}$. Holding n fixed and increasing s is analogous to holding s fixed and lowering n, and the analog of the upper critical dimension, at which ϕ^4 becomes marginal, is $s = n/2$.[5] Thus $[\lambda]$ itself is the analog of the parameter $\epsilon = 4 - n$ in ordinary ϕ^4 theory, and in some formulas we emphasize this by writing quantities in terms of ϵ.

Having defined dimensionless couplings in (4.12), we can now recast (4.11) as

$$\mathbb{Q}_{p^n} \qquad \begin{aligned} \bar{r}_{\rm soft} &= p^s \left[\bar{r} + \bar{\lambda} \frac{N+2}{6} \frac{1}{\zeta(n)} \frac{1}{1+\bar{r}} \right] \\ \bar{\lambda}_{\rm soft} &= p^\epsilon \left[\bar{\lambda} - \bar{\lambda}^2 \frac{N+8}{6} \frac{1}{\zeta(n)} \frac{1}{(1+\bar{r})^2} \right]. \end{aligned} \tag{4.14}$$

These are the recursion relations which define the renormalization of the p-adic $O(N)$ model through one loop.

4.2.4 A non-renormalization theorem

Note that we didn't have to worry about wave-function renormalization when working out the recursion relations (4.14). Absence of wave-function renormalization is a trivial observation at this loop order, since there is no way to get momentum dependence in the one-loop correction to $G^{(2)}_{ij}(k)$ even in an Archimedean

[5] The analog of the lower critical dimension is $s = n$, so IR critical behavior occurs for $n/2 < s < n$, or equivalently $s < n < 2s$ which is the analog of $2 < n < 4$ in ϕ^4 theory in $\mathbb{R}^n$.

theory. A striking point about the p-adic $O(N)$ model is that (at least in a perturbative Wilsonian approach), no wave-function renormalization ever occurs. Better yet, no diagrammatic loop correction *ever* exhibits momentum dependence, even in higher point amplitudes. That is, the effective action is always schematically of the form[6]

$\mathbb{Q}_{p^n}$
$$S = \int dk\, \frac{1}{2}\vec{\phi}(-k)|k|^s \cdot \vec{\phi}(k) + \int dx\, V_{\text{eff}}(\vec{\phi}(x))\,, \tag{4.15}$$

where $V_{\text{eff}}(\vec{\phi}(x))$ undergoes renormalization group flow but the "kinetic term" $\phi(-k)|k|^s\phi(k)$ is never renormalized, nor are any other k-dependent terms generated as they are for theories on $\mathbb{R}^n$. In other words, the renormalization group acts strictly on the purely non-derivative, local part of the action which depends on $\vec{\phi}(x)$ at one point only. This feature of the renormalization group seems to have been appreciated already for the hierarchical model [121]. It hinges on ultrametricity, as we can see by examining the first diagram whose momentum dependence would ordinarily contribute to wave-function renormalization in ϕ^4 theory, namely the underground diagram shown in figure 4.2. The loop integral is

$\mathbb{Q}_{p^n}$
$$I_{2'} = \int_{|\ell_1|=\Lambda} d\ell_1 \int_{|\ell_2|=\Lambda} d\ell_2 \int_{|\ell_3|=\Lambda} d\ell_3\, \frac{\delta(\ell_1+\ell_2+\ell_3-k)}{(\Lambda^s+r)^3}\,. \tag{4.16}$$

To see that $I_{2'}$ is actually independent of k, we use the u-substitution $\tilde{\ell}_3 = \ell_3 - k$. Ultrametricity guarantees that the map $\ell_3 \to \tilde{\ell}_3$ is a bijection from the momentum shell $|\ell_3| = \Lambda$ to itself, provided $|k| < \Lambda$. Similar arguments can be applied to general Feynman diagrams [114].

[6] By $\int dx\, V_{\text{eff}}(\vec{\phi}(x))$ we really mean a sum of powers of $\vec{\phi}(x)$, suitably contracted with $O(N)$-covariant tensors and multiplied by running couplings like r and λ, and expressed in momentum space as integrals against momentum-conserving delta functions.

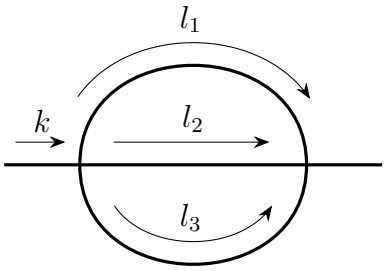

Figure 4.2: The underground diagram, the lowest order diagram that contributes to wave–function renormalization in Archimedean ϕ^4 theory.

4.2.5 Fixed point and anomalous dimensions

Finding a fixed point of the discrete RG equations (4.14) now amounts to setting $\bar{r}_{\text{soft}} = \bar{r}$ and $\bar{\lambda}_{\text{soft}} = \bar{\lambda}$. This happens, to leading order in small ϵ, at the p-adic Wilson-Fisher fixed point,

$$\mathbb{Q}_{p^n} \qquad \bar{r}_* = -\zeta(n/2)\frac{N+2}{N+8}\epsilon \log p \qquad \bar{\lambda}_* = \frac{6\zeta(n)}{N+8}\epsilon \log p\,. \tag{4.17}$$

To analyze anomalous dimensions at the fixed point, we consider perturbations

$$\mathbb{Q}_{p^n} \qquad \bar{r} = \bar{r}_* + \delta\bar{r} \qquad \bar{\lambda} = \bar{\lambda}_* + \delta\bar{\lambda}\,. \tag{4.18}$$

To linear order in $\delta\bar{r}$ and $\delta\bar{\lambda}$, the discrete RG equations become

$$\mathbb{Q}_{p^n} \qquad \begin{pmatrix} \delta\bar{r}_{\text{soft}} \\ \delta\bar{\lambda}_{\text{soft}} \end{pmatrix} = M \begin{pmatrix} \delta\bar{r} \\ \delta\bar{\lambda} \end{pmatrix}\,. \tag{4.19}$$

The explicit form of M can be worked out easily starting from (4.14) but is unenlightening. Eigenvalues of M take the form $p^{n-\Delta}$ where Δ is the dimension of a primary operator $\mathcal{O}$ in the fixed point theory. To see this, note that if ρ is the coupling dual to $\mathcal{O}$, then ρ has dimension $n-\Delta$, and we naturally define $\bar{\rho} = \rho/\Lambda^{n-\Delta}$, while $\bar{\rho}_{\text{soft}} = \rho/(\Lambda/p)^{n-\Delta} = p^{n-\Delta}\bar{\rho}$. By straightforward calculation, we see that the dimensions from (4.19) to leading order in small ϵ take the form

$$\mathbb{Q}_{p^n} \qquad \Delta_{\text{irr}} = n + \epsilon \qquad \Delta_{\text{rel}} = s - \frac{6}{N+8}\epsilon\,. \tag{4.20}$$

For higher order expansions in ϵ, we refer the reader to [122, 123]. We may naturally suppose that Δ_{irr} controls the approach of a discrete flow from the free $O(N)$ model to the p-adic Wilson-Fisher fixed point, while Δ_{rel} is the dimension of a mass-like operator which generically drives trajectories away from the fixed point.

4.3 Large N methods

Methods based on the Hubbard-Stratonovich transformation have been developed, notably in [134, 135], which resum an infinite set of diagrams of the $O(N)$ model at fixed order in large N and allow a determination of critical exponents at the Wilson-Fisher fixed point which are known exactly as functions of ϵ and to a few orders in large N. Whereas Wilsonian methods are significantly different for field theories defined over $\mathbb{Q}_{p^n}$ than for field theories defined over $\mathbb{R}^n$, the large N methods work nearly identically in the two cases. We will illustrate this by working out the leading non-trivial results for anomalous dimensions in ϕ^4 theory.

4.3.1 Action

We start with an informal introduction to the methods of [134, 135]. We are interested in a conformally invariant theory, and so we will naively turn off the relevant mass deformation while keeping the ϕ^4 interaction. The action (4.5) becomes

$$S = \int dx \left[\frac{1}{2} \phi^i(x) D^s \phi^i(x) + \frac{\lambda}{4!} \left(\phi^i(x) \phi^i(x) \right)^2 \right] . \tag{4.21}$$

Here and below, integrals are over all of $\mathbb{Q}_{p^n}$, or all of $\mathbb{R}^n$, unless indicated otherwise, and ϕ^i takes values in $\mathbb{R}^N$.

Acting with D^s in position space is, by definition, the same as multiplying by

$|k|^s$ in momentum space:

$$\int dx\, \chi(kx)^* D^s \phi^i(x) \equiv |k|^s \phi^i(k)\,. \tag{4.22}$$

A Fourier integral of fundamental importance is

$$\int dk\, \chi(kx)|k|^s = \frac{1/\Gamma(-s)}{|x|^{n+s}} + \text{contact terms}\,. \tag{4.23}$$

We have previously defined Fourier transforms over $\mathbb{Q}_{p^n}$ in (4.7). For $\mathbb{R}^n$, we set $\chi(kx) = e^{2\pi i \vec{k}\cdot\vec{x}}$. Thus, relative to standard conventions in quantum field theory, our wave numbers $\vec{k}$ always include an extra factor of $1/2\pi$.[7]

In the case of p-adic numbers, a sufficient prescription for the contact terms is for them to be just a delta function, so that we recover the Vladimirov derivative:

$\mathbb{Q}_{p^n}$
$$D^s \phi^i(x) \equiv \frac{1}{\Gamma(-s)} \int dy\, \frac{\phi^i(y) - \phi^i(x)}{|y-x|^{n+s}}\,. \tag{4.24}$$

Some of the good properties of the Vladimirov derivative are explained, for instance, in Appendix B of [32]. The Vladimirov derivative should be understood to act on functions which can be approximated as piecewise constant functions with compact support.

In the case of $\mathbb{R}^n$, the contact terms have in general a more complicated structure, including both delta functions and derivatives of delta functions. At a formal level, we can let s remain a continuously variable parameter in the real case. The theories so obtained have bilocal terms in position space, as in [126, 127]. When s is a positive even integer, we recover locality:

$\mathbb{R}^n$
$$D^s \phi^i(x) = \Box^{s/2}\, \phi^i(x) \qquad \text{for } s = 2, 4, 6, \ldots, \tag{4.25}$$

where

$\mathbb{R}^n$
$$\Box \equiv -\frac{1}{(2\pi)^2} \sum_{j=1}^{n} \partial_j^2\,. \tag{4.26}$$

[7] Restoring dimensions by writing a plane wave as $e^{i\vec{p}\cdot\vec{x}/\hbar}$, where now $\vec{p}$ is the momentum, the current conventions can be understood as arising from setting $h \equiv 2\pi\hbar = 1$ rather than following the usual practice of setting $\hbar = 1$.

The general expression (4.22) is consistent with (4.25) because $1/\Gamma_{\mathbb{R}^n}(-s)$ has zeros at $s = 2, 4, 6, \ldots$. (Actually, (4.25) is equally valid at $s = 0$, where $1/\Gamma_{\mathbb{R}^n}(-s)$ also has a zero, but this is not an interesting case because then the "kinetic" term is identical to the mass term.)[8]

The Hubbard-Stratonovich trick is to replace

$$\frac{\lambda}{4!}(\phi^i\phi^i)^2 \to \frac{\lambda}{4!}(\phi^i\phi^i)^2 - \frac{3}{2\lambda N}\left(\sigma - \frac{\lambda\sqrt{N}}{6}\phi^i\phi^i\right)^2 = \frac{1}{2\sqrt{N}}\sigma\phi^i\phi^i - \frac{3\sigma^2}{2\lambda N} \quad (4.27)$$

in the action. This is permitted because we can eliminate σ by its equation of motion and recover the original action. At the level of path integration the same manipulation is still permitted, but σ must run over imaginary rather than real values in order to have a convergent integral in the σ direction. Next we assume that λN runs to large values, so that the $\sigma^2/\lambda N$ term in (4.27) may be neglected. Thus we arrive at the modified action

$$S = \int dx \left[\frac{1}{2}\phi^i(x)D^s\phi^i(x) + \frac{1}{2\sqrt{N}}\sigma\phi^i\phi^i\right]. \quad (4.28)$$

We may alternatively understand (4.28) as arising from a non-linear sigma model where for each x, $\phi^i(x)$ is constrained to lie on a sphere S^{N-1} of fixed radius; then σ is the Lagrange multiplier that enforces the constraint, and there is an extra term linear in σ whose role is to fix the radius of the S^{N-1}—or in diagrammatic terms, to eliminate any tadpole for σ.

[8]The explicit factors of 2π in (4.26) imply a normalization of the kinetic term that is different from the one normally used in field theory: For $\mathbb{R}^n$ with $s = 2$, our kinetic term is $S_{\text{kin}} = \int_{\mathbb{R}^n} dx\, \frac{1}{8\pi^2}(\partial\phi^i)^2$ instead of the more standard $S_{\text{kin}} = \int_{\mathbb{R}^n} dx\, \frac{1}{2}(\partial\phi^i)^2$. This means that our field ϕ^i includes an extra factor of 2π compared with standard conventions, and as a result, powers of 2π will show up in all our position space Green's functions that do not match the literature. More precisely: explicit factors of 2π altogether disappear from Green's functions when we follow our conventions faithfully, including the use of $\Gamma_{\mathbb{R}^n}$ (defined in (4.4)) rather than Γ_{Euler}.

4.3.2 Leading order propagators

A two-point function for ϕ^i can be read off from (4.28) at tree level:

$$\Gamma^{(0)}_{\phi\phi}(k) = |k|^s \qquad G^{(0)}_{\phi\phi}(k) = \frac{1}{|k|^s} \qquad G^{(0)}_{\phi\phi}(x) = \frac{1/\Gamma(s)}{|x|^{n-s}}\,. \tag{4.29}$$

All these two-point functions include a factor of δ^{ij} which we suppress. All position space correlators should be understood as subject to correction by contact terms. The 1PI two-point amplitude for σ gets its first contribution at one loop as shown in figure 4.3:

$$\Gamma^{(1)}_{\sigma\sigma}(x) = -\frac{1/\Gamma(s)^2}{2|x|^{2n-2s}}\,. \tag{4.30}$$

The explicit sign in (4.30) comes from the convention that field configurations

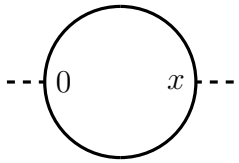

Figure 4.3: The vacuum polarization diagram for the σ field. Dashed lines correspond to the σ field, and solid lines correspond to the ϕ field.

are weighted by $e^{-\Gamma}$. The $1/2$ is a symmetry factor, and the rest of the amplitude is the square of $G^{(0)}_{\phi\phi}(x)$. A factor of N for the sum over indices in the ϕ^i loop is offset by two factors of $1/\sqrt{N}$, one from each vertex. Straightforward Fourier transforms lead to

$$G^{(1)}_{\sigma\sigma}(k) = -\frac{2}{\mathrm{B}(n-s,n-s)}|k|^{2s-n} \qquad G^{(1)}_{\sigma\sigma}(x) = -2\frac{\Gamma(2s)}{\mathrm{B}(n-s,n-s)}\frac{1}{|x|^{2s}}\,. \tag{4.31}$$

From $G^{(0)}_{\phi\phi}(x) \propto 1/|x|^{n-s}$ we conclude $\Delta_\phi = \frac{n-s}{2} + \mathcal{O}(1/N)$, which for $\mathbb{Q}_{p^n}$ trivially agrees with the conclusion of the non-renormalization theorem of section 4.2.4, which indicates that Δ_ϕ receives no corrections from its free field value.

This agreement is trivial because we're only looking at tree-level contributions to $G_{\phi\phi}(x)$ thus far.

From $G^{(0)}_{\sigma\sigma}(x) \propto 1/|x|^{2s}$ we conclude $\Delta_\sigma = s + \mathcal{O}(1/N)$. We identify σ itself as the relevant deformation, so from (4.20) we see that we already have agreement between $\Delta_{\rm rel}$ and Δ_σ to leading order in small ϵ and large N. Our computations in section 4.3.5 will extend this agreement to the next order: that is, we will find

$$\Delta_\sigma = s - \frac{6}{N}\epsilon + \mathcal{O}(1/N^2) + \mathcal{O}(\epsilon^2)\,. \tag{4.32}$$

First, however, we will show that Δ_ϕ receives no correction through $\mathcal{O}(1/N)$.

4.3.3 Self-energy diagram I: Momentum space methods

The self-energy correction to the 1PI two-point function for ϕ^i is given by the diagram in figure 4.4, whose amplitude is

$$\Gamma^{(2)}_{\phi\phi}(k) = -\frac{1}{N}\int d\ell\, G^{(0)}_{\phi\phi}(\ell) G^{(1)}_{\sigma\sigma}(k-\ell) = \frac{2/N}{\mathrm{B}(n-s,n-s)}\int d\ell\, |\ell|^{-s}|k-\ell|^{2s-n}\,. \tag{4.33}$$

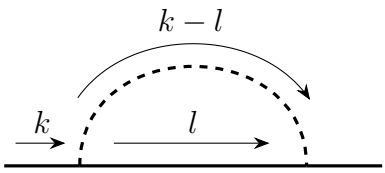

Figure 4.4: The self energy diagram for the ϕ field.

Evidently we must investigate the divergence properties of the integral. It helps to introduce functions

$$\pi_t(k) \equiv |k|^{t-n} \tag{4.34}$$

for any complex number t. These functions are multiplicative characters on $\mathbb{Q}_{p^n}$,[9] but are also of course well defined on $\mathbb{R}^n$ despite there being no obvious notion of multiplicative characters there (unless $n = 1$ or 2, where we have $\mathbb{R}$ or $\mathbb{C}$ respectively, both of which are fields). The Fourier transform of $\pi_t(k)$ is $\hat{\pi}_t(x) \equiv \Gamma(t)|x|^{-t}$ up to contact terms, so the obvious identity $\hat{\pi}_{t_1}(x)\hat{\pi}_{t_2}(x) = \mathrm{B}(t_1, t_2)\hat{\pi}_{t_1+t_2}(x)$ becomes in Fourier space

$$(\pi_{t_1} * \pi_{t_2})(k) \equiv \int d\ell\, |\ell|^{t_1-n}|k-\ell|^{t_2-n} = \mathrm{B}(t_1, t_2)\pi_{t_1+t_2}(k) = \mathrm{B}(t_1, t_2)|k|^{t_1+t_2-n}\,, \tag{4.35}$$

The integral in (4.35) converges provided $t_1 > 0$, $t_2 > 0$, and $t_1 + t_2 < n$. Outside this triangular region, we need to consider some regularization.

Suppose $t_1 > 0$, $t_2 > 0$, but $t_1 + t_2 > n$, so that the integral in (4.35) has an ultraviolet divergence. In $\mathbb{Q}_{p^n}$, imposing a hard momentum cutoff leads to

$$\mathbb{Q}_{p^n} \qquad \int_{|\ell|\le\Lambda} d\ell\, |\ell|^{t_1-n}|k-\ell|^{t_2-n} = \mathrm{B}(t_1, t_2)|k|^{t_1+t_2-n} + \frac{\zeta(t_1+t_2-n)}{\zeta(n)}\Lambda^{t_1+t_2-n}\,, \tag{4.36}$$

provided $|k| < \Lambda$. To obtain (4.36), the simplest method is to split the integral into regions where $|\ell|$ and $|k-\ell|$ are constant, and then the integral becomes a discrete sum which can be performed exactly. What is notable about (4.36) is that the result is the sum of two terms: the expression $|k|^{t_1+t_2-n}\mathrm{B}(t_1, t_2)$ that we got through formal manipulations in (4.35), plus the $k = 0$ result. Applying (4.36) to (4.33), we now find for $\mathbb{Q}_{p^n}$ the result

$$\mathbb{Q}_{p^n} \qquad \Gamma^{(2)}_{\phi\phi}(k) = \frac{2/N}{\mathrm{B}(n-s, n-s)}\left[|k|^s \mathrm{B}(n-s, 2s) + \frac{\zeta(s)}{\zeta(n)}\Lambda^s\right]. \tag{4.37}$$

The divergent piece can be canceled by a counterterm $S_{\mathrm{ct}} \propto \int dx\, \Lambda^s \phi^i \phi^i$. The absence of wave-function renormalization is due to the fact that the divergent part of $\Gamma^{(2)}_{\phi\phi}(k)$ has no k-dependence. In particular, we don't see an anomalous dimension for ϕ^i (at this level) because there is no term proportional to $|k|^s \log(\Lambda/|k|)$.

[9] Given a field K, a multiplicative character $\pi : K^\times \to \mathbb{C}^\times$ satisfies $\pi(xy) = \pi(x)\pi(y)$.

There is only a finite renormalization of the two-point function for ϕ:

$$\mathbb{Q}_{p^n} \qquad \Gamma^{(0)}_{\phi\phi}(k) + \Gamma^{(2)}_{\phi\phi}(k) = \left[1 + \frac{2}{N}\frac{\mathrm{B}(n-s,2s)}{\mathrm{B}(n-s,n-s)}\right]|k|^s \,. \tag{4.38}$$

The case of $\mathbb{R}^n$ is harder because there is no such exact formula as (4.36), owing to the possibility of subleading divergences. Focusing on the case where the leading divergence is quadratic,

$$\begin{aligned}\mathbb{R}^n \qquad \int_{|\ell|\le\Lambda} d\ell\, |\ell|^{t_1-n}|k-\ell|^{2-t_1} &= \frac{2}{\zeta(n)}\left[\frac{\Lambda^2}{2} - \frac{(t_1-n)(2-t_1)}{2n}k^2\log\frac{\Lambda}{|k|} + (\text{finite})\right] \\ &= \frac{(t_1-n)(2-t_1)}{n\zeta(n)}k^2\log|k| + (\text{non-universal})\,,\end{aligned} \tag{4.39}$$

where $k^2 = |k|^2 = \sum_{i=1}^n k_i^2$ and we restrict $0 < t_1 < n+2$ to avoid infrared divergences. In (4.39), "finite" means terms which remain finite as $\Lambda \to \infty$ with k held fixed. The precise way in which we impose the cutoff doesn't affect the terms shown; for instance, we could have integrated instead over the region $|k-\ell| \le \Lambda$. The logarithmic term is particularly robust, in that even a rescaling of Λ does not affect it. This is the familiar scheme independence of leading logarithmic terms, which we emphasize in the second line by picking out the $k^2\log|k|$ behavior explicitly and folding the $k^2\log\Lambda$ term along with the Λ^2 term into the "non-universal" part. These divergent terms can be canceled by local counterterms. Of course, all this is textbook renormalization procedure, worthy of note here only as a segue into a more formal method to extract the same leading logarithmic term which will generalize conveniently to the p-adic context in section 4.3.5. This more formal method is to "regularize" by shifting one of the exponents of the integral and then treating that shift as small:

$$\begin{aligned}\mathbb{R}^n \qquad \int d\ell\, |\ell|^{t_1-n}|k-\ell|^{2-t_1-\delta} &= \mathrm{B}(t_1, n+2-t_1-\delta)|k|^{2-\delta} = \mathrm{B}(t_1,-2+\delta)|k|^{2-\delta} \\ &= \frac{(t_1-n)(2-t_1)}{n\zeta(n)}\left[-\frac{1}{\delta} + \log|k|\right]k^2 + (\text{finite})\,.\end{aligned} \tag{4.40}$$

The first line of (4.40) is rigorously valid when $t_1 - n - 2 < \delta < -2$. To reach the second line of (4.40), we analytically continue in δ past the singularity of $\mathrm{B}(t_1, -2+\delta)$ at $\delta = -2$ to the next singularity, at $\delta = 0$. Evidently, the $k^2 \log|k|$ term matches what was found in (4.39). In applications of (4.40) and related analytic continuations to diagrammatic amplitudes, we must be careful to shift dimensions at the level of the Feynman rules. Our choice is to shift exponents associated with the σ propagator.

The contrast between $\mathbb{R}^n$ and $\mathbb{Q}_{p^n}$ is clear from the position of poles in the Beta function. If we tried the same manipulation as (4.40) for the p-adics, we would get a finite result and no $\log|k|$ term because there is no singularity in $\mathrm{B}_{\mathbb{Q}_{p^n}}(t_1, -2+\delta)$ at $\delta = 0$; but $\mathrm{B}_{\mathbb{R}^n}(t_1, -2+\delta)$ does have such a pole on account of the infinite sequence of poles in $\Gamma_{\mathbb{R}^n}(t)$.[10] If, on the other hand, we were considering an integral like $\int d\ell\, |\ell|^{t_1-n}|k-\ell|^{-t_1}$ which is logarithmically divergent, then a $\log|k|$ term would come out of any sensible regularization procedure regardless of whether the integral is over $\mathbb{R}^n$ or $\mathbb{Q}_{p^n}$. In the approach where we shift one exponent, the $\log|k|$ term would be associated with a pole in $\mathrm{B}(t_1, \delta)$ at $\delta = 0$, which is present equally for $\mathrm{B}_{\mathbb{R}^n}$ and $\mathrm{B}_{\mathbb{Q}_{p^n}}$.

With (4.39) or (4.40) in hand, we can calculate the anomalous dimension for ϕ^i in the standard setup of a local field theory on $\mathbb{R}^n$: Setting $s = 2$ and keeping only the universal leading logarithmic term, we have

$$\mathbb{R}^n \qquad \Gamma^{(0)}_{\phi\phi}(k) + \Gamma^{(2)}_{\phi\phi}(k) = k^2 - \frac{4/N}{\mathrm{B}(n-2, n-2)} \frac{4-n}{n\zeta(n)} k^2 \log|k| = |k|^{n-2\Delta_\phi}\,, \tag{4.41}$$

[10] It is intriguing to note that the same contrast between analytic properties of $\Gamma_{\mathbb{R}}$ and $\Gamma_{\mathbb{Q}_p}$ is responsible for the presence of infinitely many states in the Archimedean string spectrum, whereas the standard p-adic string construction gives only a tachyon. We will return to this line of thought further in section 4.5.

where

$\mathbb{R}^n$
$$\Delta_\phi = \frac{n-2}{2} + \frac{2/N}{\mathrm{B}(n-2,n-2)} \frac{4-n}{n\zeta(n)} + \mathcal{O}(1/N^2)\,. \tag{4.42}$$

This result is exact in $\epsilon = 4 - n$, but if we wish to compare with standard perturbation theory we can expand in small ϵ:

$\mathbb{R}^n$
$$\Delta_\phi = \frac{n-2}{2} + \frac{\epsilon^2}{4N} + \mathcal{O}(\epsilon^3) + \mathcal{O}(1/N^2)\,. \tag{4.43}$$

It is possible to unify our perspective somewhat by writing a formula for Δ_ϕ which is valid equally for $\mathbb{R}^n$ and $\mathbb{Q}_{p^n}$:

$$\Delta_\phi = \frac{n-s}{2} + \frac{1}{N} \operatorname*{Res}_{\delta} \frac{\mathrm{B}(n-s,-s+\delta)}{\mathrm{B}(n-s,n-s)} + \mathcal{O}(1/N^2)\,, \tag{4.44}$$

where we understand Res_z as picking out the residue at a pole at $z = 0$ of a meromorphic function of z:

$$\operatorname*{Res}_{z} f(z) \equiv \oint_0 \frac{dz}{2\pi i}\, f(z)\,. \tag{4.45}$$

This unified perspective suggests in $\mathbb{R}^n$ that $s = 2$ may not be as special as we normally think—and that in particular, any positive even s will give rise to constructions similar to the Wilson-Fisher fixed point, obtained (one might assume) from local Gaussian theories by adding a ϕ^4 term. We follow up this idea in section 4.4. When applied to $\mathbb{Q}_{p^n}$ (assuming $s > 0$), (4.45) tells us correctly that the anomalous dimension vanishes since $\mathrm{B}(n-s,-s+\delta)$ is finite at $\delta = 0$. Although the expression (4.44) appears to be merely a repackaging of previous results, it does highlight the origin of the anomalous dimension and suggests the possibility of extending to more general base fields and/or more interesting multiplicative characters.

4.3.4 Self-energy diagram II: Position space methods

The evaluation of the 1PI self-energy diagram is trivial in position space:

$$\Gamma^{(2)}_{\phi\phi}(x) = -\frac{1}{N} G^{(0)}_{\phi\phi}(x) G^{(1)}_{\sigma\sigma}(x) = \frac{2}{N} \frac{\Gamma(2s)/\Gamma(s)}{\mathrm{B}(n-s,n-s)} \frac{1}{|x|^{n+s}}\,. \tag{4.46}$$

In $\mathbb{Q}_{p^n}$ we can straightforwardly combine $\Gamma^{(2)}_{\phi\phi}(x)$ with $\Gamma^{(0)}_{\phi\phi}(x) = \frac{1/\Gamma(-s)}{|x|^{n+s}}$ to obtain the finite renormalization factor appearing already in (4.38). In $\mathbb{R}^n$ this fails because $\Gamma^{(0)}_{\phi\phi}(x) = \Box\,\delta(x)$. A more effective method is to investigate the contribution of the self-energy graph to the connected two-point function:

$$G^{(2)}_{\phi\phi}(x) = -\frac{2/N}{\Gamma(s)\mathrm{B}(s,s)\mathrm{B}(n-s,n-s)} I_3(x)\,, \tag{4.47}$$

where we define

$$I_3(x) \equiv \int dx_1 dx_2\, \frac{1}{|x_1|^{n-s}|x_{12}|^{n+s-\delta}|x-x_2|^{n-s}}\,, \tag{4.48}$$

where $x_{12} = x_1 - x_2$. Anticipating possible divergences, we've already introduced as a regulator a shift δ in one of the exponents. We have coordinated the normalization of δ in (4.48) with the normalization we used in (4.40): in both cases, we're effectively sending $\Delta_\sigma \to \Delta_\sigma - \delta/2$ while holding all other quantities fixed.

Because $I_3(x)$ is the convolution of three power laws, it is easily evaluated using (4.35). (We don't mean to pass to Fourier space; we mean to apply (4.35) as is with k variables replaced with x variables.) The result is

$$I_3(x) = \frac{\mathrm{B}(s,s)\mathrm{B}(2s,-s+\delta)}{|x|^{n-s-\delta}} \stackrel{\delta}{=} \frac{\mathrm{B}(s,s)\mathrm{B}(n-s,-s+\delta)}{|x|^{n-s-\delta}} \tag{4.49}$$

In the second step, $\stackrel{\delta}{=}$ means that the last expression differs from the first only by terms which are finite as $\delta \to 0$. In the current case, this delta-equality is true provided s avoids special values such as 0, n, and $n/2$. Thus we arrive at

$$\begin{aligned} G^{(0)}_{\phi\phi}(x) + G^{(2)}_{\phi\phi}(x) &\stackrel{\delta}{=} \frac{1/\Gamma(s)}{|x|^{n-s}}\left[1 - \frac{2}{N}\frac{\mathrm{B}(n-s,-s+\delta)}{\mathrm{B}(n-s,n-s)}|x|^\delta\right] \\ &\stackrel{\delta}{=} \frac{1/\Gamma(s)}{|x|^{n-s}}\left[1 - \frac{2}{N}\left(\operatorname*{Res}_{\delta}\frac{\mathrm{B}(n-s,-s+\delta)}{\mathrm{B}(n-s,n-s)}\right)\left(\frac{1}{\delta} + \log|x|\right)\right]. \end{aligned} \tag{4.50}$$

As before, we drop the divergent $1/\delta$ piece, understanding that its effects can be offset by a local counterterm. Comparing (4.50) with the expected power law

$G_{\phi\phi}(x) \propto 1/|x|^{2\Delta_\phi}$, we arrive at

$$\gamma_\phi \equiv \Delta_\phi - \frac{n-s}{2} = \frac{1}{N} \operatorname*{Res}_{\delta} \frac{\mathrm{B}(n-s, -s+\delta)}{\mathrm{B}(n-s, n-s)} + \mathcal{O}(1/N^2)\,. \tag{4.51}$$

This is easily seen to agree with (4.44) provided we stipulate $s > 0$. For $\mathbb{R}^n$ (and $s = 2$ as we always stipulate for the Archimedean case) it also agrees with the standard result [134, 135]

$$\mathbb{R}^n \qquad \gamma_\phi = \frac{n-4}{N} \frac{2^{n-3}}{\pi^{3/2}} \frac{\Gamma_{\text{Euler}}\left(\frac{n-1}{2}\right)}{\Gamma_{\text{Euler}}\left(\frac{n}{2}+1\right)} \sin\frac{\pi n}{2} + \mathcal{O}(1/N^2)\,. \tag{4.52}$$

4.3.5 Corrections to the σ propagator

In order to arrive at (4.32), we need to find contributions to $\Gamma_{\sigma\sigma}(x)$ at order $1/N$.[11] There are three diagrams which contribute: D_1, D_2, and D_3 as shown in figure 4.5. The first is easy because the only logarithmic divergence arises from the self-energy subdiagram, and it can be tracked by replacing the two-loop diagram with the one-loop diagram in figure 4.3, only with the tree-level propagators $G^{(0)}_{\phi\phi}(x)$ replaced by

$$G^{(0)}_{\phi\phi}(x) + G^{(2)}_{\phi\phi}(x) \stackrel{\delta}{=} \frac{1/\Gamma(s)}{|x|^{n-s}} \left[1 - 2\gamma_\phi \left(\frac{1}{\delta} + \log|x|\right)\right]\,, \tag{4.53}$$

where we have rewritten (4.50) in compact form. We remember that γ_ϕ is $\mathcal{O}(1/N)$ and vanishes for $\mathbb{Q}_{p^n}$. Thus, following through the manipulations of section 4.3.2, we find

$$\Gamma^{(1)}_{\sigma\sigma}(x) + \Gamma^{(D_1)}_{\sigma\sigma}(x) \stackrel{\delta}{=} -\frac{1/\Gamma(s)^2}{2|x|^{2n-2s}} \left[1 - 4\gamma_\phi \left(\frac{1}{\delta} + \log|x|\right)\right]\,, \tag{4.54}$$

implying that diagram D_1 contributes $\gamma_\sigma^{(D_1)} = -2\gamma_\phi$ to the anomalous dimension

$$\gamma_\sigma \equiv \Delta_\sigma - s\,. \tag{4.55}$$

[11] After the discussion of section 4.3.4 one might expect that carrying through to $G_{\sigma\sigma}(x)$ is necessary in order to avoid comparing power laws to contact terms in the case of $\mathbb{R}^n$. This is not a problem because in $\Gamma^{(1)}_{\sigma\sigma,\mathbb{R}^n}(x) \propto 1/|x|^{2n-4}$ we allow ourselves to analytically continue in n—and the only points of concern are the upper and lower critical dimensions, $n = 4$ and 2.

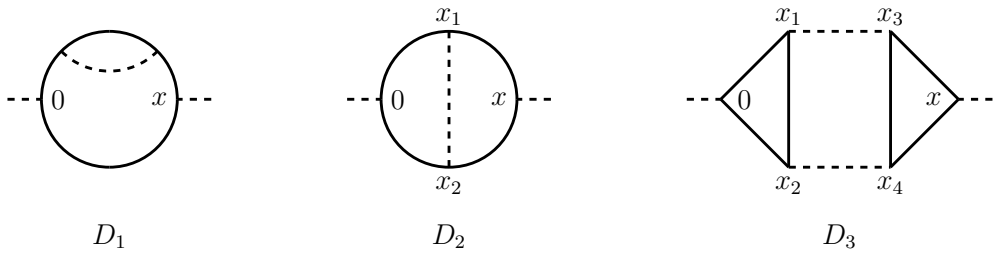

Figure 4.5: The three position space diagrams that contribute to $1/N$ corrections to the anomalous dimension of the σ field.

To get the contributions to γ_σ from D_2 and D_3 we need only isolate their leading logarithmic terms and add those terms to (4.54).

The second diagram contributes

$$\Gamma^{(D_2)}_{\sigma\sigma}(x) = -\frac{1}{2N}\left(\frac{1}{\Gamma(s)}\right)^4\left(-2\frac{\Gamma(2s)}{\mathrm{B}(n-s,n-s)}\right) I_{D_2}(x)\,. \tag{4.56}$$

The leading sign is the usual one for 1PI diagrams; the $1/2$ is a symmetry factor; $1/N$ comes from index summation together with four $\sigma\phi\phi$ vertices; the remaining prefactors come from the four $G^{(0)}_{\phi\phi}$ propagators and the one internal $G^{(1)}_{\sigma\sigma}$ propagator; and

$$\begin{aligned} I_{D_2}(x) &= \int dx_1 dx_2\, \frac{1}{|x_1|^{n-s}|x_1-x|^{n-s}|x_{12}|^{2s-\delta}|x_2|^{n-s}|x_2-x|^{n-s}} \\ &\stackrel{\delta}{=} \mathrm{B}(s,s)\mathrm{B}(\delta,\delta)|x|^{2s-2n+\delta}\,. \end{aligned} \tag{4.57}$$

The second equality in (4.57) takes a little work to justify, and we postpone a derivation to section 4.3.7. Combining (4.56) and (4.57) we see that

$$\begin{aligned} \Gamma^{(D_2)}_{\sigma\sigma}(x) &\stackrel{\delta}{=} \frac{1}{N}\frac{\mathrm{B}(\delta,\delta)}{\Gamma(s)^2\mathrm{B}(n-s,n-s)}|x|^{2s-2n+\delta} \\ &\stackrel{\delta}{=} \frac{1/N}{\Gamma(s)^2}|x|^{2s-2n}\left(\operatorname*{Res}_\delta \frac{\mathrm{B}(\delta,\delta)}{\mathrm{B}(n-s,n-s)}\right)\left[\frac{1}{\delta}+\log|x|\right]\,, \end{aligned} \tag{4.58}$$

from which we deduce in turn the contribution to the anomalous dimension

$$\gamma^{(D_2)}_\sigma = -\frac{1}{N}\operatorname*{Res}_\delta \frac{\mathrm{B}(\delta,\delta)}{\mathrm{B}(n-s,n-s)}\,. \tag{4.59}$$

The third diagram contributes

$$\Gamma^{(D_3)}_{\sigma\sigma}(x) = -\frac{1}{2N}\left(\frac{1}{\Gamma(s)}\right)^6\left(-2\frac{\Gamma(2s)}{\mathrm{B}(n-s,n-s)}\right)^2 I_{D_3}(x) \tag{4.60}$$

where

$$\begin{aligned} I_{D_3}(x) &= \int dx_1 dx_2 dx_3 dx_4 \, \frac{1}{|x_1|^{n-s}|x_2|^{n-s}|x_{12}|^{n-s}} \times \frac{1}{|x_{13}|^{2s-\delta/2}|x_{24}|^{2s-\delta/2}} \\ &\qquad \times \frac{1}{|x_3-x|^{n-s}|x_4-x|^{n-s}|x_{34}|^{n-s}} \\ &\overset{\delta}{=} \mathrm{B}(s,s)^2\mathrm{B}(n-s,n-2s)\mathrm{B}(\delta,\delta)|x|^{2s-2n+\delta}\,. \end{aligned} \tag{4.61}$$

The first and third factors in the integrand of (4.61) come from the $G^{(0)}_{\phi\phi}$ propagators running around the triangular loops. The second factor comes from the internal $G^{(1)}_{\sigma\sigma}$ propagators.[12]

$$\begin{aligned} \Gamma^{(D_3)}_{\sigma\sigma}(x) &\overset{\delta}{=} -\frac{2/N}{\Gamma(s)^2}\frac{\mathrm{B}(n-s,n-2s)\mathrm{B}(\delta,\delta)}{\mathrm{B}(n-s,n-s)^2}|x|^{2s-2n+\delta} \\ &\overset{\delta}{=} -\frac{2/N}{\Gamma(s)^2}|x|^{2s-2n}\left(\operatorname*{Res}_{\delta}\frac{\mathrm{B}(n-s,n-2s)\mathrm{B}(\delta,\delta)}{\mathrm{B}(n-s,n-s)^2}\right)\left[\frac{1}{\delta}+\log|x|\right], \end{aligned} \tag{4.62}$$

from which we deduce in turn

$$\gamma^{(D_3)}_{\sigma} = \frac{2}{N}\operatorname*{Res}_{\delta}\frac{\mathrm{B}(n-s,n-2s)\mathrm{B}(\delta,\delta)}{\mathrm{B}(n-s,n-s)^2}\,. \tag{4.63}$$

Putting the contributions from D_1, D_2, and D_3 together, we arrive at the anomalous dimension

$$\begin{aligned} \gamma_\sigma &= \gamma^{(D_1)}_\sigma + \gamma^{(D_2)}_\sigma + \gamma^{(D_3)}_\sigma + \mathcal{O}(1/N)^2 \\ &= \frac{1}{N}\operatorname*{Res}_{\delta}\left[-2\frac{\mathrm{B}(n-s,-s+\delta)}{\mathrm{B}(n-s,n-s)} + \left(-1+2\frac{\mathrm{B}(n-s,n-2s)}{\mathrm{B}(n-s,n-s)}\right)\frac{\mathrm{B}(\delta,\delta)}{\mathrm{B}(n-s,n-s)}\right] \\ &\qquad + \mathcal{O}(1/N^2)\,. \end{aligned} \tag{4.64}$$

[12]The alert reader may be surprised that we chose $\Delta_\sigma \to \Delta_\sigma - \delta/4$ as a regulator in the $G^{(1)}_{\sigma\sigma}$ propagators in (4.61), in contrast to our previous strategy $\Delta_\sigma \to \Delta_\sigma - \delta/2$. We made this new choice because there are two $G^{(1)}_{\sigma\sigma}$ propagators, and we wanted the added x dependence arising from the regulator to be $|x|^\delta$ rather than $|x|^{2\delta}$. Our new choice does not affect the leading logarithmic term: The leading terms in a small δ expansion involve a factor $\frac{1}{\delta}+\log|x|$, whereas if we had stuck with $\Delta_\sigma \to \Delta_\sigma - \delta/2$ we would have found $\frac{1}{2\delta}+\log|x|$.

The first term in square brackets comes from D_1 and vanishes for $\mathbb{Q}_{p^n}$. For $\mathbb{R}^n$ and $s = 2$ we recover from (4.64) the result of [134, 135]:

$\mathbb{R}^n$
$$\gamma_\sigma = 4\frac{(n-1)(n-2)}{n-4}\gamma_\phi + \mathcal{O}(1/N^2)\,. \tag{4.65}$$

If we pass to the limit of small ϵ, (4.64) becomes

$$\gamma_\sigma = -\frac{6}{N}\epsilon + \mathcal{O}(1/N^2) + \mathcal{O}(\epsilon^2)\,. \tag{4.66}$$

The result (4.66) is valid equally for $\mathbb{R}^n$ and $\mathbb{Q}_{p^n}$, and for $\mathbb{Q}_{p^n}$ we see that it agrees with (4.32). If one further expands (4.64) to third order in ϵ for $\mathbb{Q}_{p^n}$, the result is found to agree with the ϵ expansion in [122, 123]. If instead we expand about the lower critical dimension and define $\tilde{\epsilon} = n - s$, then equation (4.64) says that

$$\gamma_\sigma = \mathcal{O}(\tilde{\epsilon}^2)\,. \tag{4.67}$$

This result is also valid equally for $\mathbb{R}^n$ and $\mathbb{Q}_{p^n}$, though the agreement is non-trivial: different terms in (4.64) cancel to make the term linear in $\tilde{\epsilon}$ vanish.

4.3.6 Position space integrals I: The star-triangle identity

Two useful tools for evaluating position space diagrams are the convolution integral (4.35), which we rewrite here:

$$\int dy\, |x|^{t_1-n}|y-x|^{t_2-n} = \mathrm{B}(t_1,t_2)|x|^{t_1+t_2-n}\,, \tag{4.68}$$

and the star-triangle identity of [138],[13] which can be written compactly as

$$\int dx \prod_{i=1}^{3} |x-x_i|^{t_i-n} = \mathrm{B}(t_1,t_2)\prod_{i=1}^{3}|y_i|^{-t_i} \qquad \text{if} \qquad \sum_{i=1}^{3} t_i = n\,, \tag{4.69}$$

[13] Originally in [138] the star-triangle identity was stated for $\mathbb{R}^3$ as

$$\int d^3t\, |t-x|^a|t-y|^b|t-z|^c = \pi^{3/2}\frac{\Gamma_{\text{Euler}}(\frac{a+3}{2})\Gamma_{\text{Euler}}(\frac{b+3}{2})\Gamma_{\text{Euler}}(\frac{c+3}{2})}{\Gamma_{\text{Euler}}(-a/2)\Gamma_{\text{Euler}}(-b/2)\Gamma_{\text{Euler}}(-c/2)}|x-y|^{-3-c}|y-z|^{-3-a}|z-x|^{-3-b}$$

provided $a+b+c = -6$. The somewhat complicated prefactor is precisely $\mathrm{B}_{\mathbb{R}^3}(a+3, b+3)$.

where we define

$$y_1 \equiv x_{23} \qquad y_2 \equiv x_{31} \qquad y_3 \equiv x_{12}\,. \tag{4.70}$$

The formulas (4.68)-(4.69) are valid equally for $\mathbb{R}^n$ or $\mathbb{Q}_{p^n}$. Note that it does not matter which two of t_1, t_2, and t_3 we supply as arguments to B in (4.69). The integrals (4.68) and (4.69) are rigorously valid only when the integrals converge. Provided we set $t_3 = n - t_1 - t_2$, the region of convergence for the integrals both in (4.68) and (4.69) can be characterized by the constraints $t_i > 0$ for all i. Outside this region, we must be prepared to shift exponents (while preserving the constraint $\sum_{i=1}^3 t_i = n$) and cancel divergences against local counterterms, as seen in detail in sections 4.3.3 and 4.3.4 for the self-energy diagram.

In $\mathbb{Q}_{p^n}$, it is possible to evaluate the integral in (4.69) explicitly even when $\sum_{i=1}^3 t_i \neq n$. Due to the "tall isosceles" property of ultrametric spaces, for any three non-coincident points x_1, x_2 and x_3, the linear combinations y_i defined in (4.70) form the sides of a triangle, such that up to relabeling y_i, we always have $|y_1| = |y_2| \geq |y_3|$. With this choice of y_is, the integral in (4.69) can be worked out in general to give

$$\mathbb{Q}_{p^n} \qquad \int dx \prod_{i=1}^{3} |x - x_i|^{t_i - n} = \mathrm{B}(t_1, t_2)|y_2|^{t_3 - n}|y_3|^{t_1 + t_2 - n} + \mathrm{B}(t_3, t_1 + t_2 - n)|y_2|^{t_1 + t_2 + t_3 - 2n}. \tag{4.71}$$

The integral converges provided $t_i > 0$ for all i, and $t_1 + t_2 + t_3 < 2n$. From the right hand side of (4.71), we observe that the integral has poles at $t_i = 0$ for all i, at $t_1 + t_2 + t_3 = 2n$, and at $t_1 + t_2 = n$. Remarkably in $\mathbb{R}^n$, numerics reveal (4.71) (more precisely the $\mathbb{R}^n$ version constructed from $\mathrm{B}_{\mathbb{R}^n}$) holds approximately as long as the L^2 norms satisfy $|y_1| \approx |y_2| > |y_3|$, although it is no longer an exact identity like it is in $\mathbb{Q}_{p^n}$.

4.3.7 Position space integrals II: Symmetric deformations

In order to find the anomalous dimension of the σ field by evaluating Feynman diagrams, it is necessary to introduce a regulator to the scaling of the position space σ propagator. But when introducing this regulator, the condition $\sum_{i=1}^{3} t_i = n$ in equation (4.69) is no longer satisfied, and so the star-triangle identity cannot immediately be applied to equations (4.57) and (4.61). [14] There is, however, a way around this obstacle [139]. Essentially the idea consists in considering instead of the integrals $I_{D_2}(x)$ and $I_{D_3}(x)$ other integrals that differ from them only by terms that are finite in the $\delta \to 0$ limit, but to which the star-triangle identity can be applied. Suppose, in (4.57), that we introduce yet another regulator η and consider the following integral:

$$I_{D_2}(x,\eta) = \int dx_1 dx_2 \, \frac{1}{|x_1|^{n-s-\eta}|x_1-x|^{n-s-\eta}|x_{12}|^{2s-\delta}|x_2|^{n-s+\eta}|x_2-x|^{n-s+\eta}}. \tag{4.72}$$

The deformation is depicted diagrammatically in figure 4.6. Because of the symmetrical manner in which η has been introduced, it is clear that $I_{D_2}(x,\eta)$ is invariant under the transformation $\eta \to -\eta$. For this reason, and because this Feynman diagram has at most single poles in the regulators, the Taylor expansion of $I_{D_2}(x,\eta)$ in η must assume the following form,

$$I_{D_2}(x,\eta) = I_{D_2}(x) + f_2(x)\eta^2 + f_4(x)\eta^4 + ... \tag{4.73}$$

where $f_i(x)$ are some functions that have at most single poles in δ. It is clear then, that if we set $\eta = \frac{\delta}{2}$, then $I_{D_2}(x,\eta)$ will only differ from $I_{D_2}(x)$ by terms that tend to zero as $\delta \to 0$. But $I_{D_2}(x,\frac{\delta}{2})$ can be evaluated exactly via equations

[14] The more general identity written in (4.71) can still be employed—we present an alternate derivation of (4.57) using this identity in the next section.

(4.69) and (4.68).

$$\begin{aligned} I_{D_2}(x) &\stackrel{\delta}{=} I_{D_2,\delta}(x) = \int \frac{dx_1}{|x_1|^{n-s-\frac{\delta}{2}}|x_1-x|^{n-s-\frac{\delta}{2}}} \frac{dx_2}{|x_{12}|^{2s-\delta}|x_2|^{n-s+\frac{\delta}{2}}|x_2-x|^{n-s+\frac{\delta}{2}}} \\ &\stackrel{\delta}{=} \mathrm{B}(s,s)|x|^{2s-n-\delta} \int \frac{dx_1}{|x_1|^{n-\delta}|x_1-x|^{n-\delta}} = \mathrm{B}(s,s)\mathrm{B}(\delta,\delta)|x|^{2s-2n+\delta}. \end{aligned} \tag{4.74}$$

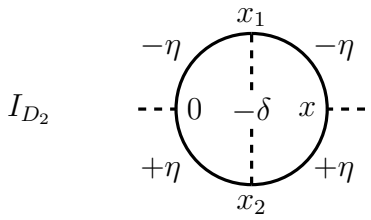

Figure 4.6: The symmetric deformation of I_{D_2} that allows the integral to be exactly evaluated without disturbing the leading behavior in δ. η is eventually set to $\delta/2$.

This method of finding the leading order behavior of a Feynman diagram by symmetrically changing the scaling of internal propagators and invoking equations (4.69) and (4.68) can also be used to derive equation (4.61) in the following manner, represented diagrammatically in figure 4.7:

$$\begin{aligned} I_{D_3}(x) &\stackrel{\delta}{=} \int \frac{dx_2\,dx_3}{|x_2|^{n-s-\frac{\delta}{2}}|x_3-x|^{n-s-\frac{\delta}{2}}} \int \frac{dx_1}{|x_1|^{n-s+\frac{\delta}{2}}|x_{12}|^{n-s}|x_{13}|^{2s-\frac{\delta}{2}}} \\ &\qquad \times \int \frac{dx_4}{|x_{24}|^{2s-\frac{\delta}{2}}|x_{34}|^{n-s}|x_4-x|^{n-s+\frac{\delta}{2}}} \\ &\stackrel{\delta}{=} \mathrm{B}(s,s)^2 \int \frac{dx_2\,dx_3}{|x_2|^{2n-3s}|x_2-x|^{s}|x_{23}|^{2s-\delta}|x_3|^{s}|x_3-x|^{2n-3s}} \\ &\stackrel{\delta}{=} \mathrm{B}(s,s)^2 \int \frac{dx_3}{|x_3|^{s-\frac{\delta}{2}}|x_3-x|^{2n-3s-\frac{\delta}{2}}} \frac{dx_2}{|x_2|^{2n-3s+\frac{\delta}{2}}|x_{23}|^{2s-\delta}|x_2-x|^{s+\frac{\delta}{2}}} \\ &\stackrel{\delta}{=} \mathrm{B}(s,s)^2\mathrm{B}(n-s,n-2s)|x|^{2s-n-\delta} \int \frac{dx_3}{|x_3|^{n-\delta}|x_3-x|^{n-\delta}} \\ &= \mathrm{B}(s,s)^2\mathrm{B}(n-s,n-2s)\mathrm{B}(\delta,\delta)|x|^{2s-2n+\delta}\,. \end{aligned} \tag{4.75}$$

After the second step we recognize the remaining integral as similar to I_{D_2}, but with different (and slightly less constrained) exponents. We represent this di-

agrammatically on the right side of figure 4.7 by showing a diagram with the topology of D_2 but with the exponents taken from the second line of (4.75). The third step, then, is to shift these exponents *again* in imitation of how we evaluated I_{D_2}. It may not be entirely evident that the scaling dimensions are altered in a symmetrical manner in the third step in (4.75), but changing variables by letting $x_2 \to -\tilde{x}_2$ and $\tilde{x}_3 \to x_3 + x$ clearly shows that this is indeed the case.

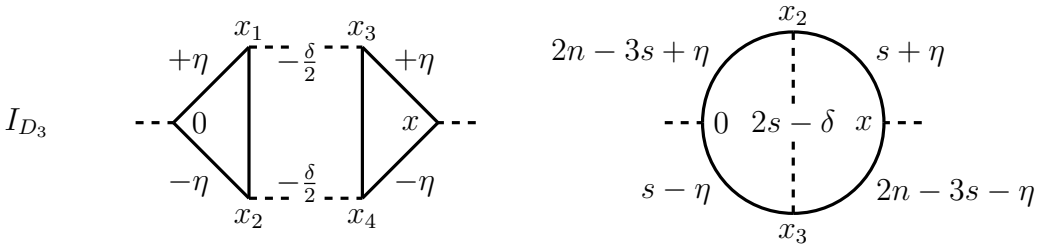

Figure 4.7: The symmetric deformations that allow I_{D_3} to be exactly evaluated without disturbing the leading behavior in δ. η is set to $\delta/2$ in both cases.

4.3.8 Position space integrals III: Direct evaluation in $\mathbb{Q}_{p^n}$

We now present an alternate derivation of (4.57) which is applicable in $\mathbb{Q}_{p^n}$ and relies on a direct application of the identity in (4.71). Using the identity to perform the integral over x_1 in (4.57), we obtain

$$\mathbb{Q}_{p^n} \qquad I_{D_2}(x) = \int dx_2 \, \frac{1}{|x_2|^{n-s}|x-x_2|^{n-s}} \, f(|x|,|x_2|,|x-x_2|)\,, \tag{4.76}$$

where

$$\mathbb{Q}_{p^n} \quad f(|x|,|x_2|,|x-x_2|) = \begin{cases} \dfrac{\mathrm{B}(s,s)}{|x_2|^{2s-\delta}|x|^{n-2s}} + \dfrac{\mathrm{B}(2s-n,n-\delta)}{|x_2|^{n-\delta}} & \text{if } |x_2| > |x| \\ \dfrac{\mathrm{B}(s,s-\delta)}{|x|^{n-s}|x_2|^{s-\delta}} + \dfrac{\mathrm{B}(s,\delta-s)}{|x|^{n-\delta}} & \text{if } |x_2| < |x| \\ \dfrac{\mathrm{B}(s,s-\delta)}{|x|^{n-s}|x-x_2|^{s-\delta}} + \dfrac{\mathrm{B}(s,\delta-s)}{|x|^{n-\delta}} & \text{if } |x_2| = |x|\,. \end{cases} \tag{4.77}$$

Splitting into the three cases displayed in (4.77), the x_2 integral in (4.76) is seen to reduce to the following three simple kinds of integrals (with the convergence condition on the exponent shown in parenthesis):

$$\begin{aligned}
&\int_{|y|>|z|} dy\,|y|^{t-n} = |z|^t \frac{1}{p^{-t}-1}\left(1-\frac{1}{p^n}\right) && (t<0)\\
\mathbb{Q}_{p^n} \qquad &\int_{|y|<|z|} dy\,|y|^{t-n} = |z|^t \frac{1}{p^{t}-1}\left(1-\frac{1}{p^n}\right) && (t>0)\\
&\int_{|y|=|z|} dy\,|y-z|^{t-n} = |z|^t \left(-\frac{1}{p^n}+\frac{1}{1-p^{-t}}\left(1-\frac{1}{p^n}\right)\right) && (t>0)\,.
\end{aligned} \tag{4.78}$$

Plugging (4.77) in (4.76) and using (4.78) to evaluate the x_2 integrals, we end up with the final result

$$\mathbb{Q}_{p^n} \qquad I_{D_2}(x) \stackrel{\delta}{=} \mathrm{B}(s,s)\mathrm{B}(\delta,\delta)|x|^{2s-2n+\delta}\,, \tag{4.79}$$

where as usual, $\stackrel{\delta}{=}$ means equality up to terms which are finite in the limit $\delta \to 0$. Though the computation is more cumbersome, the above procedure can also be used to directly evaluate $I_{D_3}(x)$ as well as any other Feynman diagram over the p-adics since the integrals always reduce to sums of geometric series.

4.4 Higher derivative $O(N)$ models on $\mathbb{R}^n$

So far, in order to compare with standard results in the literature, we have generally set $s = 2$ when considering the $O(N)$ model on $\mathbb{R}^n$. One could reasonably ask, what happens if we lift this restriction? The large N results, summarised in section 4.1 in equations (4.1) and (4.2)-(4.3) remain valid. For generic s, $g_\phi(\delta)$ has no pole at $\delta = 0$. As for $\mathbb{Q}_{p^n}$, this is associated with having only a finite renormalization of $G_{\phi\phi}$ rather than an anomalous dimension. For $\mathbb{Q}_{p^n}$ we understand this as a consequence of the non-renormalization argument of [114], following

quite generally from ultrametricity. In $\mathbb{R}^n$ a non-local kinetic term is not expected to be renormalized [140] due to the fact that Wilsonian renormalization leads to correction terms polynomial in momenta—in other words local derivative couplings in position space which do not affect the non-local kinetic piece. (This reasoning is equally valid in $\mathbb{Q}_{p^n}$, but due to the ultrametricity of the p-adic norm a stronger version holds: As discussed in section 4.2.4, no derivative couplings are *ever* generated.) Theories with a non-local kinetic term in $\mathbb{R}^n$ were already studied in [126, 127]. Fisher, Ma and Nickel [126] considered precisely the theory described by (4.1) in $\mathbb{R}^n$ and computed critical exponents in the ϵ expansion and at large N, in the range $n/2 < s < 2$. The large N results presented in (4.2)-(4.3) find perfect agreement with the anomalous dimensions γ_ϕ and γ_σ extracted from the critical exponents:

$$\begin{aligned}
&\eta = 2 - s + 2\gamma_\phi = 2 - s + \mathcal{O}(1/N^2) \\
\mathbb{R}^n \quad &\frac{1}{\gamma} = \left(\frac{s - 2\gamma_\phi}{n - s - \gamma_\sigma}\right)^{-1} = 1 - \frac{2s-n}{s} - \frac{8}{N}\frac{\Gamma_{\text{Euler}}(\frac{s}{2})^2\Gamma_{\text{Euler}}(n-s)}{s\,\Gamma_{\text{Euler}}(s-\frac{n}{2})\Gamma_{\text{Euler}}(\frac{n}{2})\Gamma_{\text{Euler}}(\frac{n-s}{2})^2} \\
&\qquad\qquad \times \left[\frac{\Gamma_{\text{Euler}}(\frac{s}{2})\Gamma_{\text{Euler}}(n-s)\Gamma_{\text{Euler}}(\frac{n}{2}-s)\Gamma_{\text{Euler}}(\frac{3s-n}{2})}{\Gamma_{\text{Euler}}(s)\Gamma_{\text{Euler}}(n-\frac{3s}{2})\Gamma_{\text{Euler}}(s-\frac{n}{2})\Gamma_{\text{Euler}}(\frac{n-s}{2})} - \frac{1}{2}\right] + \mathcal{O}(1/N^2).
\end{aligned} \tag{4.80}$$

In (4.80), η and γ are critical exponents computed in [126], while γ_ϕ and γ_σ are obtained from (4.2)-(4.3). Generically for $s \geq 2$, the local kinetic term $\sim (\partial\phi)^2$, generated from Wilsonian considerations, becomes more relevant and dominates the non-local kinetic piece, resulting in a non-vanishing anomalous dimension for ϕ found by setting $s = 2$ in (4.2)-(4.3). The discontinuity in γ_ϕ at $s = 2$ can be removed by accounting for the competition between the local kinetic term induced from renormalization and the non-local kinetic piece, with the local kinetic term argued to become more relevant at $s = s_\star < 2$ in such a way that γ_ϕ is continuous along s [127, 140] (see also [141, 142, 143, 91]). In this chapter, however, we have concerned ourselves with a $(\phi^i\phi^i)^2$ deformation as shown in (4.1) with all other

n	5	6	7
$N\gamma_\phi$	$\frac{48}{35\pi^2}$	0	$-\frac{128}{315\pi^2}$
$N\gamma_\sigma$	$-\frac{1408}{105\pi^2}$	$-\frac{14}{3}$	$-\frac{15872}{315\pi^2}$

Table 4.1: Anomalous dimension predictions for $s = 4$.

relevant deformations appropriately tuned away, and the results presented in (4.2)-(4.3) are valid as long as that continues to hold.

Perhaps a more interesting question is what happens when $s = 4$, or 6, or some larger even number. At precisely these values, the original model (4.1) recovers locality. It is then a higher derivative version of the $O(N)$ model. Let's consider the case $s = 4$ for the sake of a focused discussion. Then

$$\mathbb{R}^n \qquad S = \int dx \left[\frac{1}{2}(\Box\,\phi^i)^2 + \frac{\lambda}{4!}(\phi^i\phi^i)^2\right], \tag{4.81}$$

from which it follows that

$$\mathbb{R}^n \qquad [\phi^i] = \frac{n-4}{2} \qquad\qquad [\lambda] = 8 - n\,, \tag{4.82}$$

and so we see that the upper critical dimension is $n = 8$, while the lower critical dimension is $n = 4$. Between the upper and lower critical dimension, the interaction term $(\phi^i\phi^i)^2$ is relevant, so it triggers a renormalization group flow which we may suspect leads to a new critical theory in the infrared—provided relevant deformations are appropriately tuned away. Precisely this sort of flow was considered in $8 - \epsilon$ dimensions in [130], and the infrared critical theory was referred to as a Lifshitz point. Setting $s = 4$ in (4.2)-(4.3) leads to the predictions for the anomalous dimensions at Lifshitz points shown in table 4.1, up to $\mathcal{O}(1/N^2)$ corrections to both γ_ϕ and γ_σ in each case.

These results were anticipated in [144]; in fact, results were given there for

fixed $s = 4$ and arbitrary $n \in (4, 8)$ in the form

$$\eta_{\ell 4} = 4 - s + 2\gamma_\phi\Big|_{s=4} = \frac{1}{N}\frac{(8-n)}{n(n+2)}\frac{3\times 2^{n-2}}{\pi^{3/2}}\frac{\Gamma_{\text{Euler}}(\frac{n-3}{2})}{\Gamma_{\text{Euler}}(\frac{n}{2})}\sin\frac{\pi n}{2} + \mathcal{O}(1/N^2)$$

$\mathbb{R}^n$
$$\gamma_\ell = \frac{s-2\gamma_\phi}{n-s-\gamma_\sigma}\bigg|_{s=4} = \Big(\frac{n}{4}-1\Big)^{-1} - \frac{1}{N}\frac{\Gamma_{\text{Euler}}(n-4)}{\Gamma_{\text{Euler}}(\frac{n}{2})\Gamma_{\text{Euler}}(\frac{n}{2}-2)^2\Gamma_{\text{Euler}}(4-\frac{n}{2})} \times\Big(\frac{n}{4}-1\Big)^{-2}\left[1+\frac{(10-n)(n-5)}{3}+\frac{3(n-6)(n-8)}{4(n+2)}\right]+\mathcal{O}(1/N^2). \tag{4.83}$$

In (4.83), $\eta_{\ell 4}$ and γ_ℓ are quantities defined and computed in [144]. Explicit expression in terms of Γ_{Euler} can be derived for γ_ϕ and γ_σ starting from (4.2)-(4.3) with s set equal to 4, and when this is done, perfect agreement with (4.83) is found.

The expressions for γ_ϕ and γ_σ that we gave in (4.2)-(4.3) go smoothly to zero at both the upper and lower critical dimensions. At the upper critical dimension, the natural expectation is that the only fixed point is the Gaussian theory, and turning on λ causes us to run logarithmically away from it. At the lower critical dimension (namely four), the physics may be richer, and we recover the four-dimensional sigma-model considered in [129], where the value given for the anomalous dimension of ϕ in an ϵ-expansion matches the $s = 4$ case of the $1/N$ result (4.2)-(4.3). We comment further on the lower critical dimension at the end of section 4.4.2.

4.4.1 A bound on the higher derivative action

To properly understand the field theory (4.81), we should list the relevant deformations: for $n \geq 6$,

$\mathbb{R}^n$
$$S_{\text{rel}} = \int dx\left[\frac{w}{2}\phi^i\,\Box\,\phi^i + \frac{r}{2}\phi^i\phi^i\right], \tag{4.84}$$

where $[w] = 2$ and $[r] = 4$. (Of course, $\phi^i \Box \phi^i = -(\partial\phi^i)^2/(2\pi)^2$ up to a total derivative which we can discard.) With these extra terms added, the action may no longer be everywhere nonnegative, and one might wonder about runaway instabilities. The aim of this section is to provide an estimate which shows that by adding a suitable constant term to the lagrangian, we can make it once again nonnegative. This is the sense in which the action is bounded below. While the estimates we give are fairly trivial, they are worthwhile to see given the prevalence of instabilities and ghosts in higher derivative theories after passing to a Hamiltonian or Lorentzian setting.

For $n < 6$, $O(N)$ singlet operators schematically of the form $\phi^2(\partial\phi)^2$ become relevant as well, and we can proceed to $\phi^4(\partial\phi)^2$ operators when we have $n < 5$. Such a large assortment of terms would complicate the story too much for us to give simple estimates, so let's stipulate $n \geq 6$ in this section.

We may bring the action into a form considered for example in [145, 146] by trading w and r for two mass parameters, m_1 and m_2:

$$\mathbb{R}^n \qquad S + S_{\text{rel}} = \int dx \left[\frac{1}{2}\phi^i q(\Box)\phi^i + \frac{\lambda}{4!}(\phi^i\phi^i)^2\right] \tag{4.85}$$

where

$$\mathbb{R}^n \qquad q(\Box) = (\Box + m_1^2)(\Box + m_2^2)\,. \tag{4.86}$$

We can assume $m_1^2 < m_2^2$ without loss of generality, but we cannot necessarily assume that the m_i^2 are positive. Aficionados of Pauli-Villars regulators will immediately recognize (4.86) and the consequent tree-level momentum space propagator:

$$\mathbb{R}^n \qquad G^{(0)}_{\phi\phi}(k) = \frac{1}{(k^2 + m_1^2)(k^2 + m_2^2)} = \frac{1}{m_2^2 - m_1^2}\left(\frac{1}{k^2 + m_1^2} - \frac{1}{k^2 + m_2^2}\right)\,. \tag{4.87}$$

The Pauli-Villars strategy is to let the $1/k^4$ behavior of this propagator improve UV behavior, and then at the end of a computation take m_2 large while m_1 remains finite. (Normally in a Pauli-Villars context one would rescale ϕ by a power of $m_2^2 - m_1^2$ to get rid of the $1/(m_2^2 - m_1^2)$ prefactor in the last expression in (4.87).) The minus sign on the $1/(k^2 + m_2^2)$ term in (4.87) is understood as an indication of ghosts (i.e. negative norm states in the Hilbert space) in a canonical quantization approach. Indeed, pathological features of higher derivative scalar field theories have been explored extensively: see for example [145, 147, 146, 148] and references therein. Typical pathologies hinge on a Hamiltonian construction in which one sees an instability along the lines of Ostrogradsky's theorem [149], and/or failures of reflection positivity [145] that lead to negative norm states in a canonical quantization approach. In a Euclidean quantum field theory setting, these pathologies may prove less significant as long as we do not attempt canonical quantization. Instead, we should form a Euclidean path integral

$$Z = \int_{\mathbb{R}^n} \mathcal{D}\phi \, e^{-S[\phi] - S_{\text{rel}}[\phi]} \,, \tag{4.88}$$

and then what matters is that the total action should be bounded below and that it should not have flat or nearly flat directions that prevent convergence. Boundedness can be demonstrated explicitly, as follows.

$$\begin{aligned} \left| \int_{\mathbb{R}^n} dx \, \frac{1}{2}(m_1^2 + m_2^2)\phi^i \, \Box \, \phi^i \right| &\leq \left(\int dx \, \frac{1}{4\xi}(m_1^2 + m_2^2)^2 \phi^i \phi^i \right)^{1/2} \left(\int dx \, \xi (\Box \, \phi^i)^2 \right)^{1/2} \\ &\leq \int dx \left[\frac{\xi}{2}(\Box \, \phi^i)^2 + \frac{1}{8\xi}(m_1^2 + m_2^2)^2 \phi^i \phi^i \right] , \end{aligned} \tag{4.89}$$

where the first inequality is Cauchy-Schwarz and the second is the arithmetic-geometric mean inequality, and ξ is any positive real number. Plugging (4.89)

into (4.85), we arrive at

$$S + S_{\text{rel}} \geq \int_{\mathbb{R}^n} dx \left[\frac{1-\xi}{2} (\Box \phi^i)^2 - \frac{1}{8} \left(\frac{1-\xi}{\xi} (m_1^2 + m_2^2)^2 + (m_1^2 - m_2^2)^2 \right) \phi^i \phi^i + \frac{\lambda}{4!} (\phi^i \phi^i)^2 \right]. \tag{4.90}$$

We must choose $\xi \in (0,1)$ in order to get the derivative term on the right hand side of (4.90) to be positive definite, so as to make the lower bound strong when the ϕ^i are highly oscillatory. Choosing $\xi \in (0,1)$ makes the mass term on the right hand side of (4.90) negative, which seems like the beginning of an instability; but as long as $\lambda > 0$ the overall value of the lagrangian density is bounded below. We could adjust the lagrangian density by a constant term (which is after all a relevant deformation) to achieve an action which can be shown to be nonnegative through the approach outlined in (4.89)-(4.90). In short, the situation is no worse than the case of the usual $O(N)$ model on $\mathbb{R}^n$ with negative mass squared. It should be borne in mind that the inequalities might be far from sharp. So the actual behavior of $S + S_{\text{rel}}$ could be somewhat better than we have demonstrated.

4.4.2 Qualitative features of renormalization group flows

Starting from the free massless higher derivative theory $S_0 = \int dx \, \frac{1}{2} (\Box \phi^i)^2$, let's consider what renormalization group flows there must be, indicating in each case what the likeliest outcome is in the infrared. For simplicity we avoid consideration of deformations which lead to soft or spontaneous breaking of translational or rotational symmetry on $\mathbb{R}^n$. We assume that $n > 4$ so that the dimension of ϕ^i is positive, and we assume $n < 8$ so that we have relevant deformations, namely ϕ^2, $(\partial\phi)^2$, or ϕ^4, where we omit $O(N)$ indices for brevity. Let's consider in turn the deformations with respect to each:

- Deforming only by ϕ^2 with a positive coefficient looks boring in the sense that it can only lead to a theory in which there are no light degrees of freedom. We exclude the case of adding $-\phi^2$ to the action because then there really would be a runaway instability.

- Deforming only by $(\partial\phi)^2$—where again to avoid instability we must insist on a positive coefficient—leads trivially to the massless two-derivative Gaussian theory, with action (proportional to) $\int dx\, \frac{1}{2}(\partial\phi)^2$. We say "trivially" because there are no loop diagrams. All we are doing is setting $m_2 \neq 0$ in (4.86) while keeping $m_1^2 = 0$. The only non-trivial Green's function is the two-point function $G_{\phi\phi}(k) \propto \frac{1}{k^2} - \frac{1}{k^2+m_2^2}$, the same as for a free massless scalar plus a Pauli-Villars regulator. Passing to the regime $|k| \ll m_2$ amounts to excising the Pauli-Villars part of the propagator.

- Deforming by $(\partial\phi)^2$ and ϕ^4, with positive coefficients for each, while tuning the coefficient of ϕ^2, should enable us to again reach massless two-derivative Gaussian theory. The key point is that $(\partial\phi)^2$ is more relevant than the original $(\Box\,\phi)^2$ term, so the latter drops out; and in the new dimension counting based on $(\partial\phi)^2$, the interaction term ϕ^4 is irrelevant, so it too should attenuate away as we proceed toward the infrared. In the process, ϕ^2 terms are generated, so to wind up at the free massless Gaussian theory rather than a massive theory we must tune ϕ^2.

  We could also take the Pauli-Villars point of view and reason that our deformed theory in this case is a Pauli-Villars regularization of the usual two-derivative $O(N)$ model. Since we are above the upper critical dimension of this two-derivative theory, the transition from the disordered state to the ordered state must be described by mean field theory, i.e. the massless two-derivative Gaussian theory.

- Deforming by ϕ^4 with a positive coefficient while tuning both $(\partial\phi)^2$ and ϕ^2 should enable us to reach new conformal theories whose anomalous dimensions for integer n are listed in table (4.1). Deforming only by ϕ^4 doesn't make sense because loop effects will presumably generate $(\partial\phi)^2$ and ϕ^2. If we don't tune the ϕ^2 term, we'll wind up with a massive theory, while if we don't tune the $(\partial\phi)^2$ term we could wind up with the two-derivative Gaussian theory.

  Below $n = 6$, new relevant $O(N)$ singlets appear: the aforementioned $\phi^2(\partial\phi)^2$ operators. Their coefficients might also need to be tuned in order to arrive at the new conformal field theories whose existence we are hypothesizing. Relevant operators of this type may be relatively harmless since their dimensions are always higher than the operator ϕ^4 which is driving the flow.

Altogether, four-derivative ϕ^4 theory should augment the space of fixed points of the $O(N)$ model as indicated in figure 4.8. If this picture is accepted, the next natural question is what happens at the lower critical dimension. In the case of two-derivative theories, the key point for $N > 1$ is that non-linear sigma models (NLσM) on S^{N-1} become renormalizable in $n = 2$—though for $N > 2$ they are asymptotically free rather than conformal. In the case of $N = 1$, the symmetry group is $\mathbb{Z}_2$, and we obtain the $c = 1/2$ minimal model as the continuum limit of 2d Ising. In other words, the NLσMs (or, for $N = 1$, the $c = 1/2$ minimal model) are at the terminus of the line of Wilson-Fisher fixed points as we proceed downward in dimension.

Proceeding by analogy, we might expect in $n = 4$ some new way of realizing $O(N)$ symmetry in a renormalizable field theory. The obvious candidate is a NLσM on S^{N-1}, where the kinetic term is $(\Box\,\phi^i)^2$ with $\phi^i\phi^i$ constrained to be equal to 1. Exactly such a theory is considered in [129], and the Beta function

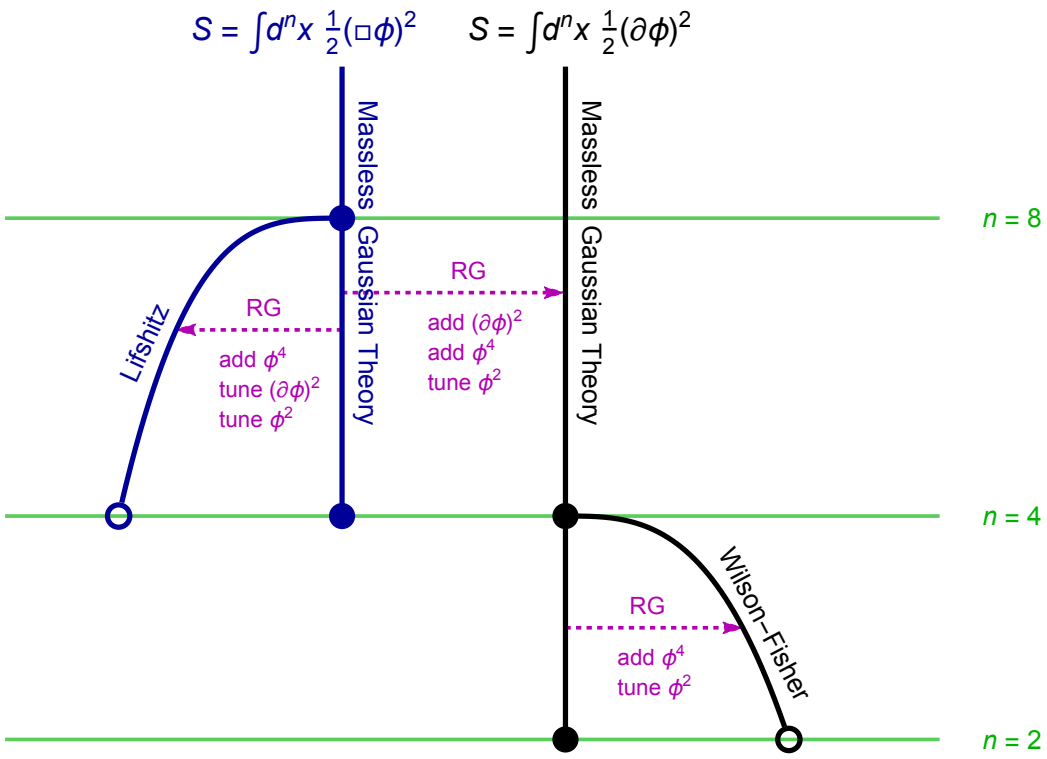

Figure 4.8: The four-derivative extension of the space of fixed points of ϕ^4 theory.

computed there accords with the natural expectation that for N large enough (larger than 2) the theory is asymptotically free in the ultraviolet and confining in the infrared. Since the NLσM construction is unavailable for $N = 1$, we are thrown back on the more abstract proposal that there could be some four-dimensional Euclidean conformal field theory whose natural degrees of freedom we don't know but which realizes a global $\mathbb{Z}_2$ symmetry.

It is of course tempting not to stop with ϕ^4 theory; as in two-derivative theories one can consider higher powers of ϕ, leading to new branches of fixed points that fork off the Gaussian theory at dimensions that are successively closer to $n = 4$ as one raises the power of ϕ. Such fixed points are called multicritical in the two-derivative context because one has to tune several relevant operators to hit the infrared fixed point. They are thought to connect to minimal models in the lower critical dimension [150]. Multicriticality will be even more pronounced for

four-derivative theories, because the list of relevant operators proliferates quickly as we head toward $n = 4$ and includes an assortment of two-derivative operators. Let us nonetheless conjecture that multicritical versions of Lifshitz fixed points above $n = 4$ exist for the $O(N)$ model, and that for $N = 1$ they are continuously connected with new conformal field theories in $n = 4$ which are analogs of unitary minimal models. These new theories, both in $n = 4$ and in higher dimensions, may be amenable to treatment via the conformal bootstrap, similar to [151]. If all this is true, then one might hope that other classic field theory constructions in $n = 2$ generalize to higher derivative theories in $n = 4$; in such a case, we clearly have a lot of work to do to understand what the full picture of four-dimensional Euclidean field theories really comprises!

One also need not stop with four-derivative theories. The next case to consider is $\phi\Box^3\phi$ theory. The upper critical dimension (where ϕ^4 becomes marginal) is 12, and the lower critical dimension is 6. It is easy to read off from (4.2)-(4.3) the anomalous dimensions of ϕ and ϕ^2 at conjectural fixed points anywhere between $n = 6$ and 12. The list of relevant deformations will be even more extensive than in the four-derivative case, and correspondingly one must expect quite a complex picture of possible renormalization group flows. Problems with canonical quantization and Ostrogradsky instabilities are likely to be ubiquitous in all the higher derivative theories we are considering, but as Euclidean path integral field theories they are probably well defined due to bounds along the lines of section 4.4.1. In fact, by studying the analytical structure of the conformal blocks of generalized free CFTs (unitary and non-unitary) and nearby Wilson-Fisher critical points, the authors in [152, 153] derive expressions for the first terms of the anomalous dimensions of classes of scalar operators in an ϵ-expansion, and their results for γ_ϕ and γ_{ϕ^2} in theories with (in our notation) $s = d/2$ exactly matches (4.2)-(4.3) in arbitrary dimension.

4.4.3 A lattice implementation

Just as ordinary two-derivative ϕ^4 theory (with real-valued ϕ, i.e. $N = 1$) is realized as a continuum limit of the Ising model with nearest neighbor interactions, we might expect four-derivative ϕ^4 theory to be realized as a continuum limit of an Ising model with next-to-nearest neighbor interactions. We have in mind particularly a lattice action along the lines of the anisotropic next-to-nearest neighbor Ising model (ANNNI for short) [154, 155], but as isotropic as the underlying lattice allows:

$$S = K \sum_{\vec{x} \in \mathbb{Z}^n} (\Box \, \sigma_{\vec{x}})^2 + J \sum_{\vec{x} \in \mathbb{Z}^n} \sum_{\vec{y} \sim \vec{x}} (\sigma_{\vec{x}} - \sigma_{\vec{y}})^2 \,, \tag{4.91}$$

where we define a lattice laplacian

$$\Box \, \sigma_{\vec{x}} = \sum_{\vec{y} \sim \vec{x}} (\sigma_{\vec{x}} - \sigma_{\vec{y}}) \,. \tag{4.92}$$

The notation $\sum_{\vec{y} \sim \vec{x}}$ means that we hold $\vec{x}$ fixed and sum over all $\vec{y}$ which are nearest neighbors of $\vec{x}$, which is to say $2n$ nearest neighbors when we work on the lattice $\mathbb{Z}^n$. With the action (4.91) in hand, we can define a partition function

$$Z = \sum_{\sigma} e^{-S} \,, \tag{4.93}$$

where the sum is over all possible spin configurations. If we set $K = 0$, then according to standard reasoning, there is a phase transition between ordered and disordered phases that occurs at a special value of J, and it will have mean field theory critical exponents when $n > 4$ because $n = 4$ is the upper critical dimension of two-derivative ϕ^4 theory. But if $4 \leq n < 8$, we should be able to find a critical point not described by mean field theory by tuning both K and J. Instead, the critical point should be described by the endpoint of a renormalization group flow from the massless four-derivative Gaussian theory, triggered by ϕ^4 deformation and with the relevant operators ϕ^2 and $(\partial\phi)^2$ appropriately tuned—the Lifshitz point of [130]. A caveat, as previously noted, is that as one

gets close to the lower critical dimension, additional relevant operators appear, so it is conceivable that more lattice quantities must be tuned than just K and J. For $n \geq 6$ this should not be a problem.

Similar lattice constructions can obviously be given for $N > 1$ theories. We could even construct next-to-next-to-nearest neighbor models which should give Lifshitz-like critical points in dimensions between 6 and 12—but the computational difficulties associated with lattices in such large dimensions, not to mention the number of tunings required to suppress relevant directions, seem likely to make anything beyond next-to-nearest neighbor models impractical. The recent work [156] indicates that $n = 5$ lattice simulations of the Ising model on a large enough lattice to see scaling behavior are accessible with modern computational methods. So it should be possible to do a direct search on the lattice for non-mean-field critical behavior in (4.91) in $n = 4$, 5, and maybe 6. It would also be interesting to study finite-range Ising models on the Bethe lattice, whose recursive structure often leads to exactly solvable models and whose exponential growth mimics infinite dimension [157, 158]. Such studies might eventually lead us back to the p-adics through the holographic relation of the Bethe lattice (also called the Bruhat–Tits tree) with coordination number $p + 1$ to the p-adic numbers $\mathbb{Q}_p$ on the boundary.

4.5 Discussion

The main technical result of the chapter, summarized in (4.2)-(4.3), is the expression of anomalous dimensions γ_ϕ and γ_σ as residues of meromorphic functions which are simple rational combinations of the "local" Beta function, $g_\phi(\delta)$ and $g_\sigma(\delta)$ of a quantity δ at $\delta = 0$, where δ is understood as a shift in the dimension of the Hubbard-Stratonovich field σ that we impose as a regulator and then

remove at the end of the calculation. These meromorphic functions come from diagrammatic amplitudes of the form

$$I_{V,m}(z_a) = \int d^V x \left(\prod_{a=1}^{m} \prod_{i=1}^{V} \frac{1}{|x_i - z_a|^{\delta_{ia}}} \right) \left(\prod_{i \neq j} \frac{1}{|x_{ij}|^{\delta_{ij}}} \right) \tag{4.94}$$

where $x_{ij} = x_i - x_j$. V is the number of internal vertices, each at a spatial location x_i. The notation $\int d^V x$ means that we are integrating x_i over all space; and "space" here could be $\mathbb{R}^n$ or $\mathbb{Q}_{p^n}$. The number of external vertices is m, each at a spatial location z_a. Based on the Feynman rules for the particular theory under consideration (the $O(N)$ model in our case), we are able to assign values to the exponents δ_{ij} and δ_{ia} which are linear functions of the regulator δ. Then $I_{V,m}(z_a)$ becomes a meromorphic function of δ, and a linear combination of several such functions, each deriving from a different diagram, gives us the meromorphic functions $g_\phi(\delta)$ and $g_\sigma(\delta)$ that we are eventually interested in.

In general, such integrals give complicated answers. However, there are particular cases where the answer simplifies. If $m = 2$ and $V = 1$, then $I_{V,m}$ is just a convolution, so the answer is expressed naturally in terms of the appropriate variant of the Beta function together with a power of z_{12}. If $m = 3$ and $V = 1$, then the same thing happens again provided the exponents obey a sum rule: This is the star-triangle identity (4.69). The striking point about $O(N)$ model calculations, at least to the order we have exhibited here, is that all the amplitudes of interest for the computation of anomalous dimensions are expressible as products of the local Beta function times power-law functions of the z_a, in both $\mathbb{R}^n$ and $\mathbb{Q}_{p^n}$.[15]

There is an interesting connection between the amplitudes $I_{V,m}$ and string

[15]Final expressions for the functions $g_\phi(\delta)$ and $g_\sigma(\delta)$ involve factors of $\mathrm{B}(n-s, n-s)$ in the denominator for a special reason: this particular Beta function appears in the leading order propagator for σ. In other words, negative powers of $\mathrm{B}(n-s, n-s)$ appear in the meromorphic functions only because they appear in the coefficients we must use to combine the $I_{V,m}(z_a)$ into 1PI amplitudes.

scattering amplitudes. The Beta function appears in the star-triangle identity precisely as it appears in four-point scattering amplitudes of tachyons, i.e. the Veneziano or Virasoro-Shapiro amplitude.[16] The star-triangle identity is in fact a generalization of the way one obtains the Veneziano amplitude by integration over the position of one vertex operator over the boundary of the string. The sum rule on the exponents is understood in this context as related to momentum conservation plus the on-shell condition for external string states. Generalizations of the Veneziano amplitude to integrations over all of $\mathbb{R}^n$ were considered in [159], while generalizations to integrations over $\mathbb{Q}_p$ are the foundation of p-adic string theory [65, 66, 48]. If we add more internal vertices, then in the string theory context, instead of a four-point scattering amplitude, we would be considering a higher point amplitude—still at tree level. Might we understand the expression of the $I_{V,m}$ integrals we need for anomalous dimensions in the $O(N)$ models in terms of products of Beta functions as a consequence of a factorization property of string amplitudes?

The analogy between diagrammatic amplitudes in scalar field theory and string scattering helps our intuition in understanding why the anomalous dimension γ_ϕ vanishes for the $O(N)$ model defined over $\mathbb{Q}_{p^n}$, but not for the usual $O(N)$ model defined over $\mathbb{R}^n$. We saw in section 4.3.3 that after canceling a quadratic divergence with local counterterms, the amplitude in the p-adic case had no further divergences, but in the Archimedean case a logarithm appeared that gave rise to the anomalous dimension. From the point of view of meromorphic functions, we wound up with an integral I_D that located us at a pole in the Archimedean case which would be understood in string scattering terms as

[16] We should bear in mind that our $\mathrm{B}_{\mathbb{R}}(t_1, t_2)$ is not the same as $\mathrm{B}_{\mathrm{Euler}}(t_1, t_2)$; rather, $\mathrm{B}_{\mathbb{R}}(t_1, t_2)$ is a crossing-symmetric combination of Euler Beta functions. Thus when we refer to the Veneziano amplitude, we really mean the crossing-symmetric combination without Chan-Paton factors. See, for example, equation (2.4) in chapter 2 where we referred to $\mathrm{B}_{\mathbb{R}}$ as B_∞.

an infinitely sharp resonance due to the exchange of a first-excited string state (where tachyons are counted as the unexcited state). The absence of a pole in the p-adic case implies the vanishing of γ_ϕ and corresponds to the fact that the p-adic string has only one state in its spectrum, namely the tachyon. In general we would like to associate divergences in field theory with on-shell divergences in string scattering amplitudes.

Once we express diagrammatic amplitudes in the form (4.94), it is natural to consider a large generalization, in which we replace $\mathbb{R}^n$ or $\mathbb{Q}_{p^n}$ with some homogeneous space—not necessarily Archimedean. The propagators $1/|x|^{2\Delta}$ would then naturally be replaced by representations of a group which fixes a point in the homogeneous space.[17] For $\mathbb{R}^n$ equipped only with conformal structure rather than full metrical structure, this group would consist of dilations and rotations around the origin, so on top of $1/|x|^{2\Delta}$ we could get a factor depending only on the direction of x and providing a unitary representation of the rotation group. In common parlance, we could consider operators with spin. For $\mathbb{Q}_{p^n}$, the natural notion replacing spin hinges on multiplicative characters, as remarked in [59]; so in place of $1/|x|^{2\Delta}$ we would have $\theta(\hat{x})/|x|^{2\Delta}$ where $\hat{x} \equiv x|x|$ is a unit in $\mathbb{Q}_{p^n}$ and θ is a unitary multiplicative character of the group of units. It seems likely that there are significant generalizations of the Beta functions we have used, related to convolving generalized propagators. Star-triangle identities and more general diagrammatic amplitudes may be similarly capable of generalization, and the important question becomes what kind of meromorphic functions appear and how their poles translate into anomalous dimensions, or appropriate generalizations

[17] The group of interest is generally *not* the full group preserving a point. For instance, in the case of $\mathbb{R}^n$ equipped only with conformal structure, special conformal transformations are excluded even though they preserve the origin. If G admits an Iwasawa decomposition $G = KAN$, and M is the subgroup of K comprising elements which commute with all of A, then on the homogeneous space G/MAN the generalized propagators would be representations of M and A. See the related discussion in [160].

thereof. It would be fascinating to try to extend standard quantum field theoretic notions of locality and renormalizability to this more general setting.

Chapter 5

Conclusion and outlook

In this thesis we developed a non-Archimedean version of the (Euclidean) AdS/CFT correspondence (chapter 2), pointed out striking connections with the usual Archimedean AdS/CFT, and described simple bulk theories (chapters 2-3) and boundary theories (chapters 3-4) in some detail. The version of the correspondence we focussed on involved a bulk which had the fixed geometry of the Bruhat–Tits tree (an infinite regular graph without cycles of fixed coordination number $p^n + 1$, and the isometry group $\mathrm{PGL}(2, \mathbb{Q}_{p^n})$) and a boundary manifold constructed from $\mathbb{Q}_{p^n}$, the unramified field extension of the p-adic numbers. Chapters 2 and 3 provided a proof of principle for the non-Archimedean correspondence by exhibiting one of the touchstones of holography: Bulk Feynman diagrams on the Bruhat–Tits tree compute correlators which have the transformation properties of correlators in a conformal field theory with the global conformal group $\mathrm{PGL}(2, \mathbb{Q}_{p^n})$. A natural question to ask is: How does the Lorentzian version of the non-Archimedean AdS/CFT work? The causal structure of a Lorentzian space-time is not entirely obvious in the non-Archimedean setting because norms on a field are Euclidean (in particular, $|x| = 0 \Leftrightarrow x = 0$). Thus one can't have, for example, light-like directions. Perhaps one can look outside field norms, but

then does the Bruhat–Tits tree need to be replaced with some other construction, and do we still have p-adic numbers on the boundary?

It was clear throughout this dissertation, that the discreteness of the bulk, and the ultrametric nature of the boundary manifold resulted in a calculationally accessible framework for probing the (Euclidean) AdS/CFT correspondence. Recent interest in tensor network realizations of AdS/CFT has stemmed from developing a sufficiently simple framework for understanding how holography works in practice, *i.e.* how exactly is the bulk encoded in the boundary theory. Thus recent progress in relating the p-adic AdS/CFT framework to tensor network constructions [59, 60] provides a promising venue for furthering our understanding of holography.

A surprising property of the three-point function we found in chapters 2-3 may be summarized as the following remarkable adelic product. Setting $n = 1$ in (2.144), and for $x_i \in \mathbb{Q}$,

$$\prod_{v=p,\infty} \frac{\langle \mathcal{O}(x_1)\mathcal{O}(x_2)\mathcal{O}(x_3)\rangle_v}{(-\eta_v g_3)} = \frac{\zeta_{\mathbb{A}}(\Delta)^3 \zeta_{\mathbb{A}}(3\Delta-1)}{2\zeta_{\mathbb{A}}(2\Delta-1)^3}\,, \tag{5.1}$$

where the adelic zeta function $\zeta_{\mathbb{A}}$ is defined in (1.47). A more general adelic product for three-point correlators of scalar operators of arbitrary scaling dimensions may be obtained from (3.12) with the structure constants given by (3.22)-(3.24). The surprising observation that all coordinate dependence drops out of the adelic product is true only for $n = 1$, because we could employ the adelic product identity (1.44). Despite the fact that the adelic product in (5.1) doesn't work for $n \neq 1$, it is clear from the expressions for the structure constants that they have identical functional forms (for general n) when expressed in terms of local zeta functions. We demonstrate further evidence in this direction at the level of the four-point function in chapter 3. This suggests a deep connection between the Archimedean and non-Archimedean formulations which we do not fully under-

stand, but which offers a new vantage point into the workings of AdS/CFT.

To make the product in (5.1) work for general n, we would need a product rule like the one in (1.44) which works with multi-dimensional coordinates. One possible way out is to start with an algebraic number field K of degree n, and *then* complete it at its finite (non-Archimedean) and infinite (Archimedean) places. The local fields so constructed are no longer $\mathbb{Q}_p$ and $\mathbb{R}$. The Archimedean completion is some embedding of K in $\mathbb{C}$, while the non-Archimedean completions are $\mathfrak{p}$-adic numbers, where $\mathfrak{p}$ is a prime ideal in the ring of integers of K (see, for example [161, 162, 163] for expository accounts). It would be very interesting to develop a $\mathfrak{p}$-adic AdS/CFT correspondence based on the non-Archimedean completion of general algebraic number fields, such that the three-point function admits an adelic identity similar to (5.1), but for any n. Could such a construction be more similar to higher dimensional $\text{AdS}_{n+1}/\text{CFT}_n$ correspondence, than the one developed in this thesis?

We saw in chapters 2 and 3 that p-adic AdS/CFT shares several features of a low dimensional AdS/CFT correspondence, such as the structure of the isometry group. However, it seems to lack a key feature of low dimensional CFTs: local conformal invariance and the infinite dimensional Virasoro algebra. A p-adic field theory may be defined on a space which is an n-dimensional vector space over the p-adics $\mathbb{Q}_p$, by for example, considering the unramified extension $\mathbb{Q}_{p^n}$. Unlike the Archimedean case, nothing special happens at low values of n. In the Archimedean case, the boundary space has a field structure only when $n = 1$ or $n = 2$ (corresponding to the field of $\mathbb{R}$ and $\mathbb{C}$, respectively). No further field extensions of $\mathbb{R}$ are possible. The dimensions $n = 1$ and $n = 2$ are also the dimensions when conformal symmetry in the Archimedean case is enhanced to the full Virasoro symmetry. In the p-adics, the ability to construct field extensions of $\mathbb{Q}_p$ doesn't terminate at $n = 2$; one can consider field extensions

of any higher degree as well. Is this a hint that a (non-Archimedean) version of Virasoro symmetry is present at all values of n [72]? Or none? An important related question is what, if any, are the Virasoro generators in a p-adic CFT.

Considerable simplifications occur in p-adic CFTs due to the lack of derivatives in the operator product expansions, as discussed in chapter 3. This leads, for example, to a very simple closed-form expression for the four-point functions, due to the fact that the conformal block decomposition does not involve derivatives of primary operators, or any descendants in the intermediate channels. Moreover, as discussed in chapter 3, there are only finitely many single poles present in the intermediate channels of the conformal block decomposition, as opposed to infinitely many of them in the Archimedean case. However, a comparison between the precise coefficients accompanying the poles reveals remarkable adelic similarities. This is a hint that perhaps a simpler adelic story exists for the four-point function *before* one sums over all the poles. Thus developing a p-adic version of the Mellin amplitudes story [164, 165], where at least all poles associated with the multi-trace exchanges are factored out, may be a desirable next step.

In chapter 3, we also took the first steps towards identifying a dual pair of theories. We constructed a minimal bulk action which reproduced the two-, three- and four-point functions of scalar operators of the free $O(N)$ model. We tuned various couplings in the bulk theory to force a match between the bulk and boundary calculations for the normalizations of the two- and three-point functions. We had one final tunable parameter available to force a match between the bulk and the boundary for the functional form of the four-point function. With no additional parameter available to be tuned, it wasn't guaranteed that the overall coefficient of the holographically obtained four-point function, which depended on the already tuned bulk couplings, would agree with the normalization of the four-point function obtained via field theoretic methods on the boundary. That

the coefficients were found to agree can be seen as the first example of a duality test in the non-Archimedean AdS/CFT correspondence. Owing to the simplistic nature of non-Archimedean AdS/CFT, further tests which constrain the bulk action should be within reach. For example, it would be interesting to extend the match to higher point correlators. However, an understanding of symmetry principles which guide the construction of the bulk is missing.

The story in the Archimedean case also differs significantly. The bulk dual of the free $O(N)$ model is a Vasiliev higher spin theory, as discussed in chapter 1. In this dissertation, we have restricted ourselves to just scalar fields in the bulk, and scalar operators on the boundary. The construction of local conserved currents in a p-adic field theory, for example the analog of the infinitely many higher spin conserved currents in the free Archimedean $O(N)$ model, is lacking. Correspondingly, the description of gauge fields in the bulk is lacking as well. More generally, it would be highly desirable to learn how to describe spinning degrees of freedom in the bulk and the boundary theories. At least in the boundary theory, this will likely involve the inclusion of more general multiplicative characters as suggested in section 4.5 (see also discussions in [68, 166, 167, 59]). With this in hand, one would be able study many more rich and interesting theories such as the non-Archimedean versions of various gauge theories.

A connected, but seemingly hard task is the bulk description of spin fields. Recently in [32], some progress was made towards extending the bulk constructions of this thesis to include fluctuating gravity. The key idea involves considering fluctuations in the lengths of edges on the Bruhat–Tits tree, as the graviton degree of freedom, and also involves a graph-theoretic notion for the Ricci scalar (which does not depend on defining holonomies on a lattice). The operator dual to the edge-length fluctuations was found to share some properties with the stress-tensor, but lacked many others, such as a notion of spin. However, multiplicative

characters were not included in the analysis, which perhaps explains why a spin structure is lacking. Nevertheless, a discrete version of Einstein equations could be written, whose exact solutions included, other than the Bruhat–Tits tree itself, certain discrete graphs with cycles (the simplest example being a tree with one cycle). Roughly, a tree with a single cycle is understood as the quotient of the Bruhat–Tits tree with a Schottky subgroup (see [59] and references therein), and corresponds to a negatively curved bulk geometry with a black hole. These results seem to be suggest we are headed in the right direction but are missing one or two key ideas to arrive at a satisfactory (non-Archimedean) description of fluctuating geometry.

Moving on to field theory, in chapter 4 we studied the renormalization group flows of an interacting p-adic quantum field theory, and computed the anomalous dimensions of low lying operators in the ϵ-expansion as well as the $1/N$ expansion in large N, at the interacting fixed point. The large N methods admitted mostly a simultaneous treatment of Archimedean and non-Archimedean theories, and this was apparent in the expressions obtained for the anomalous dimensions, which had a universal form, independent of the choice of the local field.

Anomalous dimensions are related to critical exponents which can be measured in experimental systems and checked against predictions from a CFT which lies in the same universality class. If a non-Archimedean version of the CFT exists as well, then we have an infinite number of anomalous dimensions (one for every prime p, and one for the place at infinity) associated with some operator. Presumably, the one measured experimentally is associated with the Archimedean anomalous dimension, but we know the non-Archimedean anomalous dimensions are related to the Archimedean one via a universal formula in terms of residues of meromorphic functions constructed out of local zeta functions. This begs the question: Do non-Archimedean anomalous dimensions have any physical inter-

pretation, *i.e.* can they be measured directly in experiments?

This leads to a philosophical question about the non-Archimedean framework advanced in this thesis. Is it just a convenient mathematical construction, or does it have a physical significance of its own? We have shown in this thesis hints of connections between Archimedean and non-Archimedean theories via some adelic relations, but so far it is not clear if we can build purely adelic theories (perhaps even those that describe our Nature) where no norm (Archimedean or non-Archimedean) is preferred over another.

References

[1] **Particle Data Group** Collaboration, C. Patrignani *et. al.*, "Review of Particle Physics," *Chin. Phys.* **C40** (2016), no. 10 100001.

[2] **ATLAS** Collaboration, G. Aad *et. al.*, "Observation of a new particle in the search for the Standard Model Higgs boson with the ATLAS detector at the LHC," *Phys. Lett.* **B716** (2012) 1–29, 1207.7214.

[3] **CMS** Collaboration, S. Chatrchyan *et. al.*, "Observation of a new boson at a mass of 125 GeV with the CMS experiment at the LHC," *Phys. Lett.* **B716** (2012) 30–61, 1207.7235.

[4] **Virgo, LIGO Scientific** Collaboration, B. P. Abbott *et. al.*, "Observation of Gravitational Waves from a Binary Black Hole Merger," *Phys. Rev. Lett.* **116** (2016), no. 6 061102, 1602.03837.

[5] **Virgo, LIGO Scientific** Collaboration, B. P. Abbott *et. al.*, "GW151226: Observation of Gravitational Waves from a 22-Solar-Mass Binary Black Hole Coalescence," *Phys. Rev. Lett.* **116** (2016), no. 24 241103, 1606.04855.

[6] **VIRGO, LIGO Scientific** Collaboration, B. P. Abbott *et. al.*, "GW170104: Observation of a 50-Solar-Mass Binary Black Hole Coalescence at Redshift 0.2," *Phys. Rev. Lett.* **118** (2017), no. 22 221101.

[7] **Super-Kamiokande** Collaboration, Y. Fukuda *et. al.*, "Evidence for oscillation of atmospheric neutrinos," *Phys. Rev. Lett.* **81** (1998) 1562–1567, `hep-ex/9807003`.

[8] **SNO** Collaboration, Q. R. Ahmad *et. al.*, "Measurement of the rate of $\nu_e + d \to p + p + e^-$ interactions produced by ^8B solar neutrinos at the Sudbury Neutrino Observatory," *Phys. Rev. Lett.* **87** (2001) 071301, `nucl-ex/0106015`.

[9] **SNO** Collaboration, Q. R. Ahmad *et. al.*, "Direct evidence for neutrino flavor transformation from neutral current interactions in the Sudbury Neutrino Observatory," *Phys. Rev. Lett.* **89** (2002) 011301, `nucl-ex/0204008`.

[10] G. Veneziano, "Construction of a crossing - symmetric, Regge behaved amplitude for linearly rising trajectories," *Nuovo Cim.* **A57** (1968) 190–197.

[11] J. Scherk and J. H. Schwarz, "Dual Models for Nonhadrons," *Nucl. Phys.* **B81** (1974) 118–144.

[12] T. Yoneya, "Connection of Dual Models to Electrodynamics and Gravidynamics," *Prog. Theor. Phys.* **51** (1974) 1907–1920.

[13] M. B. Green and J. H. Schwarz, "Anomaly Cancellation in Supersymmetric D=10 Gauge Theory and Superstring Theory," *Phys. Lett.* **B149** (1984) 117–122.

[14] E. Witten, "String theory dynamics in various dimensions," *Nucl. Phys.* **B443** (1995) 85–126, `hep-th/9503124`.

[15] P. Horava and E. Witten, "Heterotic and type I string dynamics from eleven-dimensions," *Nucl. Phys.* **B460** (1996) 506–524, hep-th/9510209.

[16] P. Horava and E. Witten, "Eleven-dimensional supergravity on a manifold with boundary," *Nucl. Phys.* **B475** (1996) 94–114, hep-th/9603142.

[17] C. M. Hull and P. K. Townsend, "Unity of superstring dualities," *Nucl. Phys.* **B438** (1995) 109–137, hep-th/9410167.

[18] T. Banks, W. Fischler, S. H. Shenker, and L. Susskind, "M theory as a matrix model: A Conjecture," *Phys. Rev.* **D55** (1997) 5112–5128, hep-th/9610043.

[19] J. Polchinski, "Dirichlet Branes and Ramond-Ramond charges," *Phys. Rev. Lett.* **75** (1995) 4724–4727, hep-th/9510017.

[20] G. 't Hooft, "Dimensional reduction in quantum gravity," in *Salamfest 1993:0284-296*, pp. 0284–296, 1993. gr-qc/9310026.

[21] L. Susskind, "The World as a hologram," *J. Math. Phys.* **36** (1995) 6377–6396, hep-th/9409089.

[22] J. M. Maldacena, "The Large N limit of superconformal field theories and supergravity," *Int. J. Theor. Phys.* **38** (1999) 1113–1133, hep-th/9711200.

[23] S. S. Gubser, I. R. Klebanov, and A. M. Polyakov, "Gauge theory correlators from noncritical string theory," *Phys. Lett.* **B428** (1998) 105–114, hep-th/9802109.

[24] E. Witten, "Anti-de Sitter space and holography," *Adv. Theor. Math. Phys.* **2** (1998) 253–291, hep-th/9802150.

[25] N. Arkani-Hamed and J. Trnka, "The Amplituhedron," *JHEP* **10** (2014) 030, 1312.2007.

[26] H. W. Hamber, "Quantum Gravity on the Lattice," *Gen. Rel. Grav.* **41** (2009) 817–876, 0901.0964.

[27] J. Ambjorn, J. Jurkiewicz, and R. Loll, "Lattice quantum gravity: An Update," *PoS* **LATTICE2010** (2010) 014, 1105.5582.

[28] M. Dupuis, J. P. Ryan, and S. Speziale, "Discrete gravity models and Loop Quantum Gravity: a short review," *SIGMA* **8** (2012) 052, 1204.5394.

[29] S. S. Gubser, "Evolution of segmented strings," *Phys. Rev.* **D94** (2016), no. 10 106007, 1601.08209.

[30] D. Vegh, "Segmented strings from a different angle," 1601.07571.

[31] S. S. Gubser, S. Parikh, and P. Witaszczyk, "Segmented strings and the McMillan map," *JHEP* **07** (2016) 122, 1602.00679.

[32] S. S. Gubser, M. Heydeman, C. Jepsen, M. Marcolli, S. Parikh, I. Saberi, B. Stoica, and B. Trundy, "Edge length dynamics on graphs with applications to p-adic AdS/CFT," 1612.09580.

[33] O. Aharony, S. S. Gubser, J. M. Maldacena, H. Ooguri, and Y. Oz, "Large N field theories, string theory and gravity," *Phys. Rept.* **323** (2000) 183–386, hep-th/9905111.

[34] Y. Nakayama, "Scale invariance vs conformal invariance," *Phys. Rept.* **569** (2015) 1–93, 1302.0884.

[35] Y. Nakayama, "Interacting scale invariant but nonconformal field theories," *Phys. Rev.* **D95** (2017), no. 6 065016, 1611.10040.

[36] P. Breitenlohner and D. Z. Freedman, "Positive Energy in anti-De Sitter Backgrounds and Gauged Extended Supergravity," *Phys. Lett.* **B115** (1982) 197–201.

[37] I. R. Klebanov and E. Witten, "AdS / CFT correspondence and symmetry breaking," *Nucl. Phys.* **B556** (1999) 89–114, hep-th/9905104.

[38] J. McGreevy, "Holographic duality with a view toward many-body physics," *Adv. High Energy Phys.* **2010** (2010) 723105, 0909.0518.

[39] I. R. Klebanov and A. M. Polyakov, "AdS dual of the critical O(N) vector model," *Phys. Lett.* **B550** (2002) 213–219, hep-th/0210114.

[40] S. Giombi, "Higher Spin CFT Duality," in *Proceedings, Theoretical Advanced Study Institute in Elementary Particle Physics: New Frontiers in Fields and Strings (TASI 2015): Boulder, CO, USA, June 1-26, 2015*, pp. 137–214, 2017. 1607.02967.

[41] M. A. Vasiliev, "Nonlinear equations for symmetric massless higher spin fields in (A)dS(d)," *Phys. Lett.* **B567** (2003) 139–151, hep-th/0304049.

[42] S. S. Gubser and I. R. Klebanov, "A Universal result on central charges in the presence of double trace deformations," *Nucl. Phys.* **B656** (2003) 23–36, hep-th/0212138.

[43] E. Witten, "Multitrace operators, boundary conditions, and AdS / CFT correspondence," hep-th/0112258.

[44] S. A. Hartnoll, "Lectures on holographic methods for condensed matter physics," *Class. Quant. Grav.* **26** (2009) 224002, 0903.3246.

[45] S. S. Gubser and A. Karch, "From gauge-string duality to strong interactions: A Pedestrian's Guide," *Ann. Rev. Nucl. Part. Sci.* **59** (2009) 145–168, 0901.0935.

[46] B. Dragovich, A. Yu. Khrennikov, S. V. Kozyrev, I. V. Volovich, and E. I. Zelenov, "p-Adic Mathematical Physics: The First 30 Years," *Anal. Appl.* **9** (2017) 87–121, 1705.04758.

[47] S. S. Gubser, J. Knaute, S. Parikh, A. Samberg, and P. Witaszczyk, "p-adic AdS/CFT," *Commun. Math. Phys.* **352** (2017), no. 3 1019–1059, 1605.01061.

[48] L. Brekke, P. G. O. Freund, M. Olson, and E. Witten, "Nonarchimedean String Dynamics," *Nucl. Phys.* **B302** (1988) 365–402.

[49] F. Q. Gouvêa, *p-adic Numbers*. Springer, 1997.

[50] Y. I. Manin, "p-Adic automorphic functions," *Journal of Mathematical Sciences* **5** (1976), no. 3 279–333.

[51] A. Samberg, "p-adic AdS/CFT," in *Recent Mathematical Developments in Quantum Field Theory 2016* (A. Abdelmalek, H. Stefan, K. Christoph, and L. Gandalf, eds.), vol. 13, pp. 2069–2122, Oberwolfach Rep., July, 2016.

[52] S. S. Gubser, "p-adic AdS/CFT," in *Strings 2016* (J. Maldacena, H. Ooguri, H. Babak, S. Li, W. Song, and H. Lin, eds.), Adv. Theor. Math. Phys., 2017.

[53] S. S. Gubser, "A p-adic version of AdS/CFT," 1705.00373.

[54] D. Harlow, S. H. Shenker, D. Stanford, and L. Susskind, "Tree-like structure of eternal inflation: A solvable model," *Phys. Rev.* **D85** (2012) 063516, 1110.0496.

[55] B. Swingle, "Entanglement Renormalization and Holography," *Phys. Rev.* **D86** (2012) 065007, 0905.1317.

[56] B. Swingle, "Constructing holographic spacetimes using entanglement renormalization," 1209.3304.

[57] X.-L. Qi, "Exact holographic mapping and emergent space-time geometry," 1309.6282.

[58] F. Pastawski, B. Yoshida, D. Harlow, and J. Preskill, "Holographic quantum error-correcting codes: Toy models for the bulk/boundary correspondence," *JHEP* **06** (2015) 149, 1503.06237.

[59] M. Heydeman, M. Marcolli, I. Saberi, and B. Stoica, "Tensor networks, p-adic fields, and algebraic curves: arithmetic and the $\mathrm{AdS}_3/\mathrm{CFT}_2$ correspondence," 1605.07639.

[60] A. Bhattacharyya, L.-Y. Hung, Y. Lei, and W. Li, "Tensor network and (p-adic) AdS/CFT," 1703.05445.

[61] D. Vegh, "The broken string in anti-de Sitter space," 1508.06637.

[62] N. Callebaut, S. S. Gubser, A. Samberg, and C. Toldo, "Segmented strings in AdS_3," *JHEP* **11** (2015) 110, 1508.07311.

[63] D. Vegh, "Colliding waves on a string in AdS_3," 1509.05033.

[64] D. Vegh, "Segmented strings coupled to a B-field," 1603.04504.

[65] P. G. O. Freund and M. Olson, "Nonarchimedean Strings," *Phys. Lett.* **B199** (1987) 186–190.

[66] P. G. O. Freund and E. Witten, "Adelic String Amplitudes," *Phys. Lett.* **B199** (1987) 191.

[67] L. Brekke and P. G. O. Freund, "p-adic numbers in physics," *Phys. Rept.* **233** (1993) 1–66.

[68] A. V. Zabrodin, "Nonarchimedean Strings and Bruhat-Tits Trees," *Commun. Math. Phys.* **123** (1989) 463–483.

[69] L. Brekke, P. G. O. Freund, E. Melzer, and M. Olson, "Adelic strings N point amplitudes," *Phys. Lett.* **B216** (1989) 53–58.

[70] D. Ghoshal, "p-adic string theories provide lattice discretization to the ordinary string worldsheet," *Phys. Rev. Lett.* **97** (2006) 151601.

[71] A. A. Gerasimov and S. L. Shatashvili, "On exact tachyon potential in open string field theory," *JHEP* **10** (2000) 034, `hep-th/0009103`.

[72] J.-L. Gervais, "p-adic Analyticity and Virasoro Algebras for Conformal Theories in More Than Two Dimensions," *Phys. Lett.* **B201** (1988) 306.

[73] L. O. Chekhov, A. D. Mironov, and A. V. Zabrodin, "Multiloop Calculations in P-adic String Theory and Bruhat-Tits Trees," *Commun. Math. Phys.* **125** (1989) 675.

[74] Y. I. Manin and M. Marcolli, "Holography principle and arithmetic of algebraic curves," *Adv. Theor. Math. Phys.* **5** (2002) 617–650, `hep-th/0201036`.

[75] Y. I. Manin, "Three-dimensional hyperbolic geometry as ∞-adic Arakelov geometry," *Inventiones Mathematicae* **104** (1991), no. 1 223–243.

[76] W. Mueck and K. S. Viswanathan, "Conformal field theory correlators from classical scalar field theory on AdS(d+1)," *Phys. Rev.* **D58** (1998) 041901, hep-th/9804035.

[77] D. Z. Freedman, S. D. Mathur, A. Matusis, and L. Rastelli, "Correlation functions in the CFT(d) / AdS(d+1) correspondence," *Nucl. Phys.* **B546** (1999) 96–118, hep-th/9804058.

[78] E. D'Hoker, D. Z. Freedman, S. D. Mathur, A. Matusis, and L. Rastelli, "Graviton exchange and complete four point functions in the AdS / CFT correspondence," *Nucl. Phys.* **B562** (1999) 353–394, hep-th/9903196.

[79] N. Bao, C. Cao, S. M. Carroll, A. Chatwin-Davies, N. Hunter-Jones, J. Pollack, and G. N. Remmen, "Consistency conditions for an AdS multiscale entanglement renormalization ansatz correspondence," *Phys. Rev.* **D91** (2015), no. 12 125036, 1504.06632.

[80] J. M. Maldacena, "Wilson loops in large N field theories," *Phys. Rev. Lett.* **80** (1998) 4859–4862, hep-th/9803002.

[81] S.-J. Rey and J.-T. Yee, "Macroscopic strings as heavy quarks in large N gauge theory and anti-de Sitter supergravity," *Eur. Phys. J.* **C22** (2001) 379–394, hep-th/9803001.

[82] R. J. Baxter, *Exactly solved models in statistical mechanics*. Academic Press Limited, 24-28 Oval Road, London NW1 7DX, 1982.

[83] Y. M. Zinoviev, "Ising model on the generalized Bruhat-Tits tree," *Commun. Math. Phys.* **130** (1990) 433–440.

[84] S. S. Gubser and S. Parikh, "Geodesic bulk diagrams on the Bruhat-Tits tree," 1704.01149.

[85] P. Dutta, D. Ghoshal, and A. Lala, "On the Exchange Interactions in Holographic p-adic CFT," 1705.05678.

[86] E. Hijano, P. Kraus, E. Perlmutter, and R. Snively, "Witten Diagrams Revisited: The AdS Geometry of Conformal Blocks," *JHEP* **01** (2016) 146, 1508.00501.

[87] E. Melzer, "Nonarchimedean Conformal Field Theories," *International Journal of Modern Physics A* **04** (1989), no. 18 4877–4908.

[88] S. Bosch, U. Güntzer, and R. Remmert, *Non-Archimedean analysis. A systematic approach to rigid analytic geometry*, vol. 261 of *Grundlehren der Mathematischen Wissenschaften*. Springer, 1984.

[89] M. F. Paulos, J. Penedones, J. Toledo, B. C. van Rees, and P. Vieira, "The S-matrix Bootstrap I: QFT in AdS," 1607.06109.

[90] O. Aharony, L. F. Alday, A. Bissi, and E. Perlmutter, "Loops in AdS from Conformal Field Theory," 1612.03891.

[91] C. Behan, L. Rastelli, S. Rychkov, and B. Zan, "A scaling theory for the long-range to short-range crossover and an infrared duality," 1703.05325.

[92] F. A. Dolan and H. Osborn, "Conformal four point functions and the operator product expansion," *Nucl. Phys.* **B599** (2001) 459–496, hep-th/0011040.

[93] B. Czech, L. Lamprou, S. McCandlish, B. Mosk, and J. Sully, "A Stereoscopic Look into the Bulk," *JHEP* **07** (2016) 129, 1604.03110.

[94] E. D'Hoker and D. Z. Freedman, "Supersymmetric gauge theories and the AdS / CFT correspondence," in *Strings, Branes and Extra Dimensions: TASI 2001: Proceedings*, pp. 3–158, 2002. hep-th/0201253.

[95] H. Liu, "Scattering in anti-de Sitter space and operator product expansion," *Phys. Rev.* **D60** (1999) 106005, hep-th/9811152.

[96] A. Petkou, "Conserved currents, consistency relations and operator product expansions in the conformally invariant O(N) vector model," *Annals Phys.* **249** (1996) 180–221, hep-th/9410093.

[97] E. Sezgin and P. Sundell, "Holography in 4D (super) higher spin theories and a test via cubic scalar couplings," *JHEP* **07** (2005) 044, hep-th/0305040.

[98] M. A. Vasiliev, "Higher spin gauge theories in four-dimensions, three-dimensions, and two-dimensions," *Int. J. Mod. Phys.* **D5** (1996) 763–797, hep-th/9611024.

[99] M. R. Gaberdiel and R. Gopakumar, "An AdS_3 Dual for Minimal Model CFTs," *Phys. Rev.* **D83** (2011) 066007, 1011.2986.

[100] M. R. Gaberdiel and R. Gopakumar, "Minimal Model Holography," *J. Phys.* **A46** (2013) 214002, 1207.6697.

[101] X. Bekaert, J. Erdmenger, D. Ponomarev, and C. Sleight, "Quartic AdS Interactions in Higher-Spin Gravity from Conformal Field Theory," *JHEP* **11** (2015) 149, 1508.04292.

[102] C. Sleight and M. Taronna, "Higher Spin Interactions from Conformal Field Theory: The Complete Cubic Couplings," *Phys. Rev. Lett.* **116** (2016), no. 18 181602, 1603.00022.

[103] X. Bekaert, J. Erdmenger, D. Ponomarev, and C. Sleight, "Towards holographic higher-spin interactions: Four-point functions and higher-spin exchange," *JHEP* **03** (2015) 170, 1412.0016.

[104] R. Gopakumar, A. Kaviraj, K. Sen, and A. Sinha, "A Mellin space approach to the conformal bootstrap," 1611.08407.

[105] S. S. Gubser, C. Jepsen, S. Parikh, and B. Trundy, "$O(N)$ and $O(N)$ and $O(N)$," 1703.04202.

[106] M. Nishida and K. Tamaoka, "Geodesic Witten diagrams with an external spinning field," 1609.04563.

[107] A. Castro, E. Llabrés, and F. Rejon-Barrera, "Geodesic Diagrams, Gravitational Interactions & OPE Structures," 1702.06128.

[108] E. Dyer, D. Z. Freedman, and J. Sully, "Spinning Geodesic Witten Diagrams," 1702.06139.

[109] H.-Y. Chen, E.-J. Kuo, and H. Kyono, "Anatomy of Geodesic Witten Diagrams," 1702.08818.

[110] C. Sleight and M. Taronna, "Spinning Witten Diagrams," 1702.08619.

[111] M. A. Vasiliev, "Consistent equation for interacting gauge fields of all spins in (3+1)-dimensions," *Phys.Lett.* **B243** (1990) 378–382.

[112] M. A. Vasiliev, "More on equations of motion for interacting massless fields of all spins in (3+1)-dimensions," *Phys.Lett.* **B285** (1992) 225–234.

[113] F. J. Dyson, "Existence of a phase transition in a one-dimensional Ising ferromagnet," *Commun. Math. Phys.* **12** (1969) 91–107.

[114] E. Yu. Lerner and M. D. Missarov, "Scalar Models of p-adic Quantum Field Theory and Hierarchical Models," *Theor. Math. Phys.* **78** (1989) 177–184.

[115] K. G. Wilson, "Renormalization group and critical phenomena. 1. Renormalization group and the Kadanoff scaling picture," *Phys. Rev.* **B4** (1971) 3174–3183.

[116] K. G. Wilson, "Renormalization group and critical phenomena. 2. Phase space cell analysis of critical behavior," *Phys. Rev.* **B4** (1971) 3184–3205.

[117] K. G. Wilson and J. B. Kogut, "The Renormalization group and the epsilon expansion," *Phys. Rept.* **12** (1974) 75–200.

[118] L. P. Kadanoff, "Scaling laws for Ising models near T_c," *Physics* **2** (1966) 263–272.

[119] P. M. Bleher and J. G. Sinai, "Investigation of the critical point in models of the type of Dyson's hierarchical models," *Comm. Math. Phys.* **33** (1973), no. 1 23–42.

[120] P. M. Bleher and Y. G. Sinai, "Critical indices for Dyson's asymptotically-hierarchical models," *Comm. Math. Phys.* **45** (1975), no. 3 247–278.

[121] P. M. Bleher and P. Major, "Critical Phenomena and Universal Exponents in Statistical Physics. On Dyson's Hierarchical Model," *Ann. Probab.* **15** (04, 1987) 431–477.

[122] M. D. Missarov and R. G. Stepanov, "Critical Exponents in p-Adic ϕ^4-Model," *AIP Conf. Proc.* **826** (2006) 129–139.

[123] M. D. Missarov and R. G. Stepanov, "Epsilon-expansion in the N-component ϕ^4 model," *Theor. Math. Phys.* **146** (2006) 304–320.

[124] M. Missarov, "p-Adic Renormalization Group Solutions and the Euclidean Renormalization Group Conjectures," *P-Adic Numbers, Ultrametric Analysis, and Applications* **4** (2012), no. 2 109–114.

[125] S. Giombi and X. Yin, "Higher Spin Gauge Theory and Holography: The Three-Point Functions," *JHEP* **09** (2010) 115, 0912.3462.

[126] M. E. Fisher, S.-k. Ma, and B. G. Nickel, "Critical Exponents for Long-Range Interactions," *Phys. Rev. Lett.* **29** (1972) 917–920.

[127] J. Sak, "Recursion Relations and Fixed Points for Ferromagnets with Long-Range Interactions," *Phys. Rev. B* **8** (Jul, 1973) 281–285.

[128] M. F. Paulos, S. Rychkov, B. C. van Rees, and B. Zan, "Conformal Invariance in the Long-Range Ising Model," *Nucl. Phys.* **B902** (2016) 246–291, 1509.00008.

[129] E. Gava and R. Jengo, "A four-dimensional nonlinear σ-model," *Nucl. Phys.* **B140** (1978) 510–524.

[130] R. M. Hornreich, M. Luban, and S. Shtrikman, "Critical Behavior at the Onset of $\vec{k}$-Space Instability on the λ Line," *Phys. Rev. Lett.* **35** (Dec, 1975) 1678–1681.

[131] A. Michelson, "Phase diagrams near the Lifshitz point. I. Uniaxial magnetization," *Phys. Rev. B* **16** (Jul, 1977) 577–584.

[132] S. A. Brazovskii, "Phase transition of an isotropic system to a nonuniform state," *Journal of Experimental and Theoretical Physics* **68** (1975) 175.

[133] W. Selke, "The ANNNI model – Theoretical analysis and experimental application," *Physics Reports* **170** (Nov., 1988) 213–264.

[134] A. N. Vasiliev, Yu. M. Pismak, and Yu. R. Khonkonen, "Simple Method of Calculating the Critical Indices in the $1/N$ Expansion," *Theor. Math. Phys.* **46** (1981) 104–113.

[135] A. N. Vasiliev, Yu. M. Pismak, and Yu. R. Khonkonen, "$1/N$ Expansion: Calculation of the Exponents η and ν in the Order $1/N^2$ for Arbitrary Number of Dimensions," *Theor. Math. Phys.* **47** (1981) 465–475.

[136] I. M. Gelfand, M. I. Graev, and I. I. Pyatetskii-Shapiro, *Representation Theory and Automorphic Functions*. Saunders, 1969.

[137] H. Kleinert and V. Schulte-Frohlinde, *Critical properties of ϕ^4-theories*. World Scientific, 2001.

[138] M. D'Eramo, L. Peliti, and G. Parisi, "Theoretical predictions for critical exponents at the λ-point of bose liquids," *Lettere al Nuovo Cimento Series 2* **2** (10, 1971) 878–880.

[139] M. Ciuchini, S. E. Derkachov, J. A. Gracey, and A. N. Manashov, "Computation of quark mass anomalous dimension at $O(1/N_f^2)$ in quantum chromodynamics," *Nucl. Phys.* **B579** (2000) 56–100, `hep-ph/9912221`.

[140] J. Honkonen and M. Yu. Nalimov, "Crossover between field theories with short range and long range exchange or correlations," *J. Phys.* **A22** (1989) 751–763.

[141] M. Chiara Angelini, G. Parisi, and F. Ricci-Tersenghi, "Relations between Short Range and Long Range Ising models," *Phys. Rev.* **E89** (Jan., 2014) 062120, 1401.6805.

[142] E. Brezin, G. Parisi, and F. Ricci-Tersenghi, "The Crossover Region Between Long-Range and Short-Range Interactions for the Critical Exponents," *Journal of Statistical Physics* (Aug., 2014) 1407.3358.

[143] N. Defenu, A. Trombettoni, and A. Codello, "Fixed-point structure and effective fractional dimensionality for O(N) models with long-range interactions," *Phys. Rev.* **E92** (2015), no. 5 052113, 1409.8322.

[144] R. Hornreich, M. Luban, and S. Shtrikman, "Critical exponents at a Lifshitz point to O(1/N)," *Physics Letters A* **55** (1975), no. 5 269 – 270.

[145] S. W. Hawking, "Who's afraid of (higher derivative) ghosts?," in *Quantum field theory and quantum statistics: essays in honour of the sixtieth birthday of ES Fradkin. V. 2.* Hilger, 1985.

[146] F. J. de Urries and J. Julve, "Ostrogradski formalism for higher derivative scalar field theories," *J. Phys.* **A31** (1998) 6949–6964, hep-th/9802115.

[147] K. Jansen, J. Kuti, and C. Liu, "The Higgs model with a complex ghost pair," *Phys. Lett.* **B309** (1993) 119–126, hep-lat/9305003.

[148] S. W. Hawking and T. Hertog, "Living with ghosts," *Phys. Rev.* **D65** (2002) 103515, hep-th/0107088.

[149] M. V. Ostrogradski, "Mémoire sur les équations différentielles relatives au problème des isopérimetres," *Mem. Ac. St. Petersbourg VI* **4** (1850) 385.

[150] A. B. Zamolodchikov, "Conformal Symmetry and Multicritical Points in Two-Dimensional Quantum Field Theory. (In Russian)," *Sov. J. Nucl. Phys.* **44** (1986) 529–533.

[151] F. Kos, D. Poland, D. Simmons-Duffin, and A. Vichi, "Bootstrapping the O(N) Archipelago," *JHEP* **11** (2015) 106, 1504.07997.

[152] F. Gliozzi, A. Guerrieri, A. C. Petkou, and C. Wen, "Generalized Wilson-Fisher critical points from the conformal OPE," *Phys. Rev. Lett.* **118** (2017), no. 6 061601, 1611.10344.

[153] F. Gliozzi, A. L. Guerrieri, A. C. Petkou, and C. Wen, "The analytic structure of conformal blocks and the generalized Wilson-Fisher fixed points," *JHEP* **04** (2017) 056, 1702.03938.

[154] R. J. Elliott, "Phenomenological Discussion of Magnetic Ordering in the Heavy Rare-Earth Metals," *Phys. Rev.* **124** (1961) 346–353.

[155] M. E. Fisher and W. Selke, "Infinitely Many Commensurate Phases in a Simple Ising Model," *Phys. Rev. Lett.* **44** (1980) 1502–1505.

[156] B. Berche, R. Kenna, and J. C. Walter, "Hyperscaling above the upper critical dimension," *Nucl. Phys.* **B865** (2012) 115–132.

[157] T. P. Eggarter, "Cayley trees, the Ising problem, and the thermodynamic limit," *Phys. Rev.* **B9** (1974) 2989–2992.

[158] E. Muller-Hartmann and J. Zittartz, "New Type of Phase Transition," *Phys. Rev. Lett.* **33** (1974) 893–897.

[159] R. C. Brower and P. Goddard, "Generalized Virasoro models," *Lett. Nuovo Cim.* **1S2** (1971) 1075–1081.

[160] A. Gadde, "In search of conformal theories," 1702.07362.

[161] K. Conrad, "Ostrowski's theorem for number fields." http://www.math.uconn.edu/~kconrad/blurbs/gradnumthy/ostrowskinumbfield.pdf.

[162] D. Prasad, "Lectures on algebraic number theory." www.math.tifr.res.in/~dprasad/ant.pdf, 2001.

[163] C. Singh Dalawat, "A first course in Local arithmetic," 0903.2615.

[164] J. Penedones, "Writing CFT correlation functions as AdS scattering amplitudes," *JHEP* **03** (2011) 025, 1011.1485.

[165] A. L. Fitzpatrick, J. Kaplan, J. Penedones, S. Raju, and B. C. van Rees, "A Natural Language for AdS/CFT Correlators," *JHEP* **11** (2011) 095, 1107.1499.

[166] A. V. Marshakov and A. V. Zabrodin, "New p-adic string amplitudes," *Mod. Phys. Lett.* **A5** (1990) 265.

[167] P. Ruelle, E. Thiran, D. Verstegen, and J. Weyers, "Adelic String and Superstring Amplitudes," *Mod. Phys. Lett.* **A4** (1989) 1745.